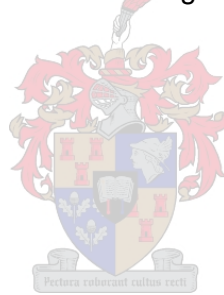


Towards Design Rules for Reinforced Strain Hardening Cement Composites (R/SHCC) in bending

Susanna Aletta Engelbrecht



Dissertation presented for the degree of Doctor in the Philosophy of Engineering at Stellenbosch University

Prof. G.P.A.G. van Zijl

March 2018

DECLARATION

By submitting this thesis electronically, I declare that the entirety of the work contained therein is my own, original work, that I am the authorship owner thereof (unless to the extend explicitly otherwise stated) and that I have not previously in its entirety or in part submitted it for obtaining any qualification.

March 2018

VERKLARING

Deur hierdie tesis elektronies in te lewer verklaar ek dat die geheel van die werk hierin vervat, my eie, oorspronklike werk is (behalwe tot die mate uitdruklik anders aangedui) en dat ek dit nie vantevore, in the geheel of gedeeltelik, ter verkryging van enige kwalifikasie aangebied het nie.

Maart 2018

ABSTRACT

Strain Hardening Cement Composites (SHCC) are cement-based materials with remarkable characteristics. Its strain hardening ability under tension enables it to carry increased loads, after the material has cracked. Combined with conventional reinforcement, this material has been demonstrated to have remarkable damage tolerance under severe loading conditions. SHCC has also been proven to show very small crack widths under service conditions. This is a very attractive characteristic for durability.

There are very few design guidelines for using R/SHCC as a structural material, though its properties and characteristics have been widely studied. This study aims at providing the structural designer with an analytical design model for designing flexural members constructed from R/SHCC. The design model aims to be universal and applicable to most types of strain hardening cement based materials.

The base design model is derived from first principles, using existing knowledge of the materials' behaviour under uniaxial tension and compression. Both tensile and compressive responses are simplified into bilinear approximations in order to simplify the calculations. Even with this simplification, the base design model is calculated in three phases to incorporate the various stadia that the material undergoes under flexural bending. Phase one represents the elastic phase where the cement matrix has not yet cracked. Phase two starts with the onset of cracking in the tensile zone. During Phase 2, the compression part of the member is still assumed to be elastic as the compressive strain has not passed the ultimate compressive strain limit. This limit is set as the boundary where the compressive behaviour changes from elastic to plastic. The last phase starts with the compressive strain passing its plastic limit. The third phase ends with the member failing either in compression or in tension.

As the base design model is very complicated and not user friendly, it is simplified into something that can be calculated on a hand held calculator. The simplification of the design model is done by analysing a number of different scenarios with different member sizes and different amounts of reinforcement. For each one, the tensile strain in the SHCC matrix is noted and a simple relationship between the height of the flexural member and the tensile strain can be found. The position of the neutral axis and the design compressive strain can then be found from existing relationships. This simplified design model is then tested against two other SHCC materials in order to establish the universality of the design model.

During the reliability analysis, material factors are derived for the strength parameters of the material. Model factors are also derived from beam tests compared to model predictions. Twelve large beams

are tested and their load versus deflection graphs compared to the predicted loads versus deflections from the base design model.

Finally, an example design is done to show how the simplified design model, combined with its model factors, can be applied to practical design work. The amount of reinforcement needed in an R/SHCC member is then compared to that needed in a conventional R/C member of the same size and constructed of concrete with the same compressive strength. As expected the tensile reinforcement needed in the R/SHCC member is less than that needed in the conventional R/C member in bending. However, the same is not always true for the compressive reinforcement.

UITTREKSEL

Vervormingsverhardende Sementbasis Saamgestelde Materiale (SHCC) is 'n sementbasis materiaal met buitengewone eienskappe. Die vermoë om, nadat die sement matriks reeds begin kraak het steeds hoër laste te dra is een van die mees kenmerkende eienskappe van hierdie materiaal. Gekombineer met konvensionele staal bewapening, is dit bewys dat die materiaal oor uitmuntende skade tolleransie onder buitengewone las toestande beskik. Daar is ook bewys dat die materiaal baie klein kraak wydtes toon onder dienslas toestande, wat dit as 'n duursame materiaal bevestig.

Tot op hede is daar baie min ontwerpriglyne beskikbaar vir die gebruik van R/SHCC as 'n strukturele materiaal, hoewel die eienskappe en gedrag van die materiaal wyd bestudeer is. Hierdie proefskrif poog om die ontwerper te voorsien van 'n analitiese ontwerpmodel vir die ontwerp van R/SHCC strukturele elemente in hoofsaaklik buiging. Die model is universeel en toepaslik op die meeste van die verskillende tipes SHCC.

The basismodel is afgelei uit eerste beginsels en bestaande kennis van die materiaal se gedrag onder een-assige trek en druk laste. Beide die trek en druk reaksies word vereenvoudig met 'n bi-lineêre benadering in 'n poging om die berekeninge te vereenvoudig. Selfs met die vereenvoudiging moet die model steeds in drie fases bereken word sodat al die verskillende stadia wat die element in buiging ondergaan beskryf kan word. Fase een is die elastiese fase waar daar nog geen krale in die sementmatriks is nie. Fase twee begin wanneer die eerste krale in die sementmatriks vorm. Die druk deel van die element word aanvaar om steeds in 'n elastiese toestand te wees gedurende Fase twee. Dit is omdat daar aanvaar word dat die drukvervorming nog nie die limiet drempelwaarde bereik het nie. Hierdie limiet dui die grens tussen die plastiese en elastiese drukgedrag aan. Die derde en laaste fase begin wanneer die drukvervorming die plastiese limiet oorskry. Hierdie fase eindig wanneer die element faal. Die faling kan in trek of in druk wees.

Aangesien die basismodel baie gekompliseerd en nie baie gebruikersvriendelik is nie, word dit vereenvoudig tot iets wat met die hand bereken kan word. Die vereenvoudiging is gedoen deur 'n aantal verskillende moontlikhede te ondersoek waar die struktuurelement groottes en die volume staal gevarieer word. Vir elke situasie is daar 'n nota gemaak van die trek vervorming in die sement matriks en 'n eenvoudige eksponensiele vergelyking is gevind tussen die trekvervorming en die diepte van die buigelemente. Die posisie van die neutrale as en die ontwerp drukvervorming kan dan uit bestaande verhoudings bereken word. Die vereenvoudigde model word dan getoets met twee ander SHCC materiale om te bewys dat dit wel universeel is.

In 'n betroubaarheidsstudie is daar materiaalfaktore afgelei vir die sterkte eienskappe van die materiaal. Modelfaktore is ook afgelei vir elke fase van die ontwerp deur die uitkomst van toetse en die voorspelling van die model teen mekaar op te weeg. Twaalf groot balke is getoets en die gemete las teenoor die verplasing vir elkeen is vergelyk met die voorspelde las en verplasing van die basismodel.

Laastens is daar 'n voorbeeld ontwerp gedoen om aan die ontwerper te demonstreer hoe die vereenvoudigde model in 'n alledaagse ontwerp gebruik kan word. Die hoeveelheid bewapening wat die R/SHCC balk nodig is dan opgeweeg teenoor die hoeveelheid bewapening wat 'n konvensionele R/C balk nodig. Soos verwag nodig die R/SHCC balk minder trekstaal as die gewone R/C balk. Dieselfde kan egter nie in alle gevalle gesê word van die drukstaal in die onderskeie balke nie.

CONTENTS

Declaration	i
Verklaring	i
Abstract	ii
Uittreksel	iv
List of Figures	xi
List of Tables:	xv
List of Abbreviations	xvi
List of Symbols	xvii
Foreword	1
Scope	1
Overview	2
1. INTRODUCTION TO FIBER REINFORCED CONCRETE	3
1.1 Classification	3
1.2 Strain Hardening Cement Composites (SHCC)	6
1.2.1 The History of SHCC	6
1.2.2 Unique characteristics of ECC	7
1.2.3 Micromechanics	9
1.3 Durability	13
1.3.1 Introduction	13
1.3.2 Durability of Strain Hardening Cement Based Composites (SHCC)	14
1.3.3 Fundamentals of Durability Design for SHCC	15
1.3.4 Crack Control as Durability Measure	16
1.3.5 Conclusion	19
2. MATERIAL DESCRIPTION	20
2.1 Response to Tension	20
2.1.1 Material Behaviour	20
2.1.2 Test Models and Testing	23

2.1.3	Stress-Strain Relationships	24
2.1.4	Critical Parameters	25
2.2	Response to Compression	27
2.2.1	Material Behaviour	27
2.2.2	Test Program	27
2.2.3	Stress-Strain Curves	27
2.2.4	Critical Parameters	32
2.3	Conclusion	33
3.	Testing and Verification of the Model	34
3.1	Critical Parameters	34
3.1.1	Performance Function	34
3.1.2	Sensitivity to critical parameters	34
3.2	Test Program	36
3.2.1	General	36
3.2.2	Mixing and Casting	36
3.2.3	Testing	37
3.3	Minimizing Sources of Uncertainty	38
3.4	Model Predictions	42
3.4.1	First Set of Tests	42
3.4.2	Second Set of Tests	46
3.5	Interpretation of Results	49
3.5.1	First set of Tests	49
3.5.2	Second Set of Tests	49
3.6	Conclusion	50
4.	Analysis Model	51
4.1	Description	51
4.2	Formulation of the model	54
4.2.1	Phase 1 – Elastic behaviour	54

4.2.2	Phase 2 – Strain Hardening	58
4.2.3	Phase 3 – Compressive inelasticity before crack localization	60
4.3	Simplifying the model: From analytical to design model	62
4.3.1	Numerical Verification	71
4.4	Testing the Simplified Model with Different Materials	78
4.4.1	Materials used	78
4.4.2	Verification	79
4.5	Conclusion	89
5.	Deflection Model	90
5.1	Fundamental Theory of Beam Deflection	90
5.2	Linear-elastic behaviour	94
5.3	Deflection calculation for R/SHCC beams	95
5.3.1	Introduction	95
5.3.2	Phase 1 - Linear-elastic behaviour	95
5.3.3	Phase 2 – Strain Hardening	96
5.3.4	Phase Three	100
5.3.5	Tension Stiffening in R/SHCC members in flexure	100
5.3.6	Comparing the Predicted Deflected shape to the Measured Deflected shape	101
5.4	Serviceability	101
5.5	Conclusion	102
6.	Reliability	103
6.1	General	103
6.2	Material Strength	104
6.2.1	Statistical Properties of Critical Parameters	104
6.2.2	The Conversion Factor	104
6.2.3	Material Factor	105
6.2.4	Limiting Strain Values	107
6.3	Model Uncertainty	108

6.3.1	Theoretical Predictions	108
6.3.2	Interpretation of Results	111
6.4	Conclusion	114
7.	Design	116
7.1	Material Classification	116
7.2	Limitations	116
7.3	Calculations	118
7.4	Comparison with Normal R/C	123
7.5	Conclusion	128
8.	Summary, Conclusion and Recommendations	129
8.1	Summary	129
8.1.1	Introduction	129
8.1.2	Material Description	129
8.1.3	Testing and Verification of the Model	129
8.1.4	Analysis Model	130
8.1.5	Deflection Model	131
8.1.6	Reliability	131
8.1.7	Design	132
8.2	Conclusion	132
8.2.1	Compression and Tensile Response Models	132
8.2.2	Design Model	132
8.2.3	Comparing R/SHCC with R/C	133
8.3	Recommendations	133
8.3.1	Material properties	133
8.3.2	Deflection Model	134
8.3.3	Shear Design	134
9.	Bibliography	135
	Annexure A: Algorithm for calculation of numerical model	146

Annexure B: Complete Illustrative Design	150
Example 1 – Simply supported beam with line load	150
Example 2 – Roof slab with upstand beams	152
Annexure C: Verification of design Model via different materials	157

LIST OF FIGURES

Figure 1-1: Uniaxial Tensile behaviour of FRC (a) and HPFRC (b) [1]	3
Figure 1-1-2: Stress-Strain Relationships for Cement Composites.....	4
Figure 1-3: Typical Tensile Stress-Strain graph for SHCC Material.....	6
Figure 1-4: Effect of Fibre Surface Oiling content on J'_b	12
Figure 1-5: Effect of Fly Ash Content on J'_b/J_{tip}	13
Figure 2-1: Minimum Information Needed for Design on Tensile Strain Hardening Stress-Strain Response of FRP Composites [38].....	21
Figure 2-2: FRC classification model proposed by Naaman and Reinhardt (2006).....	22
Figure 2-3: a) Extensometer consisting of a frame and 2 LVDT's, b) The thin flat dumbbell shaped specimen, c) Tensile test setup in Zwick Z250 [41]	24
Figure 2-4: Tensile Stress-Strain relationship.....	25
Figure 2-5: Simplified Stress-Strain Relationship	26
Figure 2-6: Apparatus for compressive specimens [44].....	28
Figure 2-7: Compression Stress-Strain Behaviour according to Naaman and Reinhardt.....	29
Figure 2-8: Compression Stress and Strain Response showing the change from elastic to inelastic response.....	30
Figure 2-9: Compression Stress and Strain relationship showing the change from elastic to plastic response (2).....	31
Figure 2-10: Compression Stress and Strain Relationship with adjusted approximation	31
Figure 2-11: Compression Stress and Strain relationship with adjusted approximation (2).....	32
Figure 2-12: Simplified compression stress-strain relationship.....	33
Figure 3-1: Beam testing Setup.....	38
Figure 3-2: Beam 1a,b - Test results and model predictions	44
Figure 3-3: Beam 2a,b - Test Results and Model Predictions.....	45
Figure 3-4: Beam 3a,b - Test Results and Model Predictions.....	46
Figure 3-5: Balk 1a,b - Test Results and Model Predictions	47
Figure 3-6: Beam 2a,b - Test Results and Model Predictions.....	48
Figure 3-7: Beam 3a,b - Test Results and Model Predictions.....	49

Figure 4-1: Simply supported beam load and moment diagram	51
Figure 4-2a,b, and c – Progression of Stress through Phase 1 of Loading.....	52
Figure 4-3a,b, and c – Progression of Stress through Phase 2 of Loading.....	53
Figure 4-4a, and b - Progression of Stress through Phase 3 of Loading	54
Figure 4-5: Phase 1 - Stress and Strain relationship	55
Figure 4-6: Phase 2 - Stress and Strain relationship	58
Figure 4-7: Stress-Strain Relationship for Phase 3.....	60
Figure 4-8: Tensile strain in relation to the applied moments for phase 2.....	63
Figure 4-9: The distance to the neutral axis, x , in relation to the applied moment for phase 2.....	65
Figure 4-10: Tensile strain in relation to the applied moment for phase 3.....	66
Figure 4-11: The distance to the neutral axis in relation to the applied moment for phase 3.....	66
Figure 4-12: Phase 2 – Comparing estimated and applied areas of tensile reinforcement	69
Figure 4-13: Phase 2 - Comparing estimated and applied areas of compressive reinforcement....	70
Figure 4-14: Phase 3 - Comparing estimated and applied areas of tensile reinforcement	70
Figure 4-15: Phase 3 - Comparing estimated and applied areas of compressive reinforcement....	71
Figure 4-16: Phase 2 - $h = 200\text{mm}$	72
Figure 4-17: Phase 2 - $h = 250\text{mm}$	72
Figure 4-18: Phase 2 - $h = 300\text{mm}$	73
Figure 4-19: Phase 2 - $h = 400\text{mm}$	73
Figure 4-20: Phase 2 - $h = 500\text{mm}$	74
Figure 4-21: Phase 2 - $h = 600\text{mm}$	74
Figure 4-22: Phase 2 - $h = 750\text{mm}$	75
Figure 4-23: Phase 3 - $h = 200\text{mm}$	75
Figure 4-24: Phase 3 - $h = 250\text{mm}$	76
Figure 4-25: Phase 3 - $h = 300\text{mm}$	76
Figure 4-26: Phase 3 - $h = 400\text{mm}$	77
Figure 4-27: Phase 3 - $h = 500\text{mm}$	77
Figure 4-28: Phase 2 - Comparison between actual tensile strain for Materials 1, 2, and 3 for beam heights under 500mm	79

Figure 4-29: Phase 2 - Comparison between actual tensile strain for Materials 1,2, and 3 for beam height over 500mm	80
Figure 4-30: Phase 2 - Comparison between the neutral axis depth for Materials 1, 2, and 3 for beam heights under 500mm	80
Figure 4-31: Phase 2 - Comparison between the neutral axis depth for Materials 1, 2, and 3 for beam heights over 500mm	81
Figure 4-32: Phase 3 - Comparison between the actual tensile strain for Materials 1 and 2.....	81
Figure 4-33: Phase3 - Comparison between the neutral axis depth for Materials 1 and 2	82
Figure 4-34: Phase 2 - h = 200mm.....	83
Figure 4-35: Phase 2 - h = 250mm.....	83
Figure 4-36: Phase 2 - h = 300mm.....	84
Figure 4-37: Phase 2 - h = 400mm.....	84
Figure 4-38: Phase 2 - h = 500mm.....	85
Figure 4-39: Phase 2 - h = 600mm.....	85
Figure 4-40: Phase 2 - h = 750mm.....	86
Figure 4-41: Phase 3 - h = 200mm.....	86
Figure 4-42: Phase 3 - h = 250mm.....	87
Figure 4-43: Phase 3 - h = 300mm.....	87
Figure 4-44: Phase 3 - h = 400mm.....	88
Figure 4-45: Phase 3 - h = 500mm.....	88
Figure 5-1: Assumed Stress Distribution in Traditional Reinforced Concrete.....	90
Figure 5-2: Simple Beam Configurations.....	93
Figure 5-3: Schematic representation of the three phases of deflection	95
Figure 5-4: Schematic Representation of SHCC Beam Load - Deflection Phases.....	96
Figure 5-5: Schematic Representation of SHCC Beam Sectional Strain and Stress distributions..	98
Figure 5-6: Schematic Representation of SHCC Moment and Curvature Diagrams	99
Figure 5-7: Predicted Deflection vs Measured Deflection along length of beam	101
Figure 6-1: Scatter Plot showing accuracy of Phase 1 of the Base Model.....	109
Figure 6-2: Scatter Plot showing accuracy of Phase 2 of the Base Model.....	110

Figure 6-3: Scatter Plot showing the accuracy of Phase 3 of the Base Model 111

Figure 7-1: Comparison between Reinforcement needed in SHCC and normal R/C beams 127

LIST OF TABLES:

Table 1-1: Examples of crack width limitations in RC Structures for Durability (Carino and Clifton, 1995), [20].....	17
Table 3-1: Model Sensitivity	35
Table 3-2: Cube Test Results.....	39
Table 3-3: Concrete Cylinder test results - Second set of tests only.....	40
Table 3-4: Tensile test results	40
Table 3-5: Test Specimen Details	42
Table 3-6: Mix design for both test sets.....	42
Table 3-7: Test specimen details	46
Table 4-1: Material Properties.....	78
Table 6-1: Conversion Factors	105
Table 6-2: Material Factors	106
Table 6-3: Statistical Values for Model Predictions.....	113
Table 6-4: Model Factors for Phase 1, 2, and 3	114

LIST OF ABBREVIATIONS

- ACI – American Concrete Institute
- CEB/FIB – International Federation of Structural Concrete
- ECC - Engineered Cement Composites
- EC2 – Eurocode 2
- EN 1990 - Eurocode of 1990
- FRC - Fibre Reinforced Concrete
- FRCC - Fibre Reinforced Cement-based Composites
- FRP – Fibre Reinforced Plastic
- GPa - Giga Pascal
- HPFRC - High Performance FRC
- HPFRCC - High Performance Fibre Reinforced Cement Composites
- kNm – Kilo-Newton Meter
- LVDT - Linear Variable Differential Transformer
- mm - Millimetre
- MOR - Modulus Of Rupture
- MPa - Mega Pascal
- MTM – Materials Testing Machine
- NA – Neutral Axis
- N/m – Newton per Meter
- PE-ECC - Polyethylene ECC
- PET – Polyethylene Terephthalate
- PVA – Polyvinyl Alcohol
- PVA-ECC - Polyvinyl Alcohol ECC
- R/C - Reinforced Concrete
- R/ECC - Steel Reinforced ECC
- R/SHCC - Steel Reinforced SHCC
- SANS - South African National Standards
- SHCC - Strain Hardening Cement Composites
- UHPFRC – Ultra-High Performance Fibre Reinforced Concrete
- UHFRC - Ultra-High Fibre Reinforced Concrete
- WBCSD - World Business Council for Sustainable Development
- w/b – Water Binder Ratio
- 3D – Three Dimensional
- μm – Micro Meter

LIST OF SYMBOLS

- A_c - Cross sectional area of concrete
- A_f - Cross sectional area of one fibre
- A_s - Cross sectional area of tensile reinforcement
- A'_s - Cross sectional area of compressive reinforcement
- b - The width of the beam at its cross section.
- b - Correction factor or model bias
- d_f – Fibre diameter
- d - The distance to the tensile reinforcement, measured from the top of the beam.
- d' - The distance to the compressive reinforcement, measured from the top of the beam.
- E – Elasticity modulus
- E_c - Elasticity modulus of concrete
- E_{cc} – Elasticity Modulus for SHCC in compression
- E_{ct} – Elasticity Modulus for SHCC in tension
- E_d - Design value of load effects
- E_s – Elasticity Modulus for reinforcement steel
- ϵ – Strain
- f_s - Stress in the reinforcement
- f_{sc} - Reinforcement compressive stress
- f_{st} - Reinforcement tensile stress
- h - The total depth of the beam
- I – Moment of Inertia
- I_{tr} - Transformed moment of inertia of the cross section under consideration.
- J_b' - The complementary energy of the fibre bridging stress
- J_b'/J_{tip} - strain-hardening index
- J_{tip} - The matrix toughness
- K – Coefficient taking into account boundary values as well as load configurations
- $k_{d,n}$ - Design fractile estimator
- k_n - Fractile estimator
- L - The length of the proposed beam
- L_f - fibre length
- M_e - Moment at the end of the linear-elastic phase
- M_u - The ultimate moment applied to the beam
- m_X - Sample mean obtained from test data
- M_y - Moment at the end of the strain hardening phase

- P - Applied point load
- P_e – Load when the first crack is initiated
- P_y - Load when crack saturation is reached
- p_f - Probability of failure
- R - Real structural resistance
- R_d - Design value of resistance
- r_e - Experimental resistance
- r_t - Theoretical resistance
- V_f - volume fraction
- V_δ - coefficient of variation of the error term
- V_X - coefficient of variation
- w – in w/b denotes water
- x - The distance to the neutral axis measured from the top of the beam
- x - Coordinate system axis along the beams' centroid axis,
- X_d - Design value
- X_k - the characteristic value
- α - Product of several coefficients
- αE_c - Gradient of the strain hardening leg of the tension graph for SHCC.
- αL - Width of the cracked region in a flexural member
- β_R – The Reliability Index
- β_T – The Target Reliability Index
- δ - Error term or model uncertainty
- δ_0 - Crack opening corresponding to the peak bridging stress
- Δ - Deflection at the centre of the beam.
- Δ_e – Deflection when elastic limit is reached
- Δ_i - Variation for the error term
- Δy – Deflection when plastic hinge forms
- ε_{cc} - SHCC compressive strain
- ε_{ccu} - SHCC ultimate compressive strain
- ε_{cs} - Compressive strain in concrete
- ε_{ct} - SHCC tensile strain
- ε_{ct1} – SHCC tensile strain at first cracking
- ε_{ctu} - SHCC ultimate tensile strain
- ε_{sc} - Reinforcement compressive strain
- ε_{st} - Reinforcement tensile strain
- Φ - Cumulative distribution function for the standard normal distribution

- γ_M - partial resistance factor
- γ_m - material factor
- γ_{RD} - model factor
- η_d - Conversion factor
- ρ – Curvature
- ρ_m – Maximum curvature
- $\sigma(\delta)$ - Opening relation
- σ_0 - Peak bridging stress
- σ_{cc} - SHCC compressive stress
- σ_{ccu} – SHCC ultimate compressive stress
- σ_{cs} - Concrete compressive stress
- σ_{ct} - SHCC tensile stress
- σ_{ct1} - SHCC tensile stress at first cracking
- σ_{ct2} – SHCC tensile stress at the bottom most section of the tensile zone
- σ_{ctu} - SHCC ultimate tensile stress
- σ_{mu} - Tensile strength of unreinforced matrix
- σ_t - Tensile stress in the concrete at the position of the tensile reinforcement
- τ - Bond between the matrix and the fibres
- $\bar{\tau}$ - Average bond strength at the fibre matrix interface
- Ψ - Perimeter of one fibre

FOREWORD

Scope

Fibre Reinforced Concrete (FRC) has been around for almost 50 years but has been used almost exclusively in non-structural applications. These applications include mostly crack controlling applications. It is only recently that the use of this material as structural material has been motivated by developments in the industry. One such development is the continual increase in the height of buildings. These higher buildings demand either bigger structural components or better structural materials. Another development is the increased use of prefabrication of structural elements [1]. This development allows for use of materials that would not be suitable for site applications to be used in a controlled environment.

Strain Hardening Cement Composites (SHCC) are a relatively new class of fibre reinforced materials in the sense that it has been widely studied but not yet widely used. The majority of studies on this material are aimed at showing its advantages above other materials in terms of durability, strength, flexibility as well as resistance to damage. There is, however, very little information on how this material can be used in standardized structural design. This is the main reason why this material has mainly been used in experimental construction and not for general use.

The Japanese Society of Civil Engineers has published recommendations for the design of High Performance Fibre Reinforced Cement Composites, or HPFRCC [2]. This document is used in Japan as a design guideline for the construction of reinforced SHCC. However, the document does not include any actual design models, but gives guidance on the specification of the material parameters and appropriate safety factors to be used and then refers the user back to the Japanese concrete code for the design of the structure itself. In doing so it does not take into account the strain hardening nature of the material. This approach is conservative and safe, but not necessarily economically viable as this material is more expensive than normal concrete.

This study aims to provide the designer with an analytical design model for designing flexural members with reinforced SHCC. This model will take into account the material's strain hardening potential under tension, but shear behaviour is ignored. Calculating crack widths also falls outside the scope of this study. The novelty of the work lies in the design model itself and not in the methods used for its calibration and testing. The only novel models developed in this study are the base design model and the simplified design model. Existing models are used in the derivation of these two models.

Overview

In Chapter 1, a discussion of fibre reinforced concrete in general is given and then the focus moves on to Engineered Cement Composites (ECC), which is a type of SHCC. This chapter also touches on the durability of this material and its appropriateness in terms of sustainability.

Chapter 2 describes the tensile and compressive behaviour of SHCC and also gives the reader the background on how the author came up with the design model that is described in detail in Chapter 3. Here the calculations for the derivation of the design model equations are shown. This chapter also explains the simplification of the design model and the testing of it on different types of SHCC materials.

The deflection model is explained in Chapter 4 and the serviceability limit states incorporated into this deflection model are also stipulated. The verification of the design model is done in Chapter 5. The performance function and its sensitivity to critical parameters is illustrated and the beam tests and their results are discussed at the end of this chapter.

Chapter 6 discusses the reliability design of the design model. In this chapter, material factors are found for the strength properties of the material and model factors are derived for the three different phases of the design model.

Chapter 7 illustrates to the designer how this design model can be used in the structural design of flexural members. It also compares flexural members designed with reinforced SHCC to those constructed with normal reinforced concrete.

In Chapter 8 a final summary of the study is given along with the conclusions.

1. INTRODUCTION TO FIBER REINFORCED CONCRETE

The inclusion of fibres into concrete was originally done to improve concrete tensile strength and to reduce brittleness. For low fibre volumes, typically less than 1% per volume fraction, a stress-strain curve as shown in Figure 1-1a, Curve A, is possible. For moderate to high fibre volumes, $1\% \leq V_f \leq 3\%$, a stress-strain curve such as Curve B in Figure 1-1a can be achieved. Curve C could originally only be achieved for very high volumes of fibre [1].

Lately it has become possible to achieve tensile responses as shown in Figure 1-1b with low to moderate fibre volumes, $1\% \leq V_f \leq 3\%$. These materials are known as high performance fibre reinforced cement-based composites (HPFRCC). Strain Hardening Cement Composites (SHCC), one member of the HPFRCC, have significant ductility coupled with moderate tensile and compressive strengths, while ultra-high performance fibre-reinforced concretes (UHPRFC) show high tensile and compressive strengths coupled with moderate strain levels [1]. These UHPFRFC materials are typically not tensile strain hardening as is the case with SHCC.

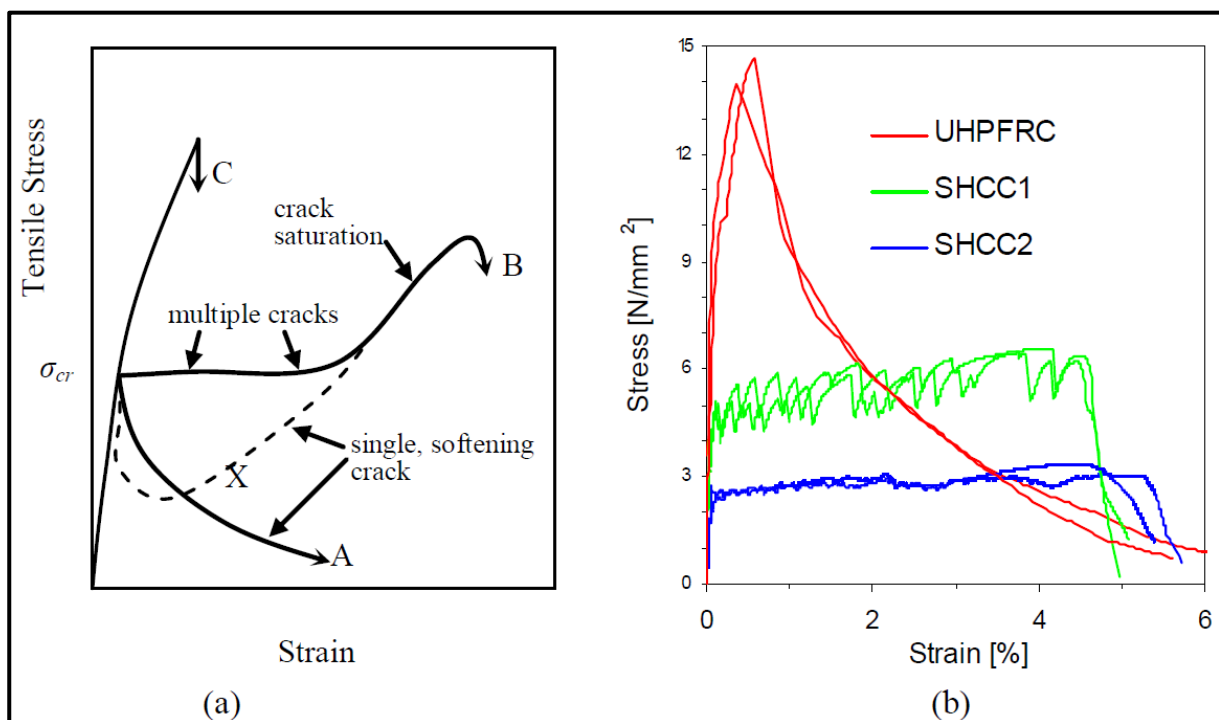


Figure 1-1: Uniaxial Tensile behaviour of FRC (a) and HPFRFC (b) [1]

1.1 Classification

There are three basic classes of fibre reinforced cement-based composites, FRCC. The first one contains less than 1% fibre per volume fraction (V_f), and utilizes the fibres to reduce shrinkage cracking in structural and non-structural elements. The second class contains between 1% and 3% fibre per volume fraction, and shows improved mechanical properties such as a higher modulus of

rupture (MOR), fracture toughness and impact resistance. The fibres in this class can be used as secondary reinforcement in structural members, such as in the partial replacement of shear steel. It can also be used to control crack widths. The third class of FRC, more commonly known as high performance FRC or HPFRC, shows increased tensile resistance, and in some cases, significant strain hardening behaviour after the first cracking. This material usually contains a high fibre volume content of $V_f \geq 3\%$. During strain hardening, the matrix undergoes multiple cracking, by means of which fracture localization is delayed. The width of these cracks needs to be controlled tightly, as that is the key to this material's durability.

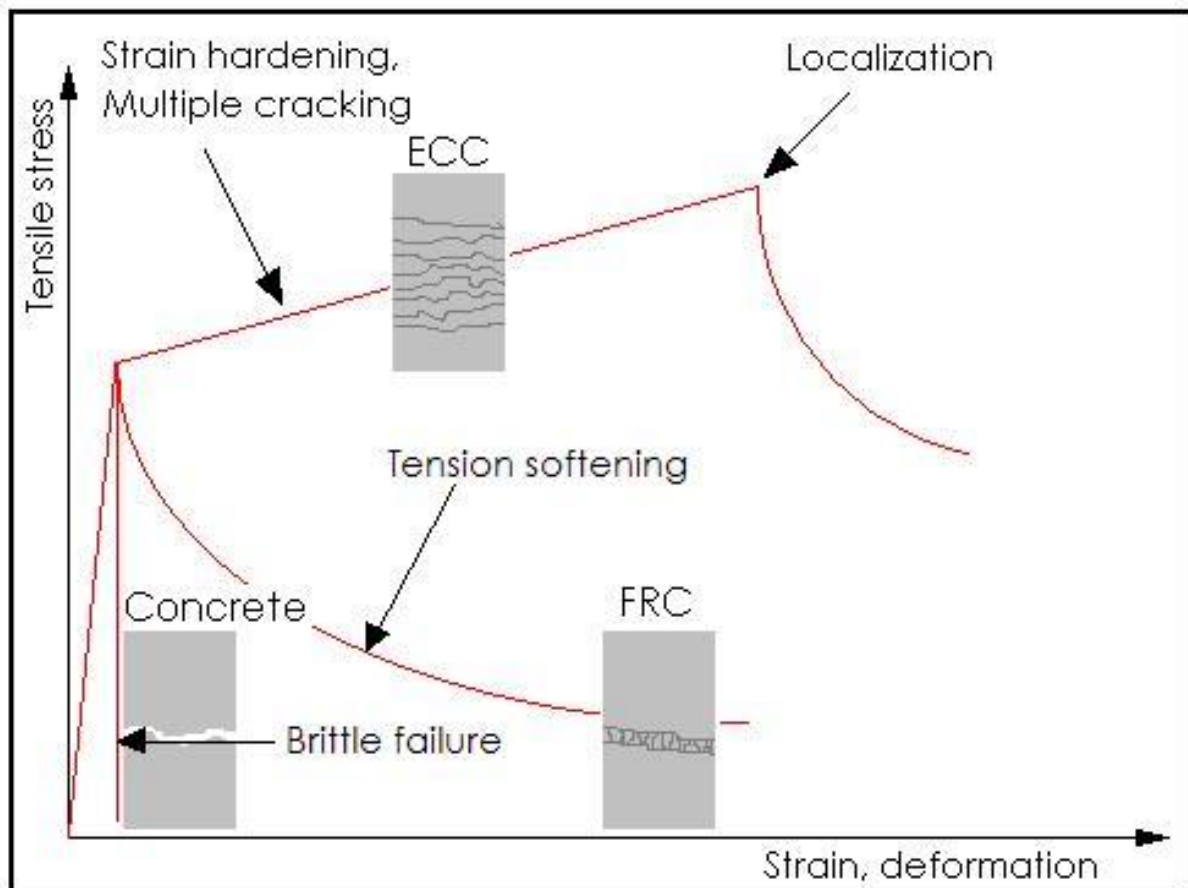


Figure 1-1-2: Stress-Strain Relationships for Cement Composites

The deformation behaviour of cement composites such as concrete, fibre reinforced concrete (FRC), and high performance fibre reinforced concrete (HPFRC) is typically distinguished according to their tensile stress-strain characteristics and post-cracking response in particular.

Recently, a new kind of fibre reinforced cement composite, known as Engineered Cement Composites (ECC) was developed. ECC represents one specific class of HPFRC, which is defined by an ultimate strength higher than its first cracking strength and the formation of multiple cracks during the inelastic deformation process. In other words, ECC is a member of the SHCC family. In

conventional FRC, the strain is dependent on the gauge length. The reason for this dependence is the formation of a single, large crack at the point of maximum tensile stress. This single crack formation is indicative of localized deformation. In SHCC, the post cracking strain, and so the deformation, is uniform on a macro scale and is considered as pseudo strain, which is a material property and independent of the gauge length.

ECC, a type of SHCC, uses a fibre content of up to 2% by volume, but shows strain hardening behaviour with strain capacities in the range of 3% - 7%. The typical ultimate tensile strength lies between 5MPa and 8MPa. Micro mechanical models, taking account of the mechanical interactions between the fibre, matrix and the interface, are used to optimize the micro structure to achieve an ultra-high ductility. As shown in Figure 1-2, brittle matrices, such as plain mortar and concrete, lose their tensile load-carrying capacity almost immediately after formation of the first matrix crack. The toughness of the cement matrices of conventional FRC is increased by the addition of fibres; however, the tensile strength and especially strain capacity beyond first cracking are not enhanced. FRC is thus considered to be a quasi-brittle material with tension softening deformation behaviour as seen in Figure 1-2.

ECC's ability to strain harden in tension rather than strain soften after first cracking, is what makes it different from FRC in general and also why it is categorized under strain hardening cement composites (SHCC). In normal FRC, the first crack continues to open up as fibres pull out or rupture and the stress carrying capacity decreases as the load increases. In SHCC, the first cracking is followed by a rising stress accompanied by an increase in strain. The strain capacity is attained through the formation of many closely spaced micro cracks, allowing for a tensile strain capacity over 300 times that of normal concrete. These cracks, which carry increasing load after first crack formation, allow the material to exhibit strain hardening behaviour, similar to many ductile metals, as seen in an experimental uni-axial tensile stress-strain curve shown in Figure 1-3. This curve was typical for the tests done during this study. This strain-hardening response gives way to the common FRC tension-softening response only after several percent of straining has been attained.

Closely related to the strain-hardening behaviour of SHCC, is the high fracture toughness of SHCC, similar to that of aluminium alloys. In addition, the material is extremely damage tolerant, and remains ductile even in severe shear loading conditions [3] [4]. The compressive strength of SHCC varies from 30 MPa to 250 MPa [3], depending on the matrix composition. Such high compressive strength SHCC is recent, typically referred to as UHP-SHCC, by the group of Prof Kuneida, now in Gifu, Japan. Note that high strength composites, termed ultra-high fibre reinforced concrete (UHFRFC), with examples such as Ductal®, SIFCON and SIMCON, have been developed which form a particular class of HPFRC's, with high fibre content (For a discussion of this particular material refer to Van Zijl, 2007) [4]. Compressive strengths of beyond 200MPa are achieved, and fibres

prevent explosive, brittle failure. Flexural strengths of up to 50MPa can be achieved. However, high to extremely high fibre contents (up to 20%) are used in UHFRC. The focus here is on low to moderate fibre contents, and high ductility, as opposed to high strength [4] [1].

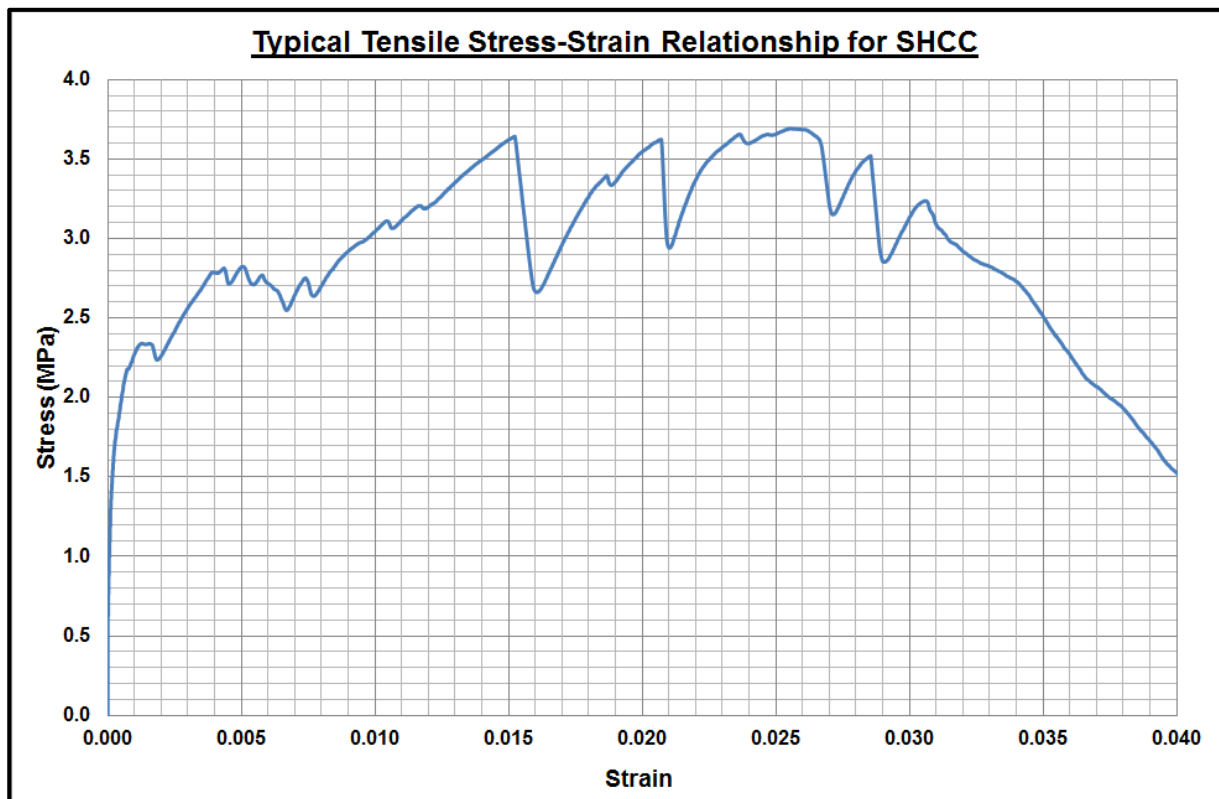


Figure 1-3: Typical Tensile Stress-Strain graph for SHCC Material

1.2 Strain Hardening Cement Composites (SHCC)

1.2.1 The History of SHCC

While ECC constituents are similar to those of fibre reinforced concrete (FRC), the distinctive strain hardening through micro-cracking is achieved through micromechanical tailoring of the constituents, along with controlled interfacial properties between these constituents. Coarse aggregates are not used in ECC, due to their unfavourable effect on fibre spreading and fibre performance. While most HPFRCC's rely on high fibre volume for high performance, ECC uses low amounts of short discontinuous fibres. This low fibre volume along with the common constituents, allows for ECC mixing with conventional equipment.

Micromechanics form the backbone of a materials design theory, and relate microscopic properties to the microstructures of a composite. It specifically allows systematic microstructure tailoring of ECC as well as material strength and ductility optimization. Microstructure tailoring can lead to composite ductility of several percent in tension which is a material property not seen before in discontinuous

fibre reinforced cement-based composites. Material strength and ductility optimization also leads to compositions that make highly flexible materials processing possible. ECC can now be cast (including self-compacting), extruded, or sprayed.

What makes ECC ideal for a broad range of applications are the advantages of high composite ductility in the hardened state and flexible processing in the fresh state. A variety of experiments have been performed to assess the performance of ECC at a structural level for both seismic and non-seismic applications. These experiments provide new insights into how the material properties increase the response performance of the structure. At the same time, constitutive models of ECC have been constructed and implemented into finite element models for prediction of structural behaviour [3]. They should be useful for examining the different uses of ECC in critical elements of a structural system, without having to do expensive experiments. These activities are important in establishing rational means of designing structures made with ECC material.

Apart from structural applications, ECC has also been researched as a protective layer for improving the corrosion durability of normal reinforced concrete structures. The typical formation of fine cracks and anti-spall properties of ECC show the potential of this material in achieving the durability function, as reported for PE-ECC (Polyethylene ECC) and PVA-ECC (Polyvinyl Alcohol ECC) [3]. ECC has also been shown to exhibit an unfamiliar kink-crack trapping behaviour when used as a repair layer in concrete structures [3]. This behaviour eliminates the deterioration mechanism of delaminating and spalling in the repair material usually seen in repaired concrete structures.

Other potential applications of ECC are in high energy absorption structures/devices, which include short columns, dampers, joints for steel elements, and connections for hybrid steel/RC structures. The isotropic energy absorption behaviour of ECC may be very useful for structures subjected to impact or 3D loading. This may include highway pavements, bridge decks, and blast resistant building core elements. Other potential targets for ECC application are structures subjected to large deformations, such as underground structures that need to conform to soil deformation and require leak prevention, permanent formwork, extruded elements with structural properties, structures reinforced with FRP (fibre reinforced plastic), and structures to store radioactive waste.

1.2.2 Unique characteristics of ECC

A number of investigations into the use of ECC in improving structural performance have been conducted in recent years, often revealing unique characteristics of ECC and R/ECC (steel reinforced ECC) in a structural context.

Among these characteristics are high damage tolerance, resistance to shear load, energy absorption, delaminating and spall resistance, and high deformability and tight crack width control

for durability. Another unique feature of ECC, its ultra-high ductility, which implies that structural failure by fracture, is significantly less likely in comparison to normal concrete or FRC.

Damage tolerance: this is the ability of the structure to sustain load carrying capacity when overloaded into the plastic strain range. Damage tolerance is a critical characteristic, as the cost of repairing infrastructure after, for example an earthquake, is quite substantial. Further to that is safety becoming more and more important.

Parra-Montesinos [5], has done a series of cyclic tests on the structural integrity of joints in hybrid steel-beam R/C column connections. The standard R/C joint experiences large crack opening, loss of bond between the axial reinforcement and the concrete, and therefore, loss of composite action, and suffers severe spalling, where the steel beam bears on the concrete. The ECC joint, however, undergoes strain-hardening with multiple micro-crack damage. There was no spalling observed in the R/ECC material which maintains its high bond efficiency despite all the shear reinforcement being removed. The R/ECC connection structurally needs no repair, not even after the imposed load and deflection are pushed to higher levels. This shows that the damage tolerance of ECC eliminates the spall failure usually seen in high stress-concentration zones where concrete and steel interact. This phenomena is very important in the current climate of safety first design. Even when this material is overloaded, it does not collapse. This could potentially save lives.

Energy Absorption: Energy absorption is used in seismic hinge zones of structures, to dissipate energy input of an earthquake. In R/C structures, the concept of a plastic hinge is introduced by ductile yielding of the steel reinforcement in seismic detailing. However, it is typical that only a small fraction of the steel actually undergoes yielding due to the disintegration of the surrounding brittle concrete. Fischer and Li (2002) [6], did cyclic flexural experiments on cantilevered elements. In their study it is clear that the R/ECC absorbs much higher energy than the R/C element despite the fact that no hoop shear reinforcement was used in the R/ECC element. This result shows high shear resistance and the effect has been demonstrated in later studies of Fischer and Li, as well. This characteristic might save costs on parking lot flat slab design where punching shear always seems to be a problem. There have not yet been any studies done to support this theory, but there is a definite possibility for thinner parking lot slabs done in R/ECC.

Resistance to delaminating and spalling: Spalling and delaminating between the old and the new concrete are the most common modes for failure in patch repair. In repairing bridge decks or pavements with overlays, reflective crack and spalling in the concrete substrate are often seen. This causes concern since it is difficult to address all modes of failure simultaneously. Strengthening the interfacial bond tends to enhance spalling while increasing the overlay strength tends to encourage

delamination, which means, the durability of concrete repair is compromised by one or the other of these failure mechanisms.

Li and co-workers (1997, 2001) [7] [8], studied the resistance of ECC repaired structures to delamination and spalling. They used a specimen overlay on top of a joint together with an initial interface defect and found that the delamination and spalling mode is eliminated by means of a kink-crack trapping process. The initial interface crack extends slightly as the load increases, but quickly kink into the ECC overlay. The crack is then trapped in the ECC by the fibres that act as reinforcement. The crack can only propagate further if the fibre is pulled out or broken and that only happens after crack saturation is reached. Crack saturation is that point where no new cracks form and the existing cracks start to open up. It is also known as crack localisation. The kink-trapping process then repeats itself, resulting in a succession of kink cracks in the ECC. Kink-trapping happens when a crack starts on the tensile face of the member and spreads inwards towards the centre of the member. However, as soon as the crack reaches a fibre, the tension is transferred from the matrix to the fibre. Now the crack can only propagate further if the fibre is pulled out or broken and so the crack is stopped. Spalling of the ECC is not observed as the kink crack does not reach the specimen surface. Delamination of the interface is also eliminated since the interface crack tip repeatedly returns into the ECC. On the other hand, the specimen with a regular FRC overlay also shows the expected kink-spall brittle fracture behaviour.

1.2.3 Micromechanics

ECC is a special member of the new breed of HPFRCC, with characteristics like high ductility and medium fibre content. Material engineering of ECC is based on the model of the relationship between material microstructures, processing, material properties, and performance, where micromechanics is highlighted as the binding link between composite mechanical performance and material microstructure properties (Li, 1993) [9]. This is state of the art work by others such as Li, and will only be described briefly here as the main interest of this paper is the structural design of R/SHCC flexural members.

The adaptation of composite constituents including fibre, matrix and interface are guided by established micromechanical models for overall performance [10]. This elevates the material design from trial-and-error empirical testing to a systematic, holistically 'engineered' combination of individual constituents. The link between microstructure and composite performance can be further extended to the structural performance level and combine the material design into a performance based design concept for structures. Seeing it this way, ECC resembles a material design approach as well as being an advanced material and thus gives an alternative degree of freedom in structural performance.

Tensile ductility is the main performance goal in ECC. Other secondary goals are high strength and elasticity modulus, tight crack width control and high durability. For most uses, a tensile strain capacity of 2% is seen as adequate. Evaluating strength, ECC should be able to compare to other normal strength concretes in terms of compressive strength. The water to binder ratio, w/b, is the main variable influencing strength of the matrix.

Studies have shown that permeability would be in the same order of good quality concrete if the crack width is below 80 – 100 μm [10]. The ECC strength is governed by the fibres from the equation:

$$\sigma_{tu} = \frac{1}{2} \tau V_f \frac{L_f}{d_f} \quad 1-1$$

Where:

- τ = bond between the matrix and the fibres
- $V_f \frac{L_f}{d_f}$ = so-called fibre factor
- V_f = fibre volumes
- L_f = fibre length
- d_f = fibre diameter
- σ_{tu} = Tensile strength of ECC

Of course τ might be influenced by the w/b (water/binder) ratio, but w/b ratio is less important in ECC.

Different fibre types can be used in ECC, but the detail composition must comply with certain criteria imposed by micromechanical considerations. This implies that the fibre, cement-based matrix, and the interface (mechanical and geometric) characteristics must be of a certain combination to be able to achieve the special behaviour of ECC. This means that ECC designs are directed by micromechanical criteria. Micromechanical formulas show that fibres with diameter (d_f) less than 50 μm are preferred, in order to attain strain-hardening with lower fibre volume fraction, V_f . For this reason polymeric fibres, generally drawn to such diameters, are preferable over steel fibres, normally in the 150-500 μm range. Steel fibres with smaller diameters can be made, but the cost escalates. Most data available today are for PVA-ECC and PE-ECC where PE stands for Polyethylene fibre.

PVA fibre was found during a search for low cost high performance fibres for ECC. The hydrophilic nature of the PVA fibres created major problems in the composite design, as the fibres are prone to rupture instead of being pulled out. This is because the fibre tends to bond strongly to the cement-based matrix. This needed careful engineering in fibre geometry, fibre/matrix interface and matrix

characteristics to attain high ductility in PVA-ECC. To help in the adapting process, micromechanical models taking into consideration the uniqueness of PVA-fibre were developed (Wang and Li).

Tensile ductility can be measured by the strain-hardening index J_b'/J_{tip} , (Wang and Li) where J_b' is the complementary energy of the fibre bridging stress versus crack opening relation $\sigma(\delta)$, and J_{tip} is the matrix toughness. The load carried by the bridging fibre is a function of the crack opening, characterised by a $\sigma(\delta)$ relationship that increases to a peak and then decreases. The peak value σ_0 , known as the fibre bridging capacity, varies from one crack plane to another due to the inevitable spatial non-uniformity in fibre dispersion [11]. For strain-hardening, J_b'/J_{tip} must be more than one and a higher J_b'/J_{tip} leads to more saturated multiple cracking. The fibre bridging complementary energy is calculated from single fibre pull-out tests and incorporating the fibre pull-out displacement-resistance response as follows:

$$J'_b = \sigma_0 \delta_0 - \int_0^{\delta_0} \sigma(\delta) d\delta \quad 1-2$$

Where:

- σ_0 = peak bridging stress
- δ_0 = crack opening corresponding to the peak bridging stress
- δ = crack opening
- $\sigma(\delta)$ = crack opening relationship

$$J_{tip} = \frac{K_m^2}{E_c} \quad 1-3$$

Where:

- J_{tip} = energy equivalent of the matrix fracture toughness, K_m
- E_c = composite elasticity modulus

The modelling of the $\sigma(\delta)$ relation is a very important element of ECC micromechanics. It not only connects the fibre, matrix and interface characteristics to J_b' , but also estimates the multiple crack width before failure. As a result of significant slip-hardening action during pull-out, PVA-fibre can be pulled out from both sides across the crack, in contrast to the one-way pull-out usually seen in steel and other polymeric fibres. Also, matrix spalling at the fibre exits has to be accounted for in the accurate estimation of crack opening. A very strong interface bond leads to fibre rupture at small crack opening, resulting in small J_b' . This is in contrast with the fact that a very weak interface may result in low bridging strength and large crack opening. A study of the parameters shows that to

reach the crack width performance target (below 80 μm) the most favourable interface properties should be in the range of 1.5 – 2.5 MPa for frictional stress, and below 1.5 N/mm for interface fracture energy, given enough fibre diameter and length for easy fibre scatter. However, without treating the PVA fibre, the bond properties are far above the optimal values.

There are two approaches taken to reduce the excessive interface bond. On the fibre side, coating the surface with oil is investigated. The frictional stress and interface fracture energy decreases significantly when the oil content is increased. This means that, J_b' increases with oiling content for a given matrix, as shown in Figure 1.4, where a fibre volume fraction of 2% is used. On the matrix side, fly ash is brought into the formula. It is found that a high volume fraction of fly ash reduces both the interface bond and matrix toughness. Figure 1.5 shows the effect of ASTM Type F fly ash content on J_b'/J_{tip} , where oiling content of 1.2% is used for fibre and the fibre volume fraction is 2.0%. Fly ash also improves the workability of the mixture and the sustainability of the material. A negative impact, however, is that high contents of fly ash lead to slower strength development at early stage. It is found that fly ash to cement at 1:2 weight ratio provides best overall performances although much higher fly ash proportions have been used successfully.

Control of the matrix properties is as important as the interface bond adapting. It is preferred that the matrix toughness is below 12 N/m and the matrix cracking strength is kept below σ_0 . Controlling the matrix flaw size distribution may become necessary to make sure that saturated multiple cracking occurs. Saturated multiple cracking can, however, be guaranteed if the matrix tensile strength without macro defects is controlled to be below the variation range of σ_0 . Using a PVA fibre volume fraction of 2% and achieving the optimal interface properties, the more desirable matrix tensile strength without macro defect is around 3MPa – 5MPa.

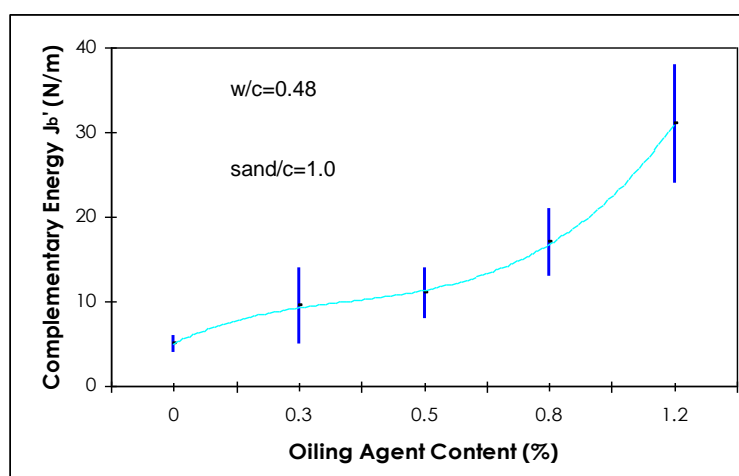


Figure 1-4: Effect of Fibre Surface Oiling content on J_b'

(Polyvinyl Alcohol Fibre Reinforced Engineered Cementitious Composites: Material Design and Performance, [10])

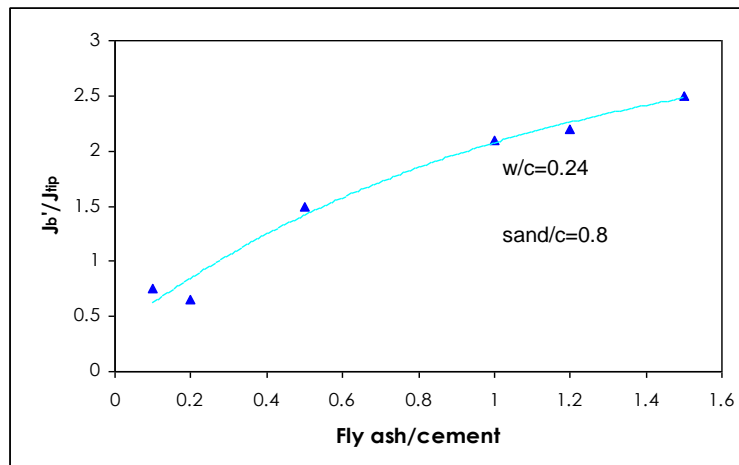


Figure 1-5: Effect of Fly Ash Content on J'_b/J'_{tip}

(Polyvinyl Alcohol Fibre Reinforced Engineered Cementitious Composites: Material Design and Performance, [10])

Traditionally, in R/C structural design, the most often used and most important material characteristic of concrete is its compressive strength. That is why the key controlling parameter for structural strength and performance is usually material strength. This means that higher material strength (normally referred to as compressive strength in the concrete literature) is expected to lead to higher structural strength, but this is only valid if the material strength property really dominates the failure mode. For example, if tensile fracture failure takes place, a high strength material does not necessarily mean higher structural strength. Then it is rather a high toughness material that is needed, and in the extreme, a ductile material like SHCC, can then lead to a higher structural strength.

1.3 Durability

1.3.1 Introduction

It is said that the production of cement, an energy intensive process, is responsible for 5% of global greenhouse gas emissions (WBCSD 2002), [12]. The need for such extensive cement production can be found in the rate at which development is taking place around the globe. Reinforced concrete is possibly the most used building material in the world, in spite of its limited durability when not properly maintained.

The limited durability of reinforced concrete results in significant amounts of infrastructure repair, rehabilitation, and replacement. The reason for this limited durability is the combination of corrosion prone reinforcement embedded in brittle, crack prone concrete. Cracks provide pathways for the ingress of harmful substances which, in time, corrode the reinforcement. Besides the fact that the

corrosion of the reinforcement tends to result in unsightly markings on the outside of the structure, it also reduces the strength of the structure. This, in turn, can lead to structural failures.

It is possible that a more environmentally friendly concrete with improved durability for new and refurbished infrastructure provides the best solution to the infrastructure decay problem, while relieving environmental concerns. Given that cracking in concrete is a major cause for the rehabilitation of infrastructure, this makes the case for a future generation of concrete that is more damage resistant, and exhibits smaller crack widths.

1.3.2 Durability of Strain Hardening Cement Based Composites (SHCC)

Strain-Hardening Cement-Based Composites (SHCC) are known for their ability to control crack widths. This ability is what gives this material its strain-hardening characteristic. Crack widths are limited by means of fibres bridging the gaps formed by cracks. The fibre bridging results in multiple micro cracks, rather than one or two larger ones. When the tensile strain, however, reaches its maximum limit, the fibres bridging the cracks will either pull out or break off, causing one or two cracks to open up. This is called crack localization and happens when the member has reached crack saturation. It is thus important when designing with SHCC to ensure that the tensile strain in the concrete does not reach its ultimate limit.

The durability of many reinforced infrastructures is negatively impacted by the tendency of concrete to crack in tension; tensile stress may be due to live load, restrained shrinkage or thermal loads. Past experiences have indicated that cracks and crack widths are difficult to control in the field by only using steel reinforcements. Given these facts, it would seem natural to look to SHCC for enhancement in structural durability [13]. Closely associated with the strain-hardening and multiple cracking behaviour is the small steady state crack width. Even at a strain of 4-5%, average crack widths of SHCC remain below 100 μ m. However, the maximum crack width can be much more than that [14].

Corrosion of steel reinforcing bars in concrete can commence when the chloride ion concentration on the rebar surface reaches a certain threshold level. By preserving low chloride ion diffusion rates after cracking, SHCC reduces chloride intrusion to effectively protect rebar from corrosion (Sahmaran et al, 2007) [15]. A second level of protection against corrosion is the anti-spalling ability of ductile SHCC. It can withstand expansive forces generated by steel corrosion. In many structures, steel reinforcing is used to control concrete crack width. Such reinforcement may be completely eliminated when SHCC replaces concrete since the crack width in SHCC is self-controlled [13].

One of the shortcomings of SHCC is the environmental penalty in higher energy and carbon footprints on a unit volume basis, associated with the incorporation of fibres and typically higher

cement content in SHCC compared with normal concrete. The higher cement content in SHCC results from the deliberate elimination of coarse aggregates used as filler material in normal concrete. It is possible to add fly ash to the mixture to save on cement content. More about this is said in the next paragraph of this chapter. Hence on a unit volume basis, the primary energy consumption of SHCC is a major concern. In the investigation of life cycle primary energy consumption and the equivalent carbon dioxide emissions for a bridge deck, Keoleian et al (2005) [16] [17], identified material production as the second largest contributor to these sustainability indicators, behind traffic alterations due to maintenance and reconstruction events. Thus it is important to consider approaches in greening SHCC, even though the enhanced durability of SHCC as discussed in the previous section should substantially reduce repair needs and therefore enhance infrastructure sustainability.

The greening of SHCC can target replacement of virgin fibre with industrial waste stream materials. SHCC is optimized for tensile ductility with a minimum amount of fibres. Even so, typical amount of fibre used is 2% by volume. Attempts at using natural fibre or recycled fibres (e.g. carpet fibres) have met with limited success, given the requirements of strong fibre bridges in maintaining composite ductility (Li et al, 2000), [8]. Replacing PVA fibres with PET (polyethylene terephthalate) fibres, manufactured from recycled plastic bottles, resulted in similar compressive strengths but lower tensile and flexural strengths due to the inferior qualities of the material [18]. There have been a few successful cases where Portland cement and silica sand have been replaced with industrial wastes. The use of fly ash lowers compressive strengths in the early stages but improves the maximum tensile strength and ductility [18]. Increasing the use of recycled aggregate increases the compressive strength and the elastic modulus, but the bond strength between the fibre and cement matrix is reduced to an unacceptable level. Of all these substitutions, only the use of fly ash shows a reduction in the carbon dioxide emissions. The only other positive outcome from using these alternatives is that there is a saving in natural resources [18].

In Chapter 4 of this study, a design method is proposed for the design of reinforced SHCC members in flexure. The aim of the model is to design a reinforced SHCC beam in such a way as to ensure that it is not just structurally safe, but also strives to keep the deflection and crack widths within an acceptable range. Since SHCC has a reputation for showing very small crack widths, there might be a saving to be made from using this material.

1.3.3 Fundamentals of Durability Design for SHCC

The ductility found in SHCC is not due to plastic deformation, but is attributed to the formation of multiple micro cracks. This indicates that the material is progressively damaged in the strain hardening range [19]. However, as long as the crack widths stay within a small enough range, the material's permeability is not really increased. There is also a possibility that the micro cracks will

close again under special environmental conditions by self-healing [19]. Therefore, it is essential to keep the micro crack widths under a certain critical width. The critical crack width for specific conditions will have to be found by means of experimental testing under those conditions.

Strains imposed on structures are in two categories. The first is the mechanical strains which are caused by imposed design loads due to the specific use of the structure. These loads are normally quite well defined and the strains can easily be found by applying the design calculations given in Chapter 4.

The second group of strains is environmentally imposed strains. These strains include thermal strains due to temperature changes, and drying shrinkage and expansion due to moisture in the environment. The environmental strains are linked to changing temperatures and seasons and are therefore cyclic in nature. Moisture shrinkage strain in SHCC can be in the order of 0.08% to 0.12%, while a temperature difference of 50°C causes a thermal strain of around 0.05% [19]. These strains are quite substantial and if the mechanical strains are added, it would be prudent to check the ultimate design strain in order to ensure that strains are kept low enough. It would seem that a structure will have to be able to withstand at least 0.2% strain before micro cracking starts, in order for the environmental strains not to affect the durability negatively [19].

1.3.4 Crack Control as Durability Measure

An important part of the durability of structures, is limiting crack widths. Cracks are the weak spots in the structure where potentially damaging salts such as chlorides can find entrance into the concrete and cause damage to the reinforcement inside and to the concrete itself [19]. This damage causes restoration and maintenance costs in the building's life cycle. By keeping the crack widths small enough, these costs can be reduced significantly and maintenance periods can be increased. Corrosion of reinforcement inside concrete structures weakens the structure and can cause premature collapse in extreme cases of weather, for instance.

An alarming trend observed in the infrastructure sector internationally is that the growth rate of the maintenance and rehabilitation expenditure is increasing. The largest source of damage may be attributed to moisture, gas and salt ingress in cement-based composites like concrete, whereby steel reinforcement is subjected to degradation processes [19]. Tight crack control has the potential of addressing these issues.

Crack width limitation or control is a well-established concept in RC design. Design standards and codes for concrete suggest limiting values for crack widths for different environments to assure durability of structures built in these environments. In Table 1-1, the various limits for some different codes are listed.

Table 1-1: Examples of crack width limitations in RC Structures for Durability (Carino and Clifton, 1995), [20]

<u>Exposure conditions</u>	<u>Tolerable crack width (mm)</u>
<u>ACI 224R, 90</u>	
Dry air or protective membrane	0.41
Humidity, moist air, soil	0.30
De-icing chemicals	0.18
Seawater and seawater spray, wetting and drying	0.25
Water retaining structures	0.10
<u>ACI 318-89</u>	
Interior	0.41
Exterior	0.33
<u>ACI 350R-89</u>	
Normal	0.27
Severe	0.22
<u>CEB/FIP Model Code 1990</u>	
Humid environment, de-icing agents, seawater	0.30

Chloride has a detrimental effect on the fibre-matrix bond of the composite and consequently the mechanical properties of SHCC (Kabele et al., 2006) [21] [22]. As shown by Mechtcherine et al., (2007) [23] cracking has a significant influence on the transport parameters of the material. It is reasonable to expect that steel-reinforced SHCC members (R/SHCC) will generally have a superior durability compared to conventional RC members subjected to the same tensile strain, due to their limited crack widths. However, the durability of the material can only be fully utilized based on an accurate prediction of the time until chloride induced corrosion begins. Altmann et al., (2008) [24], developed a fuzzy probabilistic model for chloride ingress in SHCC based on the DuraCrete model [25].

Chloride ingress and subsequent corrosion of the steel reinforcement is a critical corrosion process for R/SHCC members. To fully utilize material ductility and durability, a performance based durability design concept that is applicable to both crack-free and cracked SHCC is required. It is well known that cracks of limited widths as is present in SHCC may fully heal over time. Further investigations

into self-healing of SHCC are required to accurately model chloride ingress in the cracked material. The cracks in SHCC are not always evenly spaced. Localization of cracks has a major influence on quantification of an expected chloride diffusion coefficient at an arbitrary location in a member under tensile strain. Thus the spatial distribution as well as further properties such as length and width, as a function of the induced load or strain, needs to be investigated further. It is said that the age of the crack free material has a greater impact on the chloride ingress over the life time of the structure than the diffusion coefficient. For SHCC no information for the age factor is available, and thus significant research effort in this area is required [25]. There is new evidence of chloride-induced corrosion in R/SHCC. Chlorides enter SHCC through cracks and reach the steel within minutes or hours, despite the small crack widths mentioned earlier. However, the corrosion rate is low in cracked R/SHCC due to the small spacing of cracks [26] [27].

Stopping the ingress of harmful substances into the concrete is a primary contributor to the durability of such concrete. These harmful substances can be moisture, gas and salts and they will cause degradation of the material itself or of the reinforcement within it. The most important mechanisms of moisture ingress and migration are capillary sorption and moisture diffusion. Moisture intake is governed by capillary sorption in the near surface zone, (Neithalath, 2006) [28], while it is believed that moisture fusion is the dominant mechanism for the longer term migration of moisture in the material through micro pores (Bažant and Najjar, 1971 [29]; Neithalath, 2006 [28]). In UHPFRC, capillary absorption is reduced by matrix densification, (Kuneida et al., 2007) [30], while inherent crack control reduces diffusivity in SHCC (Lepech and Li, 2005 [31]; Sahmaran et al., 2007 [15]).

Wang et al. [32], (1997) have studied the influence of crack width on the water permeability of normal concrete. It was found that for a crack width reduction from 550 to below 100 μm , the permeability reduced by seven orders of magnitude. Li and Stang (2004) [33], found that SHCC has a similar permeability to that of normal concrete for the same width of cracks. Thus it should be possible to apply the rules of water permeability for normal concrete on SHCC.

In a study done by Paul, Rens and Van Zijl [34], it was found that the crack spacing in R/SHCC is reduced with an increase in the cover to reinforcement depth. In this study, the threshold cover depth was found to be 25mm. It was also concluded that an increased crack spacing shows a higher corrosion potential and rate than a lower crack spacing. This fact was also concluded in a more recent study by Paul and Van Zijl [27]. Higher deflection levels were also shown to decrease the crack spacing, however, it also increases the average and maximum crack widths. This fact is in accordance to theory that the higher the tensile strain, the more cracks will form until such time as crack saturation is reached. Then the first cracks to form would start opening up and crack localization would take place.

In the study done by Adendorff, Boshoff and Van Zijl [35], it was found that although the average crack width in SHCC is less than 0.1mm, the maximum crack width is far more than that. In this study, measurements were taken from direct tensile tests as well as cyclic loaded tests. Both these tests showed average crack widths less than 0.1mm, but maximum crack widths as high as 0.4mm at a tensile strain of 3%. These large cracks appear in localized areas only. This was also concluded by Van Zijl et al., (2016) [36].

It seems that, for a particular type of SHCC, containing PVA fibres in the range of $2.0\% \leq V_f \leq 2.5\%$, the crack width is arrested at a strain level of 1% and at an average value of 50 - 60 μm [19]. More cracks will appear in the structure, but it is believed that they will not exceed this width, until crack saturation is reached. This phenomenon is shown in studies done by Li and Weimann in 2003 [37], Li et al., in 2001 [38], and Wang and Li in 2006 [10].

1.3.5 Conclusion

While SHCC shows much promise in reducing the need for rehabilitation of reinforced concrete structures, developments to reduce the environmental impact of the material are required. Reducing the carbon footprint of this material will enhance its worth in the construction industry.

As cracking and crack widths are the most important aspects of durability, these properties of SHCC need to be researched in greater depth. While average crack widths are shown to be small, maximum crack widths can reach up to the normal limits set in conventional concrete structures. During this study, it was found that the crack widths at the service limit state were too small to see with the naked eye.

There are currently no models for estimating the crack widths in SHCC. The specific crack width limits that need to be applied in order to protect reinforcement against ingress of harmful substances are also lacking. In the absence of these limits, the supposedly higher durability found in R/SHCC than in normal R/C cannot be proven.

2. MATERIAL DESCRIPTION

2.1 Response to Tension

2.1.1 Material Behaviour

Strain hardening cement composites are ideal for use in structural members subjected to bending because of their strain hardening ability under tension. Strain hardening is achieved by means of multiple cracking, which delays crack localization. As with normal concrete, the material cracks under tension. In normal concrete, however, the material has lost all tensile load-carrying ability after cracking and has failed. In SHCC, the initial cracks are generally too small to be seen on the surface and are spread along the length of the element by means of the fibres in the matrix. The fibres act as reinforcement, arresting the cracks and spreading the load to the nearby matrix where more fine cracks develop and more fibre bridging takes place. This enables the material to still carry higher tensile loads even though the matrix has been damaged. When the tensile strain passes the ultimate strain value of the material, the fibres bridging a crack will either pull out or be broken off. Now crack localization has occurred, and the material has failed, and gradually loses its load carrying capacity.

The first cracking strength of the material can vary from 1MPa to 5MPa, depending on the matrix design. The first cracking strain can be anything from 0.08% to about 0.2%. The ultimate tensile strength capacity is around 3MPa to 6MPa, and is accompanied by tensile strain of around 2.0% to 5.0%. These values are true for normal strength strain hardening materials. They might be very different for higher strength materials. An UHP SHCC material is used later on in this study for checking the design model. This material has a first cracking stress of 11.8MPa with an accompanying strain of 0.000211. The ultimate tensile stress is 15MPa with an accompanying strain of 0.0039.

Naaman and Reinhardt (2006), [39], proposed a classification model for Fibre Reinforced Concrete (FRC) based on the tensile properties of the material as this is considered the most important characteristic of this material. In Figure 2-1, the minimum information needed to design a strain-hardening FRC material, according to Naaman and Reinhardt, is given diagrammatically. The number, 1, indicates the first percolation cracking point (σ_{cc} , ϵ_{cc}) or first cracking point, and the number, 2, indicates the peak stress point (σ_{pc} , ϵ_{pc}) or crack localization point. Because of the difficulty in calculating the first cracking point, Naaman and Reinhardt suggested that a minimum elastic modulus be specified. This allows the minimum coordinates of point 1 to be calculated beforehand. The actual modulus can be measured from tests but because the first cracking point is very hard to pin point, this is quite a tedious and not very accurate process.

In Visser's study [40], the elasticity modulus for normally cast SHCC was measured to be around 12.5GPa, and that of extruded SHCC around 31GPa. The extruded SHCC E modulus is high due to the air being forced out of the material during extrusion. During a previous study, elasticity modulus values of around 7GPa and 8GPa were also found, while during this study, E values of around 20GPa were found. Further to the above, it was found in a study by Van Zijl (2005) [41], that the ultimate tensile strength and strain are significantly increased upon reduction in aggregate fineness. It was also found that the strength and strain is reduced with an increase in aggregate content, without the fineness of the aggregate playing a role.

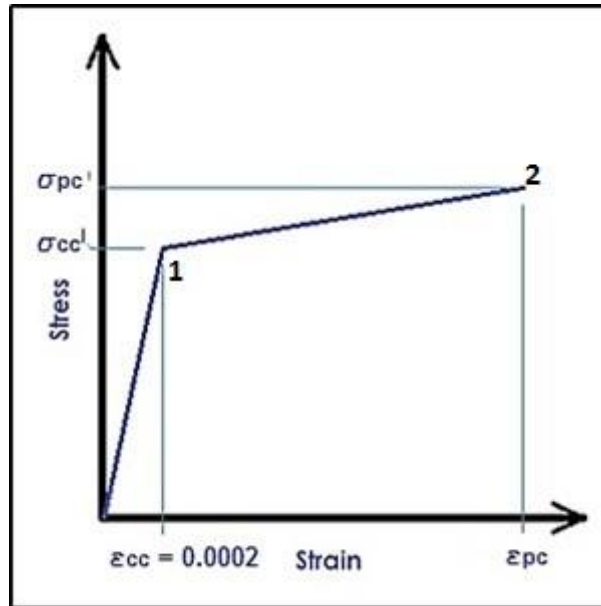


Figure 2-1: Minimum Information Needed for Design on Tensile Strain Hardening Stress-Strain Response of FRP Composites [39]

Naaman and Reinhardt assumed a minimum E value of 10.5GPa. They decided that the tensile strain could be set to a value close to that of the unreinforced matrix, and they chose $\epsilon_{cc} = 0.0002$. Then, σ_{cc} can be calculated using one of the following equations:

- $\sigma_{cc} \approx \sigma_{mu}$
- $\sigma_{cc} = E_c \epsilon_{cc}$
- $\sigma_{cc} = E_{min} \epsilon_{cc} = E_{min} 0.0002$
- $\sigma_{cc} = \sigma_{mu} (1 - V_f) + \alpha \bar{\tau} V_f \frac{\psi}{4V_f}$
- $\sigma_{cc} = \sigma_{mu} (1 - V_f) + \alpha \bar{\tau} V_f \frac{1}{d}$

Where:

- σ_{mu} = Tensile strength of unreinforced matrix
- E_c = Elastic modulus of the composite
- $E_{min} = 10.5\text{GPa}$
- $\bar{\tau}$ = Average bond strength at the fibre matrix interface
- Ψ = Perimeter of one fibre
- A_f = Cross sectional area of one fibre
- d = Fibre diameter
- α = Product of several coefficients

The first part of Reinhardt and Naaman's classification is based on the specified tensile strength or peak tensile stress after cracking, σ_{pc} , of the material (See Figure 2-2). For example, a Class T-10 composite would guarantee a post-cracking tensile strength of 10MPa. All the classes have the same required minimum level of strain at peak stress and the same minimum elastic modulus.

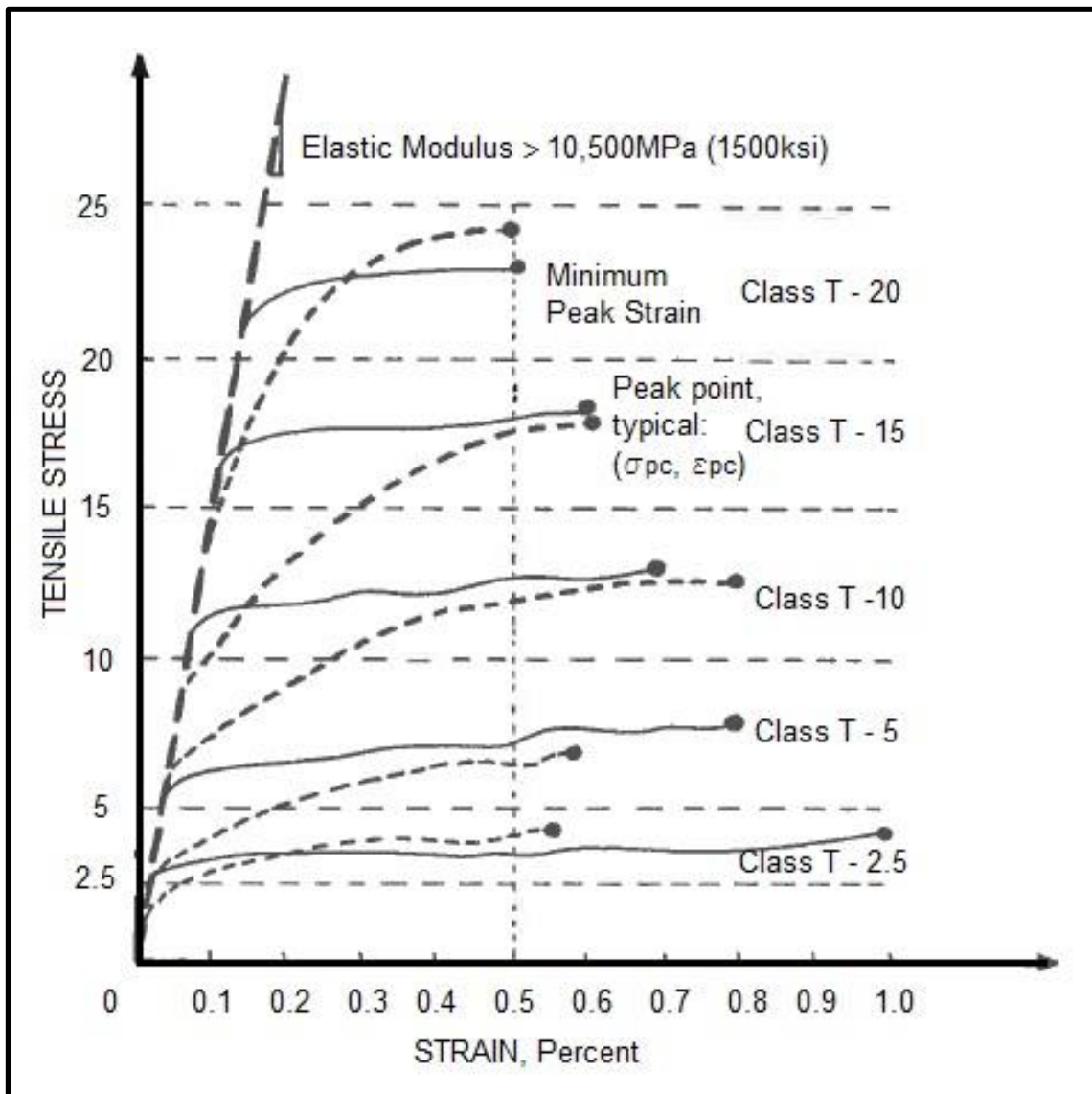


Figure 2-2: FRC classification model proposed by Naaman and Reinhardt (2006)

The second part of the classification is the minimum strain capacity at peak stress, that is, $\epsilon_{pc} \geq 0.005$. This strain level is more than twice the yield strain for normal reinforcement bars. The number is justified in that almost all failures occur when the strain in the reinforcement is significantly larger than the yield strain. This happens in under reinforced members. Naaman and Reinhardt, therefore considered it safe to specify a minimum peak strain of 0.5%. This is to ensure that the strain hardening FRC material will contribute towards crack control, ductility, energy absorption and the ultimate strength of the reinforced member. During this study, this limit was found to be low. Values of up to and more than 3% were found in a number of cases.

The minimum elasticity modulus, 10.5GPa, is the tangent modulus at the origin. It seems that almost all cement composites will be able to comply with this specification easily. By fixing this minimum value, the first cracking point, the necessity of trying to determine the exact first cracking stresses becomes less important. This will, however, not be valid for all strengths of materials and some modelling will be necessary to determine the elasticity modulus for specific strengths of SHCC. This will be especially true for the higher strength SHCC materials.

When using this classification system, it can thus be said that a Class T-10 strain-hardening FRC composite has the following properties: an ultimate tensile strength equal or higher than 10MPa, a minimum elastic modulus of 10.5GPa, and a strain at peak stress equal or higher than 0.5%.

2.1.2 Test Models and Testing

To test SHCC in uniaxial tension, it is cast in a dumbbell shape. The wider ends are used to grip the specimen and the narrow middle piece ensures that the cracks are confined to the reduced cross section piece of the dumbbell. This also simplifies the strain calculations and also ensures that the actual characteristic cracking response is captured in a known region of uniform cross-section by pre-placement of the deformation measurement devices.

The specimen is placed inside a frame which is then inserted into a materials testing machine (MTM). Openings are provided in the frame for movement measuring devices, Linear Variable Differential Transformers (LVDT), to be installed. These elements are all then connected to a data capturing system, which in turn is connected to a computer which then tracks the movement in relation to the tensile load being exerted on the specimen. The data can then be transferred into an Excel spreadsheet from where stress and strain relationships can be drawn for every specimen tested. Figure 2-3 shows a typical tensile test setup.

In recent work, and based on van Zijl et al., (2016) a larger dumbbell-shaped specimen was used in Stellenbosch, with a 40mm x 80mm cross section in the gauge region.

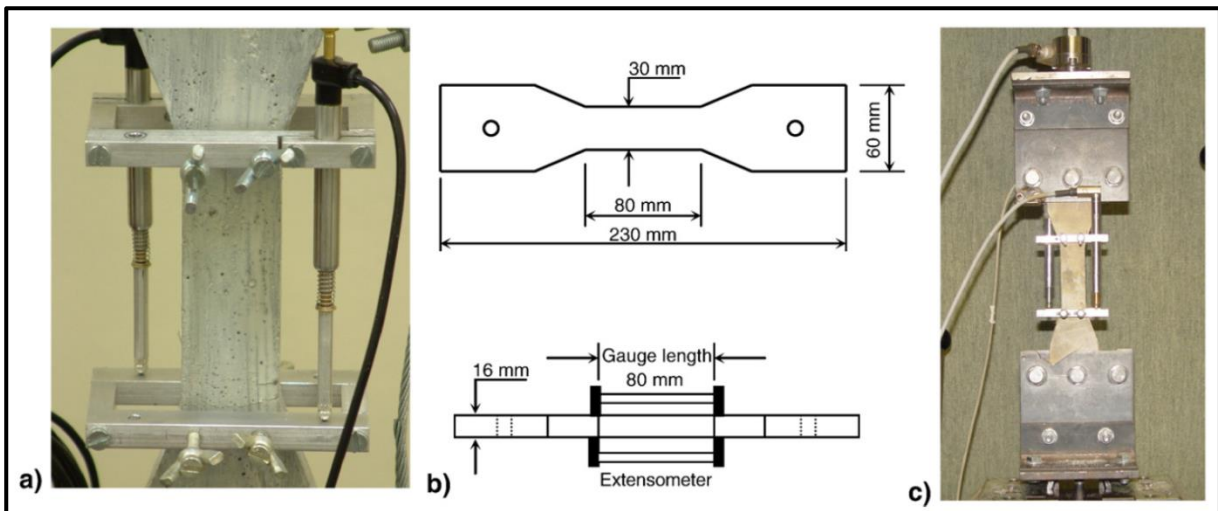


Figure 2-3: a) Extensometer consisting of a frame and 2 LVDT's. b) The thin flat dumbbell shaped specimen, c) Tensile test setup in Zwick Z250 [42]

2.1.3 Stress-Strain Relationships

Examining the stress-strain graphs produced by analysing the data from the tests done during this study, three different phases are clearly definable in the tensile response of this material as is shown in Figure 2-4. (The tests are further described in chapter 3.)

The first phase is a linearly elastic phase. It is the period from load inception until the first crack forms in the cement matrix. The elasticity modulus of the material is defined as the gradient of this part of the stress-strain graph. During this phase there are no cracks in the cement matrix and the material is assumed to be fully elastic.

The second phase is the strain hardening phase which is initiated with the first cracks appearing in the cement matrix. These cracks can be very small at first and are not necessarily visible on the surface. The specimen has now entered a plastic state. Even now, after the concrete has started cracking, the specimen is able to endure even higher loads as the strain increases. This strain hardening phase is accompanied by multiple micro cracks forming along the length of the specimen. This phenomenon is known as multiple cracking and is in turn caused by fibres in the cement matrix which act as reinforcement, arresting crack propagation as soon as it passes a fibre, and re-distributing the stresses throughout the length of the specimen. At some point, the stress will reach an ultimate level and the fibres will start pulling out or breaking off. This is then the end of phase 2 and is called crack localization.

The third phase is the failure phase. When crack localization has occurred, the member has failed in tension and under further loading the stress will gradually decrease as the strain still increases. One, or in some exceptional cases, two cracks in the matrix will now open up as the other cracks

close. This is still a ductile phase as the fibres in the matrix will keep slowing the crack's progress through the specimen.

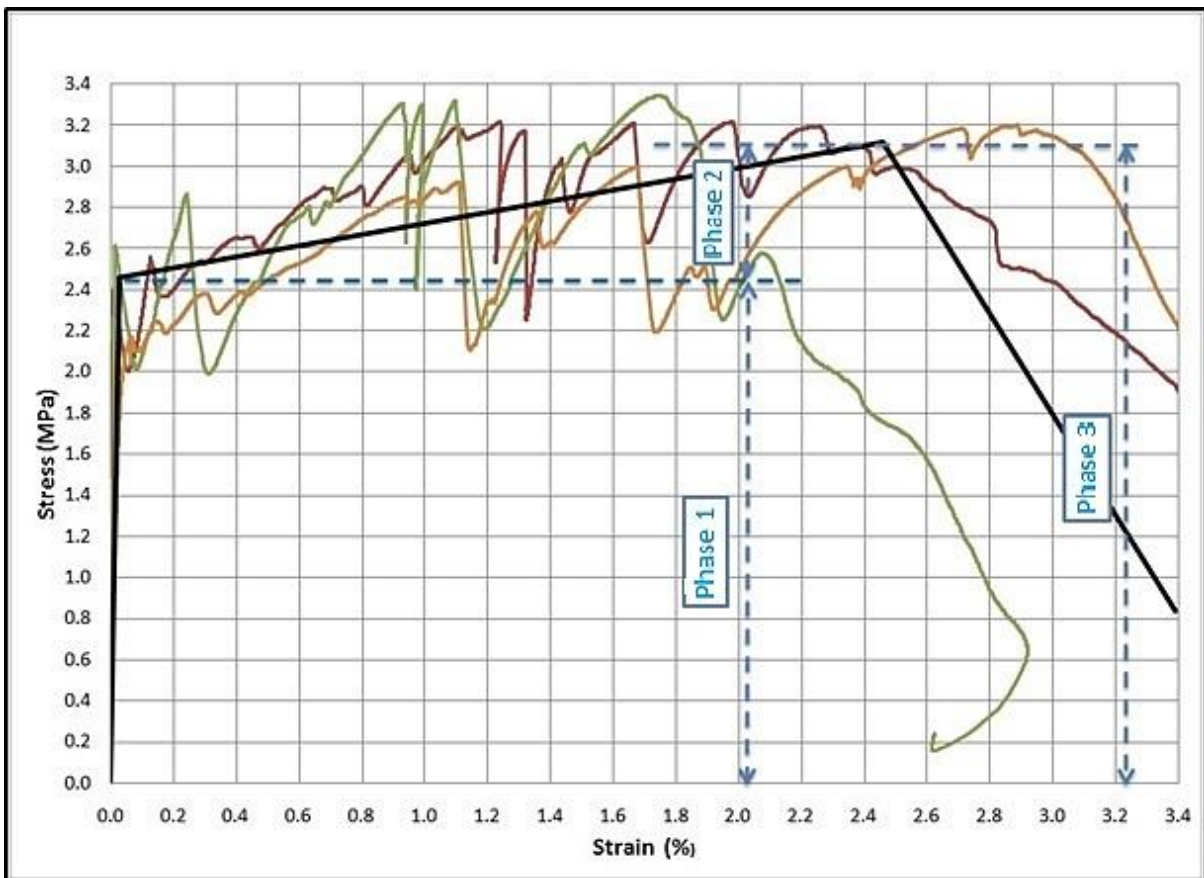


Figure 2-4: Tensile Stress-Strain relationship

2.1.4 Critical Parameters

The strain hardening characteristic of SHCC is what makes it unique from other fibre reinforced materials. As strain hardening is SHCC's most valuable characteristic, it is important to know the extent of this phase.

As was indicated earlier, strain hardening is initiated with the first crack forming in the cement matrix. Knowing the stress and strain associated with this point is necessary in order to establish the elasticity modulus for this material in tension. This point is called the first cracking point and the stress and strain associated with it is called first cracking tensile stress, σ_{ct1} , and first cracking tensile strain, ϵ_{ct1} .

The second point of interest will be the point of crack localization. The stress and strain associated with this point is called the ultimate tensile stress, σ_{ctu} , and the ultimate tensile strain, ϵ_{ctu} . When the ultimate tensile stress and strain have been reached, the material has reached the end of its strain

hardening capacity and will gradually start to loose strength as the load increases. These four parameters at the two points of interest are shown in Figure 2-5.

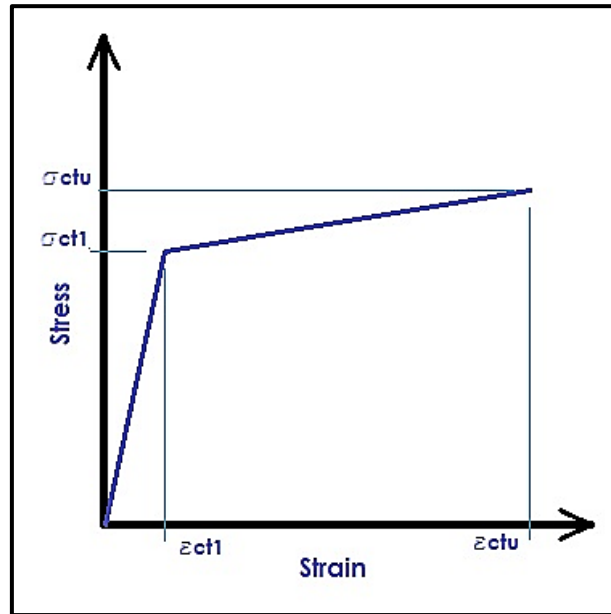


Figure 2-5: Simplified Stress-Strain Relationship

The slope of the first leg of the graph describes the elasticity modulus of the material. Elasticity modulus, E, can then be defined as:

$$E = \frac{\sigma_{ct1}}{\epsilon_{ct1}} \quad 2-1$$

Finding the slope of the second part of the graph is essential in defining the strain hardening part of the tensile behaviour. In order to make this expression more generic, it is related to the original modulus, E.

$$\alpha E = \frac{\sigma_{ctu} - \sigma_{ct1}}{\epsilon_{ctu} - \epsilon_{ct1}} \frac{\epsilon_{ct1}}{\sigma_{ct1}} \quad 2-2$$

Equations 2-1 and 2-2 are used in Chapter 4 to define the design model for reinforced SHCC in bending

2.2 Response to Compression

2.2.1 Material Behaviour

The compressive behaviour of SHCC is assumed to be similar to that of normal concrete and therefore it has not been widely studied. It is believed that the material does not have any notable strain hardening properties in compression. Its compressive behaviour is similar to that of normal concrete. Compressive strength values of between 20 and 250MPa have been found. These values are associated with elasticity modulus values of between 18 and 34GPa [43].

2.2.2 Test Program

In order to establish the correct material properties for the flexural members tested, compression tests were carried out for each of the flexural test specimens. (These tests are further described in chapter 3.) A typical test setup is shown in Figure 2-6.

The testing of the compressive strength of concrete is well established in practice, however, a challenging aspect of measuring the concrete properties of SHCC is the requirement that the strain related to the stress also need to be measured. In order to record total load-deformational response during compressive tests, a suitable mounting frame as shown in Figure 2-6 was used. The frame allows for two or three LVDT's to be mounted on it. The full load-deformational response was to be measured as well as a significant part of the post peak response. Measurement of the deformation of the post peak response was risky as the failing of the test specimen could result in damages to the movement sensors. The tests specimens were cylinders of 50mm diameter and approximately 100mm in length.

As for the tensile test the data acquired was processed via an analogue to digital converter and fed into a computer where it could be imported into an excel spreadsheet. Here it could be manipulated and the stress-strain relationship could be drawn for each test done.

2.2.3 Stress-Strain Curves

As was expected for SHCC, a very similar compressive response to that of normal concrete was found. The true curvature represents a complicated curve with the maximum compressive strength at the turn of the curve. From there it has a near linear decline as the concrete crushes and fails. This is shown in Figure 2-7.

As for normal concrete, this stress-strain response can be approximated with a parabolic expression. However, keeping the analytical solution to be developed in mind, a bi-linear approach was adopted in order to simplify the calculations. This approach was also followed by Li et al. [44]. According to them, the elasticity modulus, E , for the first part of the approximation, can be calculated as follows:

$$E = \frac{\frac{2\sigma_{ccu}}{3}}{\frac{\epsilon_{ccu}}{3}} = \frac{2\sigma_{ccu}}{\epsilon_{ccu}}$$

2-3

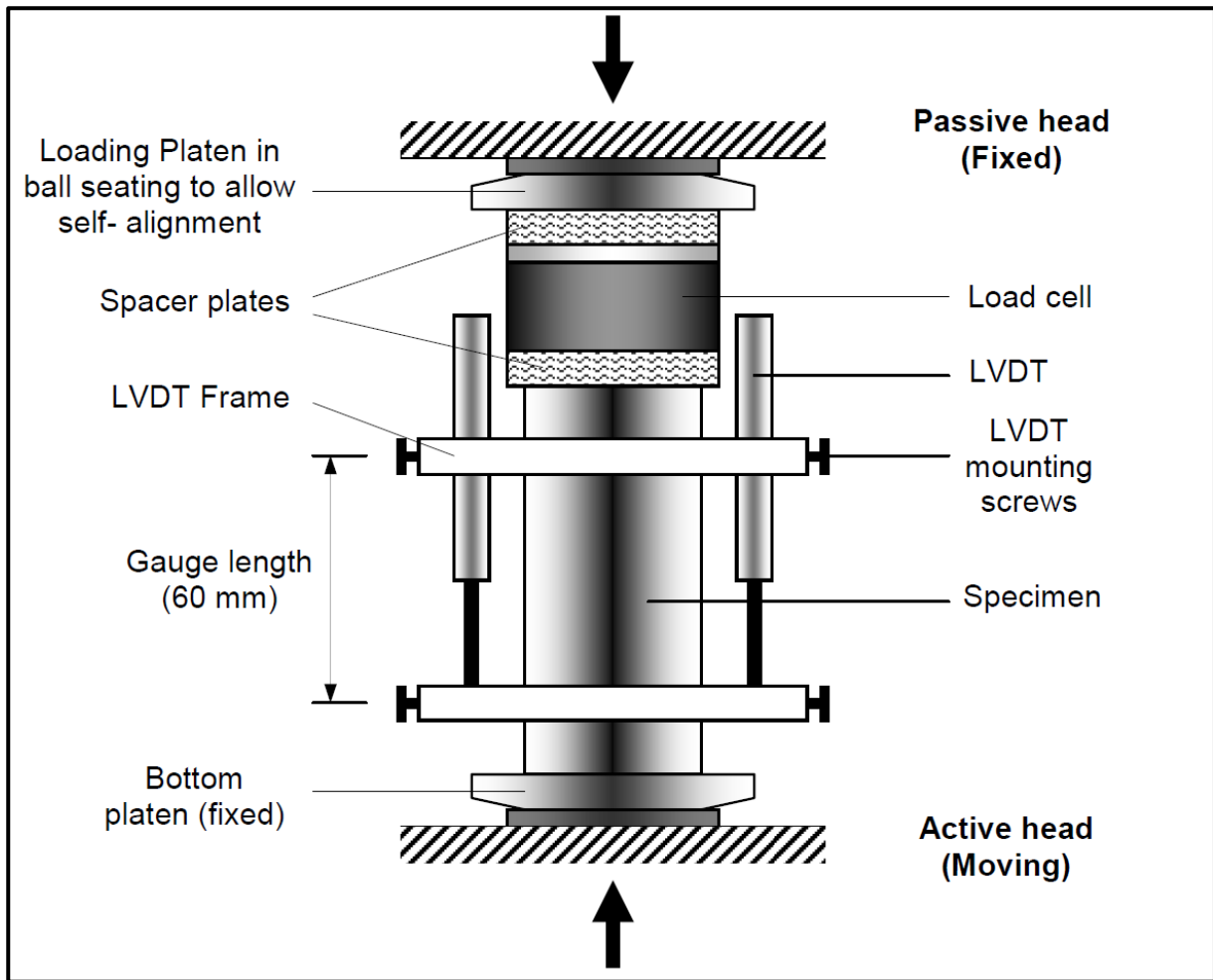


Figure 2-6: Apparatus for compressive specimens [45]

From Equation 2-3 it is clear that Li et al. [44] have assumed a stress value of 2/3 of the ultimate value to coincide with a strain value of 1/3 of the ultimate value. This approach is shown in Figure 2-7 on a single compression stress-strain curve.

To define the next part of the relationship, the slope of the second line is needed. In order to find an expression for this slope, and taking into consideration the assumed values of the starting point of this slope, it is possible to deduce the following:

$$\delta = \frac{\sigma_{ccu} - \frac{2\sigma_{ccu}}{3}}{\epsilon_{ccu} - \frac{\epsilon_{ccu}}{3}} = \frac{\frac{\sigma_{ccu}}{3}}{\frac{2\epsilon_{ccu}}{3}} = \frac{\sigma_{ccu}}{3} \frac{3}{2\epsilon_{ccu}} = \frac{\sigma_{ccu}}{2\epsilon_{ccu}}$$

2-4

If the same approach is used as for the tensile behaviour and this second slope is expressed in terms of the elasticity modulus, the following can be derived:

$$\delta E = \frac{\sigma_{ccu} \varepsilon_{ccu}}{2\varepsilon_{ccu} 2\sigma_{ccu}} = \frac{1}{4}$$

2-5

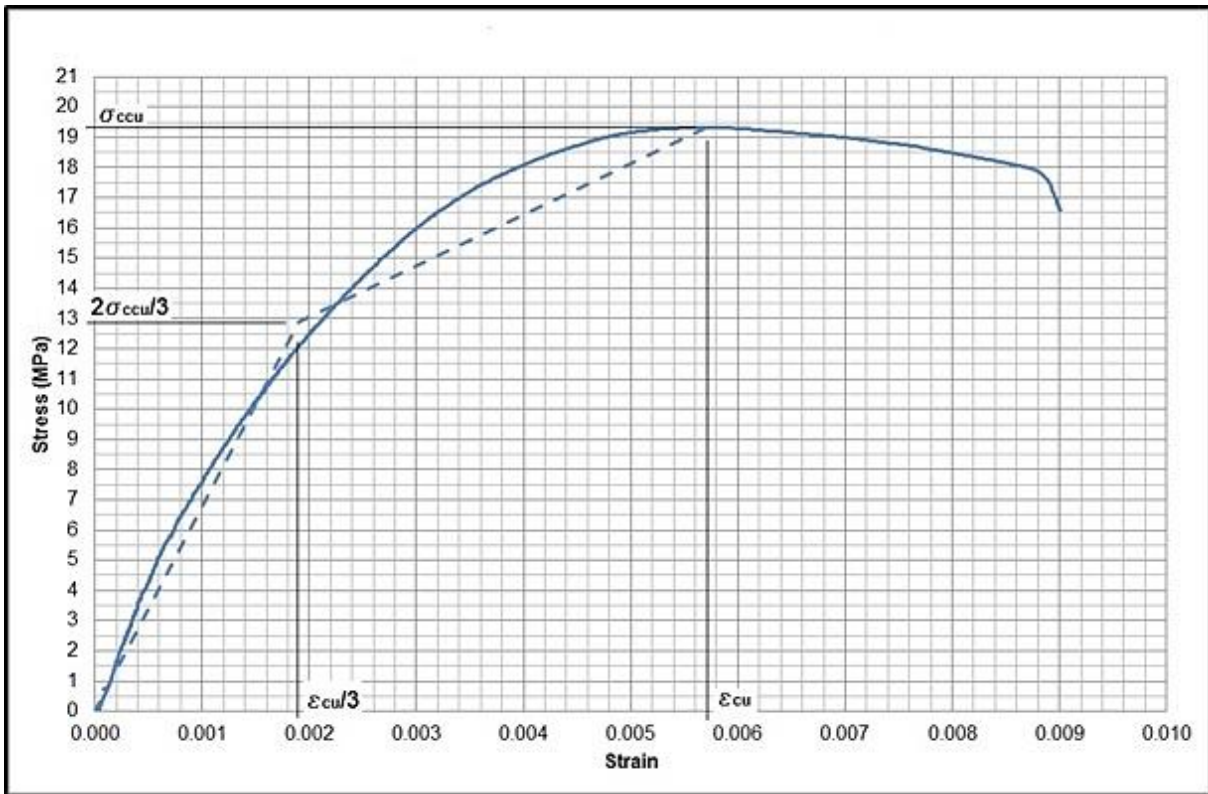


Figure 2-7: Compression Stress-Strain Behaviour according to Naaman and Reinhardt

To determine how appropriate these assumptions are, a number of compressive responses were analysed to ascertain if the cut-off point of 1/3 of the ultimate strain value for the elastic part of the compressive response is reasonable. The results of the 6 compressive tests done during this study on cylindrical specimens and reported in Table 3.3 were used for this purpose. Trend lines were used to establish the point where the compression response is no longer linear. The average strain value of these points was then used to derive a new bilinear estimate. These tests are further described in chapter 3. Two of these responses are shown in Figures 2-8 and 2-9.

Analysing Figure 2-8, it is clear that the assumed elasticity modulus of Equation 2-3, is larger than the true modulus, resulting in an over estimation of the stiffness for the compressive response. This discrepancy is much less in Figure 2-9, but it still shows an over estimation of the stiffness of the concrete in compression. It is thus clear that for some mix designs, the above assumption may be more valid than for others.

Over estimating the compression stiffness of a member can lead to un-conservative under-estimation of the deflection of the member. In order to find a more accurate solution, a two part approach was used with the first part taken as being linear. The second part was then approximated

with a polynomial curve of the second order, as this was found to fit the observed data curve best. The intersection point of these two approximations was then assumed to be the point where the elastic response ends and the plastic response starts. This was done for all the compression tests done for this study, which was a total of 6 tests.

From the number of responses tested, the average strain value of this cutting point was found to be 0.317 of the ultimate strain value. This verifies that the assumption of 0.333 of the ultimate strain value as was made by Li et al [44], was reasonable but perhaps overly simplistic.

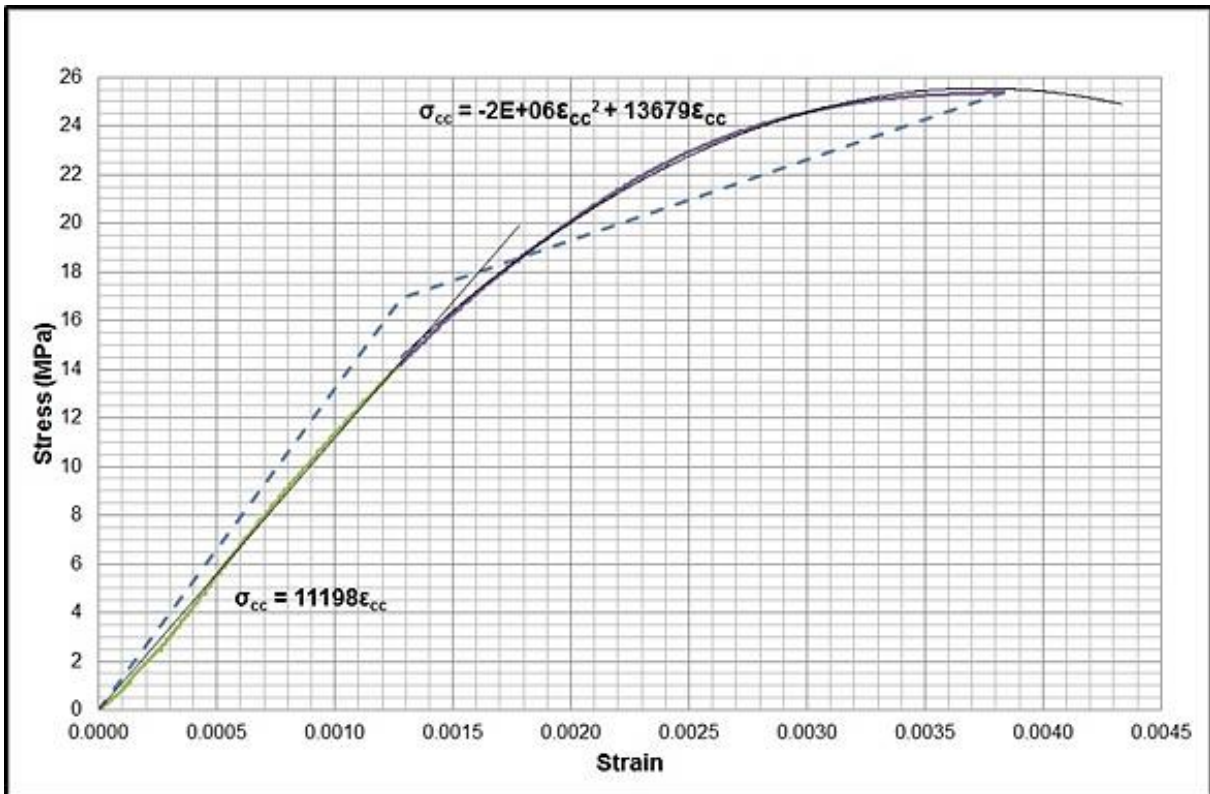


Figure 2-8: Compression Stress and Strain Response showing the change from elastic to inelastic response.

The average stress value of the cutting point was found to be 0.533 of the ultimate stress, for the data considered here. The stress value assumed by Li et al. [44], of 0.667 of the ultimate stress is considerably higher, resulting in the un-conservative stiffness estimate. This relates to Equation 2-6 below

$$E = \frac{0.533\sigma_{cu}}{0.317\epsilon_{cu}} \tag{2-6}$$

When this new approach is followed and the resulting approximation line plotted on the same graphs that were used in Figures 2-8 and 2-9, the results are given in Figures 2-10 and 2-11.

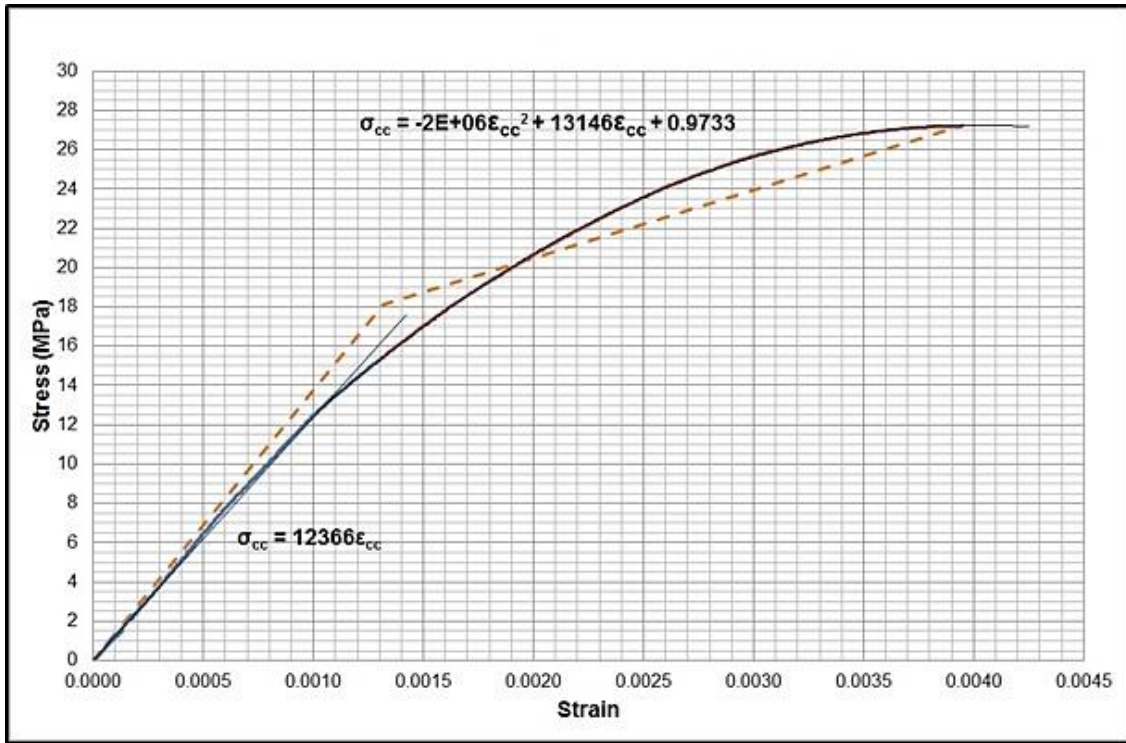


Figure 2-9: Compression Stress and Strain relationship showing the change from elastic to plastic response (2)

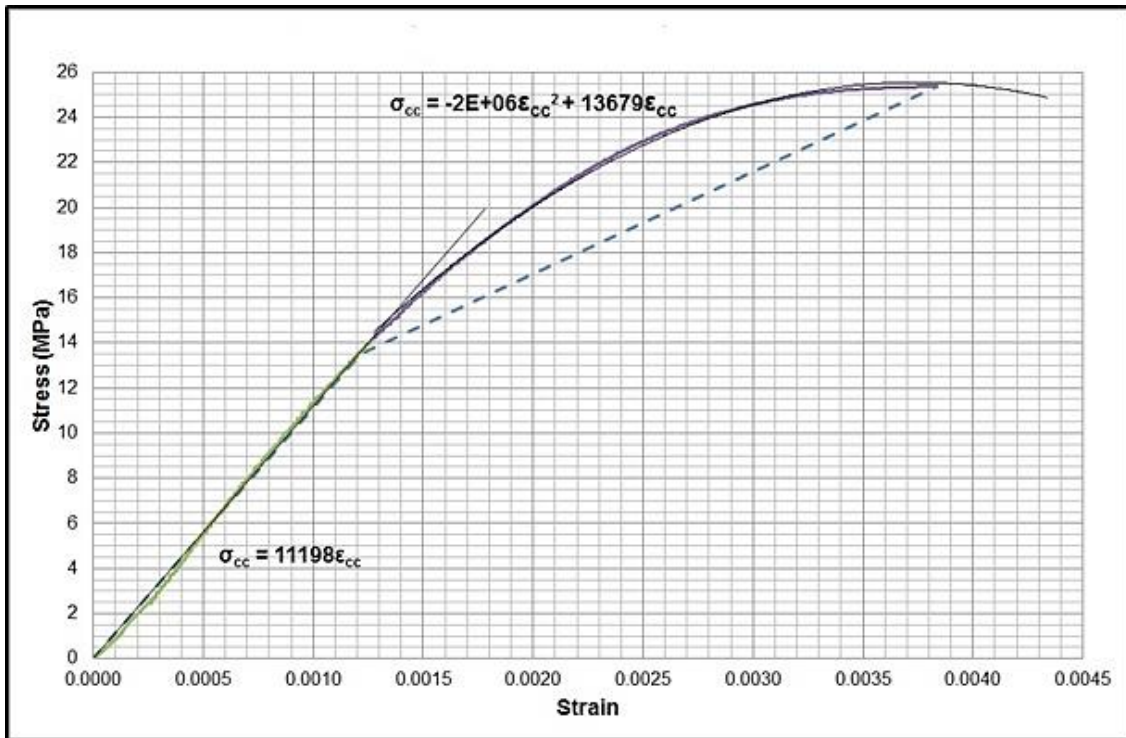


Figure 2-10: Compression Stress and Strain Relationship with adjusted approximation

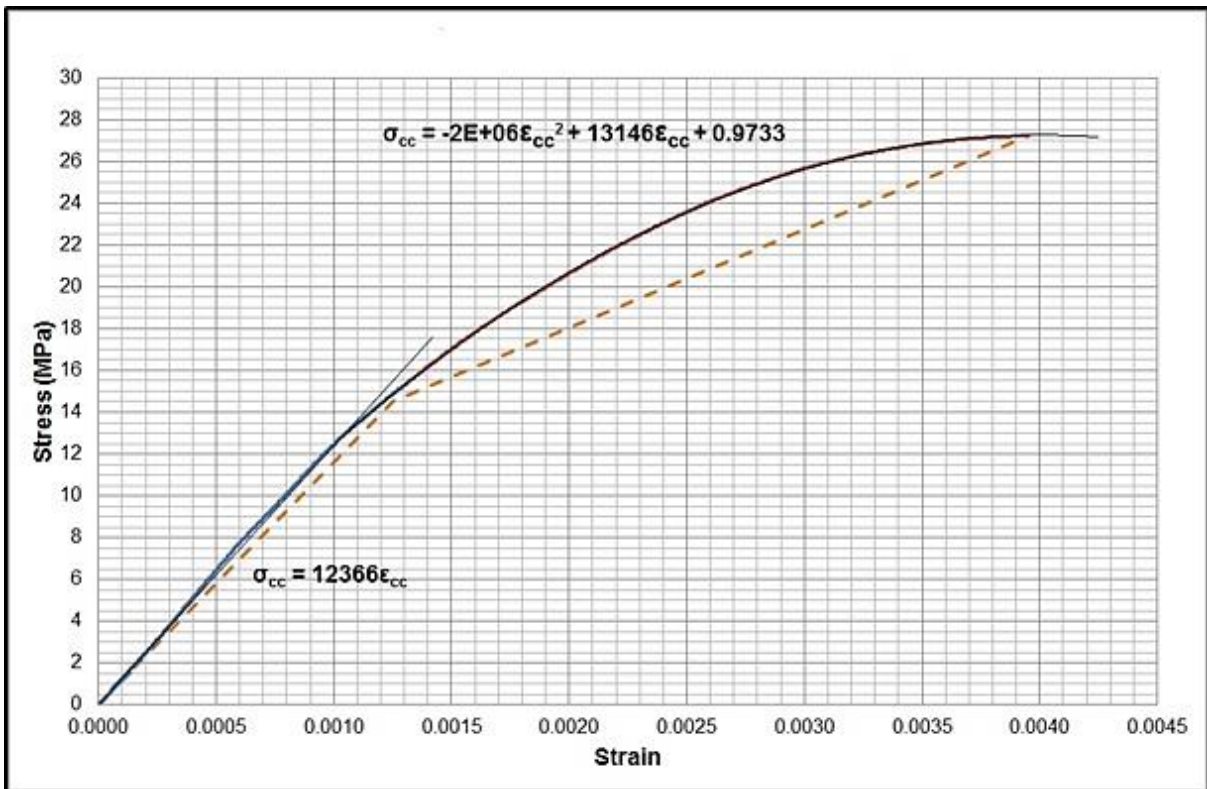


Figure 2-11: Compression Stress and Strain relationship with adjusted approximation (2)

2.2.4 Critical Parameters

The first points of interest on the compression response are the maximum stress and strain of the material under compression, and are called the ultimate compressive stress, σ_{ccu} , and ultimate compressive strain, ϵ_{ccu} . As shown in Figure 2-12, the compression model was simplified into a bi-linear approximation instead of trying to fit the rather complicated curve into the analysis model.

The above mentioned assumptions are reasonable for the materials tested. These materials included different volume fractions of fibres as well as different aggregate sizes, but were all designed to be strain hardening. These assumptions have, however, not been tested on an ultra-high performance strain hardening composite, with compressive strengths over 80MPa. Concrete materials with higher compressive strengths tend to be more brittle than those with lower compressive strengths.

In order to find an analytical solution to this problem, more data of different mix designs and different compression strengths are needed.

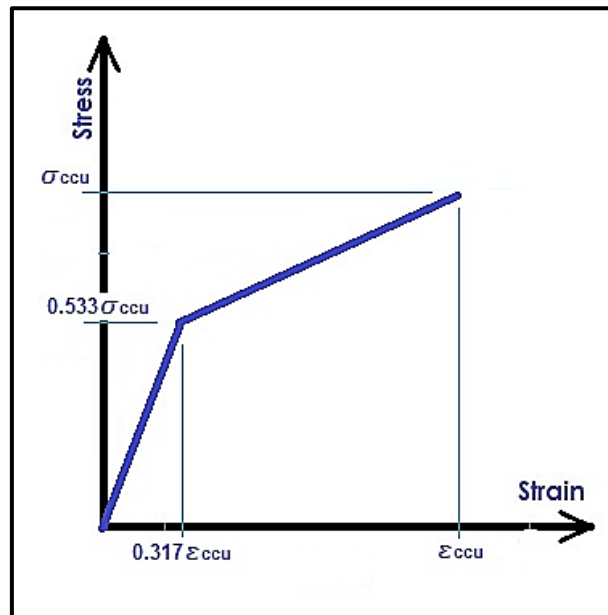


Figure 2-12: Simplified compression stress-strain relationship

2.3 Conclusion

Both the tensile and compressive behaviours of SHCC are complex and difficult to model. In order to simplify the process, a bi-linear approach was adopted in both cases. Quantifying the tensile response requires the definition of the first cracking stress and strain as well as the ultimate stress and strain. For the compression response, only the ultimate stress and strain is needed since the stress-state point marking the onset of inelastic response is expressed as fractions of the ultimate stress-strain pair.

3. TESTING AND VERIFICATION OF THE MODEL

3.1 Critical Parameters

3.1.1 Performance Function

In order to do a reliability analysis on the base design model, it is necessary to define the performance function. The performance function is defined as the applied load subtracted from the resistance and should be positive, indicating a level of safety, but no less than zero. In this case, the performance function is defined as follows:

$$P(f) = M_r - M_u$$

$$P(f) =$$

$$\frac{\varepsilon_{ct2} \left[\frac{1}{6} E_{cc} b x^3 (2\gamma^3 + 3\gamma(1-\gamma)(\gamma+1) + \delta(1-\gamma)^2(\gamma+2)) + \frac{1}{6} E_{ct} b (h-x)^3 (2\beta^3 + 3\beta(1-\beta)(\beta+1) + \alpha(1-\beta)^2(\beta+2)) + E_s (A_s (x-d)^2 + A_s (d-x)^2) \right]}{(h-x)}$$

$$\frac{PL}{4}$$

3-1

Equation 3-1 is based on the base design model, derived in Chapter 4 of this dissertation.

3.1.2 Sensitivity to critical parameters

In order to determine the critical parameters of the performance function, the sensitivity of the model with respect to its defining parameters is needed. Determining the sensitivity involves finding the partial derivative of the performance function with regard to the specific parameter under consideration. This gives the deterministic sensitivity of the model to the specific parameter. The second part of the sensitivity analysis is the statistical sensitivity, which can be represented by the standard deviation of the specific parameter. These two values must be multiplied in order to find the model's sensitivity toward this parameter [46].

As can be seen from Equation 3-1, the parameters used in the model are not base material characteristics, but rather functions of base material properties. This means that it is not possible to find the partial derivative of the resisting moment function with regard to a base material property. An alternate estimate for the deterministic sensitivity is needed. The whole model was thus taken and the base material properties increased by 10% in turn. The difference this increase made to the resistance was noted in each case. This difference in value was then used as the deterministic sensitivity of the model towards this specific material property. This could then be multiplied with the standard deviation of this material property, which was determined in the statistical analysis of the material's response to tension and compression. These values are shown in Table 3-1.

Table 3-1: Model Sensitivity

Material Property	Difference in M_r (%)	Standard deviation of material property	Model Sensitivity
ϵ_{ct1}	0.004	0.395	0.00158
σ_{ct1}	0.438	0.183	0.08015
ϵ_{ctu}	0.021	0.263	0.00552
σ_{ctu}	0.076	0.090	0.00684
ϵ_{ccu}	2.603	0.215	0.55965
σ_{ccu}	2.235	0.079	0.17657

It seems that the model is most sensitive to the compression characteristics of the material. Only the ultimate compression characteristics are used to determine the various compression elements needed for the design model. Thus there are only two material parameters involved in profiling the compressive behaviour of the element, the ultimate compressive stress and the ultimate compressive strain. It can be expected that the model will be quite sensitive to changes in said parameters.

For the part of the section of the element in tension there are four parameters used to describe the tensile behaviour of the element in bending. These are the stress and strain at first cracking, or yield stress and strain, as well as the ultimate tensile stress and the ultimate tensile strain. The yield stress and strain is used to calculate the elasticity modulus as well as the parameter α , which defines the slope of the strain hardening leg of the tensile stress – strain graph. The tensile yield strain is also used in determining the value of β , and so it would have been thought that the model would also be very sensitive to this parameter. It is, however, the least sensitive of all. That might be explained by the fact that the parameter β , is mostly constant in the third phase of the model and also very small, compared to the distance to the neutral axis or the amount of reinforcing, while α is a material property. The yield stress and strain has large standard deviations due to the difficulty in measuring these values from tests.

The standard deviation for the tensile strain values is relatively high. This phenomenon was seen in all the specimens that were tested during this study. These tests are described in the next part of this chapter. The stress values are fairly constant but the strain values vary considerably. An example is the tensile tests done along with the second set of beams. The ultimate tensile strength varies between 2.85MPa and 4.12MPa while the ultimate strain varies between 0.002 and 0.06.

3.2 Test Program

3.2.1 General

Two sets of six beams each were tested. In order to make the tests more realistic and avoid having the size effect impair the results, the test specimens were constructed to a realistic size. This meant that the experiments were quite expensive and time consuming, and so the number of tests was limited.

For each beam, a set of tensile and compressive tests were performed, in order to determine the material properties for the each specimen tested. These properties were needed as input for the model to be able to predict the response of the beam accurately. Due to limitations on the amount of moulds available for the casting of these material specimens, there were only 3 tensile specimens and 3 compressive specimens made for each beam.

The beams were designed to have both compression and tensile reinforcement as well as shear links. The shear behaviour of these elements does not form part of this study, but shear links were included to ensure that the beams failed in flexure and not in shear. It also improved the handling of the steel cages.

3.2.2 Mixing and Casting

For the first set of beams, the concrete was mixed in five batches for each beam due to the limited mixer capacity of 27 litres SHCC. The mixing time was set to 7 minutes, during which an ingredient was added roughly every minute, starting with the dry ingredients excluding the fibres, which were added last. The concrete was then carried with buckets and poured into the specially built, waterproofed, wooden formwork. After every three buckets, the concrete was compacted with a vibrating poker.

For the second set of beams, a beam and its tensile and compressive tests could be cast from one batch as the beam sizes were smaller, 200x200x2800 instead of 300x300x3000, than the first set. This was more ideal as the same mixture was used for all the tests as well as for the beam, which was not possible for the first set of beams as the volume of concrete was too much for the mixer. The mixing time was increased on these specimens as there were lumps of fibre found in the first set of beams. The mixing time was not specified but the concrete was mixed until there were no more lumps found in the mixer when testing it by hand. The casting was done in the same manner as before and the concrete was again compacted with a poker vibrator.

At first there were a few problems. Some leakage was experienced during the pouring of the first beam. This resulted in the first beams compaction being slightly less than the rest. This problem was

corrected on the following specimens by sealing the seams of the formwork with duct tape prior to applying the oil. The following beams were cast without any further problems of this nature.

The material tests made for the tensile and compression testing were cured in water for 28 days, as is the norm, while the beams were cured by covering them under wet sacking for 28 days. On site, columns are wrapped in plastic to retain as much as possible of their moisture for the curing process. Beams and slabs, however, are sprinkled with water every day. Depending on the weather and the contractor, the sprinkling sometimes happens twice daily.

3.2.3 Testing

The beams were all tested on 28 days, or as close as possible to that age. It was never more than 2 days over the 28 day limit and never under 27 days. For testing, a beam was supported at each end on a concrete block. A rubber bearing was placed between the beam and the support to prevent crushing of the support against the beam, or vice versa.

A hydraulic Instron Materials Testing Machine (MTM) of 500kN capacity was used to apply the point load in the centre of the beam specimen. The test was deflection controlled and the jack was set to push down at a speed of 10mm per minute. The jack has a maximum travel of 100mm and as that was not enough to get the specimens with the higher reinforcement content to fail, the tests were done in up to three stages. The aim was to get as complete as possible a flexural load-deflection curve for each specimen.

The deflection was measured by four LVDT's connected to a computer via an analogue to digital signal converter. They measured the relative movement in four different places on the beam, which could then be used to determine the true deflected shape of the specimen. They were positioned on the ends of the specimen, as close as possible to the support, as well as in the middle, as close as possible to the load. They could, however, not be positioned in the centre of the beam as the jack applying the load was in the way. This meant that the actual middle deflection had to be calculated using a polynomial equation of the third order. Figure 3-1 shows a photograph of the test setup.

All the test specimens were painted with lime in order to make the cracks in the surface clearer. However, for the first set, the cracks were counted and tracked manually while the beam was loaded. This proved a very difficult task and as soon as the load was lifted, because the testing machine has reached its deflection limit, some of the cracks closed up again. The cracks were not marked during the test, only measured visually. At the second set of tests, a video camera was used to film the test. The idea was that the video could be used to track the cracks in the beam as they form. However, because of the size of the beams, the video camera could not be placed in close proximity to the beam as this would have made it impossible to capture the length of the beam on the video. The

idea was that the video could afterwards be enlarged to see where and when the cracks formed. As the cracks forming in SHCC are as small as 0.1mm, it was near impossible to see when and where the first crack formed and how the cracking progressed. The picture resolution was not of a high enough standard to enable enlarging of the picture to a scale where the cracks would be clearly visible and measurable.



Figure 3-1: Beam testing Setup

The video did, however, give a very good record of the test. This was used to analyse the behaviour of the beam and also to establish what cracking could be seen in the specimens. It was found that when the beam was at its serviceability limit, no cracks could be seen on the video.

3.3 Minimizing Sources of Uncertainty

In order to minimize the uncertainty of the material parameters, tensile tests as well as compression tests were done on specimens cast from the same batch as the beam specimens. The results of these tests can be found in Tables 3-2, 3-3, 3-4. The size of the beams were also a way of minimizing the uncertainty. The size effect is well-studied in concrete, but not yet in SHCC, which means that it is an unknown. For this reason, it was opted to use beams of reasonable size, to be relevant to in-field applications.

Table 3-2: Cube Test Results

Tests specimen		Age at testing (days)	Weight (kg)	Dimensions (mmxmm)	Crushing Strength (MPa)	
Beam 1a,b (1 st set of tests)	1	28	1.71	98x100	21.122	22.485
	2	28	1.72	99x100	23.232	
	3	28	1.75	100x100	23.100	
Beam 2a,b (1 st set of tests)	1	28	1.66	100x100	20.000	21.733
	2	28	1.76	100x100	22.100	
	3	28	1.78	100x100	23.100	
Beam 3a,b (1 st set of tests)	1	28	1.74	100x100	22.400	22.691
	2	28	1.75	100x100	22.000	
	3	28	1.75	98x100	23.673	
Beam 1a (2 nd set of tests)	1	30	1.974	100x100	43.600	45.067
	2	30	2.005	100x100	49.800	
	3	30	2.023	100x100	41.800	
Beam 1b (2 nd set of tests)	1	31	1.966	100x100	41.000	44.200
	2	31	1.938	100x100	43.800	
	3	31	1.96	100x100	47.800	
Beam 2a (2 nd set of tests)	1	27	1.949	100x100	41.000	40.900
	2	27	1.978	100x100	40.700	
	3	27	1.949	100x100	41.000	
Beam 2b (2 nd set of tests)	1	27	1.959	100x100	40.600	41.367
	2	27	1.942	100x100	41.700	
	3	27	1.991	100x100	41.800	
Beam 3a (2 nd set of tests)	1	29	1.956	100x100	41.900	40.067
	2	29	1.945	100x100	38.300	
	3	29	1.962	100x100	40.000	
Beam 3b (2 nd set of tests)	1	29	1.974	100x100	51.400	45.767
	2	29	2.011	100x100	42.500	
	30	29	1.968	100x100	43.400	

Table 3-3: Concrete Cylinder test results - Second set of tests only

Test specimen	Height (mm)	Diameter (mm)	Age at testing (days)	Ultimate Strength (MPa)	Ultimate Strain	Elasticity Modulus (GPa)
Beam 1a	97.5	51	31	35.18	0.0033	17.924
Beam 1b	96.3	51	31	33.08	0.0018	30.900
Beam 2a	99.5	51	27	26.83	0.0083	5.435
Beam 2b	101	51.2	29	29.57	0.0051	9.749
Beam 3a	101	50.8	29	30.91	0.0029	17.921
Beam 3b	100	51.2	29	28.19	0.005	9.480

Table 3-4: Tensile test results

Test Specimen	Thickness (mm)	Width (mm)	Age (days)	Yield Stress (MPa)	Yield Strain	Elasticity Modulus (GPa)	Ultimate Stress (MPa)	Ultimate strain	
Beam 1 (1 st set of tests)	1	17	30	31	2.69	0.00624	0.431	3.44	0.025
	3	17	30	31	2.22	0.00547	0.406	3.03	0.026
	5	16	30	31	2.40	0.00355	0.676	3.37	0.02
	8	17	30	31	2.47	0.00458	0.539	3.02	0.014
	9	16	30	31	3.06	0.00571	0.536	3.42	0.008
Beam 2 (1 st set of tests)	1	16	30	28	2.86	0.00579	0.494	3.34	0.011
	2	17	30	28	3.14	0.00458	0.686	3.89	0.024
	4	16	30	28	2.83	0.00324	0.873	4.08	0.02
	5	16	30	28	3.9	0.00325	1.200	3.94	0.021
Beam 3 (1 st set of tests)	1	16	30	28	3.28	0.00193	1.699	3.45	0.019
	2	17	30	28	2.29	0.00255	0.898	3.44	0.048
	5	16	30	28	3.23	0.00285	1.133	3.65	0.060
	6	16	30	28	3.08	0.00274	1.124	4.12	0.032
Beam 4 (1 st set of tests)	1	16	30	28	3.58	0.00381	0.940	3.72	0.024
	2	17	31	28	2.95	0.00356	0.829	3.09	0.024
	3	18	30	28	3.23	0.00381	0.848	3.64	0.018
	4	18	31	28	2.37	0.00216	1.097	3.89	0.026
	5	17	30	28	2.23	0.00216	1.032	3.51	0.021

Beam 5 (1 st set of tests)	2	17	30	28	2.4	0.0001	24.000	3.22	0.012
	3	17	32	28	2.62	0.00014	18.714	3.35	0.017
	4	17	31	28	2.93	0.00016	18.313	3.22	0.007
	5	17	31	28	2.5	0.00015	16.667	3.61	0.039
	6	18	30	28	2.17	0.00068	3.191	3.2	0.029
Beam 6 (1 st set of	1	17	30	33	2.86	0.00009	31.777	2.87	0.002
	3	16	30	33	1.66	0.00018	9.222	2.85	0.005
	4	17	30	33	2.5	0.00107	2.336	3.08	0.017
Beam 1a (2 nd set of tests)	1	16.7	29.5	28	2.51	0.00026	9.654	3.78	0.006
	2	17	30	28	3.12	0.00011	28.363	3.78	0.006
	3	16	30	28	2.40	0.00063	3.809	3.95	0.007
	4	17.5	30.5	28	1.72	0.00017	10.118	3.27	0.004
	5	16.5	29.75	28	2.24	0.00014	16.000	3.79	0.012
	6	16.2	30	28	3.27	0.00019	17.210	4.44	0.01
Beam 2a (2 nd set of	1	17	30	27	4.4	0.00075	5.866	4.99	0.04
	4	16	30	27	3.83	0.00016	23.938	4.96	0.003
	6	18	31	27	2.72	0.00011	24.727	3.99	0.014
Beam 2b (2 nd set of	1	17	31	27	2.5	0.00026	9.615	4.32	0.013
	3	17	31	27	3.29	0.00119	2.765	3.56	0.017
	5	17	32	27	2.5	0.00012	20.833	3.62	0.014
Beam 3a (2 nd set of tests)	1	17	30.2	28	1.1	0.00013	8.462	3.41	0.005
	2	17	30.2	28	2.4	0.00059	4.068	3.68	0.018
	3	17	31.8	28	0.81	0.00031	2.613	4.04	0.01
	4	17	31.5	28	0.75	0.00006	12.5	3.2	0.01
	5	16.2	30	28	1.76	0.00021	8.381	3.14	0.006
	6	17	30	28	0.68	0.0001	6.8	3.07	0.01
Beam 3b (2 nd set of tests)	1	18	30	28	2.76	0.00005	55.2	4.22	0.005
	2	19	30	28	2.55	0.00023	11.087	3.12	0.003
	3	18	30	28	2.9	0.00013	22.308	4.43	0.007
	4	17.8	29.8	28	0.7	0.00015	4.667	3.38	0.005
	5	17.2	30.2	28	1.36	0.00016	8.500	4.01	0.019
	6	17.8	30	28	1.0	0.00015	6.667	2.93	0.004

3.4 Model Predictions

3.4.1 First Set of Tests

The flexural members to be tested are described in the next table. For each flexural member, a set of tensile and compressive test samples were also made in order to minimise uncertainties in the calibration of the base design model.

Table 3-5: Test Specimen Details

Parameters	Beam 1		Beam 2		Beam 3	
	1a	1b	2a	2b	3a	3b
Length (m)	3.0	3.0	3.0	3.0	3.0	3.4
Width (m)	0.3	0.325	0.3	0.295	0.31	0.302
Height (m)	0.28	0.28	0.275	0.275	0.28	0.275
A_s	2Y10		3Y20		2Y32+1Y16	
A_s'	2Y10		2Y10		2Y10	
Shear	R8@300mmc/c		R8@300mmc/c		R8@300mmc/c	
Test age	28 days		28 days		28 days	

The mix design for the first set of tests is shown in Table 3-6. Take note that the Y grade reinforcing has a yield strength of 450MPa, while the R grade has a yield strength of 250MPa.

Table 3-6: Mix design for both test sets

Material	Mass (kg/m ³)
CEM I 42.5	550
Fly Ash: Durapozz	650
Water	395
Agg: Console no 2	550
Fibre: PVA-Recs 15, 12mm	26
Chryso Premia	2.2
VMA	0.413

All beams showed similar flexural behaviour. During the first cycle of the press, the specimens reached and passed the first cracking strength of the specimen and so entered the tensile strain hardening zone. When the load was removed, there was a very definite elastic rebound on the deflection of the beam, but not a complete recovery.

The second cycle sometimes pushed the specimen over the ultimate strength limit, causing cracks in or near the middle of the beam to open up. All, except beams 1a and b showed buckling of the compressive steel. This happened because the stirrups were too widely spaced for the diameter of the compressive steel used in the specimen. The aim was not to test shear links and therefore the links were kept to a very minimum and in so doing they were spaced out too far. This was a mistake as when the compressive steel failed, it kinked either to the side or to the top of the specimen, breaking off the concrete cover. This then eliminated the compressive steel from the equation as it had no bond anymore with the concrete. However, this only happened after crack localization and thus tensile failure of the beam. This problem was rectified in the second set of tests where the shear link spacing was decreased when the diameter of the compressive reinforcement was small.

During the last cycle, the tensile steel ruptured in beams 1a and b. The tensile reinforcement in beams 2 and 3 could not be ruptured.

It was found that the concrete had lumps of fibres in places. This was the situation in all the specimens and could also be the reason for the easy spalling of the cover when the compressive steel failed. It was decided that the mixing of the concrete needed attention and the mixing time should possibly be lengthened for the next set of tests. This was done and the lumps of fibre were not found in the second set of tests.

The following graphs show the load versus deflection curves for the six specimens as well as the model predicted curves for each. The first graph, Figure 3-2, shows Beams 1a and 1b. Beam 1a was only put through one cycle of the press as by the end of that, one of the tensile bars had ruptured. This happened after crack localization.

Beam 1b was put through two cycles to overcome the limiting MTM stroke. It did not reach as high a load as did Beam 1a, however, the first tensile bar ruptured at a deflection twice as high as that of Beam 1a. The load at this point was roughly the same.

It is strange that two beams with almost identical physical parameters should behave so differently when tested under the exact same conditions. It was found that Beam 1a did not show a wide spread of cracks as is characteristic of this material. It started cracking in the middle and after only a few cracks along the length had formed, the first crack in the centre of the span of the beam started

opening and opened up almost to the top of the beam. It was investigated if the beam was loaded asymmetrically to have the one tensile bar snap but not the other. It was found that the side where the tensile bar stayed intact showed concrete delamination along the length of the bar. The delamination would have been assisted by the fact that the concrete showed signs of segregation, in the form of fibre lumps. The fibres were possibly not distributed evenly through the mixture and so there were weak spots in the material. The other side had no signs of delamination. This could be the reason for the one side snapping and not the other. The compressive steel in this specimen did not fail and there were no shear cracks found on the sides of the beam.

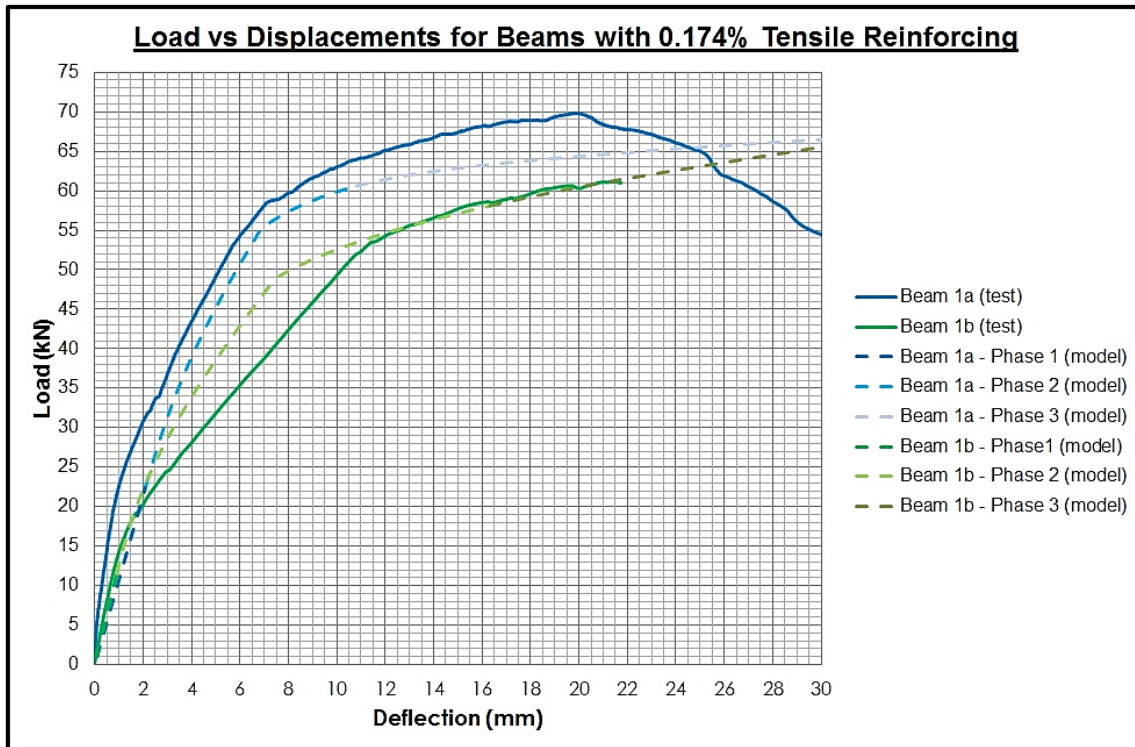


Figure 3-2: Beam 1a,b - Test results and model Predictions

Beam 1b showed similar flexural behaviour than Beam 1a. This is again due to the segregation found in the concrete.

Figure 3-3 shows the test results of Beams 2a and b compared to the model predictions of beams with similar characteristics. The two specimens showed very similar results in that the maximum loads are very close and roughly reached at the same deflection.

During the first cycle of the press, beam 2a started showing tensile cracks and crack localization. Just after crack localization was observed, the compressive steel failed and cracks were noticed on the sides and top of the specimen. It was clear that the beams had buckled after the compression reinforcement kinked. A similar observation was made with Beam 2b. Both specimens showed multiple tensile cracks along the length of the member before crack localization.

Beams 3a and b were reinforced with 2.01% tensile reinforcement and 0.174% compressive reinforcement. The shear links were the same as for the other four specimens. It is clear from the graph that these beams did not fail in bending as was the intention. After crack localization, the compressive steel failed, kinking to the top and side, pushing the concrete cover off. This again eliminated the compression reinforcing from the design equation and the beams failed in a mixture of shear and bending.

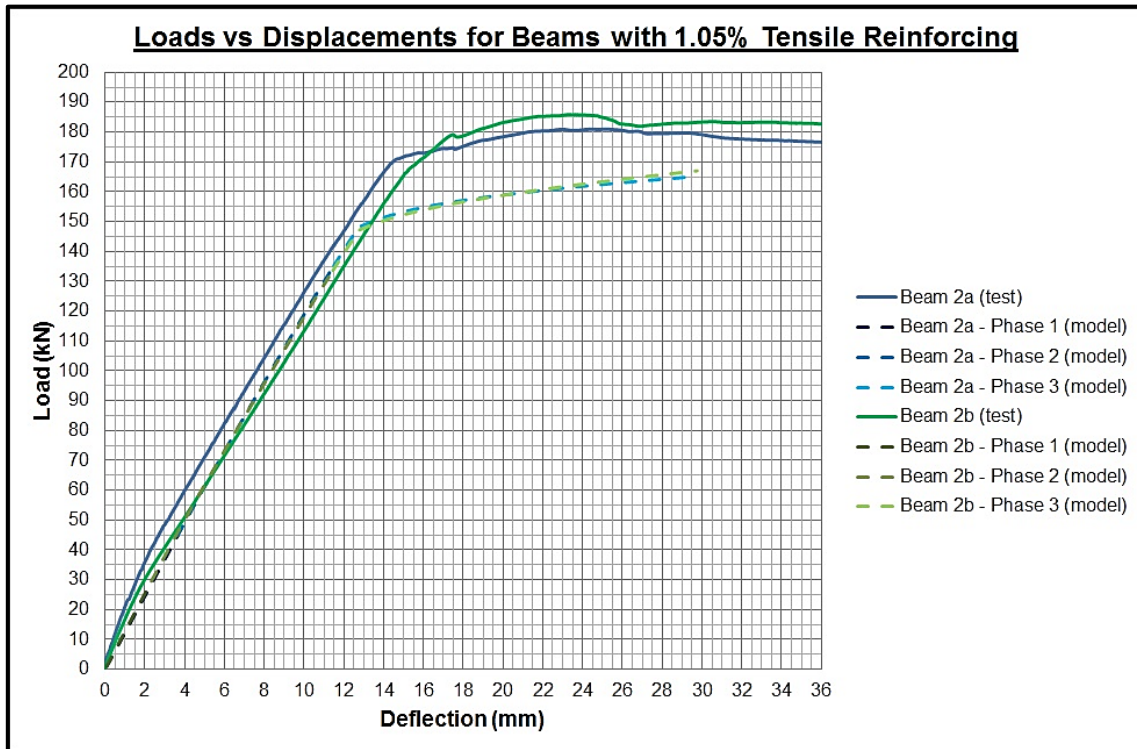


Figure 3-3: Beam 2a,b - Test Results and Model Predictions

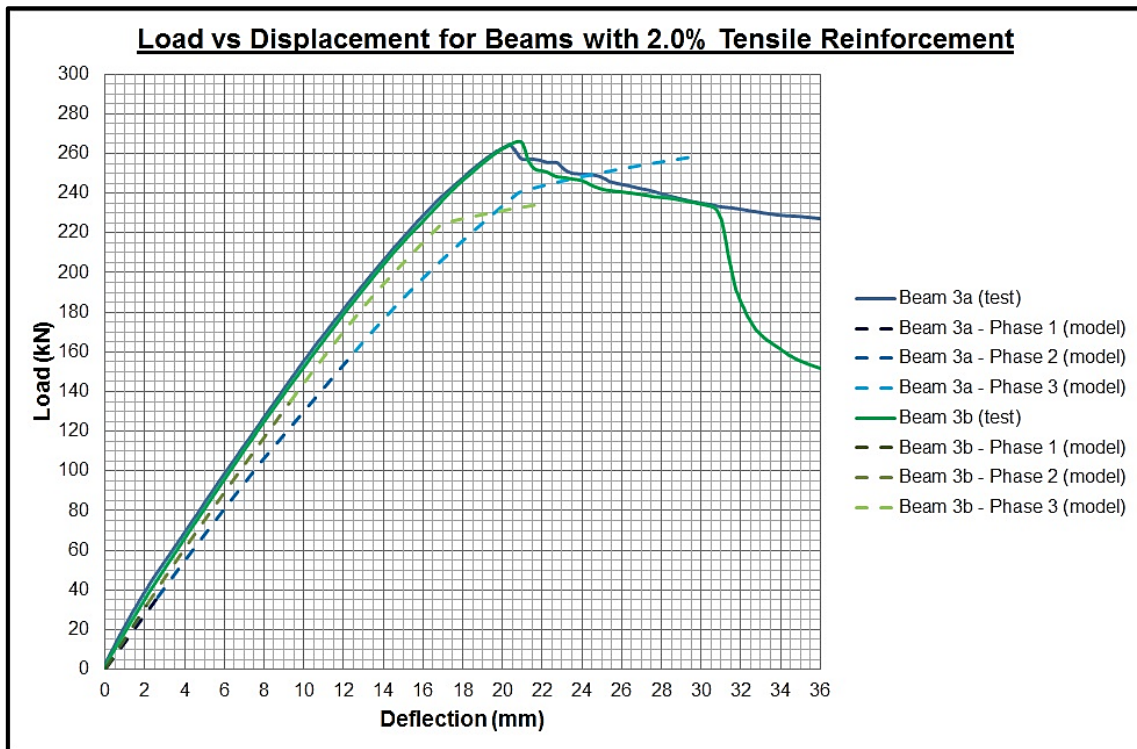


Figure 3-4: Beam 3a,b - Test Results and Model Predictions

3.4.2 Second Set of Tests

These test specimens behaved in much the same way as the first specimens had done, with the exception that there was no failing of the compressive steel this time. It was, however, noticeable that there were fewer cracks in these specimens than what were found in the previous set. This was unexpected as the concrete was mixed until no lumps were evident in the mixture to ensure that there will not be segregation as was found in the first set of tests. This trend was, however, also seen in the material tests. The specimens seemed to be more brittle than the previous set and wide spread micro cracking did not occur as was expected. The test parameters are shown in Table 3-7.

Table 3-7: Test specimen details

Parameters	Beam 1		Beam 2		Beam 3	
	1a	1b	2a	2b	3a	3b
Length (m)	2.805	2.83	2.795	2.805	2.83	2.828
Width (m)	0.205	0.205	0.205	0.200	0.203	0.205
Height (m)	0.207	0.20	0.197	0.193	0.210	0.198
A_s	2Y10		3Y20		3Y20	
A_s'	2Y10		2Y10		2Y16	
Shear	R8@150mmc/c		R8@150mmc/c		R8@250mmc/c	
Test age	28 days		28 days		28 days	

The mix design for the second set of test was the same as for the first set and can be seen in Table 3-6.

The following graphs show the load versus deflection curves for the six specimens as well as the predicted curves for each. The first graph, Figure 3-5, shows Beams 1a and 1b.

As can be seen from the graph, the two tests were similar, but not exactly the same, as can be expected due to variability of materials and the geometry of the test specimens. Beam 1a shows less deflection hardening than beam 1b. The model predictions for these two tests seem to be unconservative as the predicted deflections for a specific load is less than what was measured. It seems that there is a difference in the stiffness between the tests done and the predictions calculated which hints at the fact that the calculation of the elasticity modulus for compression and/or tension could be inaccurate. Alternatively the material properties inside the beam are different from the properties of the test specimens, which is also possible if considering that the beam is significantly larger than the test specimen which could influence the compaction and/or the fibre layout in the matrix. For this reason safety factors are applied to material properties for all construction materials.

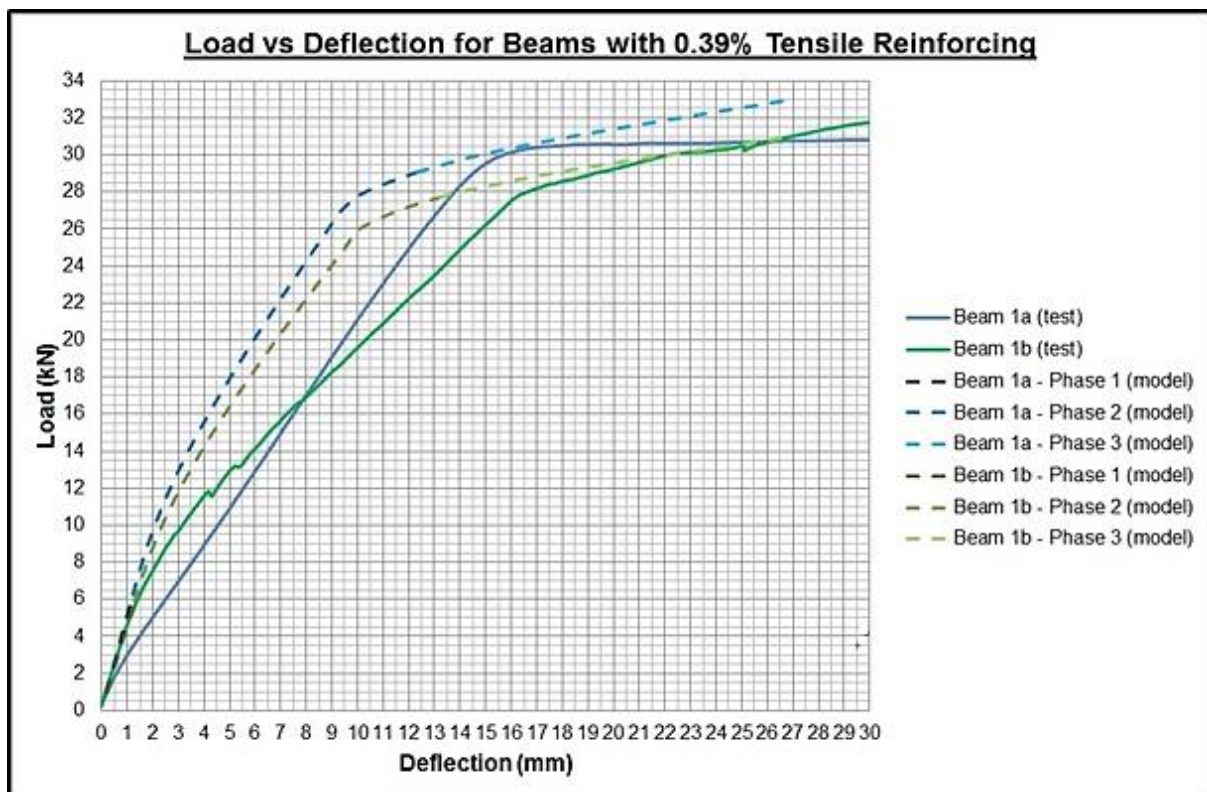


Figure 3-5: Beam 1a,b - Test Results and Model Predictions

The test result shown in Figure 3-6, are those of beams 2a and 2b. Here both the tests and the model predictions are very similar for the two beams and the model predictions are giving conservative results.

The graph in Figure 3-7 shows the test results of beams 3a and 3b compared to the model predictions for these two beams. It seems that once again the model predictions are un-conservative and that there is a difference in the stiffness of the model versus the tests done. It must be noted that these test specimens and beams 2a and 2b, were reinforced with even more tensile reinforcement than Beams 3a and 3b for the first set of tests. As the shear link spacing was reduced for beams 2a and 2b, no compressive steel failure was noted and no shear cracks were observed in either of the beams.

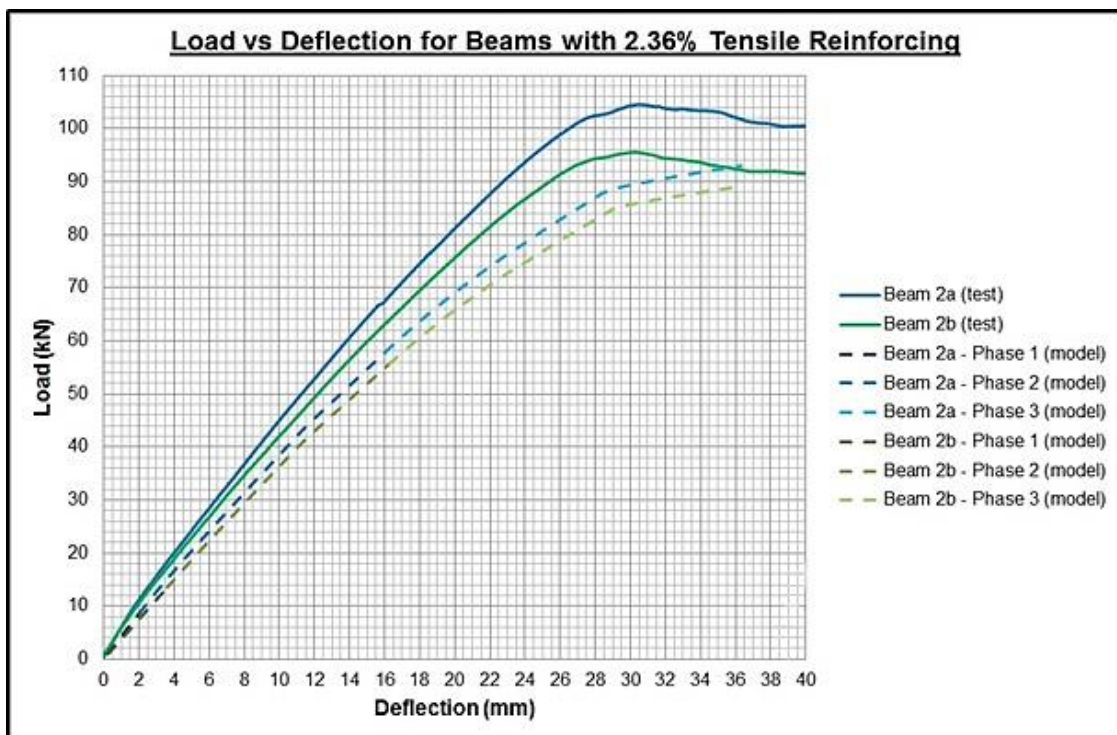


Figure 3-6: Beam 2a,b - Test Results and Model Predictions.

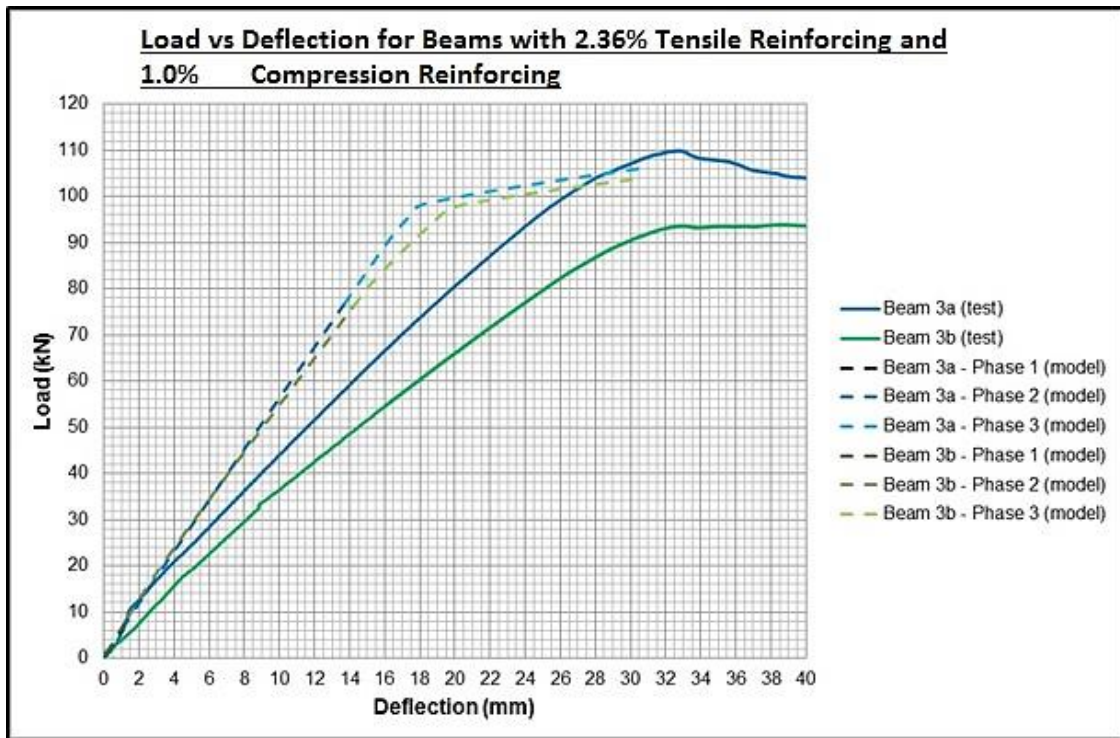


Figure 3-7: Beam 3a,b - Test Results and Model Predictions

3.5 Interpretation of Results

3.5.1 First set of Tests

The model calculates the load versus deflection only to the theoretical point where crack localization occurs. The reason for all this is that the final design equation will have to be limited to within a margin of the maximum tensile stress and strain as this is where the element will fail. Before that happens, however, the beam is bound to have exceeded the serviceability conditions for cracking and deflection.

The model predictions for the first set of tests were conservative and consistently so. The shape of the predicted model and that of the actual tests done were similar, indicating that the assumptions made on the stress and strain values for the different phases of the flexural response is fair. The failure of the compressive reinforcement influenced some of the results.

3.5.2 Second Set of Tests

For the second set of tests, the model predictions were found to be un-conservative in two of the three cases. For Beams 2a and 2b, the predictions were conservative and fairly accurate; similar to what was found for the first set of tests. However, for the other tests, the model was predicting a much less ductile behaviour than what was seen in the tests.

It can be seen that the shape of the predicted response and that of the measured response is still quite similar. Also, the ultimate load predicted shows a good relation with the ultimate load measured from the tests. The deflection, however, was predicted to be much lower than that which was measured. This lower deflection indicates that the stiffness of the test specimen was less than what was assumed in the model. This error can only come from inaccurate material properties for the specific specimens as the model shows good results for the other tests done.

3.6 Conclusion

The model seems to be most sensitive to the compression characteristics of the material used. This development is expected, as only the ultimate compression stress and strain is used to describe all the different compression characteristics.

Two sets of six beams each were tested. The test setup consisted of a simply supported beam loaded with a point load in the centre of the beam. Tensile and compression test specimens were also made for each of the beams in order to minimize the uncertainties in the prediction model. No compression strain values were measured for the first set of tests. Both tests used the same mix design but different approaches were used in the actual mixing of the material.

The first set of tests showed very good correlation with the predicted model values and even the stiffness of the material was closely predicted. The model showed mostly conservative results in this case.

For the second set of tests there seems to have been a slight difference in the stiffness of the actual material versus the stiffness assumed in the model prediction. In some instances the prediction was conservative and in others it was not. This difference is assumed to be due to uncertainties in the elasticity modulus for the material used. Further research into this characteristic of SHCC is needed in order to propose a more accurate model for the elasticity modulus for SHCC.

4. ANALYSIS MODEL

4.1 Description

The design model is based on a simply supported beam loaded with a single point load in the centre of the beam. This configuration was chosen for simplicity of the calculations but also to simplify the testing of the beams. The resisting moment equation should be applicable to all load and support configurations as it is based on an applied moment and a resisting moment.

A simply supported beam loaded in the centre with a single point load shows a sagging moment in the centre of the beam. This is shown in Figure 4-1. The maximum moment is found at the point where the load is applied, and the moment declines linearly to the sides until it reaches zero at the supports. This moment creates tension in the bottom part of the beam and compression in the top part of the beam. The two parts are separated by the neutral axis. Note that the neutral axis shown in Figure 4-1 is for the full elastic response, i.e. phase 1 of tensile and compressive response.

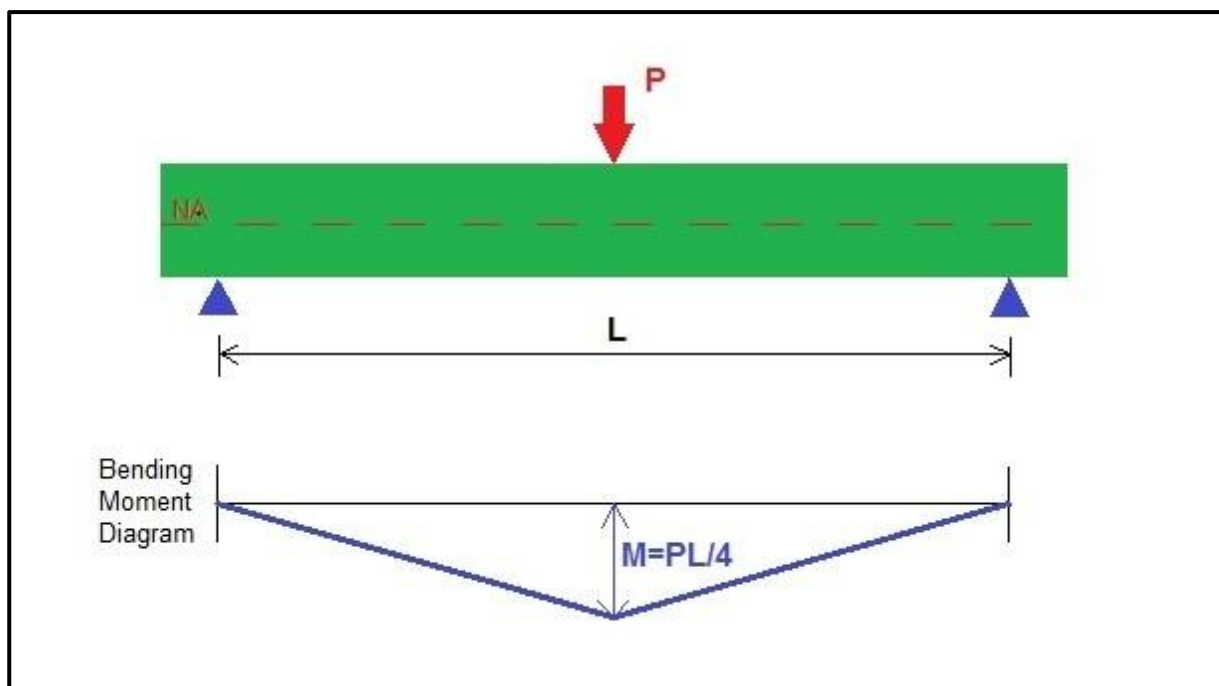


Figure 4-1: Simply supported beam load and moment diagram

The design model is based on a flexural member reinforced with tensile, compression and shear reinforcement, as is typically used in reinforced concrete structures. As is the case for normal reinforced concrete, the shear steel is not incorporated into the flexural design model, but was added to the test specimens to ensure that they do not fail in shear rather than bending, and also to facilitate the placing of the reinforcement cages.

As discussed in Chapter 2, because of the complex nature of the tensile stress-strain curvature, a bilinear approximation is used in the design model to simplify the calculations. The three phases of the tensile response can be clearly identified in Figure 2-4.

The compressive response was also simplified into a bilinear approximation. The actual shape, which is often approximated with a parabolic expression, is too cumbersome to add into the design model and so it was simplified into two straight lines, similar to what was done by Li et al. [44].

From the above approximations a base design model was derived. It was clear that a phased approach to the model calculations would be required as well. The first one represents the elastic phase of the cycle, from load inception until the first cracks form in the tensile zone of the flexural member. During this phase, which may be quite short, the compression and tensile parts of the member are assumed to behave elastically. The theoretical stress development during Phase 1 is shown in Figures 4-2a,b, and c. These figures indicate the stress situation at the start of Phase 1, during Phase 1 and at the end of Phase 1.

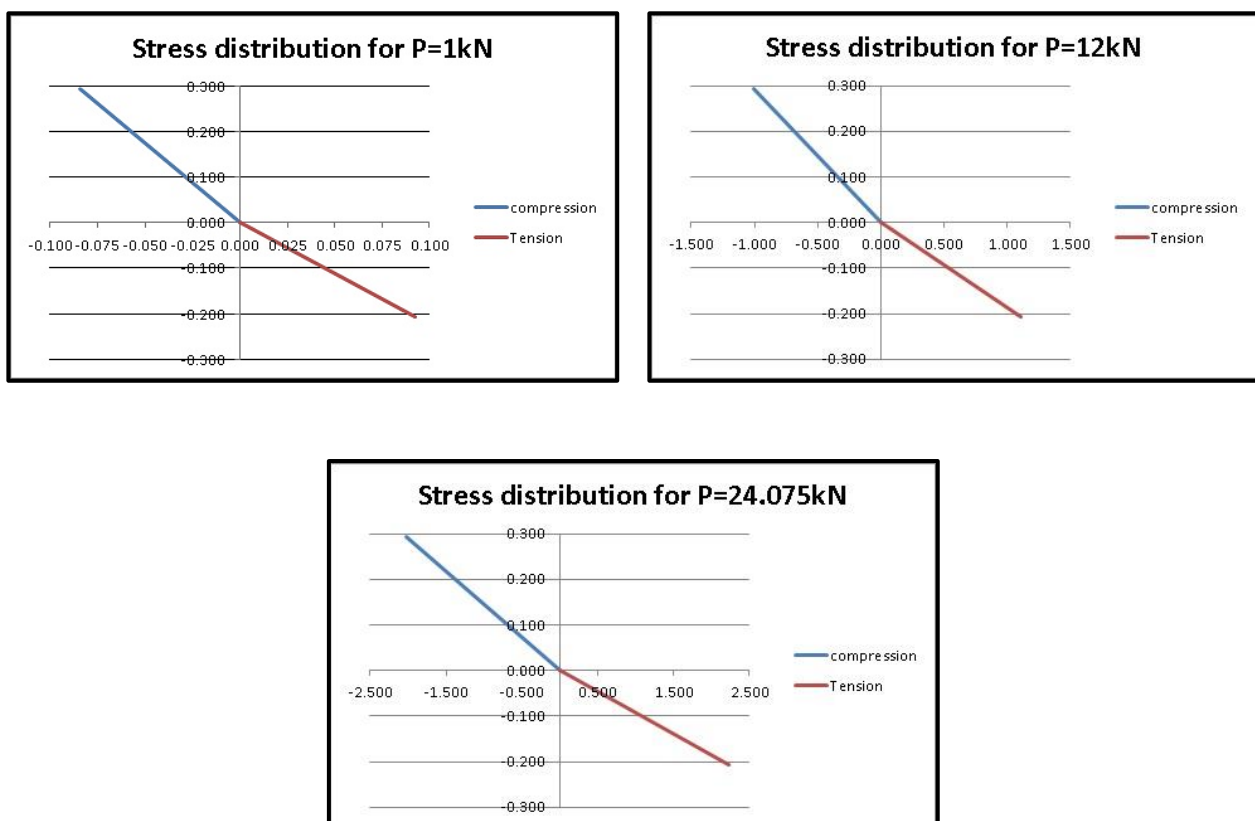


Figure 4-2a,b, and c – Progression of Stress through Phase 1 of Loading

The second phase represents the strain hardening part of the tensile cycle, but assumes that the part of the member in compression is still in its elastic phase. This was done as the first tensile cracking initiates at low strains and it is not sure whether the compressive strain has entered the inelastic phase at this time. This phase might be a material specific response as well and for some materials this second phase might not exist. This could typically happen when the ultimate compression strain for the material in question is low and so the member will either skip phase two entirely and just go straight to phase 3, or will have a very short period in phase 2 before it goes over into phase 3. For the materials tested in this study, the second phase always existed. Figure 4-3a,b, and c shows the stress progression from the start of Phase 2 until the compression strain reaches its imposed elastic limit. The beginning of Phase 2 is shown in Figure 4-2c and is thus not repeated.

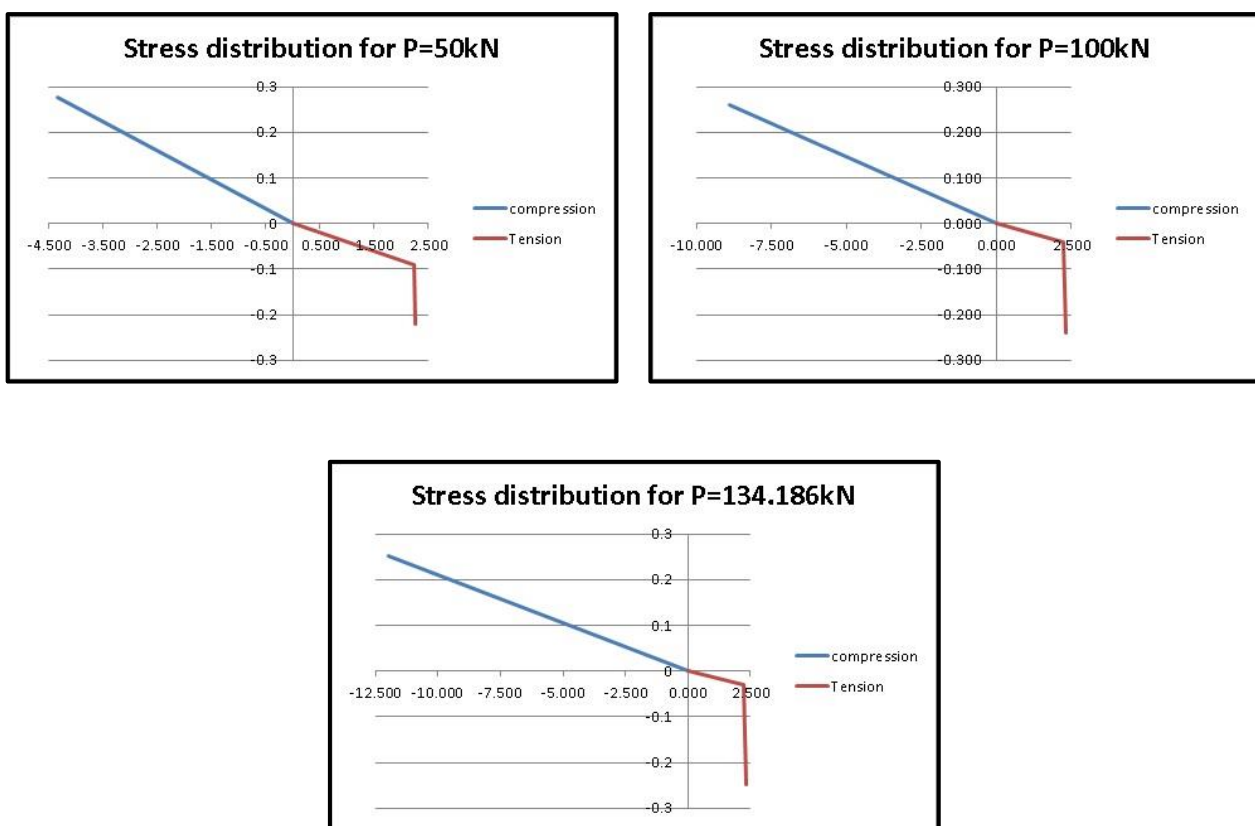


Figure 4-3a,b, and c – Progression of Stress through Phase 2 of Loading

The third and last phase assumes that the tensile part of the beam is still in its strain hardening phase, but that the compressive strain has moved past the imposed limit of $0.317\epsilon_{ccu}$. (This value is discussed in more detail in Chapter 2) This phase ends with the failure of the beam. Failure can be because of tensile crack localization, or compressive crushing, depending on the amount of reinforcement and the material characteristics. Again, this can be material specific. Materials with

very high compressive strengths might fail in tension before this phase is reached. For the purpose of this study, all materials tested comprised of all three phases. Figure 4-4a, and b shows the progression of stress through Phase 3 of loading. The beginning of Phase 3 is shown in Figure 4-3c and is thus not repeated here.

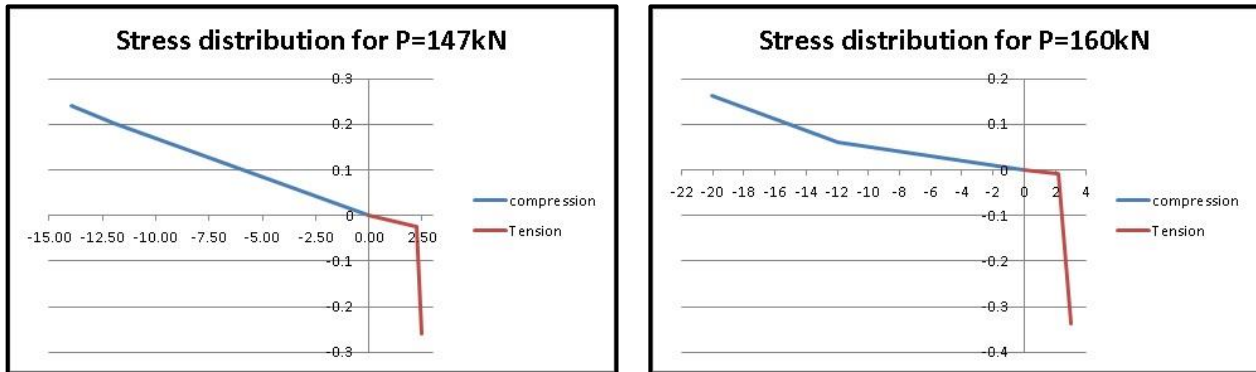


Figure 4-4a, and b - Progression of Stress through Phase 3 of Loading

4.2 Formulation of the model

4.2.1 Phase 1 – Elastic behaviour

During the elastic phase of the model, both the tensile and compression parts of the flexural member are assumed to be in the elastic state. If the load is removed during this phase, it is assumed that the member will recover completely. It is essential that no cracks have yet formed in the beam.

The model is based on sectional analysis which is illustrated in Figure 4-5. The assumption is made that a cross-section remains in a flat plane in the deformed state. This assumption allows the linear strain distribution shown in the figure. A further assumption of a perfect bond between the reinforcement steel and the SHCC matrix is made. This assumption is based on the assumption that the section is in an elastic phase and also on the knowledge that the SHCC matrix and the steel reinforcement have similar ductile behaviour. This enables the composite to act in unison and for the bond to remain intact.

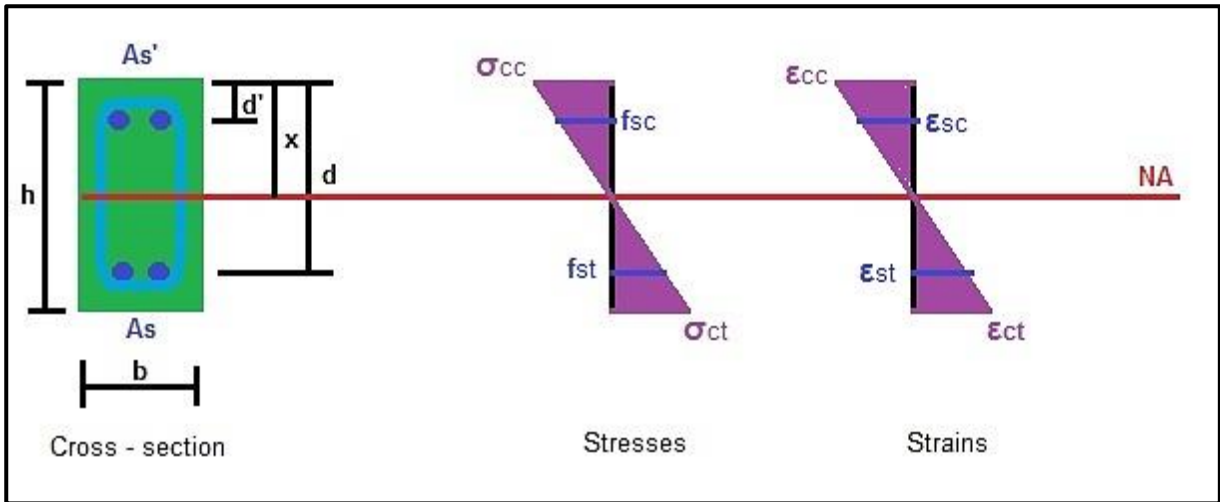


Figure 4-5: Phase 1 - Stress and Strain relationship

The elastic stress-strain responses at points in the beam are considered to be one-dimensional, whereby Poisson effects are neglected. The elastic stress-strain relations for SHCC and reinforcement steel are expressed as follows:

- $\sigma_{cc} = E_{cc}\varepsilon_{cc}$ 4-1
- $f_{sc} = E_s\varepsilon_{sc}$ 4-2
- $f_{st} = E_s\varepsilon_{st}$ 4-3
- $\sigma_{ct} = E_{ct}\varepsilon_{ct}$ 4-4

Where:

- σ_{cc} = SHCC compressive stress
- σ_{ct} = SHCC tensile stress
- f_{sc} = Reinforcement compressive stress
- f_{st} = Reinforcement tensile stress
- E_s = Elasticity modulus for reinforcement steel
- E_{cc} = Elasticity modulus for SHCC in compression
- E_{ct} = Elasticity modulus for SHCC in tension
- ε_{cc} = SHCC compressive strain
- ε_{ct} = SHCC tensile strain
- ε_{sc} = Reinforcement compressive strain
- ε_{st} = Reinforcement tensile strain

It has been discussed in chapter two, 2.1.4 and 2.2.3 that the compressive and tensile elasticity modulus differs slightly. For some materials these values might be almost the same and in other cases the differences are bigger, but to ensure that the model is applicable to all strain hardening materials, it was decided that the elastic moduli should be used in the model calculations as different entities. As the stresses and strains for the compression and tensile responses are also very different, they are also indicated by subscripts rather than simply changing the sign. This eliminates confusion when the calculations become more complex.

From Figure 4-5, the following can be deduced:

$$\varepsilon_{cc} = \frac{-x}{(h-x)} \varepsilon_{ct} \quad 4-5$$

$$\varepsilon_{sc} = \frac{-(x-d')}{(h-x)} \varepsilon_{ct} \quad 4-6$$

And, by assuming that there is no slip between the steel reinforcement and the SHCC:

$$\varepsilon_{st} = \frac{(d-x)}{(h-x)} \varepsilon_{ct} \quad 4-7$$

Where:

- x = The distance to the neutral axis measured from the top of the beam
- h = The total depth of the beam
- d = The distance to the tensile reinforcement, measured from the top of the beam.
- d' = The distance to the compressive reinforcement, measured from the top of the beam.
- b = The width of the beam at this cross section.
- A_s = The area of tensile reinforcement in the member.
- A'_s = The area of compressive reinforcement in the member.

Considering the equilibrium of forces in the cross section, we can derive the following expression:

$$\Sigma F = 0 = \frac{1}{2} \sigma_{cc} b x + A'_s f_{sc} + \frac{1}{2} \sigma_{ct} (h-x) b + f_{st} A_s$$

Substituting Equations 4-1 to 4-4 into the above, leads to:

$$0 = \frac{1}{2} E_{cc} \varepsilon_{cc} b x + E_s A'_s \varepsilon_{sc} + \frac{1}{2} E_{ct} (h-x) b \varepsilon_{ct} + E_s \varepsilon_{st} A_s \quad 4-8$$

Substituting of Equations 4-5 to 4-7, into the Equation 4-8 leads to the expression:

$$0 = -\frac{1}{2}E_{cc}b\frac{x^2}{(h-x)}\varepsilon_{ct} - E_sA'_s\frac{(x-d')}{(h-x)}\varepsilon_{ct} + \frac{1}{2}E_{ct}(h-x)b\varepsilon_{ct} + E_sA_s\frac{(d-x)}{(h-x)} \quad 4-9$$

Multiplying Equation 4-9 with $\frac{(h-x)}{\varepsilon_{ct}}$ produces:

$$0 = -\frac{1}{2}E_{cc}bx^2 - E_sA'_s(x-d') + \frac{1}{2}E_{ct}b(h-x)^2 + E_sA_s(d-x) \quad 4-10$$

Simplifying the above and changing the subject of the expression to x , a quadratic Equation for determining the position of the neutral axis in the member can be found and is given in 4-11.

$$x = \frac{E_{ct}A_c + E_s(A'_s + A_s) - \sqrt{(-E_{ct}A_c - E_s(A'_s + A_s))^2 - (E_{ct}b^2h^2 + 2bE_s(A'_sd' + A_sd))(E_{ct} - E_{cc})}}{b(E_{ct} - E_{cc})} \quad 4-11$$

Where, $A_c = bh$ and denotes the concrete area of the SHCC section.

The stress and strain, both tensile and compressive, at which the first tensile crack appears in the member, represents a transition point in the design model. This point determines the end of the elastic tensile response and so also the end of phase 1 of the model. The tensile strain was eliminated in the previous equation in order to find the position of the neutral axis.

Assuming a simply supported beam loaded in the centre with a single point load, the applied moments can be expressed as the product of the load and the length of the beam, divided by 4. Note that this can be generalized as different load configurations will require different formulas for calculating the applied moment.

By taking the equilibrium of moments around the neutral axis, the following equation can be derived.

$$\Sigma M = 0$$

$$M_u = \frac{1}{2}\sigma_{cc}bx\frac{-2x}{3} + f_{sc}\varepsilon_{sc}(-(x-d')) + \frac{1}{2}\sigma_{ct}b(h-x)\frac{2(h-x)}{3} + f_{st}\varepsilon_{st}(d-x) \quad 4-12$$

Substituting Equations 4-1 to 4-4, into this moment equilibrium equation, leads to:

$$M_u = -\frac{1}{3}E_{cc}\varepsilon_{cc}bx^2 - E_sA'_s\varepsilon_{sc}(x-d') + \frac{1}{3}E_{ct}\varepsilon_{ct}b(h-x)^2 + E_sA_s\varepsilon_{st}(d-x) \quad 4-13$$

By substituting Equations 4-5 to 4-7, into Equation 4-13 and multiplying it by $\frac{(h-x)}{\epsilon_{ct}}$, the following expression is derived:

$$\frac{M_u(h-x)}{\epsilon_{ct}} = \frac{1}{3}E_{cc}bx^3 + E_sA'_s(x - d')^2 + \frac{1}{3}E_{ct}b(h - x)^3 + E_sA_s(d - x)^2 \quad 4-14$$

By simplifying the above and rewriting, an expression for calculating the tensile strain in the member is obtained and shown in Equation 4-15:

$$\epsilon_{ct} = \frac{M_u(h-x)}{\frac{1}{3}b(E_{cc}x^3 + E_{ct}(h-x)^3) + E_s(A'_s(x-d')^2 + A_s(d-x)^2)} \quad 4-15$$

Equations 4-11 and 4-15 enable calculation of the neutral axis position in the beam from load inception until the first tensile crack appears. It is also possible to find the exact load at which the first tensile crack is supposed to appear in the beam, which enables the determination of when phase 1 of the model ends.

4.2.2 Phase 2 – Strain Hardening

The first crack has appeared in the tension zone of this flexural member and the tensile stress-strain relationship has moved on to Phase 2, the strain hardening phase. The compressive zone is assumed to still be in the elastic phase. The stress-strain relationship in the flexural member during Phase 2, is illustrated in Figure 4-6.

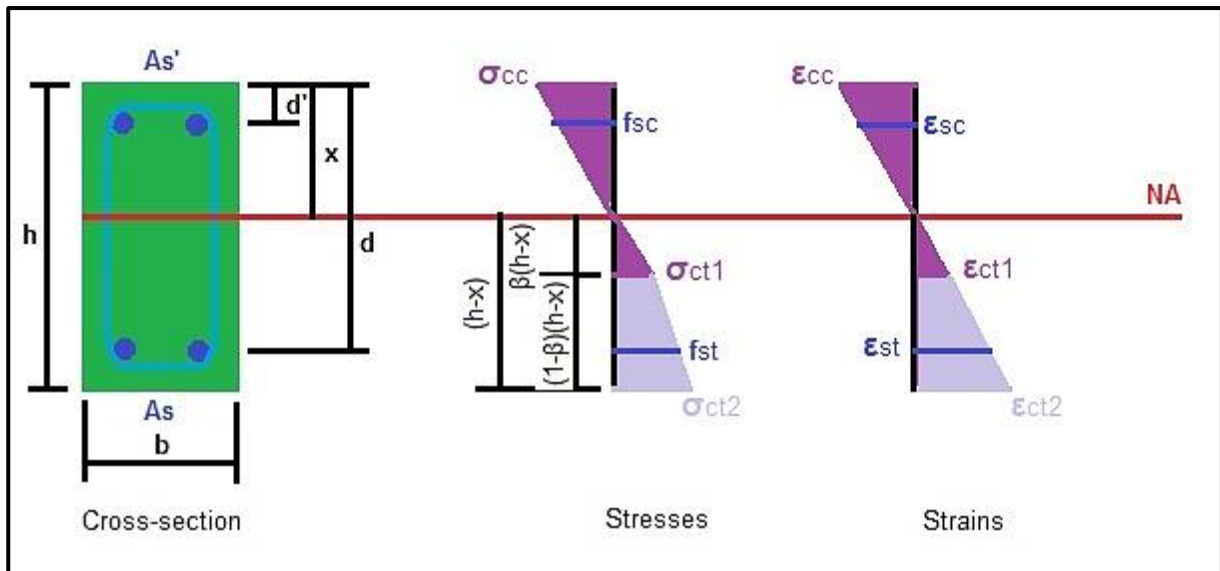


Figure 4-6: Phase 2 - Stress and Strain relationship

From Figure 4-6, the following expressions for calculating the stresses and strains in the section can be derived. Equations 4-1 to 4-7 are valid in the un-cracked part of the section. For the cracked section, the relations change to:

$$\bullet \quad \sigma_{ct2} = E_{ct} \varepsilon_{ct2} (\beta + \alpha(1 - \beta)) \quad 4-16$$

$$\bullet \quad \varepsilon_{ct1} = \beta \varepsilon_{ct2} \quad 4-17$$

$$\bullet \quad \alpha E_c = \frac{\sigma_{ctu} - \sigma_{ct1}}{\varepsilon_{ctu} - \varepsilon_{ct1}} \quad 4-18$$

Where:

- ε_{ct1} = Tensile strain at first cracking
- ε_{ct2} = Tensile strain in the bottom most section of the tensile zone
- ε_{ctu} = Ultimate tensile strain
- σ_{ct1} = Tensile stress at first cracking
- σ_{ct2} = Tensile stress at the bottom most section of the tensile zone
- σ_{ctu} = Ultimate tensile stress
- αE_c = Gradient of the strain hardening leg of the tension graph.

By following the same steps as for Phase 1 and considering equilibrium of forces in the section, quadratic Equation 4-19 for calculating the position of the neutral axis is derived.

$$x = \frac{\left[E_s(A_s + A'_s) + E_{ct}A_c g - \sqrt{(-E_s(A_s + A'_s) - E_{ct}A_c g)^2 - (2E_{ct}bg - 2E_{cc}b)(E_s(A'_s d' + A_s d) + \frac{1}{2}E_{ct}bh^2 g)} \right]}{(E_{ct}bg - E_{cc}b)} \quad 4-19$$

With:

$$g = \beta^2 + 2\beta(1 - \beta) + \alpha(1 - \beta)^2$$

This relationship is considerably more intricate than the calculation needed for the first phase of the model.

In order to find the deflections, the strains and stresses in the different parts of the flexural member are required. Equilibrium of moments around the neutral axis is used to find the following expressions:

$$\Sigma M = 0$$

$$M_u = \frac{1}{2} \sigma_{cc} b x \frac{-2x}{3} + f_{sc} A'_s (-x - d') + \frac{1}{2} \sigma_{ct1} b \beta (h - x) \frac{2\beta(h-x)}{3} + \sigma_{ct1} b (1 - \beta) (h - x) \left(\beta(h - x) + \frac{(1-\beta)(h-x)}{2} \right) + \frac{1}{2} (\sigma_{ct2} - \sigma_{ct1}) b (1 - \beta) (h - x) \left(\beta(h - x) + \frac{2(1-\beta)(h-x)}{3} \right) + f_{st} A_s (d - x) \quad 4-20$$

By following the same methodology as for Phase 1, Equation 4-21 can be deduced for calculating the tensile strain during phase 2.

$$\varepsilon_{ct2} = \frac{M_u (h - x)}{\frac{1}{3} E_{cc} b x^3 + \frac{1}{6} E_{ct} b (h - x)^3 k + E_s [A'_s (x - d')^2 + A_s (d - x)^2]} \quad 4-21$$

With:

$$k = 2\beta^3 + 3\beta(\beta + 1)(1 - \beta) + \alpha(1 - \beta)^2(\beta + 2)$$

4.2.3 Phase 3 – Compressive inelasticity before crack localization

During this phase, the tensile zone of the member is in the strain hardening phase and the compressive strain has passed the value of $0.317\varepsilon_{ccu}$. It is assumed that the compressive elastic phase has been exceeded at this level. Here it is assumed that a simple bi-linear compressive stress-strain relation occurs. This assumption is similar to that in the tensile zone of the beam and is illustrated in Figure 4-7.

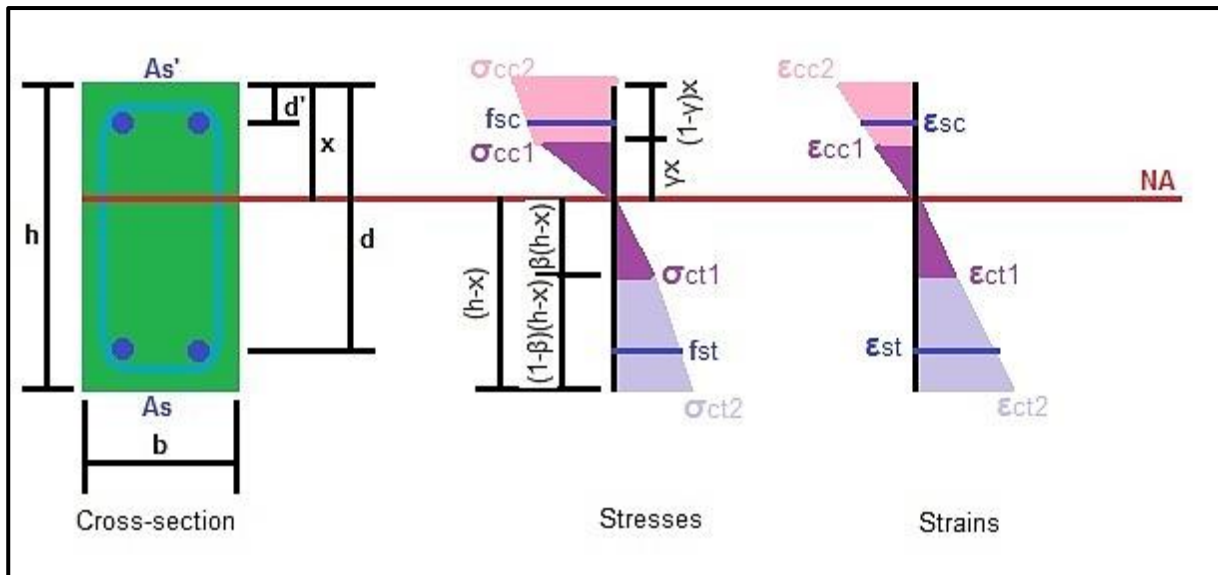


Figure 4-7: Stress-Strain Relationship for Phase 3

In the part of the section where the compressive strain exceeds 0.317 of the ultimate strain, the following relations are now valid:

- $\sigma_{cc2} = E_{cc} \varepsilon_{cc2} (\gamma + \delta(1 - \gamma)) \quad 4-22$

$$\bullet \quad \sigma_{cc1} = E_{cc}\varepsilon_{cc1} \quad 4-23$$

$$\bullet \quad \frac{\varepsilon_{cc1}}{\varepsilon_{cc2}} = \gamma \quad 4-24$$

$$\bullet \quad \varepsilon_{cc1} = \frac{-\gamma x}{(h-x)} \varepsilon_{ct2} \quad 4-25$$

$$\bullet \quad \varepsilon_{cc2} = \frac{-x}{(h-x)} \varepsilon_{ct2} \quad 4-26$$

$$\bullet \quad \delta E_{cc} = \frac{\sigma_{ccu} - \sigma_{cc1}}{\varepsilon_{ccu} - \varepsilon_{cc1}} \quad 4-27$$

By considering equilibrium of forces in the section, the position of the neutral axis can be expressed as per the quadratic Equation 4-28:

$$x = \frac{E_{ct}A_c g + E_s(A'_s + A_s) - \sqrt{(-E_{ct}A_c g - E_s(A'_s + A_s))^2 - (2E_{ct}b g - 2E_{cc}b m)\left(\frac{1}{2}E_{ct}b h^2 g + E_s(A'_s d' + A_s d)\right)}}{b(E_{ct}g - E_{cc}m)} \quad 4-28$$

With:

$$\bullet \quad g = \beta^2 + 2\beta(1 - \beta) + \alpha(1 - \beta)^2$$

$$\bullet \quad m = \gamma^2 + 2\gamma(1 - \gamma) + \delta(1 - \gamma)^2$$

This is quite an extensive expression as was expected with both stress configurations having bilinear stress-strain relations.

From moment equilibrium in the section at mid-span in this simply supported, centrally loaded beam, the expression shown in Equation 4-29 can be derived for the tensile strain in the lowest fibre.

$$\varepsilon_{ct2} = \frac{M_u(h-x)}{\frac{1}{6}E_{cc}bx^3n + \frac{1}{6}E_{ct}b(h-x)^3k + E_s(A'_s(x-d) + A_s(d-x)^2)} \quad 4-29$$

With:

$$\bullet \quad n = 2\gamma^3 + 3\gamma(1 - \gamma)(\gamma + 1) + \delta(1 - \gamma)^2(\gamma + 2)$$

$$\bullet \quad k = 2\beta^3 + 3\beta(1 - \beta)(\beta + 1) + \alpha(1 - \beta)^2(\beta + 2)$$

This base model enables prediction of the behaviour of a flexural member from load inception to crack localization or compressive crushing, whichever occurs first. This was done for the sake of completeness and to establish the behaviour of the beam over the full load-deflection response. However, for the actual design of a flexural member, this base model is too complicated and

cumbersome to use. The next part of this chapter is designated to simplifying the base model, so that it may be more suitable for structural design purposes.

4.3 Simplifying the model: From analytical to design model

The objective of this dissertation is to describe a method for calculating the reinforcement needed for a specific size of flexural member, constructed from reinforced SHCC, to withstand a specific load while still conforming to the serviceability limits set out in the applicable design standards. From the base model, this calculation is possible, but with considerable effort. The following section endeavours to simplify the design process. This simplification, however, leads to less accurate answers as some accuracy is lost in the simplification of the calculations. This is typical of design models used all over. Calibration of model uncertainty is usually done, and expressed in terms of various model and material factors. These factors typically ensure conservative resistance to actions and are calculated to acceptable levels of reliability.

When designing a flexural member, there are a number of parameters known to the designer. These parameters will include the set of loads that are to be withstood, the material that is to be used, and, to a certain extent, the size of the member. The designer must calculate the amount of reinforcement needed for the flexural member to be able to withstand the applied load. Design expressions for this purpose can be found by rewriting Equations 4-20, 4-21, 4-28, and 4-29. However, the tensile strain in the bottom of the member, the compressive strain at the top of the member, and the distance to the neutral axis still remain unknown. These parameters are needed in the calculation of the required reinforcement.

In order to simplify the model, the relationship between these three parameters and some of the known parameters, needs to be found. This is done by using the base model to analyse a number of different size fictional beams. The length of the beams were all set at 16 times their effective depth in order to conform to the rules for simply supported beams, as set out in the South African concrete design code [47]. The reinforcement in the beams were varied starting with a tensile reinforcement content of 0.1% of the concrete area and increasing to 2.5% of the concrete area. For each tensile reinforcement level, the compressive reinforcement was varied from 0.1% to equal that of the tensile reinforcement. It is very unusual to put more compression reinforcement than tensile reinforcement into a flexural member. For each one of these combinations, the ultimate load was found at which the tensile reinforcement just reaches its yield strength of 450MPa. This load was then divided by 1.4 as an estimate for the service load which was in turn used to determine the deflection in the member at mid-span. The value of 1.4 is taken as the average of the loading factors prescribed in the South African Loading code SANS 10160, which is 1.2 for dead loads and 1.6 for live loads. The assumption is made that the dead and live loads are equal in this case.

For each combination, the tensile strain, the position of the neutral axis, and the deflection was noted. (Deflections are discussed in chapter 5). Those combinations for which the deflection exceeded $L/250$ or 30mm, whichever was the smallest, were eliminated from the pool of values. Graphs were then produced via Microsoft Excel showing the relationship between the applied moment and the tensile strain, and the distance to the neutral axis respectively. This was done for Phase 2 and Phase 3 separately. It was also split into the different heights of the beams that were used for the simplification calculations. This was all done in order to keep the estimates as accurate as possible. The graphs can be seen in Figures 4-8, 4-9, 4-10, and 4-11.

Figure 4-8 shows a relationship between the tensile strain at the point of design divided by the ultimate tensile strain for the particular material, and a function consisting of the applied moment, the width of the beam, the effective depth of the beam, and the ultimate tensile stress of the particular material. It has been split into the different heights of beams for better accuracy. The relationship between the tensile strain and the function is then approximated with a power equation as is seen in Equations 4-31, 4-33, 4-35, 4-37, 4-39, 4-41, and 4-43.

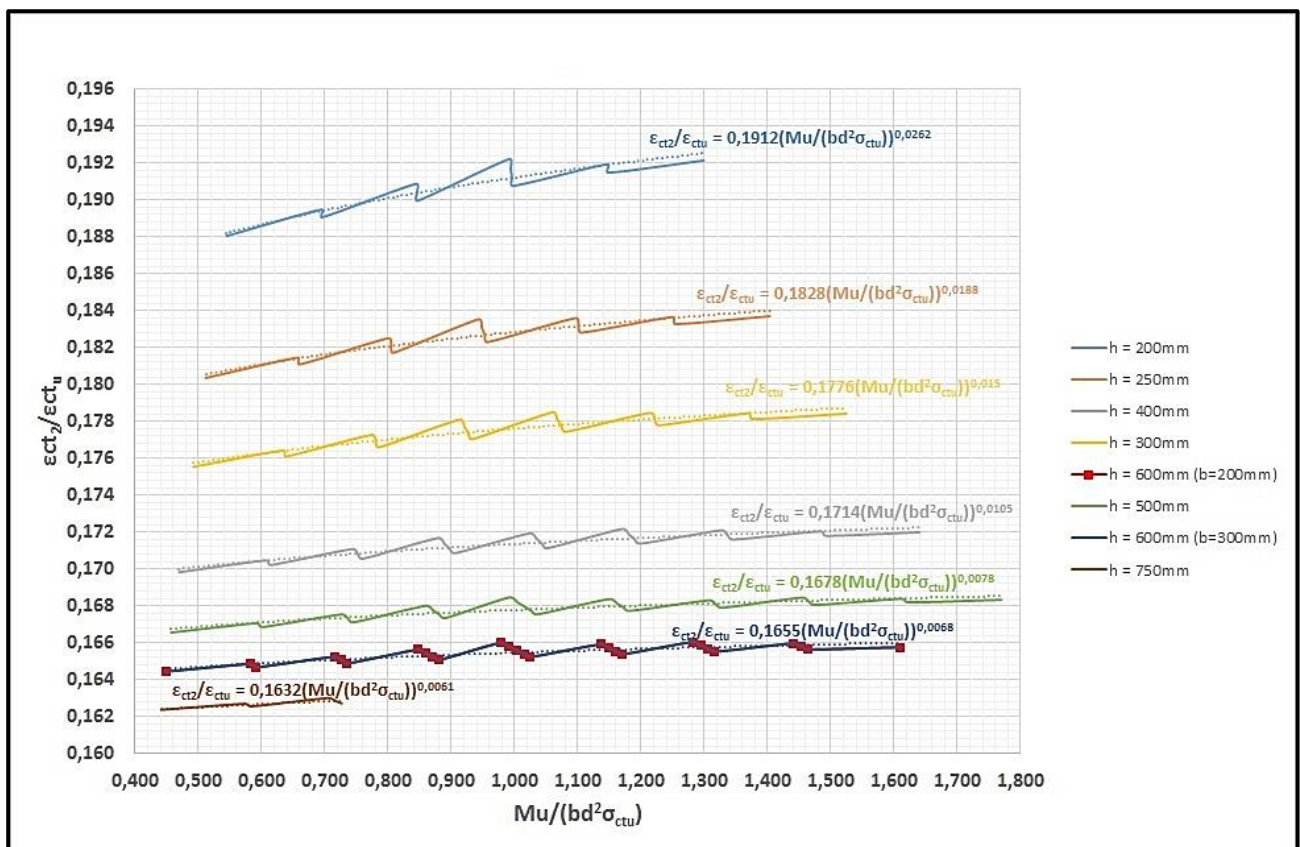


Figure 4-8: Tensile strain in relation to the applied moments for phase 2

The relationship between the distance to the neutral axis and the same function used above is shown in Figure 4-9 and Equations 4-30, 4-32, 4-34, 4-36, 4-38, 4-40, and 4-42.

For h = 200mm

$$x = 0.01512Ln\left(\frac{Mu}{bd^2\sigma_{ctu}}\right) + 0.06962 \quad 4-30$$

$$\varepsilon_{ct2} = 0.1912\left(\frac{Mu}{bd^2\sigma_{ctu}}\right)^{0.0262} 0.01456 \quad 4-31$$

For h = 250mm:

$$x = 0.017375Ln\left(\frac{Mu}{bd^2\sigma_{ctu}}\right) + 0.0884 \quad 4-32$$

$$\varepsilon_{ct2} = 0.1828\left(\frac{Mu}{bd^2\sigma_{ctu}}\right)^{0.0188} 0.01456 \quad 4-33$$

For h = 300mm:

$$x = 0.02004Ln\left(\frac{Mu}{bd^2\sigma_{ctu}}\right) + 0.10737 \quad 4-34$$

$$\varepsilon_{ct2} = 0.1776\left(\frac{Mu}{bd^2\sigma_{ctu}}\right)^{0.015} 0.01456 \quad 4-35$$

For h = 400mm:

$$x = 0.02536Ln\left(\frac{Mu}{bd^2\sigma_{ctu}}\right) + 0.3625 \quad 4-36$$

$$\varepsilon_{ct2} = 0.1714\left(\frac{Mu}{bd^2\sigma_{ctu}}\right)^{0.0105} 0.01456 \quad 4-37$$

For h = 500mm:

$$x = 0.02985Ln\left(\frac{Mu}{bd^2\sigma_{ctu}}\right) + 0.18285 \quad 4-38$$

$$\varepsilon_{ct2} = 0.1678\left(\frac{Mu}{bd^2\sigma_{ctu}}\right)^{0.0078} 0.01456 \quad 4-39$$

For h = 600mm:

$$x = 0.03768Ln\left(\frac{Mu}{bd^2\sigma_{ctu}}\right) + 0.22098 \quad 4-40$$

$$\varepsilon_{ct2} = 0.1655 \left(\frac{Mu}{bd^2\sigma_{ctu}} \right)^{0.0068} 0.01456 \quad 4-41$$

For h = 750mm:

$$x = 0.057975 \ln \left(\frac{Mu}{bd^2\sigma_{ctu}} \right) + 0.279525 \quad 4-42$$

$$\varepsilon_{ct2} = 0.1632 \left(\frac{Mu}{bd^2\sigma_{ctu}} \right)^{0.0061} 0.01456 \quad 4-43$$

Figure 4-10 illustrates the relationship between the tensile strain and the same function as was previously used. Equations 4-44, 4-46, 4-48, 4-50, and 4-52 show the relationships.

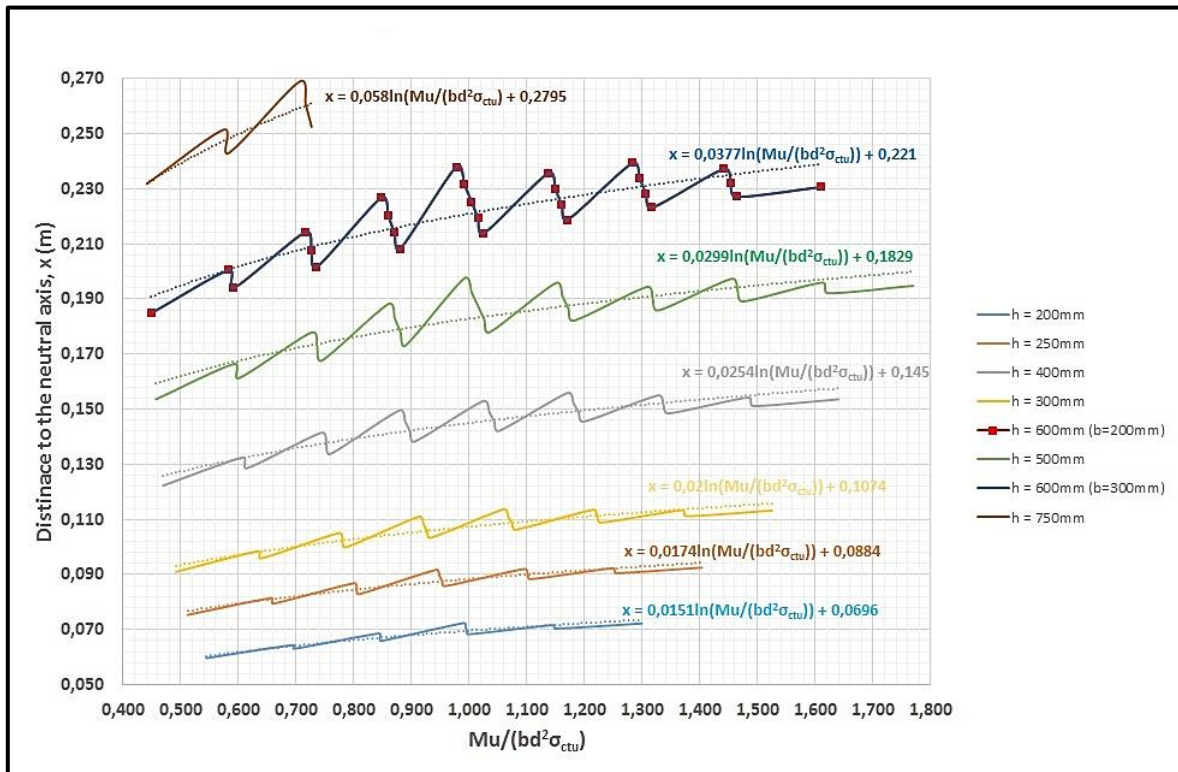


Figure 4-9: The distance to the neutral axis, x, in relation to the applied moment for phase 2

The distance to the neutral axis is again plotted against the same function as used in the previous three graphs, and is shown in Figure 4-11, and the relationship is shown in Equations 4-45, 4-47, 4-49, 4-51, and 4-53.

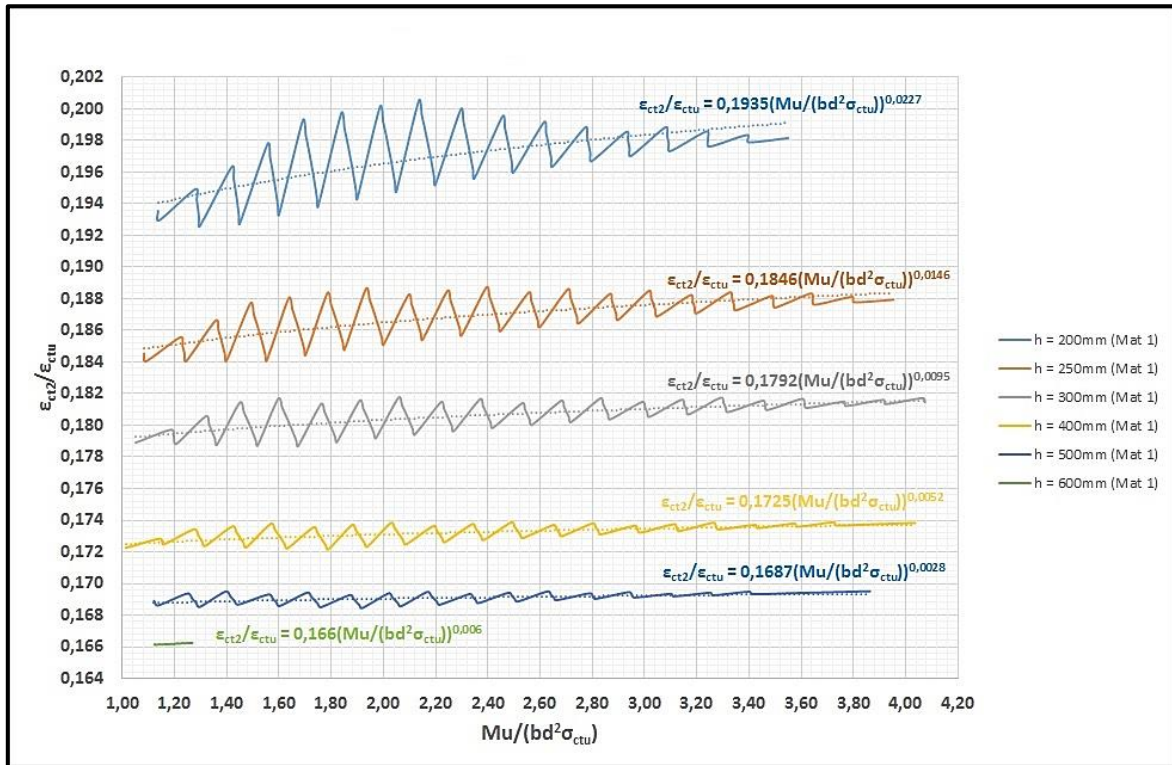


Figure 4-10: Tensile strain in relation to the applied moment for phase 3

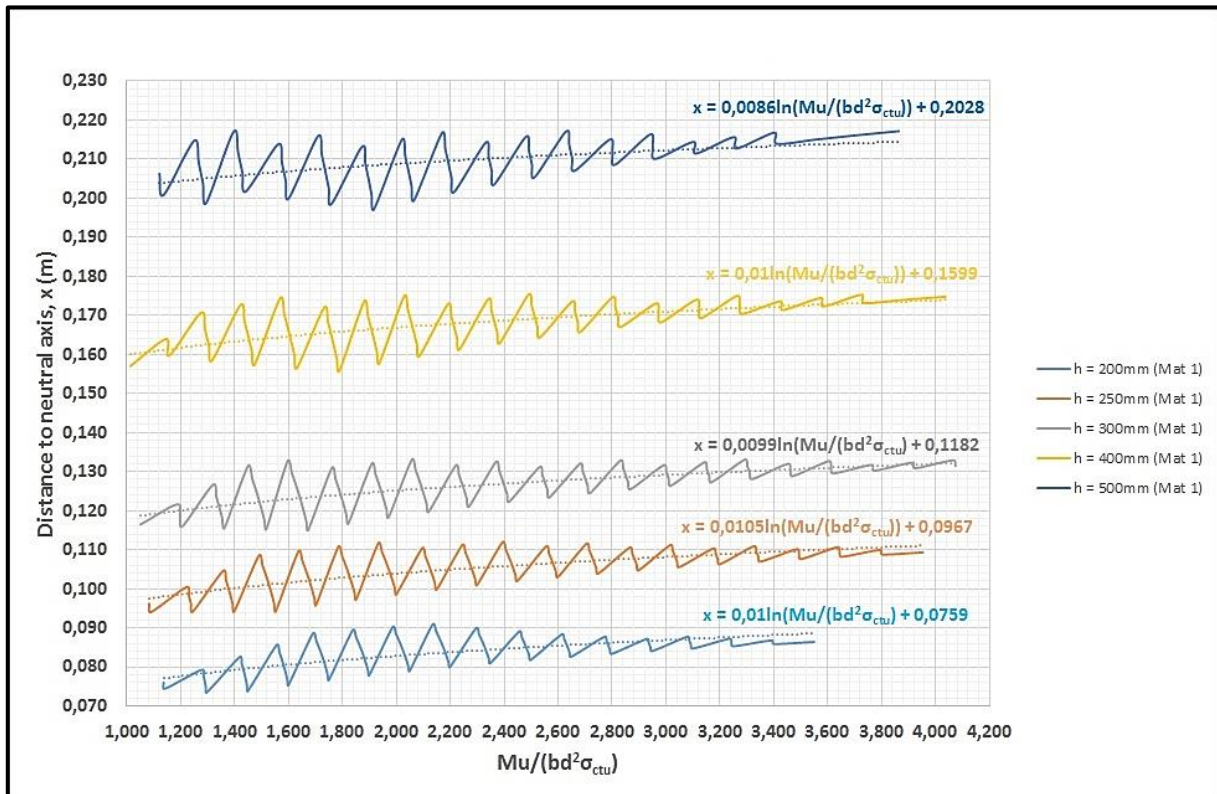


Figure 4-11: The distance to the neutral axis in relation to the applied moment for phase 3

For h = 200mm:

$$\varepsilon_{ct2} = 0.1935 \left(\frac{Mu}{bd^2\sigma_{ctu}} \right)^{0.0227} 0.01456 \quad 4-44$$

$$x = 0.01Ln \left(\frac{Mu}{bd^2\sigma_{ctu}} \right) + 0.0759 \quad 4-45$$

For h = 250mm:

$$\varepsilon_{ct2} = 0.1846 \left(\frac{Mu}{bd^2\sigma_{ctu}} \right)^{0.0146} 0.01456 \quad 4-46$$

$$x = 0.0105Ln \left(\frac{Mu}{bd^2\sigma_{ctu}} \right) + 0.0967 \quad 4-47$$

For h = 300mm:

$$\varepsilon_{ct2} = 0.1792 \left(\frac{Mu}{bd^2\sigma_{ctu}} \right)^{0.0095} 0.01456 \quad 4-48$$

$$x = 0.0099Ln \left(\frac{Mu}{bd^2\sigma_{ctu}} \right) + 0.1182 \quad 4-49$$

For h = 400mm:

$$\varepsilon_{ct2} = 0.1725 \left(\frac{Mu}{bd^2\sigma_{ctu}} \right)^{0.0052} 0.01456 \quad 4-50$$

$$x = 0.01Ln \left(\frac{Mu}{bd^2\sigma_{ctu}} \right) + 0.1599 \quad 4-51$$

For h = 500mm:

$$\varepsilon_{ct2} = 0.1687 \left(\frac{Mu}{bd^2\sigma_{ctu}} \right)^{0.0028} 0.01456 \quad 4-52$$

$$x = 0.0086Ln \left(\frac{Mu}{bd^2\sigma_{ctu}} \right) + 0.2028 \quad 4-53$$

To establish whether the design falls within Phase 2 or Phase 3, the compressive strain can be calculated from Equation 4-5. This will obviously be an iterative process as the stage will have to be guessed and the tensile strain and the distance to the neutral axis calculated, and with that

information, the compressive strain found. If the compressive strain shows the other phase from the one that was chosen up front, the first two calculations must be repeated. As a check, the compressive strain should be recalculated.

With this information, the amount of tensile reinforcement needed for a specific size beam under a specific load can be found via the following equations. For the design compressive strain less than 0.317 of the ultimate compressive strain, the design falls within Phase 2 of the model and Equations 4-54 and 4-55 should be used to calculate the tensile and compressive reinforcement needed.

$$A_s = \frac{\frac{M(h-x)}{\varepsilon_{ct2}} - \frac{1}{6}E_{cc}x^2b(3d'-x) - \frac{1}{6}E_{ct}b(h-x)^2(k(h-x)+3g(x-d'))}{E_s(d-x)(d-d')} \quad 4-54$$

$$A'_s = \frac{\frac{M(h-x)}{\varepsilon_{ct2}} - \frac{1}{6}E_{cc}x^2b(3d-x) - \frac{1}{6}E_{ct}b(h-x)^2(k(h-x)-3g(d-x))}{E_s(x-d')(d-d')} \quad 4-55$$

If the compressive strain value found from equation 4-5 is more than 0.317 times that of the ultimate compressive strain value for the material, the design falls in the third phase of the model and the following equations should be used for obtaining the tensile reinforcement.

$$A_s = \frac{\frac{M(h-x)}{\varepsilon_{ct2}} - \frac{1}{6}E_{cc}bx^2(xn-3m(x-d')) - \frac{1}{6}E_{ct}(h-x)^2b(k(h-x)+3g(x-d'))}{E_s(d-x)(d-d')} \quad 4-56$$

$$A'_s = \frac{\frac{M(h-x)}{\varepsilon_{ct2}} - \frac{1}{6}E_{cc}bx^2(xn-3m(d-x)) - \frac{1}{6}E_{ct}(h-x)^2b(k(h-x)-3g(d-x))}{E_s(x-d')(d-d')} \quad 4-57$$

With:

- $g = \beta^2 + 2\beta(1 - \beta) + \alpha(1 - \beta)^2$
- $m = \gamma^2 + 2\gamma(1 - \gamma) + \delta(1 - \gamma)^2$
- $n = 2\gamma^3 + 3\gamma(1 - \gamma)(\gamma + 1) + \delta(1 - \gamma)^2(\gamma + 2)$
- $k = 2\beta^3 + 3\beta(1 - \beta)(\beta + 1) + \alpha(1 - \beta)^2(\beta + 2)$

In order to establish the accuracy of the estimates done, the estimated tensile steel was plotted against the applied tensile steel and the same was done for the compressive steel. With *estimated* is meant that which is calculated from the formulas given above. With *applied* is meant that which was used to do develop the formulas. These comparisons are shown in Figures 4-12 and 4-13 for Phase 2 and 4-14 and 4-15 for Phase 3.

From Figures 4-13 and 4-15 it is clear that the compressive steel estimation is not as accurate as that of the tensile reinforcement. The estimates for the tensile reinforcement is slightly conservative and getting more so as the moment increases. The most probable reason for the inaccuracy of the compressive steel estimate is the fact that the stress in the compressive steel is not fixed to a certain value in the design model as is the case for the tensile reinforcement. It was noted when the stress in the compression reinforcement reached the ultimate limit and higher stresses were not allowed, but the stress was not controlled as was the stress in the tensile reinforcement. Though the stress in the compression reinforcement will not exceed the ultimate limit, it is possible that the model will over predict the compressive reinforcement due to the fact that the stress in these bars will be much less than what is ultimately allowed by the design codes.

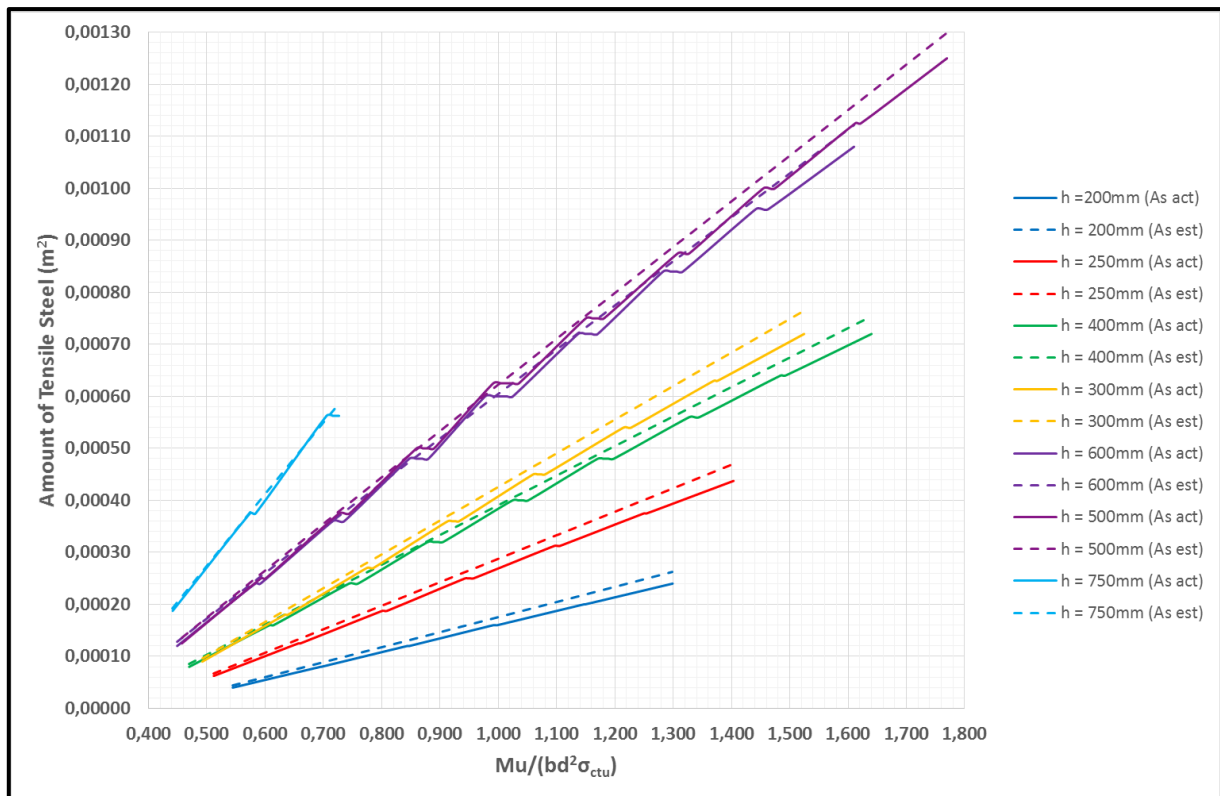


Figure 4-12: Phase 2 – Comparing estimated and applied areas of tensile reinforcement

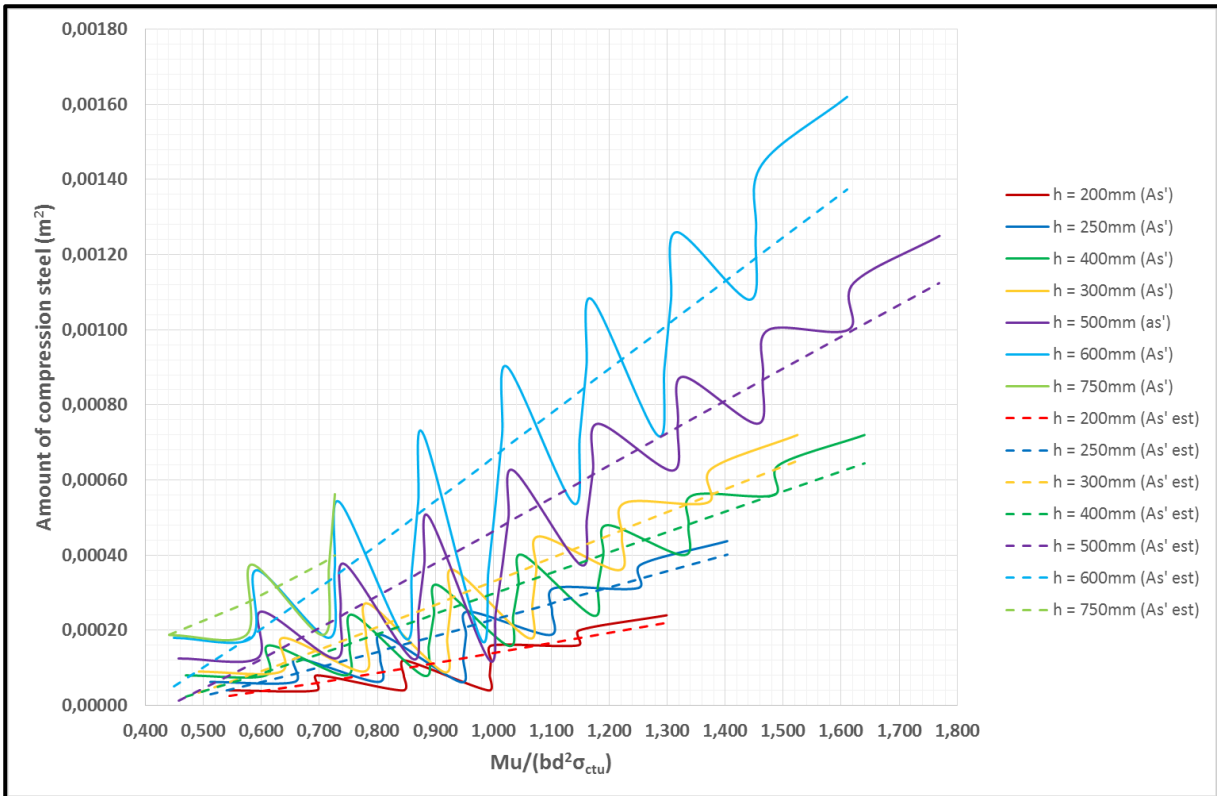


Figure 4-13: Phase 2 - Comparing estimated and applied areas of compressive reinforcement

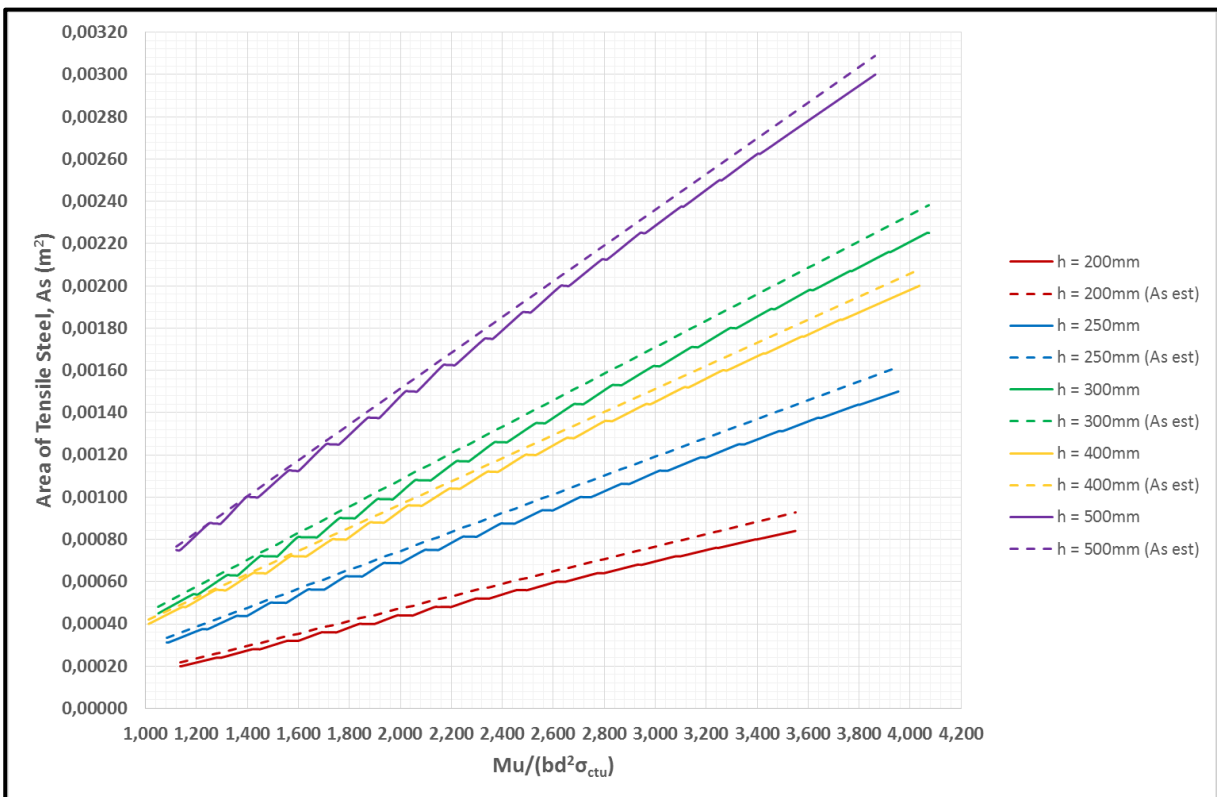


Figure 4-14: Phase 3 - Comparing estimated and applied areas of tensile reinforcement

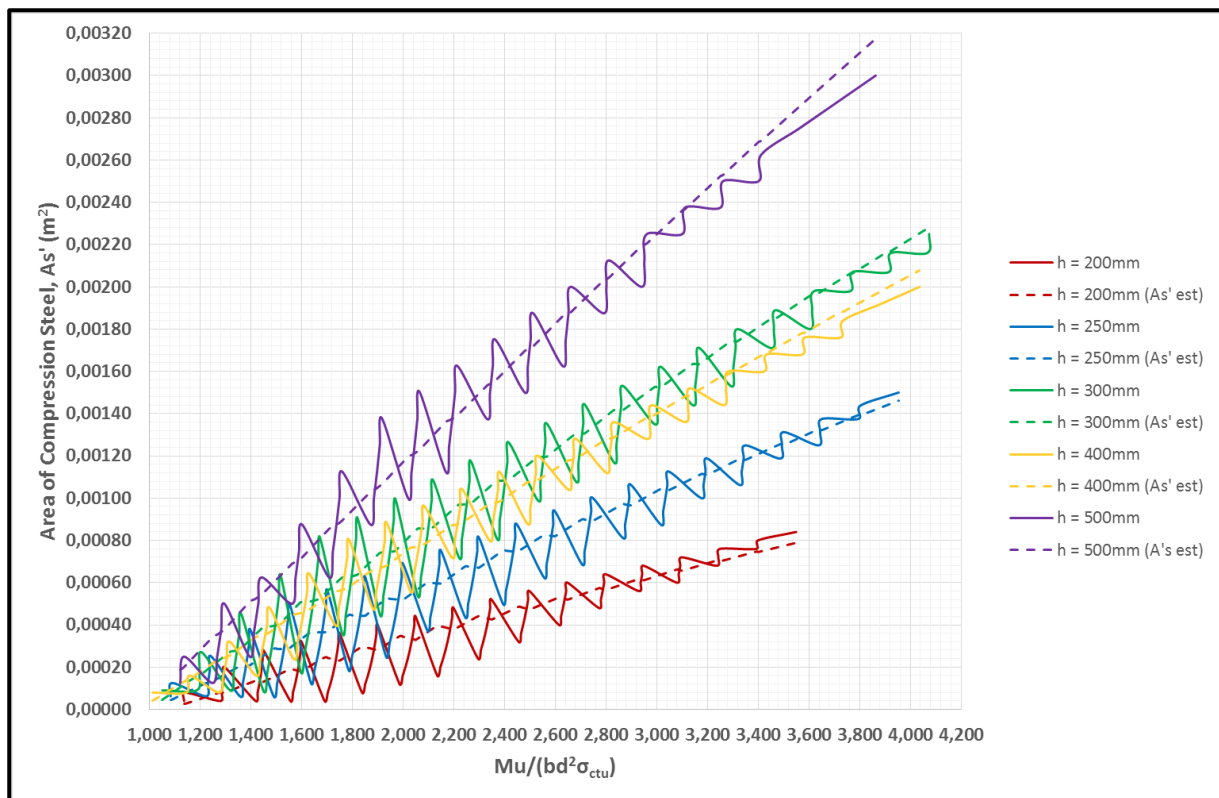


Figure 4-15: Phase 3 - Comparing estimated and applied areas of compressive reinforcement

4.3.1 Numerical Verification

In order to establish what the influence of the inaccurate estimation of the compressive reinforcement is on the resisting moment, the resisting moment was calculated using the estimated values. The model factor was then applied to the reinforcement calculations and the resisting moment recalculated with these modified reinforcement areas. In practice, the estimated reinforcement areas will be used to determine what amount of rebar must be added to a certain section. As the rebar is only found in certain diameters the actual value of reinforcement entered into the beam is normally again increased to adhere to what is practically available and possible.

To indicate the accuracy of the estimated calculations, all four moment values were plotted against each other for each height of beam evaluated. These are shown in Figures 4-16 to 4-27.



Figure 4-16: Phase 2 - h = 200mm

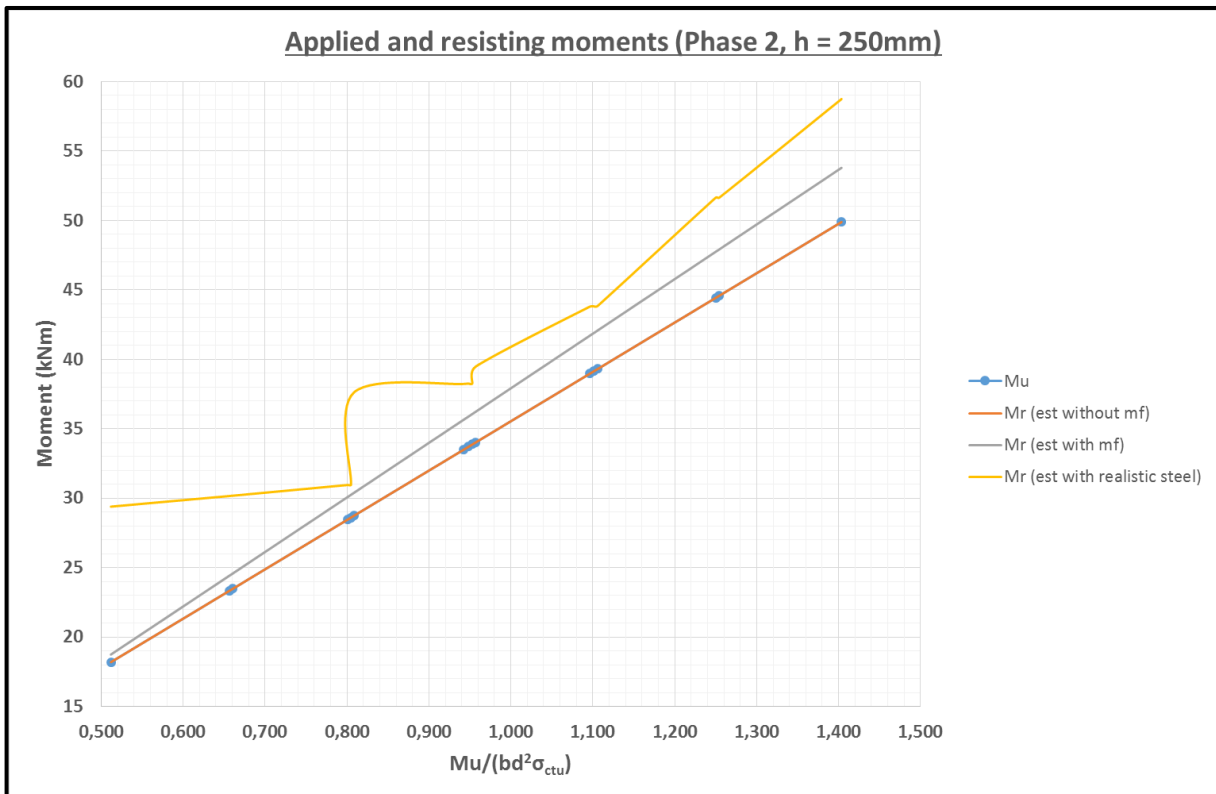


Figure 4-17: Phase 2 - h = 250mm

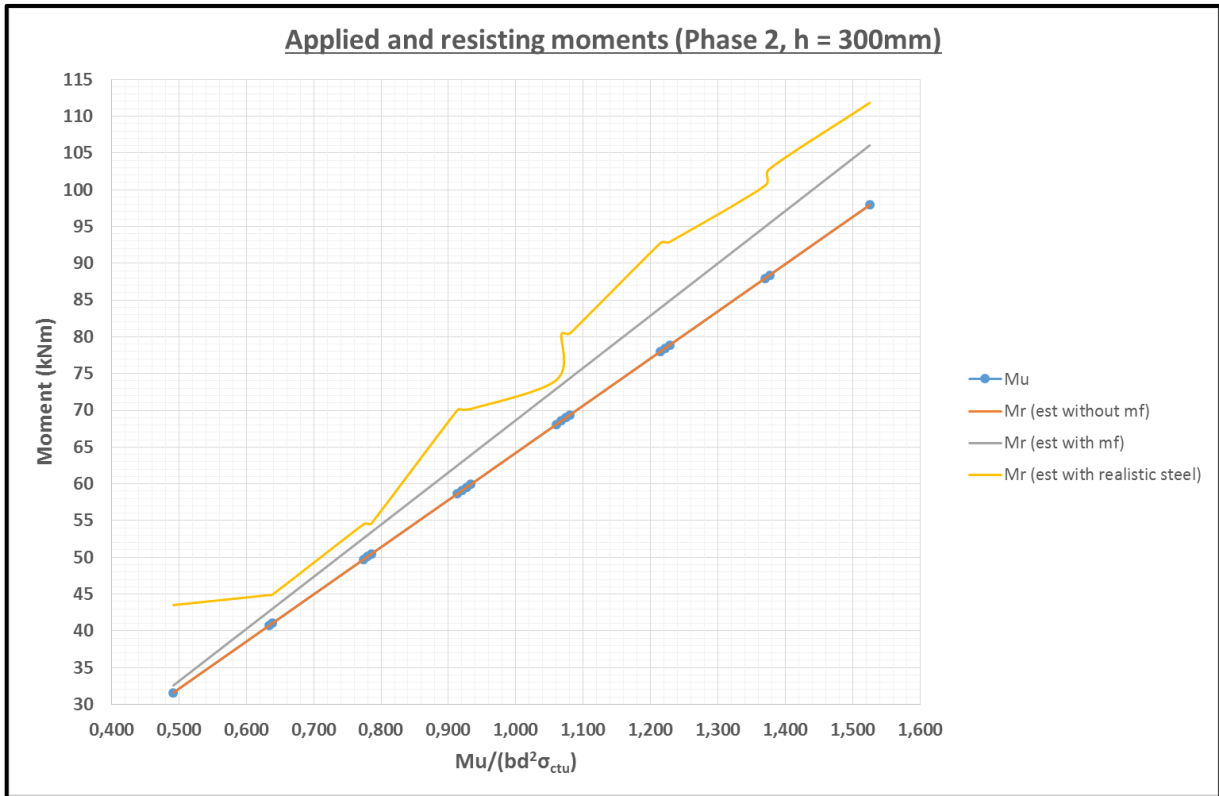


Figure 4-18: Phase 2 - h = 300mm

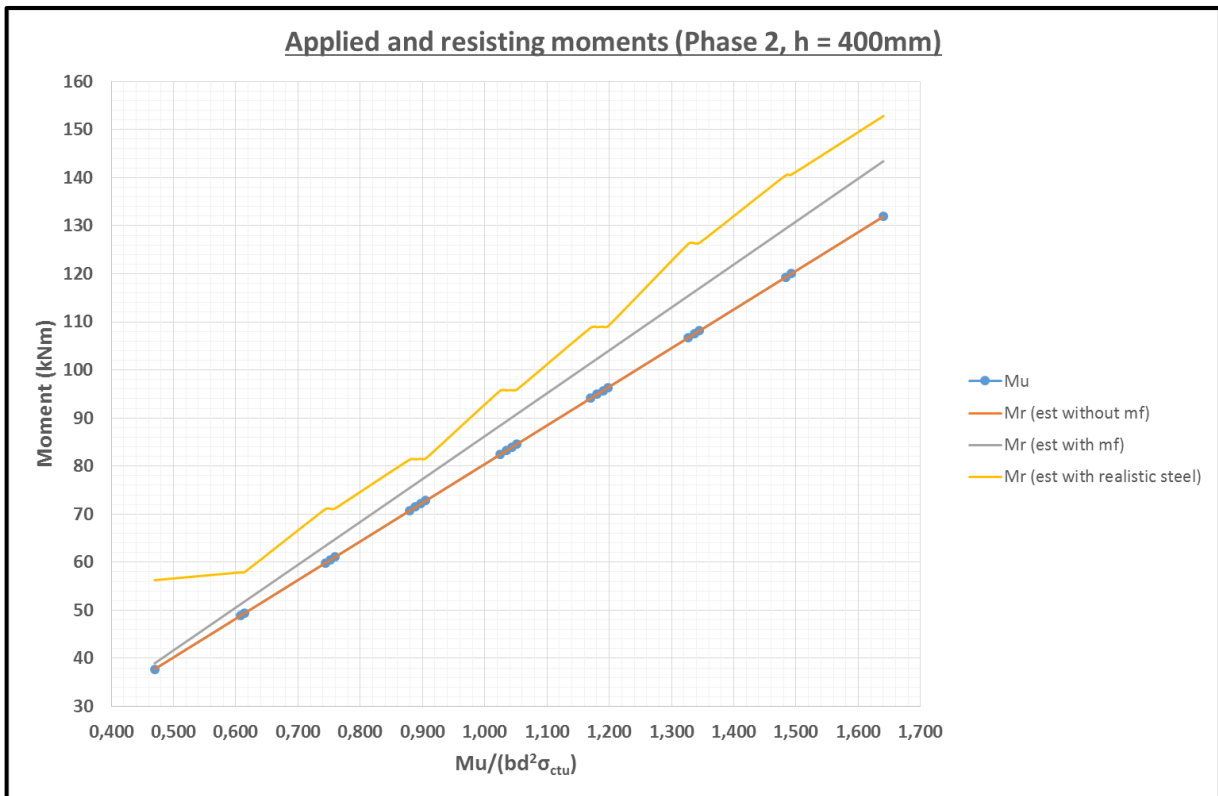


Figure 4-19: Phase 2 - h = 400mm

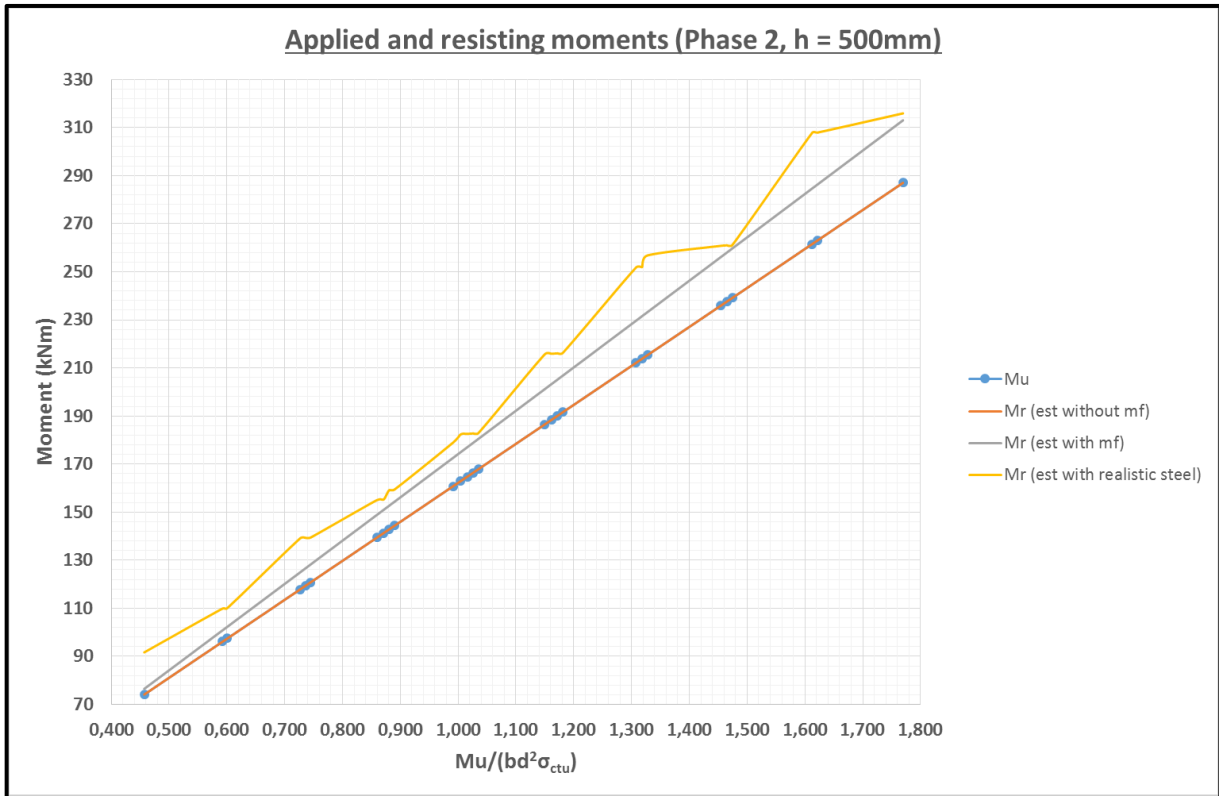


Figure 4-20: Phase 2 - h = 500mm

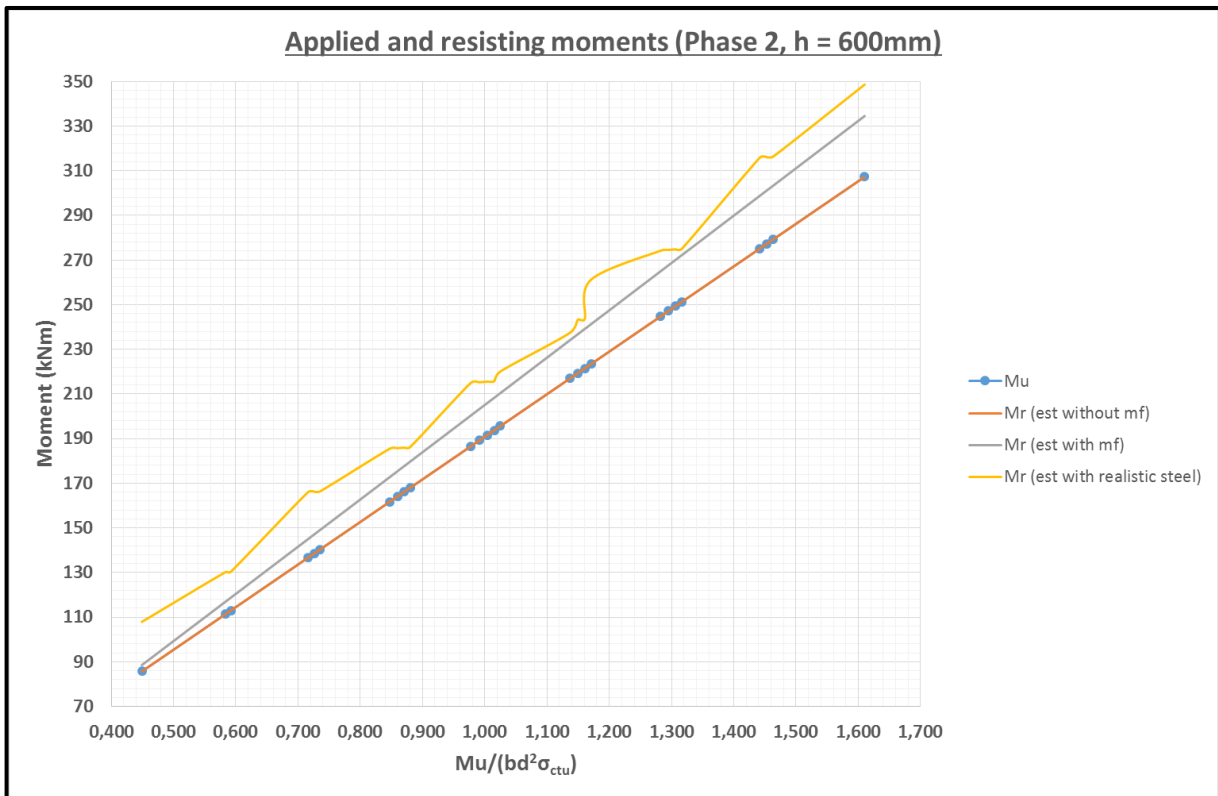


Figure 4-21: Phase 2 - h = 600mm

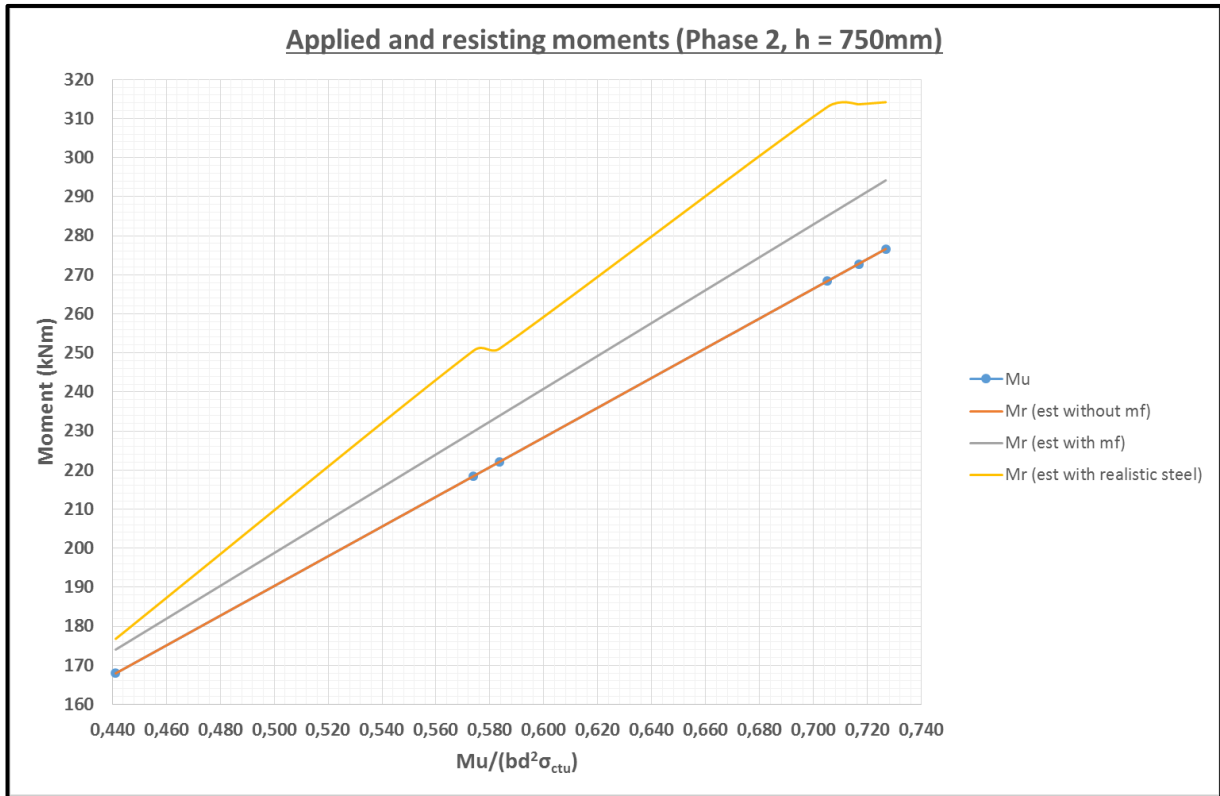


Figure 4-22: Phase 2 - h = 750mm



Figure 4-23: Phase 3 - h = 200mm

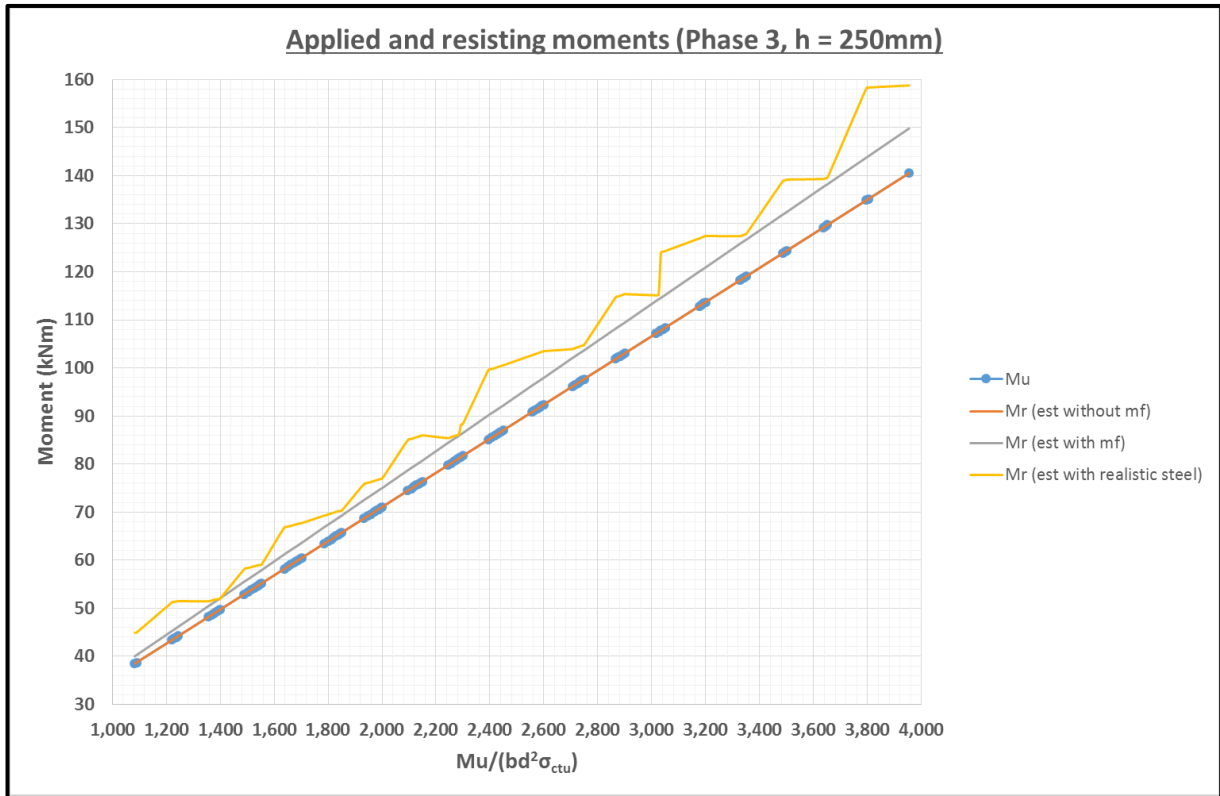


Figure 4-24: Phase 3 - h = 250mm

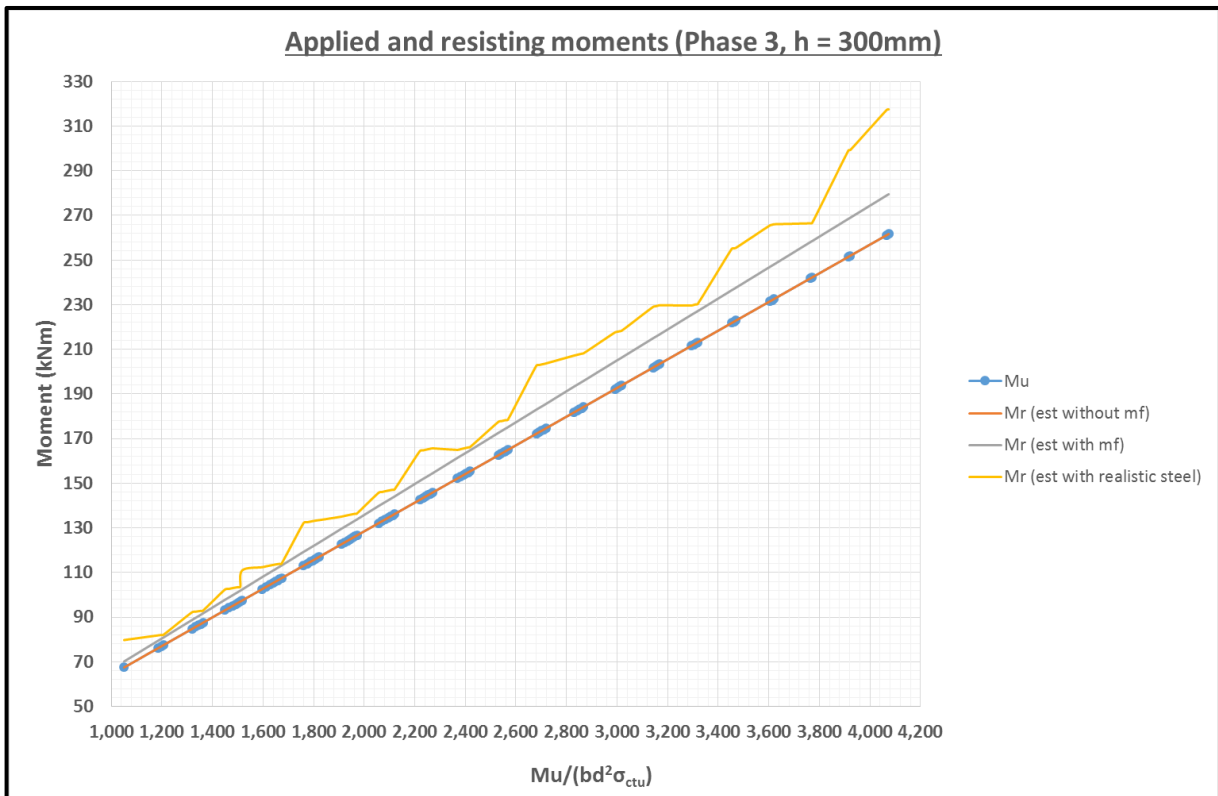


Figure 4-25: Phase 3 - h = 300mm

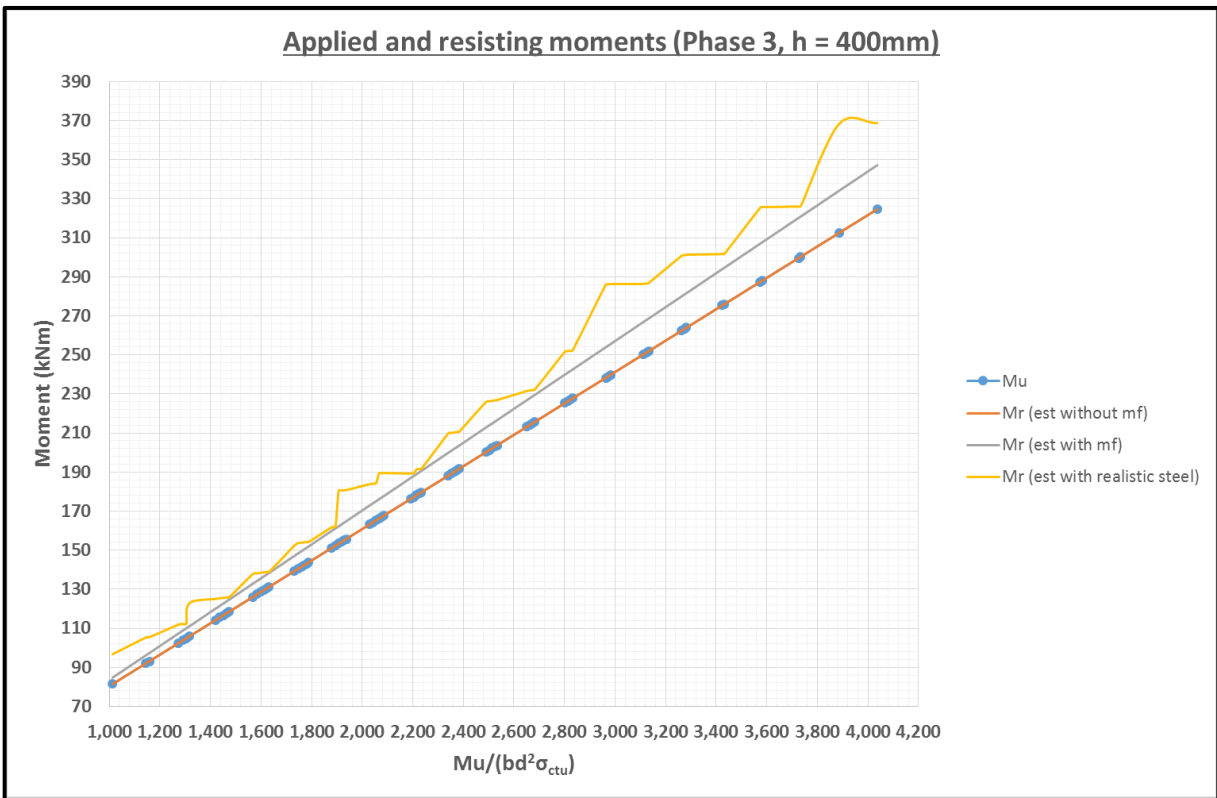


Figure 4-26: Phase 3 - h = 400mm

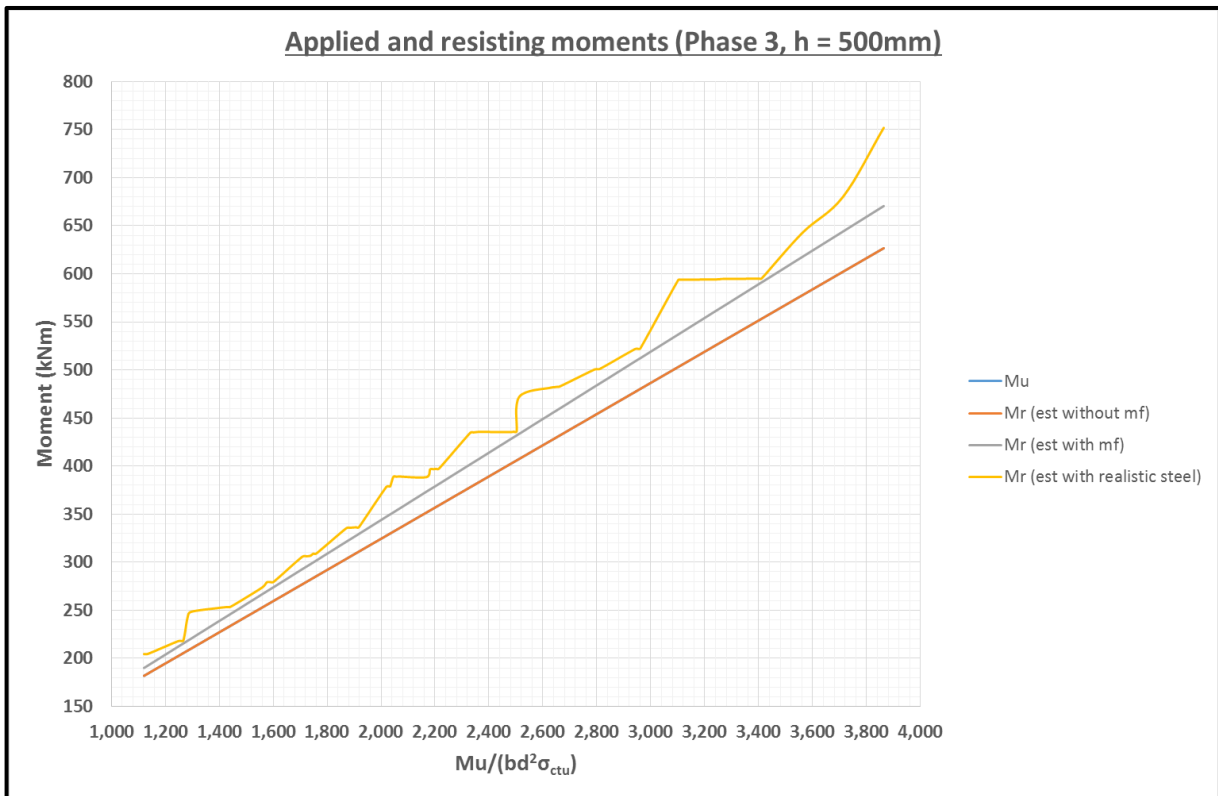


Figure 4-27: Phase 3 - h = 500mm

From the graphs it can be seen that the resisting moment without the model factor, is exactly equal to the applied moment, in spite of the inaccurate values for the compressive reinforcement. This is probably due to the fact that the tensile reinforcement is estimated slightly higher than the actual values and in most cases; the compressive reinforcement is also higher than the actual values.

When the model factor is then applied to both the tensile and the compressive reinforcement, the resisting moment becomes conservative. By incorporating the actual steel areas used the resisting moment is once again increased. Thus the simplified model can be seen as slightly conservative.

4.4 Testing the Simplified Model with Different Materials

4.4.1 Materials used

The main goal of this study is to derive an analytical model and a design model for the design of reinforced strain hardening cement composites, to be used as flexural members. The model should thus be compatible with all strain hardening materials, provided that the ultimate tensile strain is more than the strain limit of 0.00225, used for reinforcement in tension.

The material used in calibrating the model can be classified as a low strength SHCC material. The materials chosen for the testing was chosen to represent the middle and high strength SHCC materials. The material properties of the three materials are shown in Table 4-1, where Material 1 is the low strength material used in the original calibration, Material 2 is a high performance SHCC material made up with Material 1 and 3 in mind, and Material 3 represents the ultra-high strength SHCC class of materials [48].

Table 4-1: Material Properties

	Material 1	Material 2	Material 3
ϵ_{ct1}	0.000240	0.000235	0.000211
ϵ_{ctu}	0.01456	0.0127	0.0039
ϵ_{ccu}	-0.00508	-0.0053	-0.00725
σ_{ct1}	2.054MPa	3.54MPa	11.8MPa
σ_{ctu}	2.937MPa	5MPa	15MPa
σ_{ccu}	-30.559MPa	-55MPa	-250MPa
E_{ct}	8.557GPa	15GPa	55.924GPa
E_{cu}	10.112GPa	17.444GPa	57.966GPa

4.4.2 Verification

The verification of Materials 2 and 3 was done in the same way as the calibration of the model was done. For each material, a set of the same fictional beams as before, with varying sizes were reinforced with varying amounts of tensile and compressive reinforcement. For each beam, the load was found at which the tensile reinforcement would just yield. This load was then divided by 1.4 to establish the service load, which in turn was used to find the predicted deflection for the member in question. The lengths of the members were kept at exactly 16 times the effective depth of the member. Beams with deflections exceeding the lesser of $L/250$ or 30mm were again discarded. Examples of the calculations for Materials 2 and 3 can be seen in Annexure C.

For each of these beams, the tensile strain, the value of the neutral axis depth, and the deflection at the point of design was noted. Figure 4-28, 4-29, 4-30, and 4-31 shows the comparison for phases 2 and 3 between the tensile strain values and the position of the neutral axis for the three different materials.

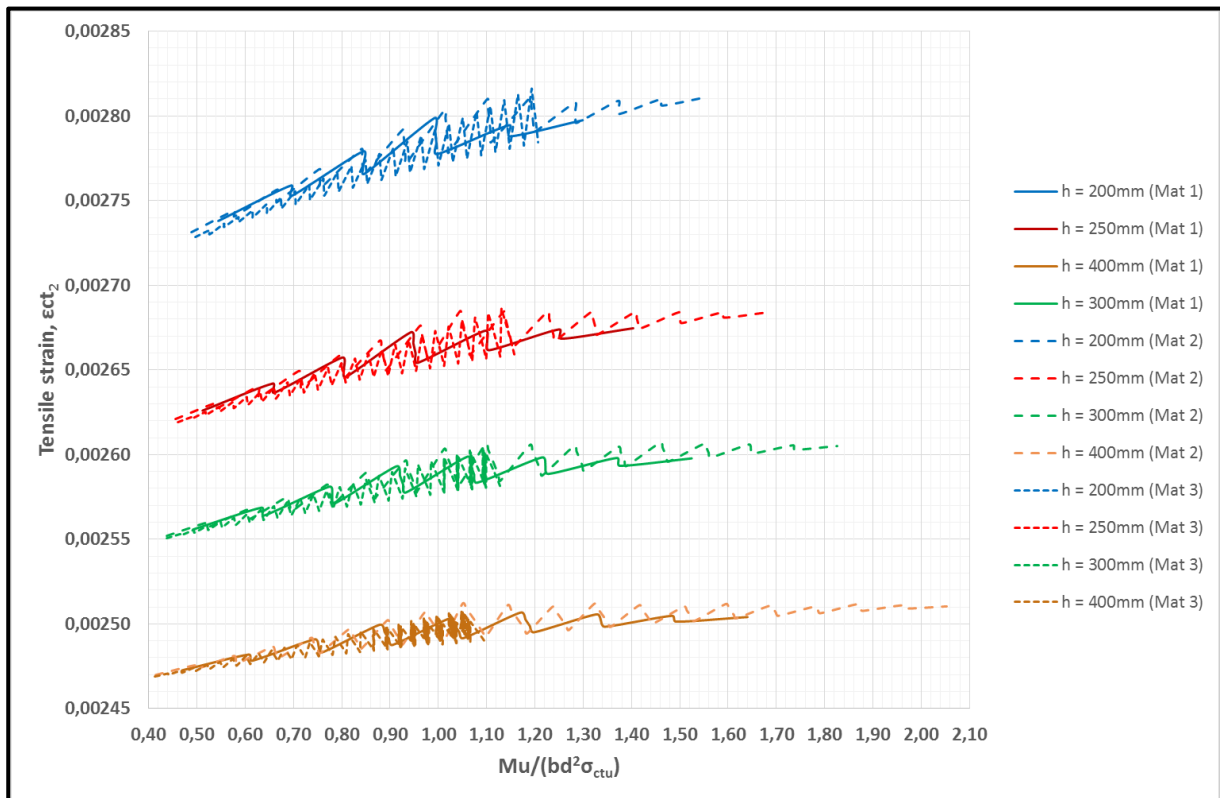


Figure 4-28: Phase 2 - Comparison between actual tensile strain for Materials 1, 2, and 3 for beam heights under 500mm

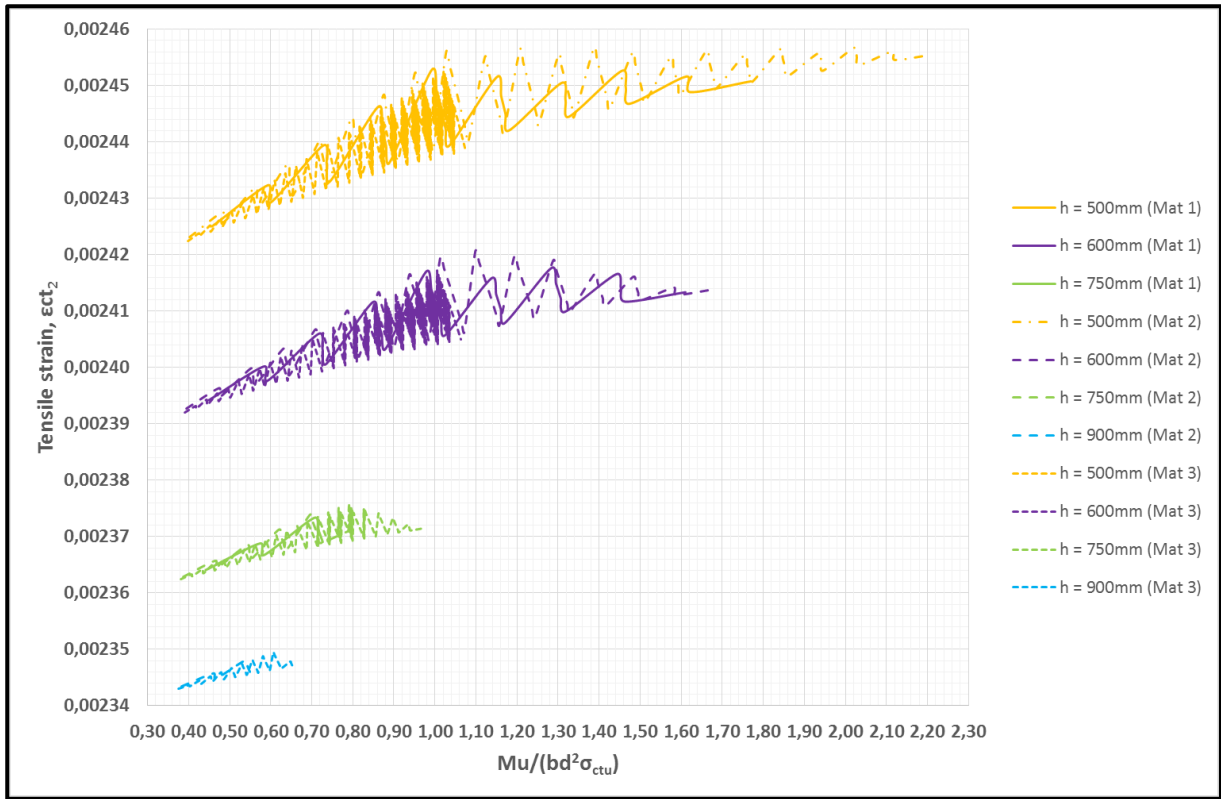


Figure 4-29: Phase 2 - Comparison between actual tensile strain for Materials 1, 2, and 3 for beam height over 500mm

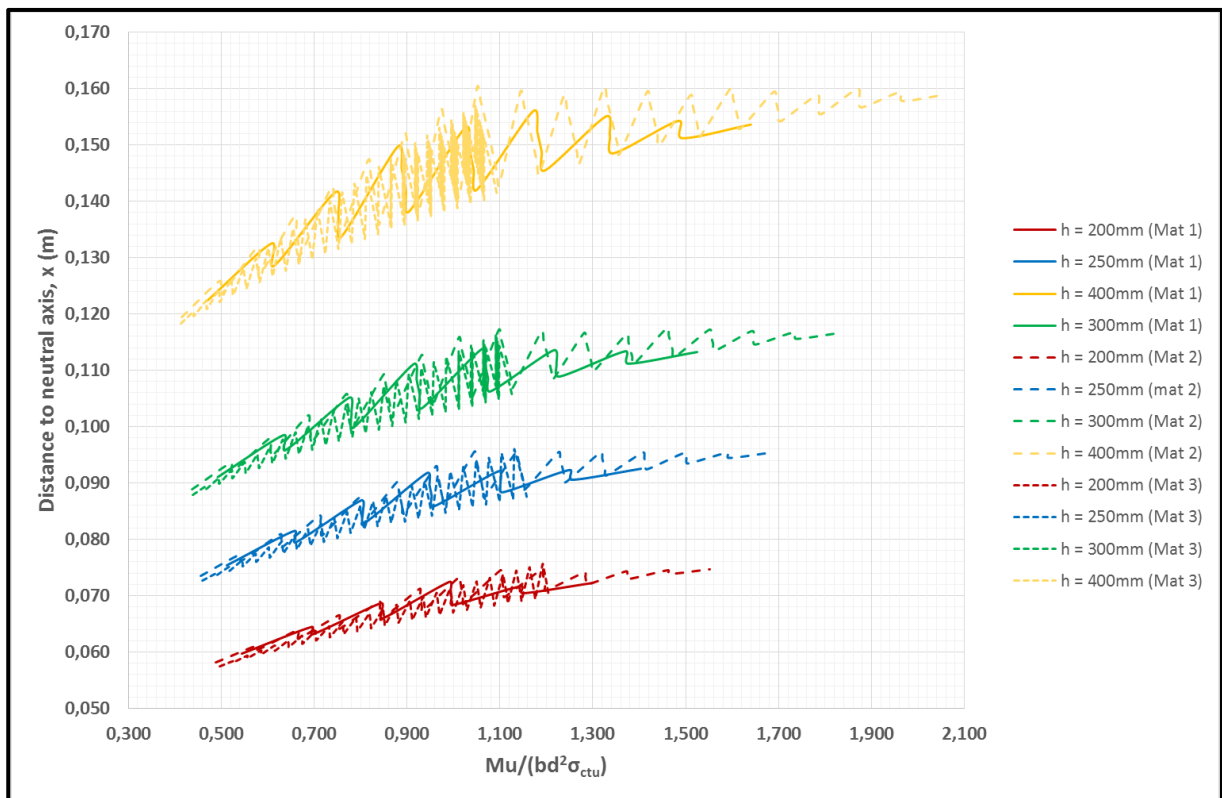


Figure 4-30: Phase 2 - Comparison between the neutral axis depth for Materials 1, 2, and 3 for beam heights under 500mm

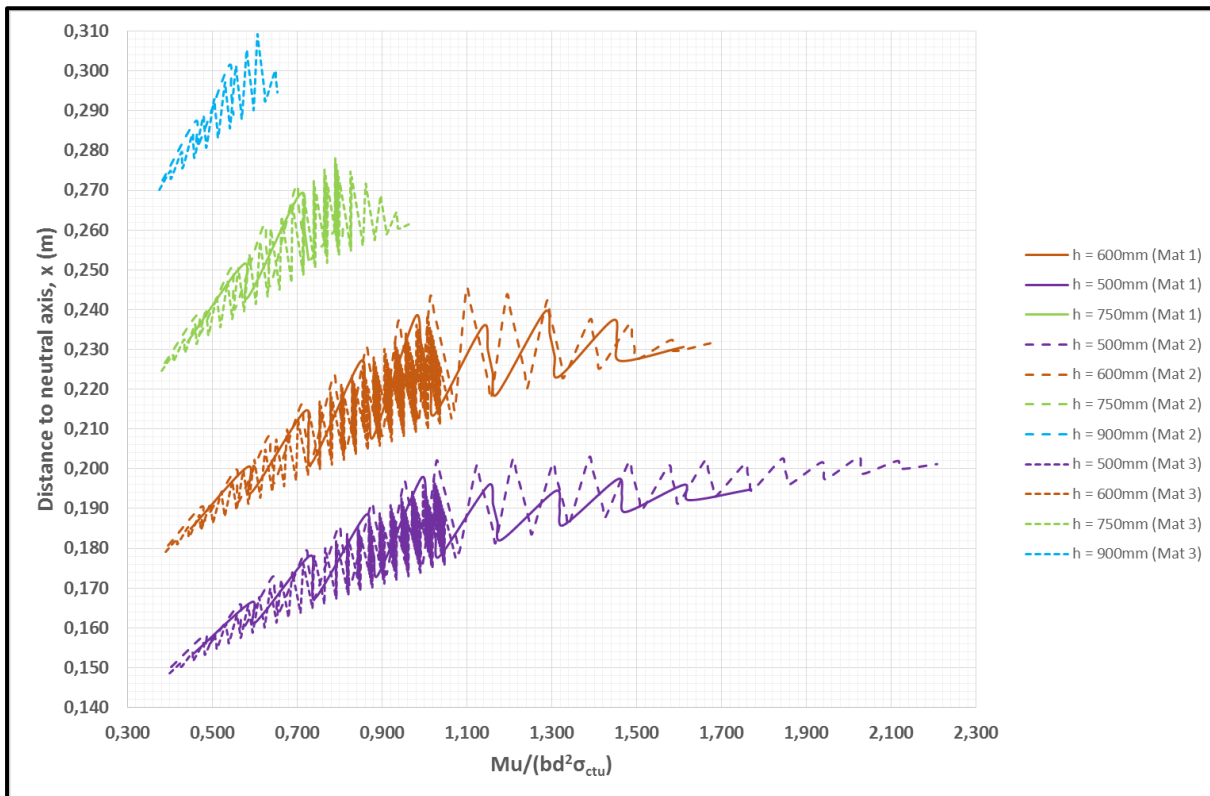


Figure 4-31: Phase 2 - Comparison between the neutral axis depth for Materials 1, 2, and 3 for beam heights over 500mm

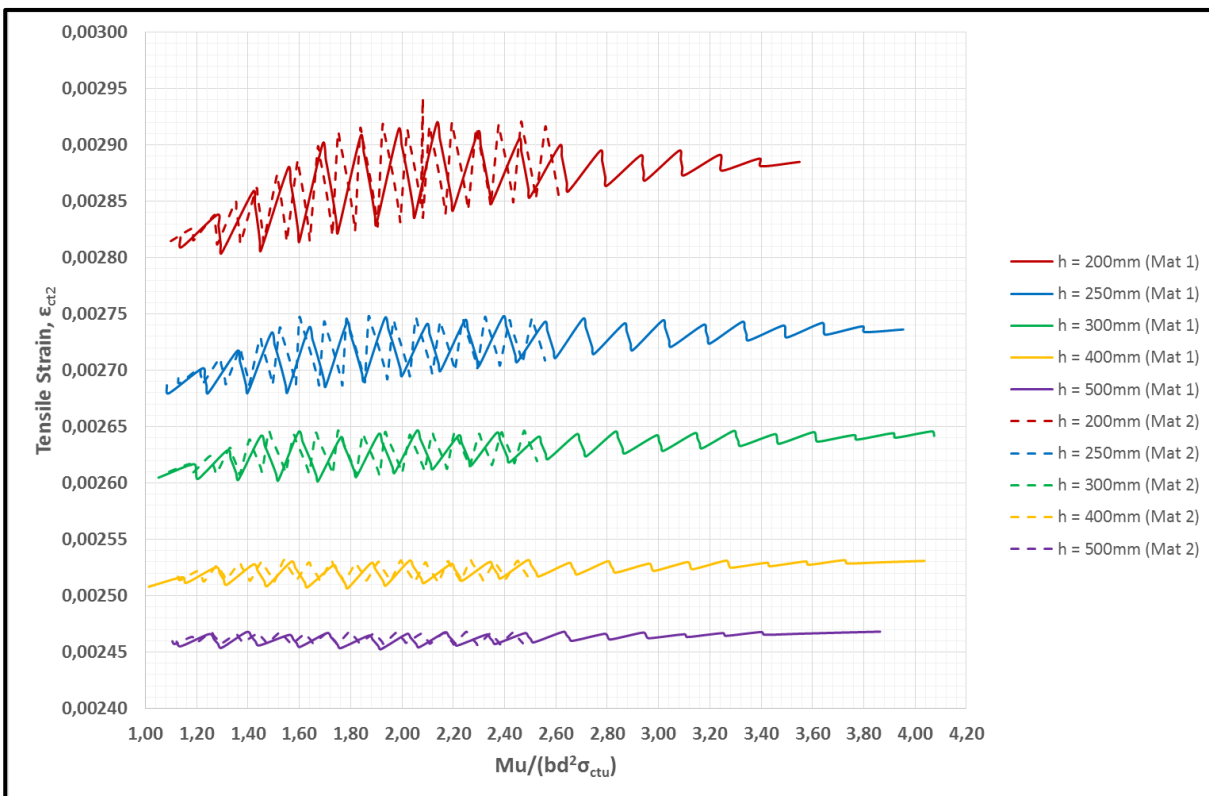


Figure 4-32: Phase 3 - Comparison between the actual tensile strain for Materials 1 and 2

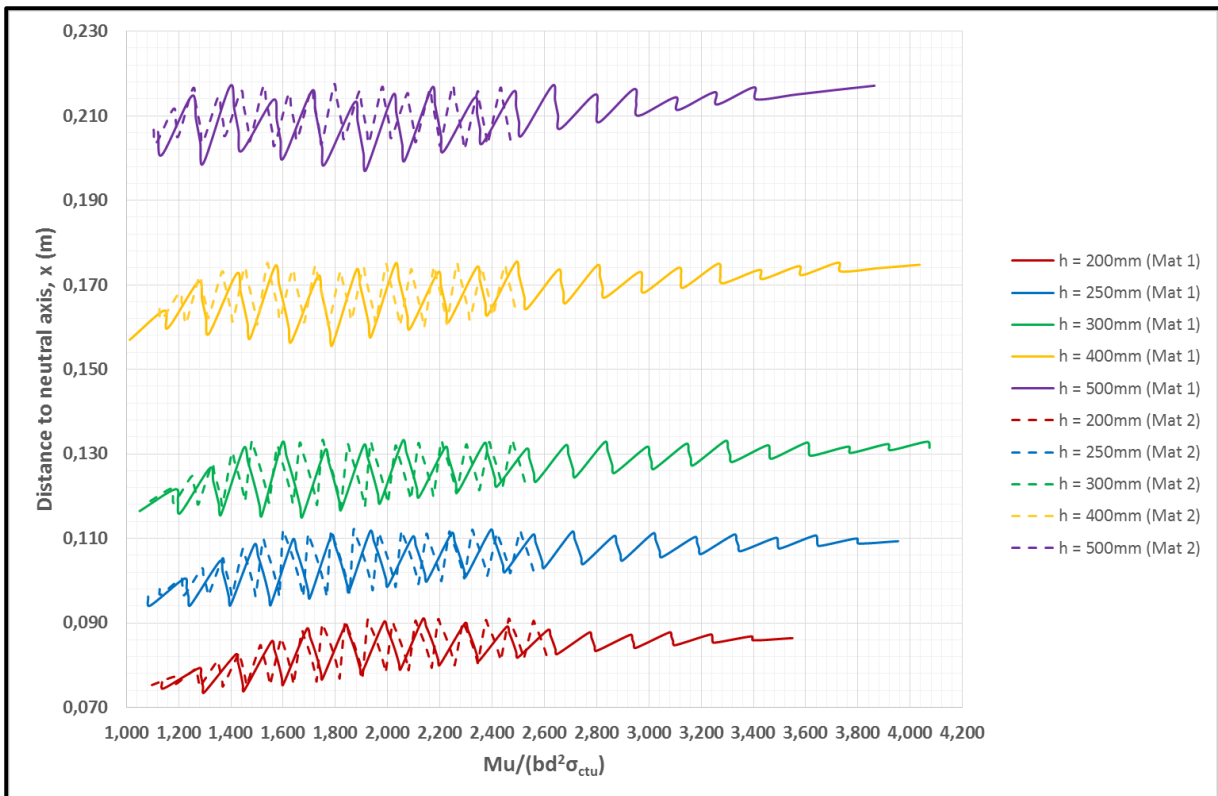


Figure 4-33: Phase3 - Comparison between the neutral axis depth for Materials 1 and 2

From the graphs it can be seen that the tensile strain values are very similar for the different materials. The same can be said for the neutral axis depths. In this light it is thus expected that the estimated values should correspond for Materials 2 and 3 as their actual values are very similar to that of Material 1. The design for Material 3 was never outside of Phase 2. This is probably due to the very high compressive strength of the material.

Figures 4-32 to 4-43 shows the comparison between the applied moments and the resisting moments for the three different materials.

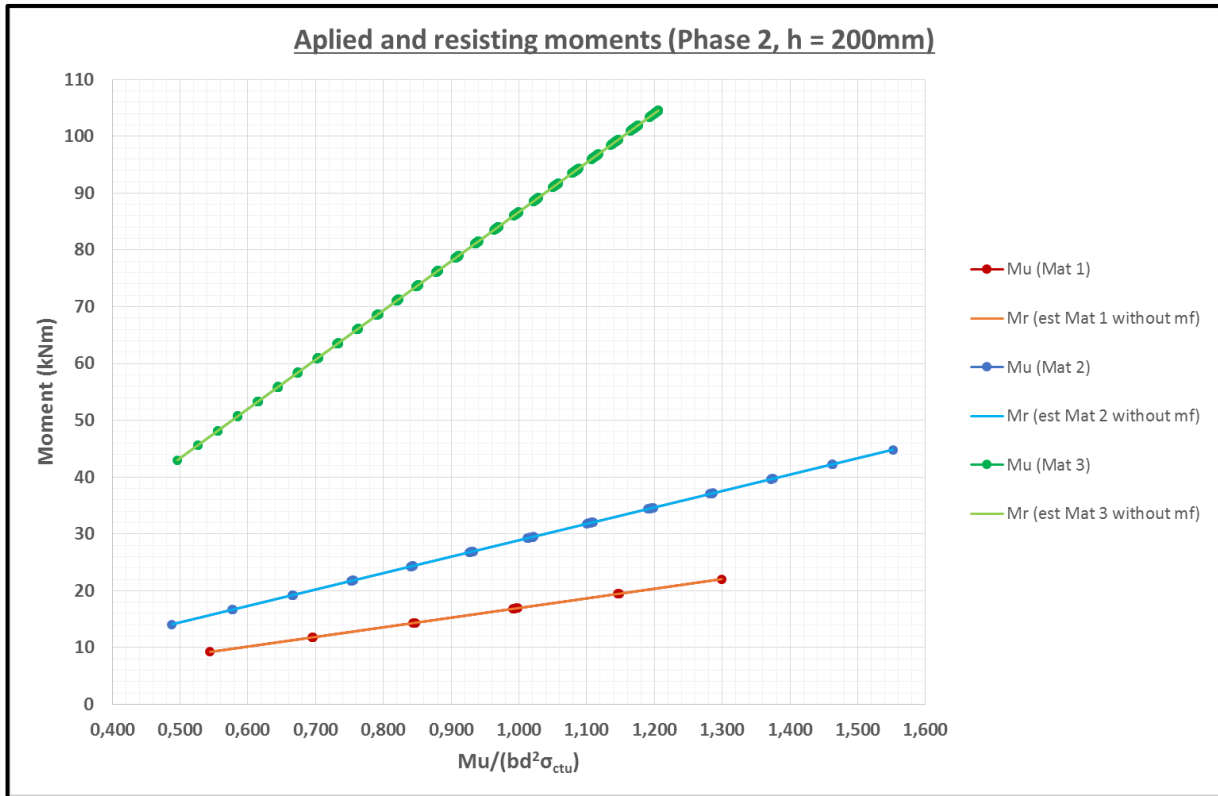


Figure 4-34: Phase 2 - h = 200mm

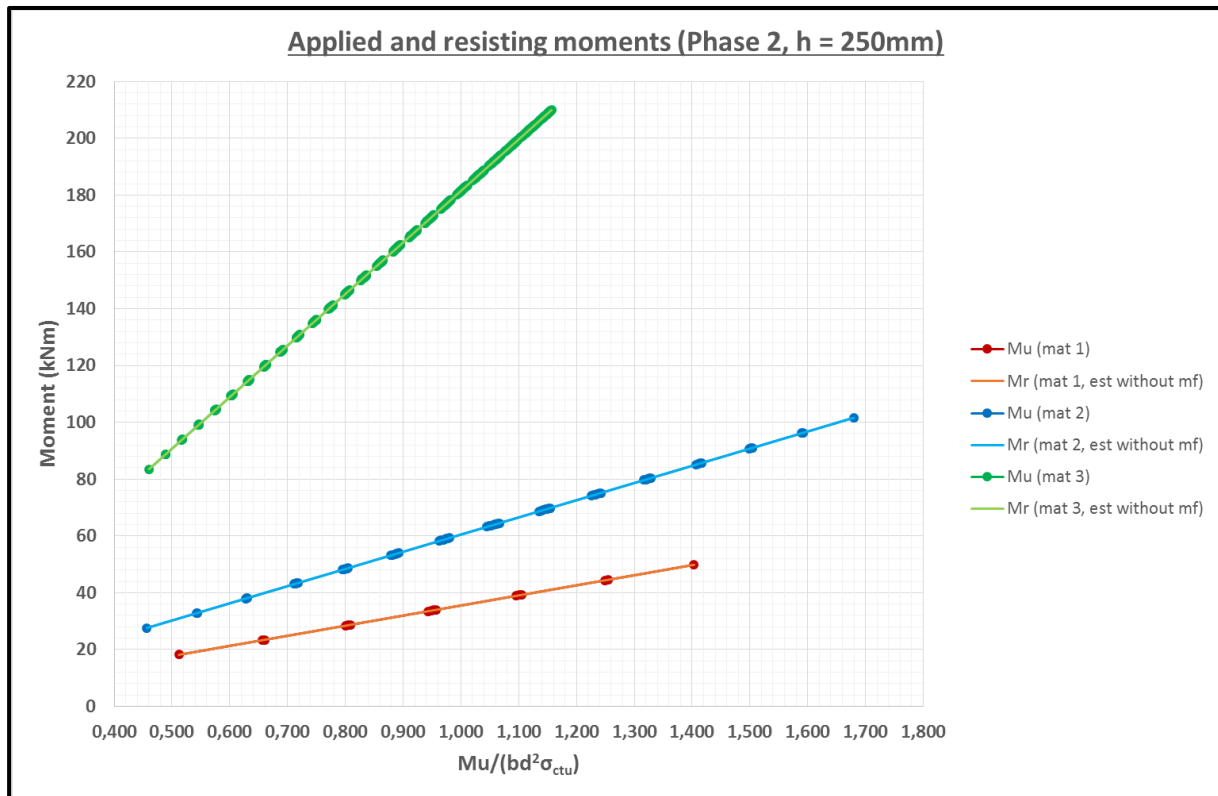


Figure 4-35: Phase 2 - h = 250mm

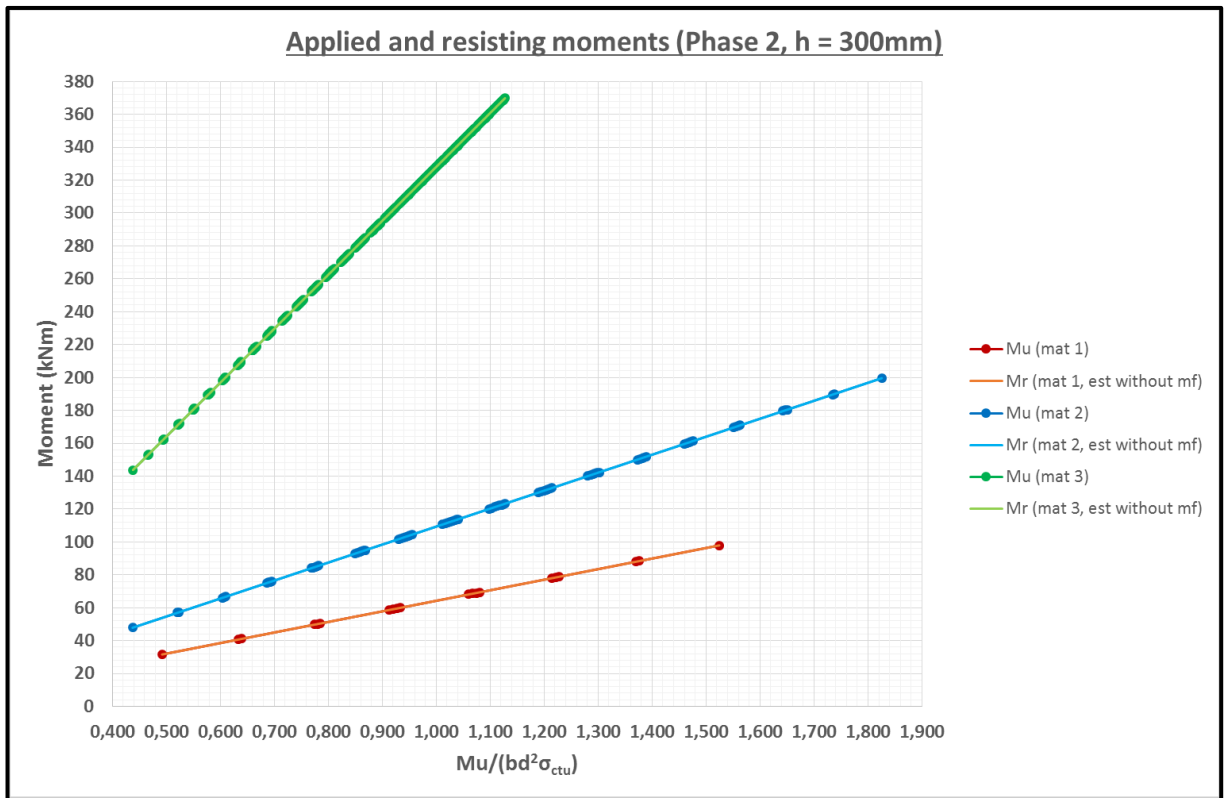


Figure 4-36: Phase 2 - h = 300mm

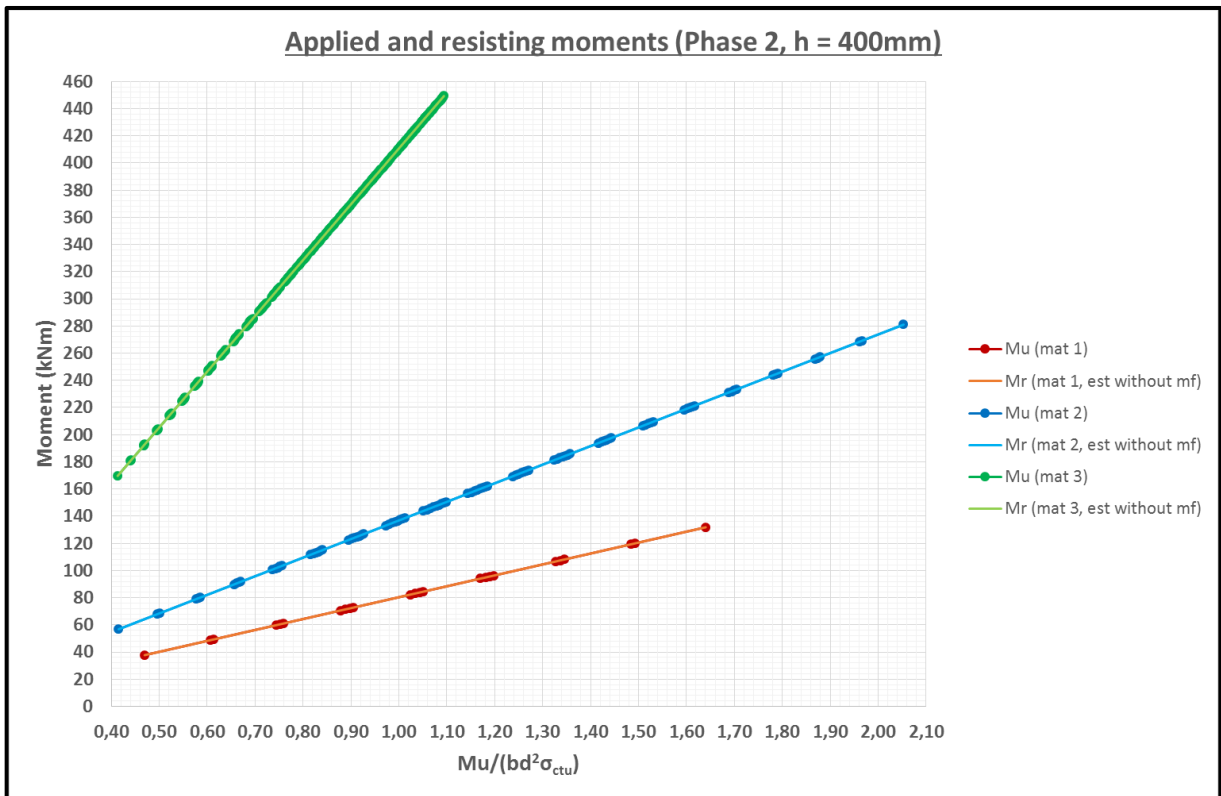


Figure 4-37: Phase 2 - h = 400mm

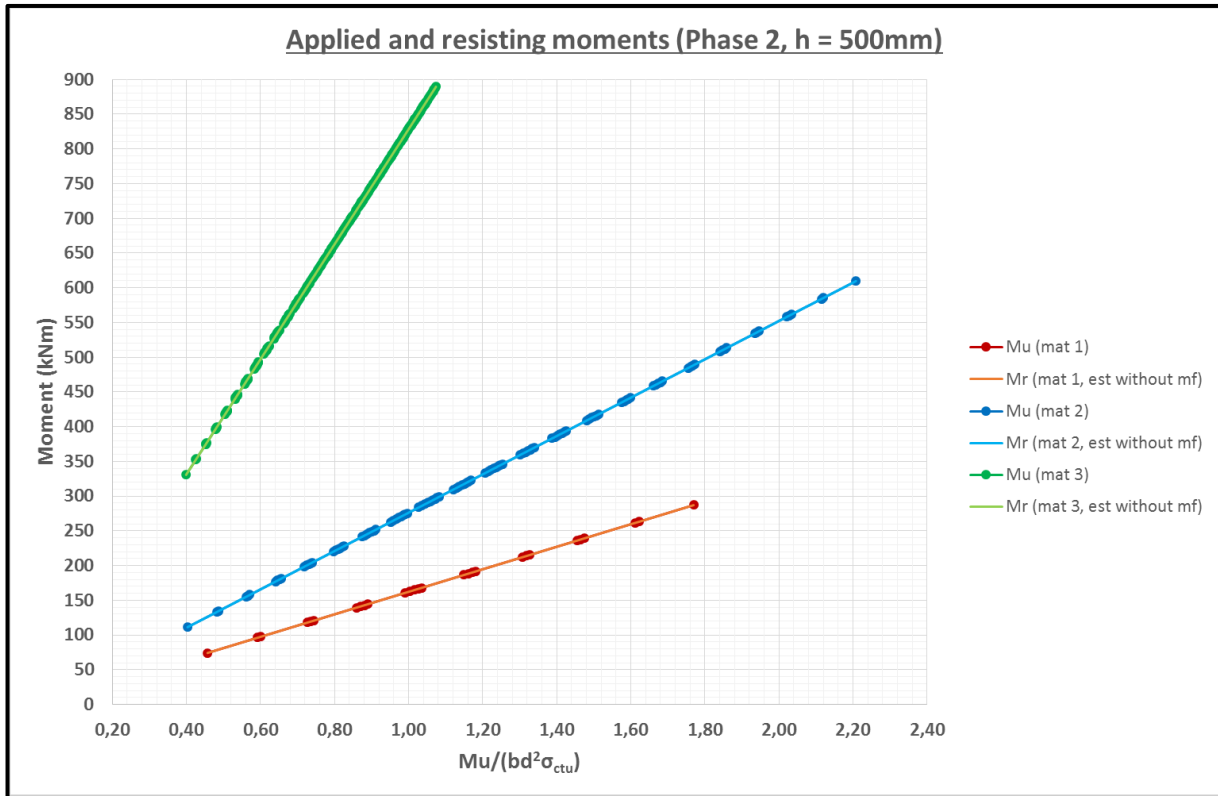


Figure 4-38: Phase 2 - h = 500mm

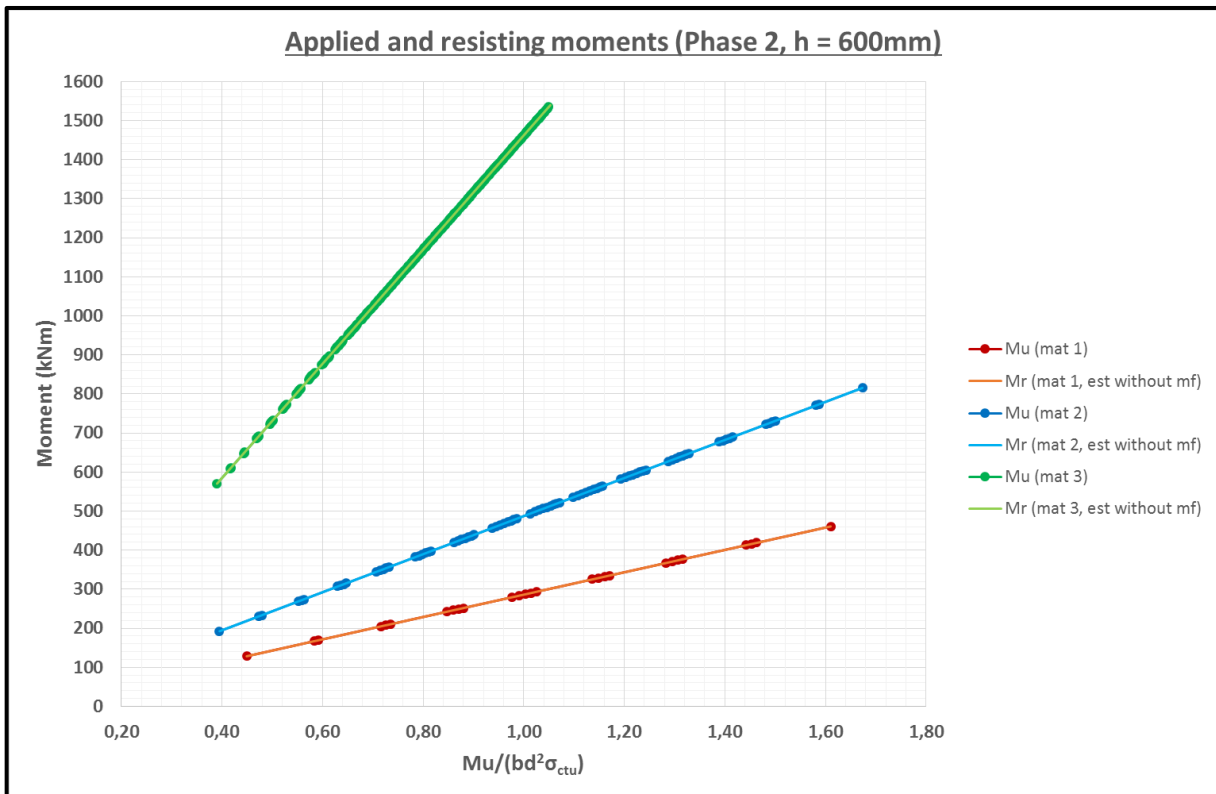


Figure 4-39: Phase 2 - h = 600mm

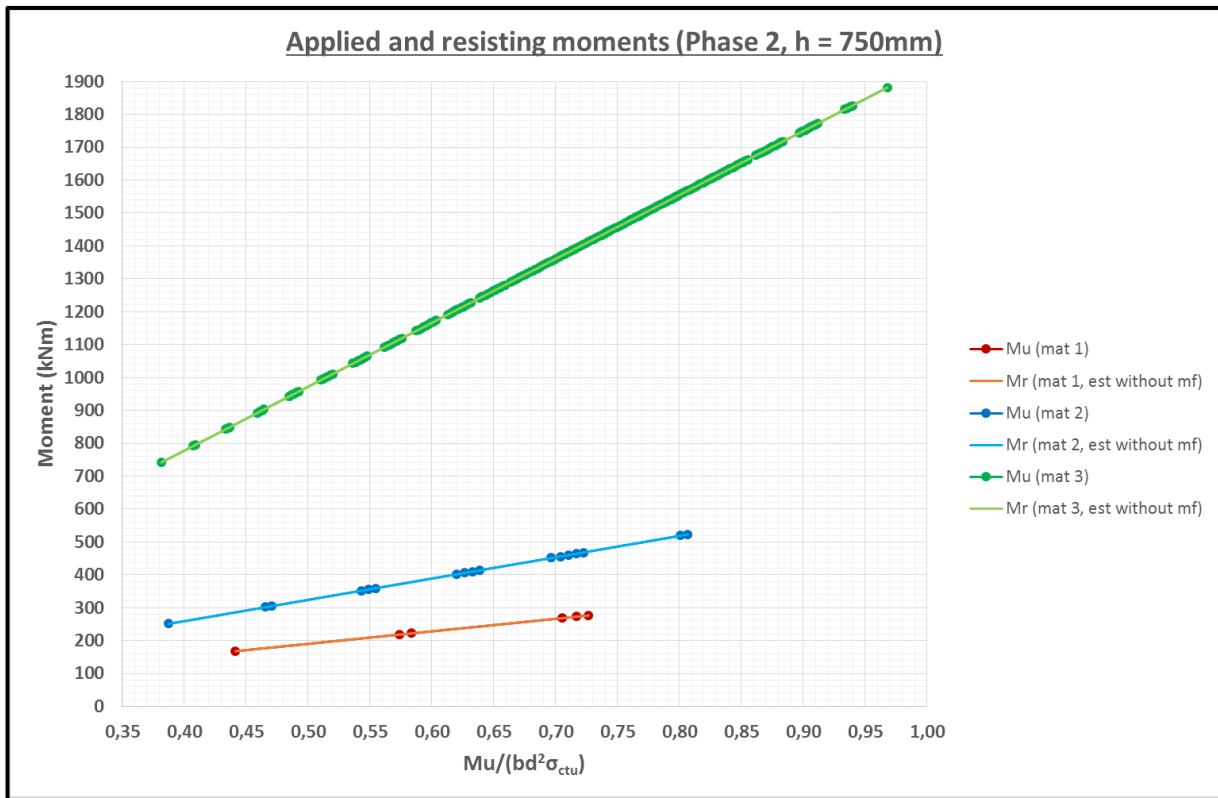


Figure 4-40: Phase 2 - h = 750mm

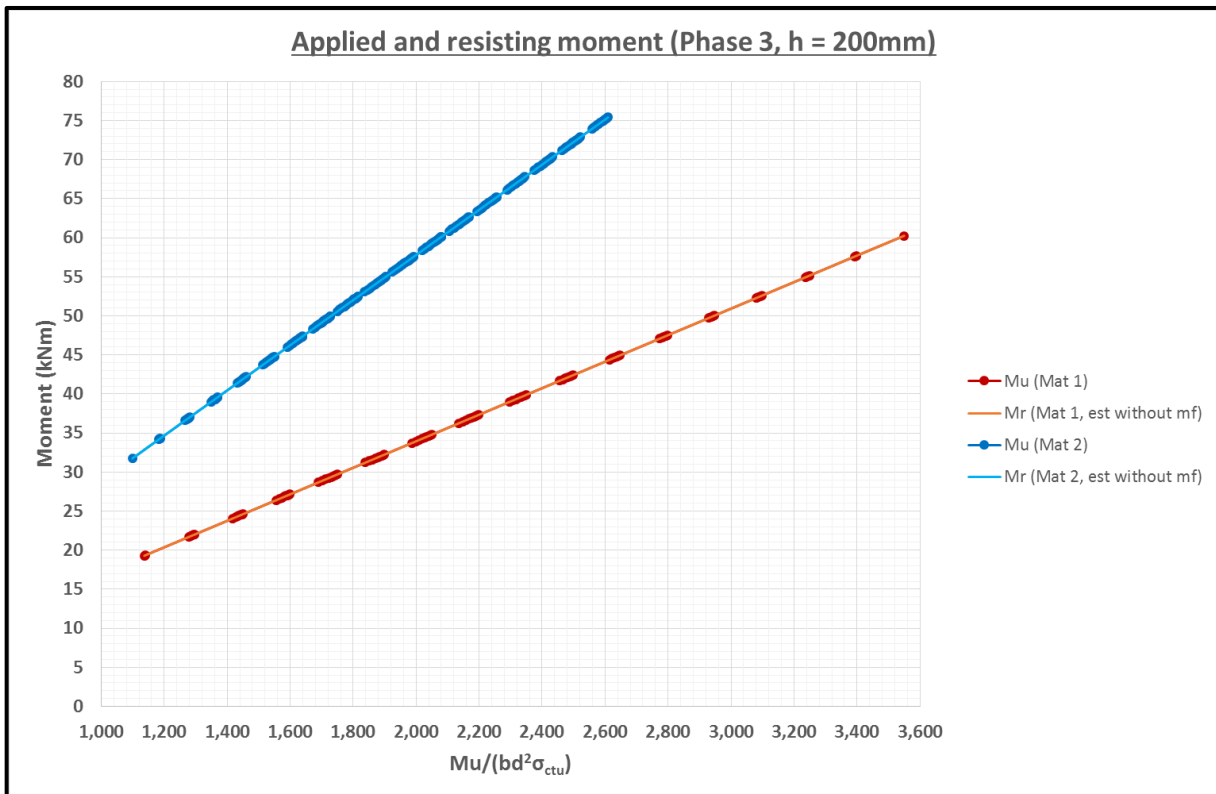


Figure 4-41: Phase 3 - h = 200mm

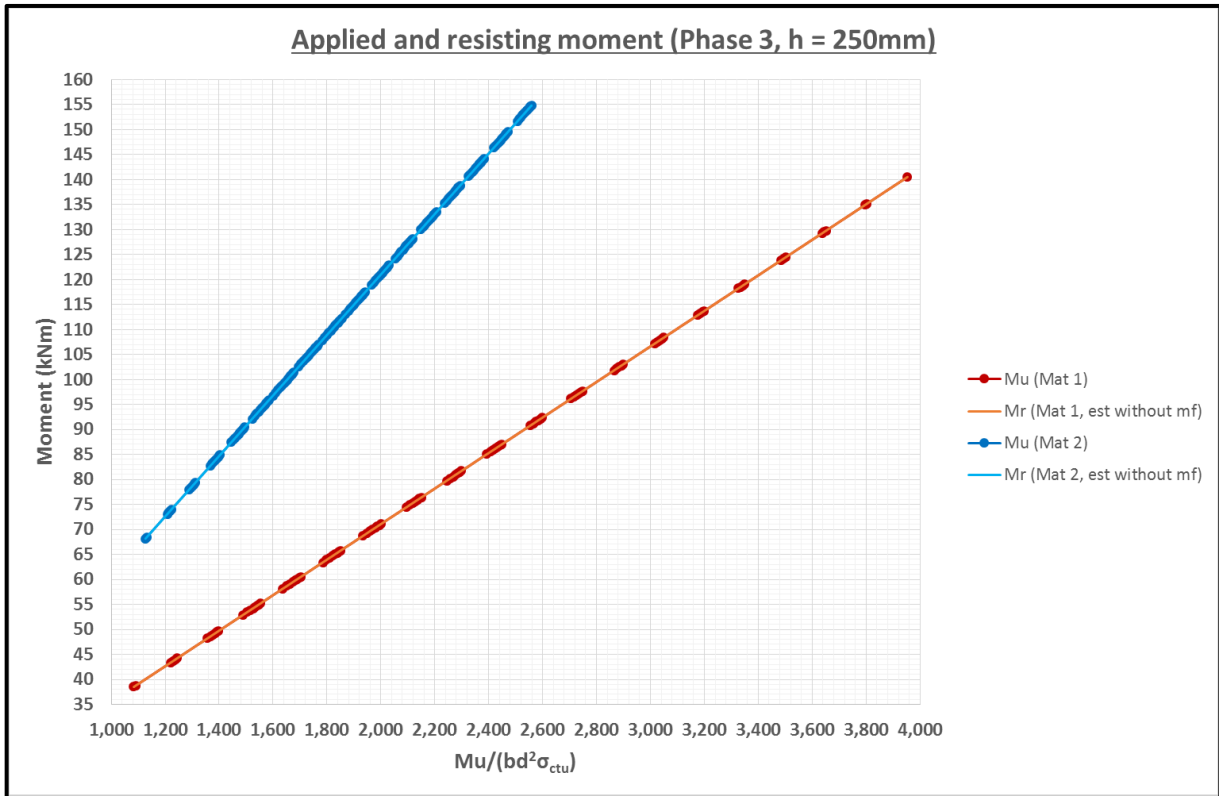


Figure 4-42: Phase 3 - h = 250mm

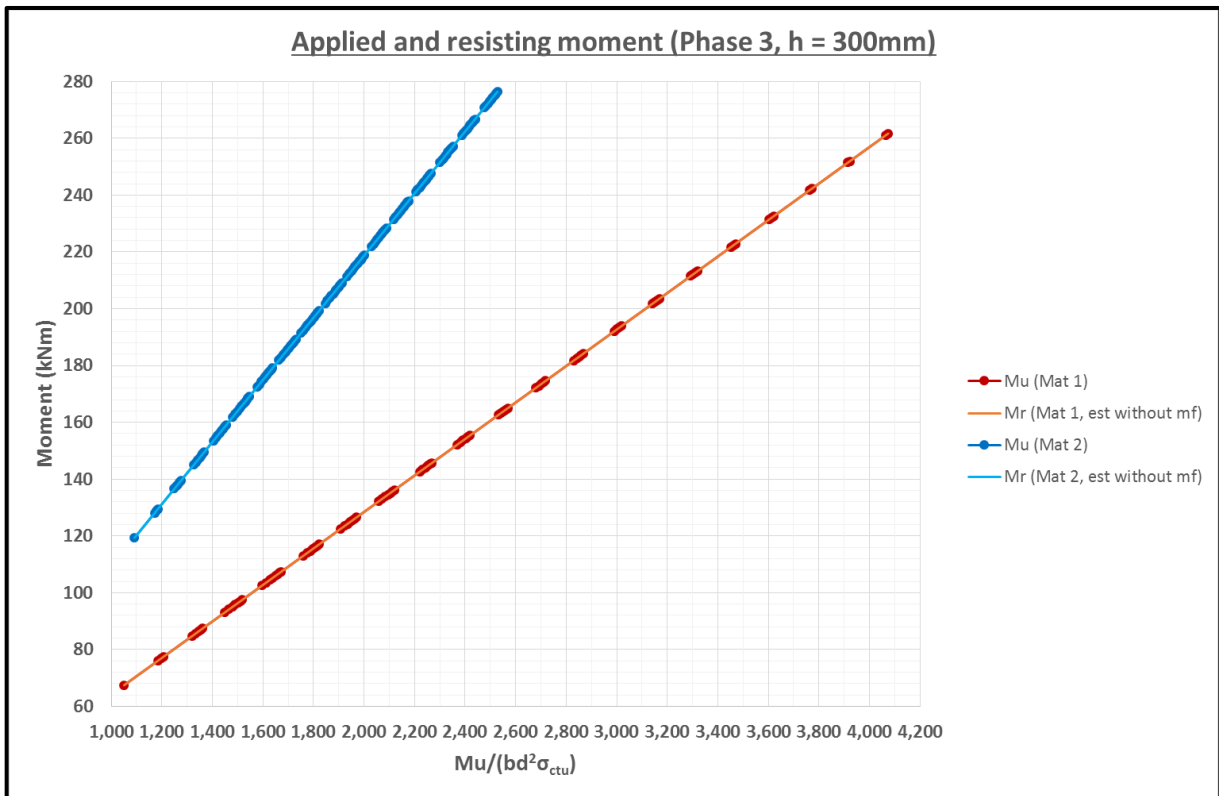


Figure 4-43: Phase 3 - h = 300mm

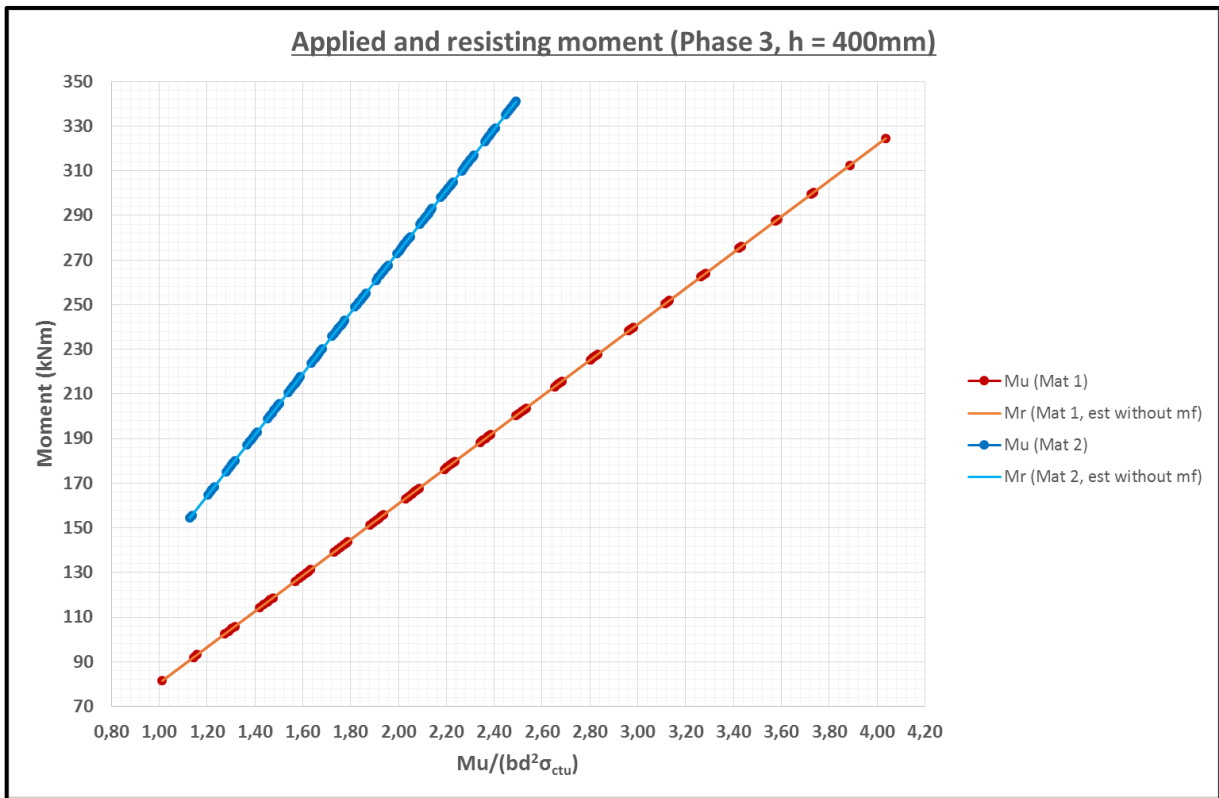


Figure 4-44: Phase 3 - h = 400mm

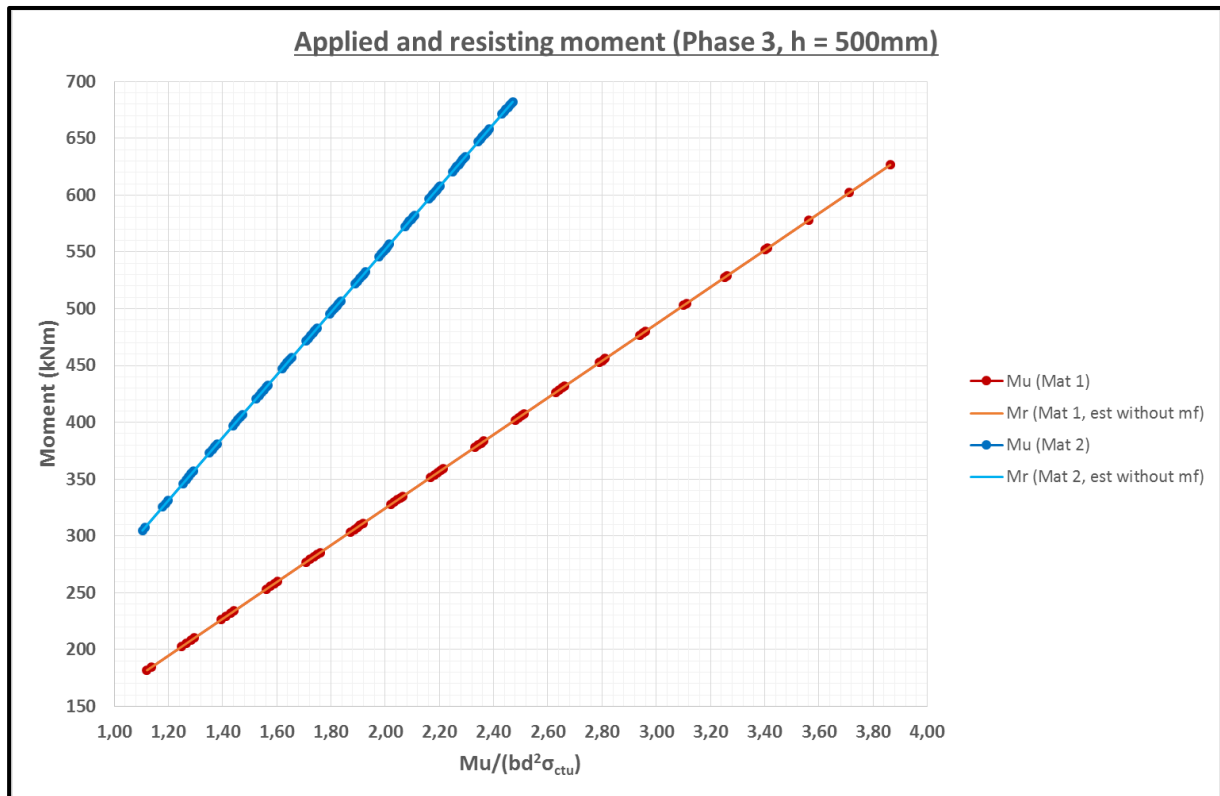


Figure 4-45: Phase 3 - h = 500mm

The accuracy found in Material 1 can be seen in Materials 2 and 3 as well. This shows that the model is applicable to any strain hardening material.

4.5 Conclusion

The original design model is based on three phases in order to incorporate the different phases of the tensile and compressive responses for this material. The first phase is known as the elastic phase and during this phase both the tensile and compressive responses are linear and no cracks have formed in the member. The second phase starts with the first cracks forming in the tensile zone of the member. This phase takes into account the tensile strain hardening of the material but assumes that the compression response is still elastic. When the compressive strain reaches the limit of 0.317 times its ultimate compressive strain, phase 2 ends and phase 3 starts. During phase 3, both responses are assumed plastic and this phase ends in either tensile crack localization or compression crushing at the top of the flexural member.

Because of the intrinsic nature of the base model, a simplified model is needed. In order to simplify the base model, certain information needs to be estimated from the base model in order to be able to establish enough information to do a flexural design. The design tensile strain value is found by calculating various different scenarios of beams and loads, and then assessing the information gathered into a single equation. When this value has been established, the distance to the neutral axis can be found by manipulating existing equations. Eventually the design compressive strain can be found from known relationships and with this information, the tensile and compressive steel can be calculated. It was found that the simplified model gives accurate results without a model factor being added to the equations. If the model factor is incorporated, a measure of conservancy is added to the answers. If the realistic steel values are used to establish the resisting moments, the safety factor on the resisting moments becomes quite big in some cases.

A major drawback of the simplified model is that it is related to the depth of the member and equations are only available for depths up to 750mm for Phase 2 design and 500mm for Phase 3 design. Interpolation can be used for values in between the available design values, but to estimate for depths higher than these are not possible at this stage.

To prove that the model is applicable to all strain hardening materials, the simplified model was tested with two more materials of different strengths. The tensile strain values were found to be remarkably similar and again the simplified model gave highly accurate results. It does show, however, that the model is applicable to other types of SHCC. More material types should be tested in order to establish a more accurate way of calculating the design tensile strain. This would improve the accuracy of the simplified model.

5. DEFLECTION MODEL

5.1 Fundamental Theory of Beam Deflection

In traditional reinforced concrete, RC, beams it is unusual to see multiple cracks forming in the tensile zone. These cracks would normally form around the point of maximum moment or, as per Figure 4-1, in the centre of the beam. It is assumed that at the crack positions, zero tensile stress is transferred by the concrete and all the tensile force is transferred by the steel reinforcement; thus assuming that the concrete loses all tensile strength as soon as it cracks. By friction transfer between the steel bars and the concrete, tensile stress builds up between the cracked sections. This implies that the tensile stress in the concrete at the level of the reinforcement may vary along the length of the beam, from zero (at the crack) to approaching the ultimate tensile strength (roughly one tenth of the concrete compressive strength) away from the crack. This means that different local curvatures, or strain distributions are found along the section height, and act in reality along the length of the RC beam. However, an average situation is normally considered, as shown in Figure 5-1, namely that a small amount, no more than 1MPa, of tensile stress is transferred by the concrete in serviceability limits states for calculating deflections in RC beams (SANS, EC2) [47] [49].

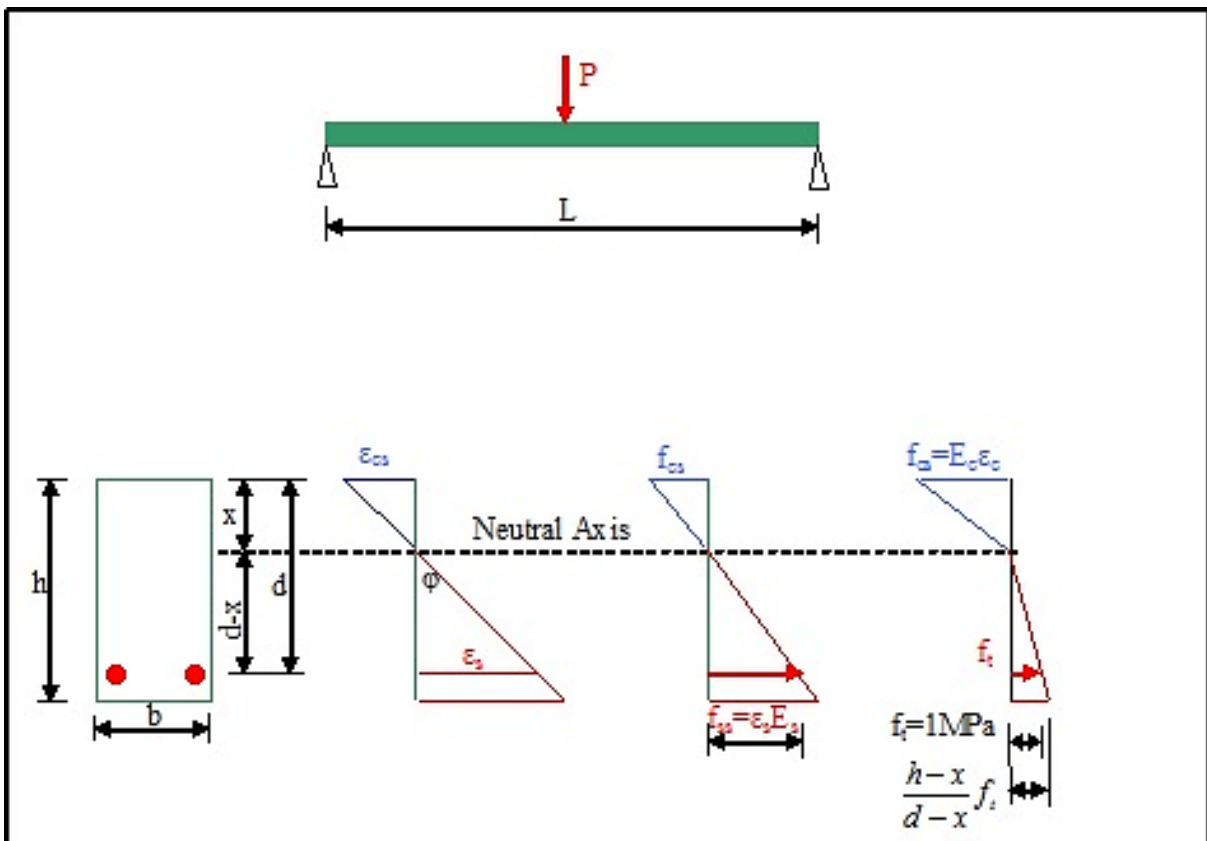


Figure 5-1: Assumed Stress Distribution in Traditional Reinforced Concrete [47]

To calculate the curvature, the equilibrium of forces is taken around the neutral axis, which can be derived from the strain distribution shown in the Figure 5-1, which in turn depend on the neutral axis depth, x . This leads to the following equation:

$$\frac{1}{2}\sigma_{cs}bx = f_sA_s + \frac{1}{2}\frac{h-x}{d-x}\sigma_t b(h-x) \quad 5-1$$

With:

- σ_{cs} = Concrete compressive stress
= $E\varepsilon_{cs}$
- b = Width of the beam
- x = Depth to the neutral axis
- f_s = Tensile stress in the reinforcement
- A_s = Area of tensile reinforcement
- h = Total depth of the beam
- d = Effective depth of the beam
- σ_t = Tensile stress in the concrete at the position of the tensile reinforcement (limited to 1MPa for normal concrete)

The sum of the moments around the neutral axis should be equal to zero. From that it can be deduced that:

$$M_u = \left(\frac{1}{2}\sigma_{cs}bx\right)\frac{2}{3}x + f_sA_s(d-x) + \frac{1}{2}\left(\frac{h-x}{d-x}f_t b(h-x)\right)\frac{2}{3}(h-x) \quad 5-2$$

With:

- M_u = applied moment

It is also known that:

$$\frac{\varepsilon_{cs}}{\varepsilon_s} = \frac{x}{d} \Rightarrow \varepsilon_{cs} = \frac{x}{d}\varepsilon_s \quad 5-3$$

$$f_s = E_s\varepsilon_s \quad 5-4$$

$$\sigma_{cs} = E_c\varepsilon_{cs} \quad 5-5$$

With:

- ε_{cs} = Compressive strain in concrete
- ε_s = Tensile strain in reinforcement
- E_s = Elasticity modulus of reinforcement
- E_c = Elasticity modulus of concrete

If Equations 5-1 and 5-2 is rewritten to take into account Equations 5-3, 5-4 and 5-5, the result is:

$$\frac{1}{2} E_c \frac{\varepsilon_s}{d} b x^2 = E_s \varepsilon_s A_s + \frac{1}{2} \frac{(h-x)^2}{d-x} b f_t \quad 5-6$$

$$\frac{1}{3} E_c \frac{\varepsilon_s}{d} b x^3 = -E_s \varepsilon_s A_s (d-x) - \frac{1}{3} \frac{(h-x)^3}{d-x} f_t b + \frac{PL}{4} \quad 5-7$$

Multiplying Equation 4-6 by $\frac{2}{3} x$ leads to the following expression:

$$\frac{1}{3} E_c \frac{\varepsilon_s}{d} b x^3 = \frac{2}{3} E_s \varepsilon_s A_s x + \frac{1}{3} \frac{(h-x)^2}{d-x} b f_t x \quad 5-8$$

Subtracting Equation 4-7 from equation 4-8:

$$E_s \varepsilon_s A_s \left(d - \frac{x}{3} \right) + \frac{1}{3} \frac{(h-x)^2}{d-x} b f_t h = \frac{PL}{4} \quad 5-9$$

The conditions involved in these equations are:

- $E_s \varepsilon_s \leq f_y$
- $f_t = \frac{d-x}{x} f_{cs} \leq 1.0$
- $f_t = \frac{d-x}{x} E_c \frac{\varepsilon_s}{d} x \leq 1.0$
- $f_t = \frac{d-x}{d} E_c \varepsilon_s \leq 1.0$

By solving Equation 5-8 and 5-9 simultaneously the depth of the neutral axis, x , can be obtained. The strain in the tensile reinforcement, ε_s , can also be found. With this information, the curvature can be calculated from Equation 5-10.

$$\rho = \frac{1}{r} = \frac{\varepsilon_s}{d-x} \quad 5-10$$

The vertical displacement of a beam can then be expressed by the differential equation:

$$\frac{d^2u}{dx^2} = \frac{1}{r} = \rho \quad 5-11$$

Where:

- x = Coordinate system axis along the beams' centroid axis,
- r = Radius of the deformed shape of the beam in flexure

Equation 5-11 can be solved by direct integration and the introduction of particular boundary values. The curvature-area method is useful for the solving of simple beam systems, for instance simply supported beams or cantilever beams, as shown in Figure 5-2.

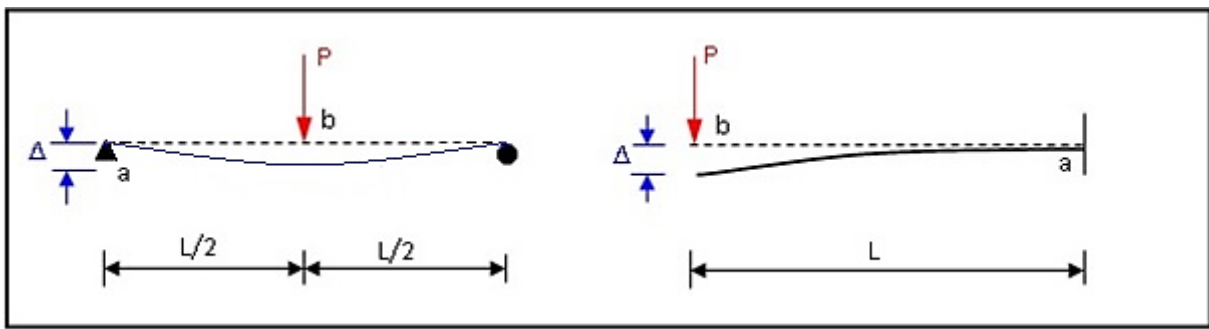


Figure 5-2: Simple Beam Configurations

With this theory it can be shown that the maximum displacements are given by:

$$\Delta = \int_a^b \frac{1}{r} x dx \quad 5-12$$

Thus, the displacement is the first moment of the curvature area between points a and b, and about point a.

Note that only time-independent deflection is considered in this study. To include time dependence, environmental strains are added to the mechanical strains to take into account shrinkage and creep. This changes the curvature. These environmental strains are mostly site specific and not dealt with here.

5.2 Linear-elastic behaviour

For linear elastic material behaviour, the curvature is given by:

$$\frac{1}{r} = \frac{M}{EI} \quad 5-13$$

It is also known that the moment along the length of the beam for a simply supported beam loaded with a point load in the centre of the beam can be calculated with Equation 5-14, where the maximum moment occurs when $x = L/2$:

$$M(x) = \frac{Px}{2} \quad 5-14$$

Likewise, the moment along the length of a cantilever beam loaded with a point load on the end of the cantilever can be calculated with Equation 5-15, where the maximum moment occurs when $x = L$:

$$M(x) = Px \quad 5-15$$

By substituting Equations 5-13 and 5-14 into 5-12, the following expression for calculating the deflection of a simply supported beam with a point load in the centre is derived:

$$\Delta = \int_0^L \frac{1/2 Px}{EI} x dx = \frac{PL^3}{48EI} \quad 5-16$$

Then, by substituting Equations 5-13 and 5-15 into 5-12, the following expression for calculating the deflection at the end of a cantilever beam, can be derived:

$$\Delta = \int_0^L \frac{Px}{EI} x dx = \frac{PL^3}{3EI} \quad 5-17$$

Often, the maximum deflection is expressed in terms of a particular curvature. This is usually the maximum curvature ρ_m at mid-span, in a simply supported beam, and at the support, in a cantilever beam. The maximum deflection is then expressed as follows:

$$\Delta = KL^2 \rho_m \quad 5-18$$

Where, K, denotes the coefficient taking into account the boundary value type as well as the load configuration.

5.3 Deflection calculation for R/SHCC beams

5.3.1 Introduction

Figure 5-3 shows the postulated schematic representation of the three different phases of deflection for a simply supported beam loaded with a single point load in the centre.

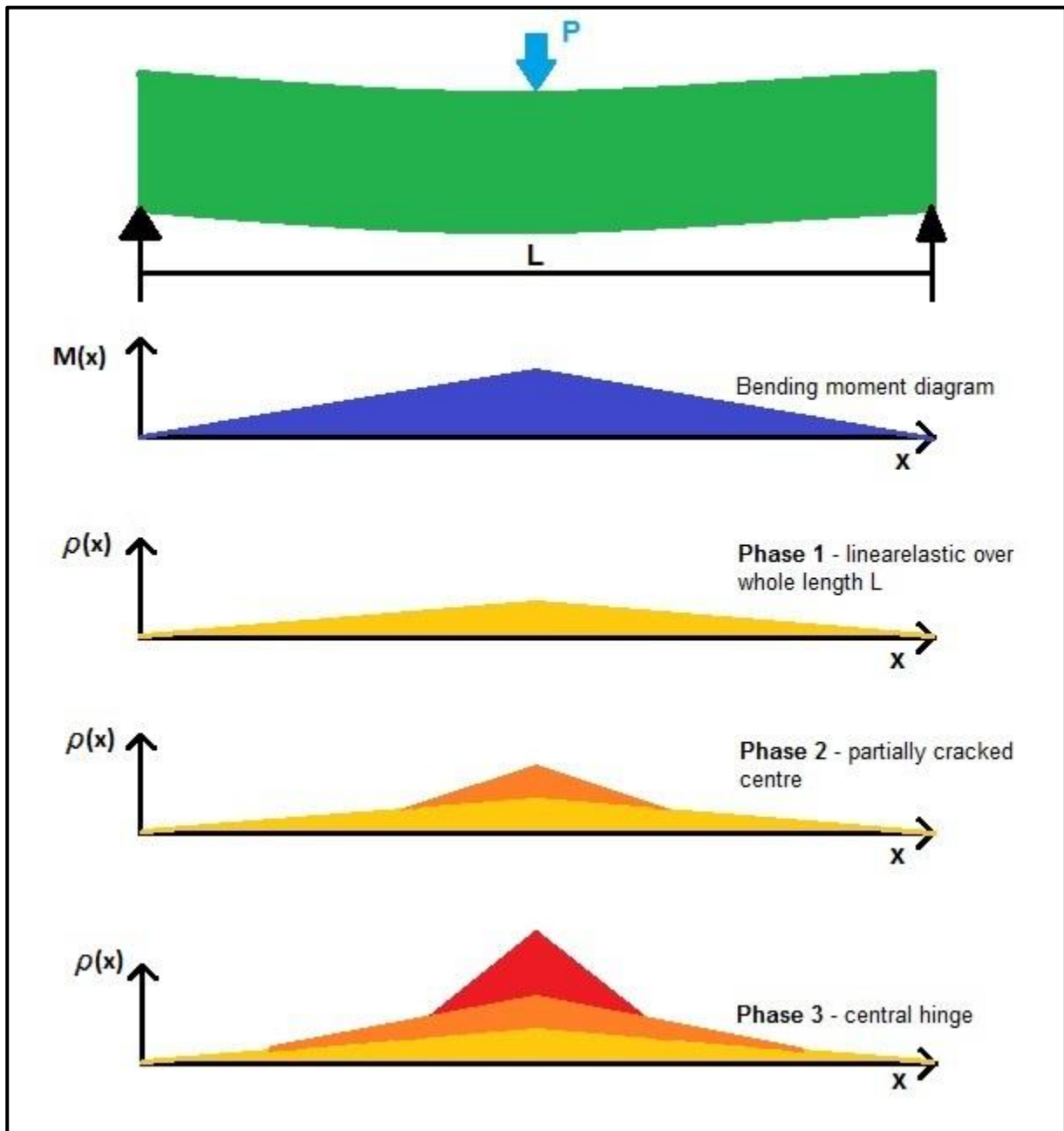


Figure 5-3: Schematic representation of the three phases of deflection

5.3.2 Phase 1 - Linear-elastic behaviour

During phase 1, the cement matrix has not cracked and so the material is assumed to behave linear-elastically. For linear-elastic material behaviour, the deflection can be calculated as for normal

concrete. The curvature can be calculated by using equation 5-13, and as the moment calculation does not change with the material type, the deflections can be calculated by using equations 5-16 and 5-17 for simply supported beams, and cantilever beams respectively.

Equation 5-19 is an expanded version of Equation 5-16

$$\Delta = \frac{PL^3}{48E_cI_{tr}} \quad 5-19$$

Where:

- Δ = Deflection at the centre of the beam.
- P = Point load applied in the centre of the beam.
- L = The effective length of the beam.
- E_c = Elasticity modulus of the cement material.
- I_{tr} = Transformed moment of inertia of the cross section under consideration.

This method was used in calculating the deflections for Phase 1 of the model predictions.

5.3.3 Phase 2 – Strain Hardening

In reinforced SHCC beams there are two main phases of deflection after the elastic limit has been reached. This is shown in Figure 5-4.

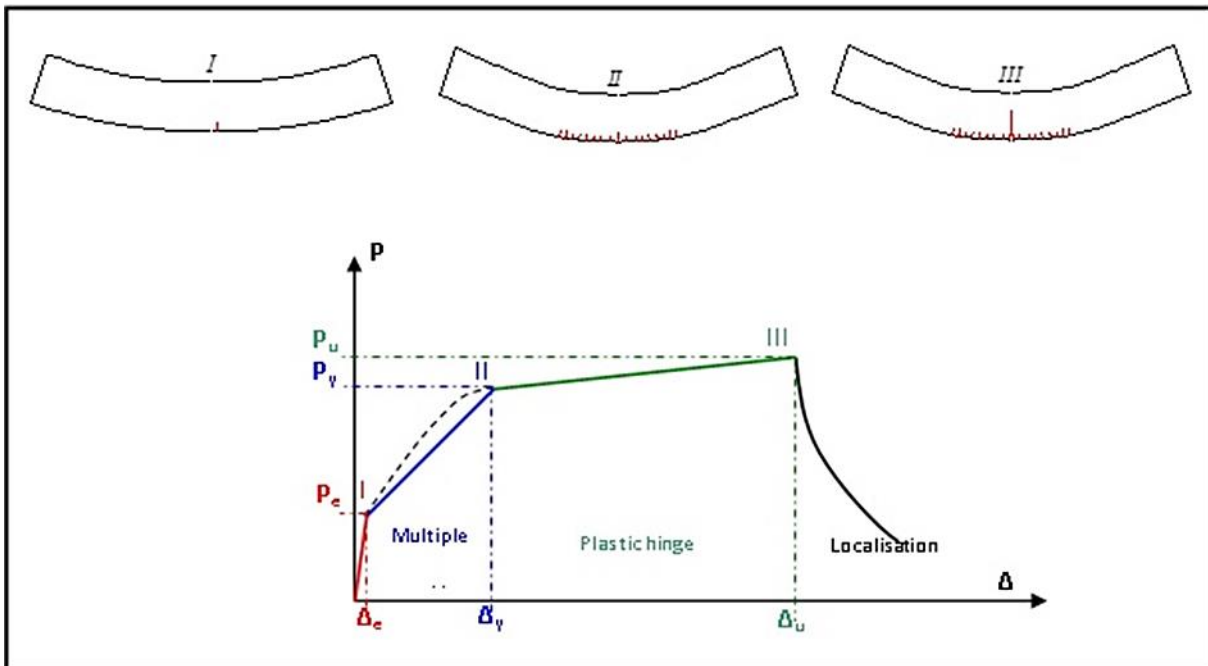


Figure 5-4: Schematic Representation of SHCC Beam Load - Deflection Phases

Micro-cracking starts after the elastic limit is reached at load P_e , with the corresponding deflection Δ_e . Because the cement matrix is now cracked, it has lost some of its stiffness. As the cracks spread along the length of the beam, the cement-based matrix is weakened or damaged. The curvature in this damaged region will differ from the curvature in the undamaged areas of the beam. The cracks do not spread along the whole length of the beam, but stop at some point, when crack saturation is reached. This phase ends with crack saturation (P_y, Δ_y) and a plastic hinge forms where crack localization occurs.

The differential Equation 5-11 and the curvature-area Equation 5-12 may be used to determine the curvature and deflection of beam elements made up of inelastic materials. The simplified expression for determining the curvature for linear-elastic materials, Equation 5-13 is no longer valid. This is because the curvature is no longer proportional to the bending moment, but depending on the local cracking behaviour of the beam. As illustrated in Figure 5-4, the curvature increases at crack locations in the beam. This increased curvature needs to be taken into account when calculating the deflection.

For design purposes, it is important to utilize the multiple cracking behaviour of SHCC. Figure 5-4 shows that this phase starts at P_e , when the first crack is initiated, and ends at P_y , when crack saturation is reached. Crack saturation is reached when all possible cracks have formed. After this, no new cracks will form, but a few existing cracks will widen up as a result of fibre pull-out and/or breakage. The strain hardening phase is the optimal phase for this material to be in, as this is where the tensile strain hardening has been activated, but the compression is still elastic. This will thus be the safest phase for design of a flexural member. This phase should thus be considered in the design for both ultimate limit state, crack width calculations, as well as serviceability limit state, deflection calculations. In Figure 4-4, an assumption is made of the strain and stress distributions at the end of the strain hardening phase at mid-span for the case of a centrally loaded simply supported beam. This point is where the maximum bending moment will occur and is also the position of the greatest curvature. This is also the case for the elastic phase, phase 1. This is not obvious because of the multiple cracking nature of SHCC, which shows uniform crack spacing and approximately uniform crack width over the entire cracked region. It is thus harder to find the point of maximum curvature, than it would be in a normal concrete element which will have one or two wide cracks at failure.

The end of the strain hardening phase is marked by the start of crack localization at mid-span, meaning the widening of the central crack, where the largest bending moment acts. For this reason the tensile strain at the furthest tensile fibre in the cross-section is indicated as ε_{tu} in Figure 5-5. The strain value is defined in Figure 5-5, where the simplified uniaxial tensile behaviour of SHCC is shown schematically.

The stress state on the compression face is unknown. It may vary, depending on the particular SHCC relation between compressive and tensile strength, beam geometry, and the level of steel reinforcement in the R/SHCC. For the flexural model, the compression was kept elastic up to the point where the compressive strain reaches 0.317 times its ultimate strain value. From this point forward, the compressive stress and strain relation is shown in Equation 4-22. This is explained in more detail in Chapter 2.

It is assumed that the strain is linear along a cross-section. This is shown in Figure 5-5. Considering the uniaxial material behaviour of SHCC, force equilibrium, and moment equilibrium, it is possible to derive the stress distributions as shown in Figure 5-5.

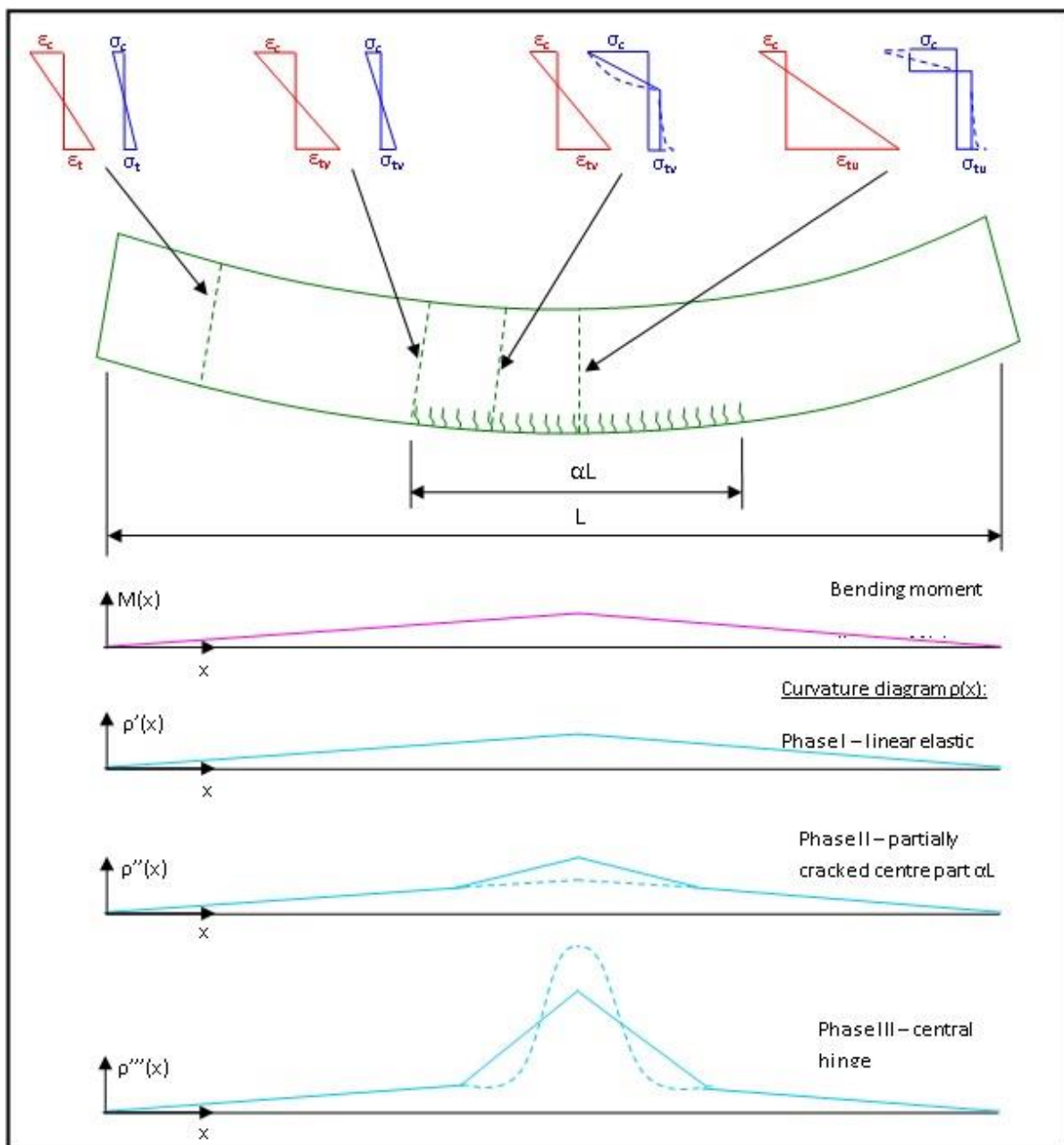


Figure 5-5: Schematic Representation of SHCC Beam Sectional Strain and Stress distributions

The width of the cracked region, αL , as indicated in Figure 5-6, can be estimated from the first cracking tensile stress σ_{ty} and the bending moment diagram in Figure 5-6. The relationship between the moment at the end of the linear-elastic phase, M_e , that is when the first cracks in the beam occurs at mid-span, and the bending moment at the end of the strain hardening phase, M_y , determines the cracked length. This is based on the assumption that all material points have equal tensile strength. Then the cracked region can be derived as:

$$\alpha = 1 - \frac{M_e}{M_y}$$

5-20

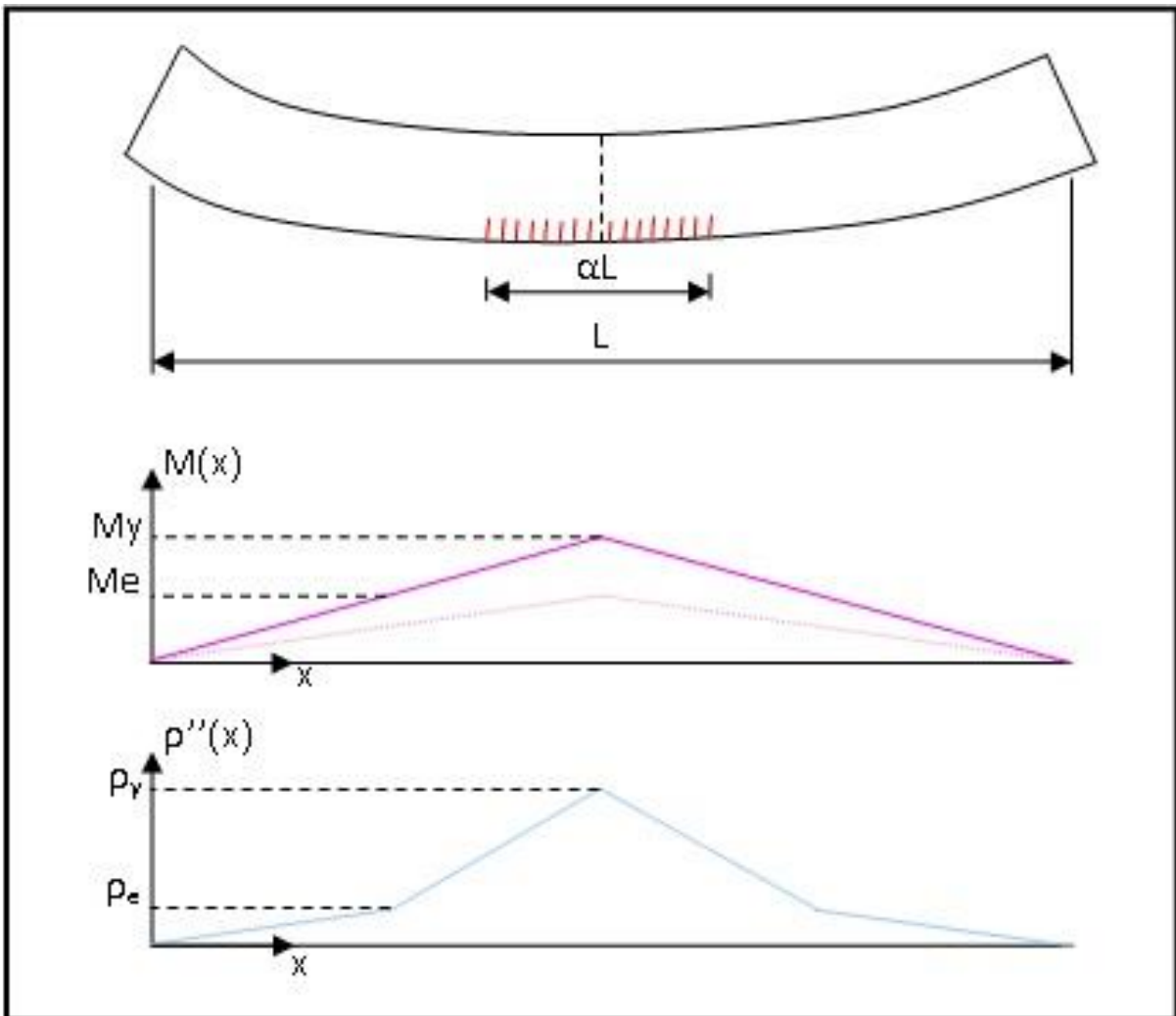


Figure 5-6: Schematic Representation of SHCC Moment and Curvature Diagrams

The simplified curvature diagram given in Figure 5-6 can be integrated by using the following relationship;

$$\epsilon_c = \frac{-x}{h-x} \epsilon_t$$

5-21

Or it can be numerically integrated by using;

$$\rho_y = \frac{\varepsilon_c}{x} \quad 5-22$$

In order to calculate the mid-span deflection, however, the simple nature of the diagram allows for analytical integration, leading to the following expression for the mid-span deflection:

$$\Delta = \frac{1}{2}\rho_e \frac{L^2}{4} \frac{2}{3}(1 - \alpha)^2 + \rho_e \frac{\alpha L}{2} \frac{L}{2} \left(1 - \frac{\alpha}{2}\right) + \frac{1}{4}(\rho_y - \rho_e) \frac{\alpha L}{2} L \left(1 - \frac{\alpha}{3}\right) \quad 5-23$$

This is the approach that was used to determine the deflection for phases 2 and 3 of the model predictions. The beam was divided into eighths and the curvature at the beginning and end of each eighth piece was calculated. The areas under these curvatures were then calculated and added as per Equation 5-23.

5.3.4 Phase Three

Phase 2 of the deflection path ends when crack saturation has occurred (P_y , Δ_y) and a plastic hinge is formed. Phase 3 of the deflection path has now started. This allows for an increase in deflection without an increase in loads, or sometimes, deflection hardening (or strain hardening) up to a loading level P_u and a mid-span deflection of Δ_u . This last ultimate stage is indicated by the start of crack localization in a single crack at mid-span. The crack patterns at the various phases are shown in Figure 5-4.

5.3.5 Tension Stiffening in R/SHCC members in flexure

A tension stiffening effect has been reported in reinforced HPFRCC [50], where the concrete material has been reported to carry tension beyond the yield strain of the mild steel reinforcement. Moreno et al [50] concluded that splitting cracks in the concrete contributes to the spreading of strain along the reinforcing bars, resulting in larger displacement capacity. These splitting cracks are normally absent in SHCC members, implying that their displacement capacity would be lower than that of normal concrete.

Moreno et al [50] also states that the ultimate fracture strain of the reinforcing bar is a function of the ability of the HPFRCC to resist or restrain splitting cracks and to prevent or allow the formation of dominant transverse cracks at specimen strains over 1%. If the formation of splitting cracks is prevented and no dominant cracks are allowed to form along the length of the length of the specimen, strain will localise in the first dominant transverse crack. This will then lead to early fracture of the steel reinforcement. If splitting cracks occur, strains are more evenly spread and several of the

multiple transverse cracks can grow wider together. This delays reinforcement fracture and higher deformation levels are possible.

5.3.6 Comparing the Predicted Deflected shape to the Measured Deflected shape

In Figure 5-7, the predicted shape of the deflection for one of the test beams was plotted against the measured shape of the deflection. The predicted deflection is conservative in all three phases of the model, over estimating the deflection by approximately 2mm. The shape of the predicted deflection is hard to calculate but the comparison is quite good in the image below.

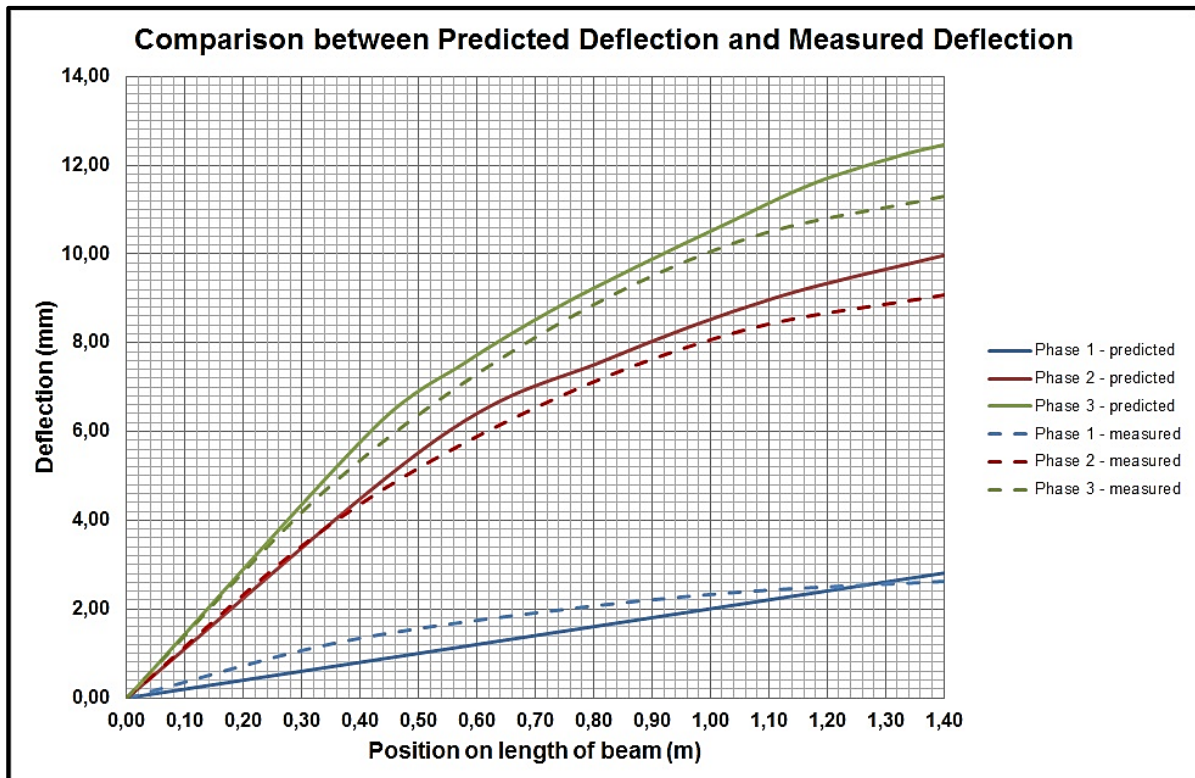


Figure 5-7: Predicted Deflection vs Measured Deflection along length of beam

5.4 Serviceability

According to SANS 10160-1:2011, serviceability limit states specify the following requirements for a structure under normal use:

- The functioning of the structure or structural members.
- The acceptability of the structure by users in terms of perceived safety and well-being
- The appearance of the structure.

All of the above hint at deflections, as excessive deflection can be the cause of a building not being able to function as intended. Doors and windows sticking in their frames and tiles popping from floors

are only a few phenomenon that will reduce the functionality of a building. Visibly sagging floors not only makes people feel unsafe, but it impacts on the aesthetics of the building.

For a flexural member to be serviceable it needs to be within the deflection limits set in the various codes used for structural design. These limits are normally set according to the sensitivity of the finishes applied to the structure and vary between countries. For instance, glass will crack when exposed to too much deflection while brickwork is more flexible and can withstand larger deflection before it starts cracking.

A general limit for deflections in slab and beam structures is $L/250$ or 30mm, whichever is the smallest. This is the limit used to calibrate the model in order to make sure that the information it gives will be both serviceable and structurally correct. When calibrating the model, a span/d limit of 16 was used, but for lengths exceeding 10m, deflection was still a problem for the weaker materials. This is assumed to be because of the ductility of the material used, as SHCC is much more ductile than normal concrete. However, the concrete code also specifies that for spans over 10m the deflection must be proved by calculation and the span/depth ratios cannot be blindly followed.

5.5 Conclusion

The deflection of the SHCC member is found by applying the same principles as for conventional RC. When the material is elastic, an elastic approach can be adopted, but for a cracked section, the deflection must be found by means of analytical or numerical integration.

Deflection calculations are important in order to establish the serviceability level of the member. Too much deflection can lead to unsightly cracking in structures and visible deflections makes occupants feel unsafe. The serviceability limits as set out for conventional concrete were adopted for SHCC in this instance.

6. RELIABILITY

6.1 General

The development of design methods needs to include measures for ensuring structural safety. This is done in the form of partial factors. Partial factors are normally calibrated on existing practice, but in the case of SHCC, reliability calibration methods will have to be used in the absence of existing practice data.

A measure of reliability is the reliability index, β_R , which is related to the probability of failure, p_f , by the following equation [46]:

$$p_f = \Phi(-\beta_R) \quad 6-1$$

Where, Φ , is the cumulative distribution function for the standard normal distribution.

In the Eurocodes, the target reliability is given by $\beta_T = 3.8$ (EN 1990). South African codes have a minimum target value reliability of $\beta_T = 3.0$ for ductile failure modes [46].

To ensure that the resistance model has an acceptable level of reliability, a partial resistance factor, γ_M , is used. The factor consists of two parts; a material factor, γ_m , to take into account the uncertainty in the material properties, and a model factor, γ_{RD} , to take into account the uncertainties in the design assumptions made when developing the model [46].

A limit state is defined as the border between a safe and an unsafe state in the structure. When considering the performance function, $g = R - E$, the safe state is represented by $g > 0$ ($R > E$), and the unsafe state is given by, $g < 0$ ($R < E$) and the limit state is shown as $g = 0$ [46]. Where R is the resistance and E is the imposed load.

In design codes, the design value method is normally used in finding the limit state expressions. This method includes finding a design value for each basic variable by making use of partial factors. An adequate design will then be one for which the limit states are not reached when the design values are used in the resistance model [46]. This can be expressed as:

$$E_d < R_d$$

Where:

- E_d = design value of load effects

- R_d = design value of resistance

6.2 Material Strength

6.2.1 Statistical Properties of Critical Parameters

The statistical properties of the critical parameters are required in order to determine acceptable levels of structural reliability. This may be done by determining characteristic values of the properties along with a reliable material factor, or by finding design values directly [46]. For the purpose of this study, it was important that the design could be used on most classes of strain hardening cement composites. It would thus be more efficient to find material factors that could be used along with characteristic values to find proper design values for the critical parameters.

It was not possible to obtain big enough sample sizes in order to derive stable values of the mean, standard deviation, and skewness of the parameters in question. Most samples contained 6 or less elements. Combining the samples was not possible in most cases as the samples were taken from different material mixes.

6.2.2 The Conversion Factor

The conversion factor represents the ratio of in situ strength of a material to the cube, or laboratory tested strength, and is thus a factor that is derived over time and by experience [46]. This factor can either be accounted for in the determination of the design material strength parameters, or in the resistance model calibration. The ideal way of determining the conversion factor is to compare results from cubes cast and tested in laboratory conditions, and core samples taken from site. As SHCC has many critical parameters, and most of them show great variation when tested, it seems necessary that there should be a conversion factor for each critical point in the model. For normal reinforced concrete, the conversion factor is taken as 0.85, and has been derived from data accumulated over years of use. This factor is then applied only to the compressive strength of the concrete, as this is the only material parameter used in design calculations.

The development of SHCC as a construction material only took place recently and no site related data exists for this material. Therefore, the conversion factor is unknown. As this material does not involve complicated mixing techniques and has the same curing procedure as normal concrete, it seems logical that the conversion factor for normal concrete could be a starting point for estimating the conversion factors needed for SHCC.

For normal concrete, the conversion factor is only applied to the concrete compressive strength. SHCC, on the other hand, has compressive as well as tensile parameters that need to be defined and there are stresses as well as strains involved. The critical points in the model are defined by the

critical parameters of the material. These are the first cracking point or yield point, defined by the tensile yield stress and strain of the material. Then there is the point of crack localization which is defined by the ultimate tensile stress and strain of the material. The last critical point is the maximum compressive strength, defined by the ultimate compressive stress and strain of the material.

All of these critical points have two critical parameters defining them. It seems inappropriate that both the parameters should have conversion factors applied to them as that would reduce the strength of the material considerably. As the conversion factor for normal reinforced concrete is only applied to the ultimate strength of the material, it seems prudent to do the same for SHCC and apply the conversion factors only to the strength parameters of the material. Based on the coefficient of variation for each of the parameters, and applying the 0.85 conversion factor to the ultimate compressive stress, the conversion factors for the rest of the strength parameters are shown in Table 6-1. The coefficient of variation was derived from the tests done for this study, as well as other data received from a colleague research student in the group [51]. All inclusive, there was about 100 tests evaluated but the sample sizes were limited to a minimum of 3 and a maximum of 9. They could not be combined as they were not done from the same batch or with the same mix, but were roughly for the same strength of material. Only the test results for tests done during this study are shown in Chapter 3.

Table 6-1: Conversion Factors

Material Property	Coefficient of Variation	Conversion Factor
σ_{ccu}	0.090	0.850
σ_{ct1}	0.196	0.390
σ_{ctu}	0.097	0.790

6.2.3 Material Factor

The material factor for a specific critical parameter is defined as the coefficient of variation of the characteristic value multiplied by its conversion factor, and divided by the design value for this particular parameter [46]. The characteristic value was taken as the 0.05 fractile of the distribution and the design value as the 0.0082 fractile [46]. All samples were taken as having a normal distribution as there were not enough elements in the samples available to define the statistical properties of the various distributions.

As per the derivation of the conversion factor, it was deemed to be overly conservative to apply a material property to the stresses as well as the strains of the material. As an alternative, it would be

better to apply the conversion and material factors to the stress or strength parameters of the material, and then impose limits on the strain parameters, rather than applying more factors. The material factors for the strength parameters are shown in Table 6-2.

Table 6-2: Material Factors

Material Property	Conversion Factor	Material Factor
σ_{ccu}	0.850	1.220
σ_{ct1}	0.390	2.833
σ_{ctu}	0.790	1.326

The values shown in Table 6-2 were calculated by finding the material factors for each sample test data available, and then calculating the average value. The material factor for each sample was found by calculating the mean, coefficient of variation, skewness, and characteristic value and then also the design value, and then dividing the characteristic value by the design value. The coefficient of variation, V_X , the characteristic value, X_k , and the design value X_d , were calculated by using the following equations:

$$V_X = \frac{1}{m_X} \sqrt{\frac{\sum(x_i - m_X)^2}{n-1}} \quad 6-2$$

$$X_k = m_X(1 - k_n V_X) \quad 6-3$$

$$X_d = \eta_d m_X(1 - k_{d,n} V_X) \quad 6-4$$

Where:

- m_X = Sample mean obtained from test data
- k_n = Fractile estimator
- η_d = Conversion factor
- $k_{d,n}$ = Design fractile estimator

The fractile estimators can be found in the EN 1990 [52] or in [46].

6.2.4 Limiting Strain Values

6.2.4.1 Compressive Strain

The strain values defining the critical points on the tension and compression responses for SHCC have a very high variation coefficient. As was indicated earlier, it seems inappropriate to impose a conversion and material factor on both the stress and the strain for compression and tension as this would lead to a very conservative design. Further to that, the high variation of the strain values would lead to very high material factors being imposed on the strain values. Combining these high factors with the factored down stress values, and the design would be ridiculously conservative. The alternative is to factor the stress values as was done in the previous part of this chapter, and then impose limits on the strain values, ensuring that they are conservative but not overly so.

Examining the compression parameters, it was found that the compression value for elasticity modulus, was quite constant. The expression for calculating this value is given in Equation 2-3. This expression involves the ultimate compressive stress as well as the ultimate compressive strain. Finding the ultimate compressive stress is not a hard task, and if the E value can be defined as a definitive value, the strain value is not hard to come by either.

From the test data available, it was found that the average value for the elasticity modulus is 14.833GPa. An average value would, however, not be a conservative approach to use. For that reason the design value was calculated, using Equations 6-2 to 6-4. The design value was found to be 8.063GPa. This means that for a SHCC mix with ultimate compressive strength of 30MPa, the ultimate strain value can be calculated as follows:

$$\sigma_{ccd} = \frac{\sigma_{ccu}}{1.220} = 24.590MPa$$

$$\varepsilon_{ccd} = 1.681 \frac{\sigma_{ccd}}{E_{ccd}} = 0.00513$$

6.2.4.2 Tensile Strain

Naaman and Reinhardt [39] proposed a classification for SHCC based on the tensile properties of the material. This classification is discussed in more detail in Chapter 2, but for clarification it is necessary to highlight a few points from their work.

Naaman and Reinhardt proposed a tensile Elasticity Modulus of 10.5GPa. Although there are indeed some materials that show a value much lower or higher than that, this value ties in very well with the average values obtained from the material test data accumulated. Calculating the elasticity modulus for the tensile response is somewhat cumbersome as it is very difficult to find the exact strain values

where yielding takes place. Limiting the E-value to something sensible makes the process of determining the yield strain so much easier, as the yield stress is much easier to find from test data. In the work by Visser (2007) [40], E-moduli determined from tensile tests and those determined from compressive tests were in close proximity, within 0.1% for cast specimens, and 12.3% for extruded specimens.

The ultimate tensile strain shows as much deviation as the yield strain, but a design value was found by analysing the available test data. An ultimate tensile strain value of 0.0246 is proposed as a maximum limit on the tensile strain. Naaman and Reinhardt, [39], proposed a value of 0.005, which seems to be very low as most of the tensile failures only happen at around 2 – 3% strain levels.

6.3 Model Uncertainty

6.3.1 Theoretical Predictions

To establish the accuracy of the design model, it was tested against the results obtained from the actual tests. See Chapter 3.4.1 and 3.4.2 for the results. The test results were also broken down into the three phases of the model to establish the accuracy of each phase separately. This shed some light on the validity of the assumptions made in each phase as well as the limits defining the three phases.

To be able to compare the model predictions with the test results, the values were plotted against one another on a graph. Figures 6-1, 6-2 and 6-3 show the different scatter plots for the three phases of the model.

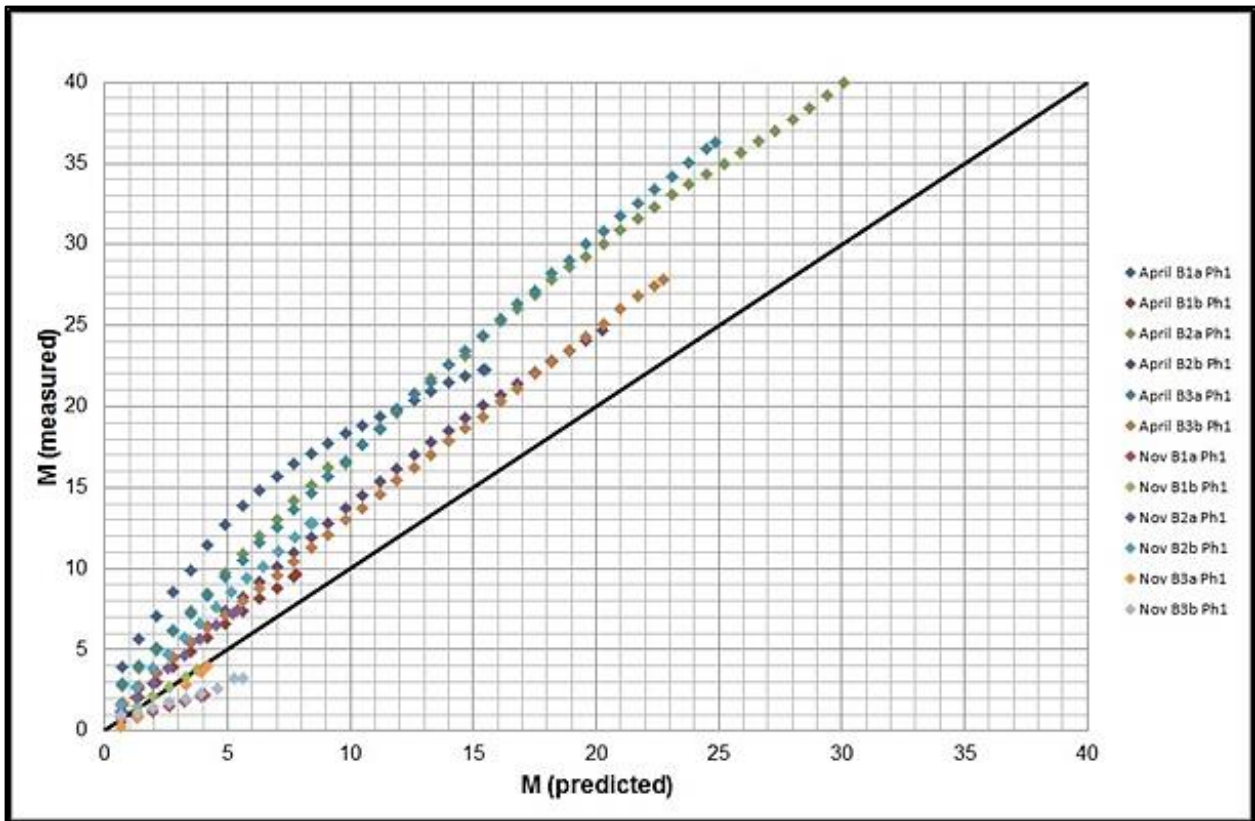


Figure 6-1: Scatter Plot showing accuracy of Phase 1 of the Base Model

From the scatter plot for Phase 1, it can be seen that the resistance moment calculated is generally lower than the actual resistance moment measured from the tests. This shows that, except in the cases of beams 1b, 3a and 3b, tested in November 2010, the model gives fairly conservative results. These were the second set of tests referred to in Chapter 3. All three these tests showed less stiffness than what was expected. (See Chapter 3, Figure 3-5, and 3-7)

From Figure 6-2 it is clear that the second phase of the model is not as conservative as was the first. All the beams tested in November, except for Beams 2a and b, are shown to have un-conservative resistance moments. This indicates that the model might need a calibration factor to ensure that the resistance moments calculated is conservative to an appropriate level of reliability. This factor will be very important as Phase 2 is where the strain hardening starts and some instances either of the serviceability limit state design or the ultimate limit state design might happen within this phase. This is dependent on the material properties as well as the design parameters.

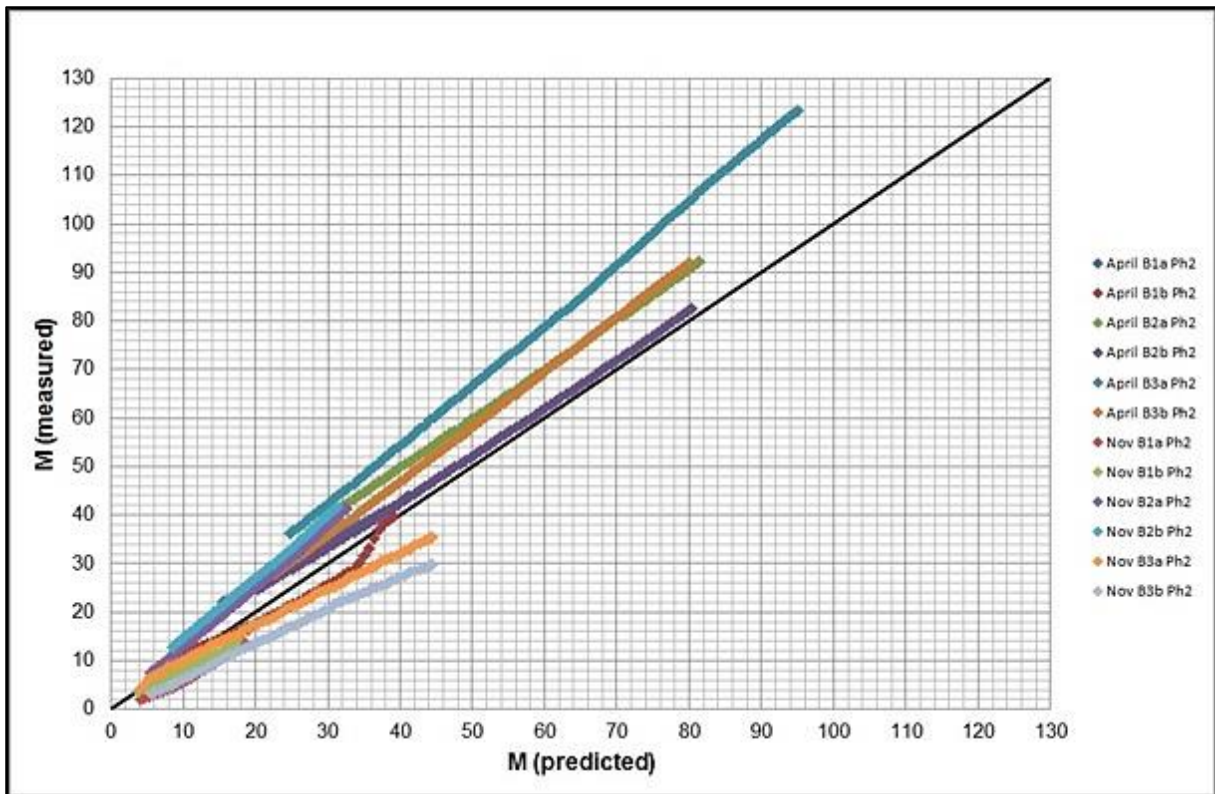


Figure 6-2: Scatter Plot showing accuracy of Phase 2 of the Base Model

The third and last phase is again more conservative in the prediction of the resistance moment. Except for Beams 3a and b, tested in November 2010, all the results are fairly conservative.

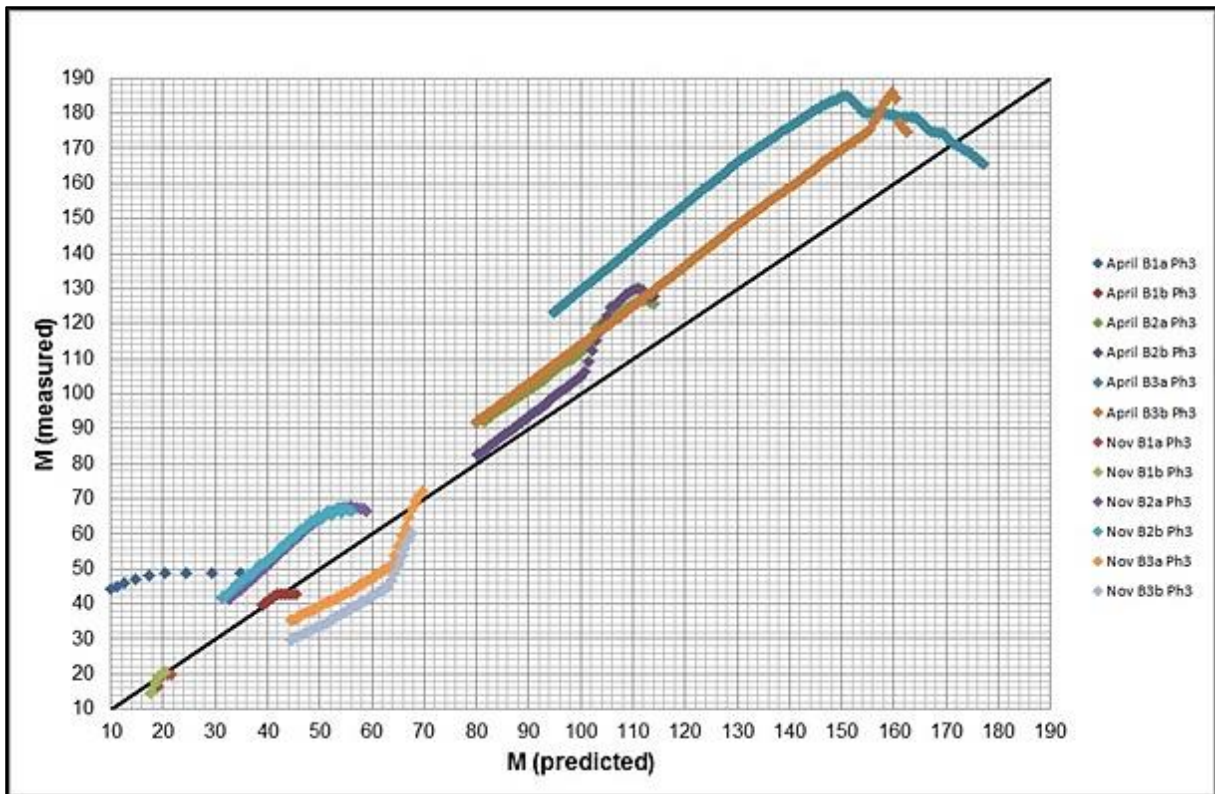


Figure 6-3: Scatter Plot showing the accuracy of Phase 3 of the Base Model

6.3.2 Interpretation of Results

From Figures 6-1, 6-2 and 6-3, it is clear that the model is non-conservative in some instances. Therefore, it is necessary to find a model factor to calibrate the resistance model so that all resistance values calculated will be conservative. In order to do that, a statistical evaluation of the above results needed to be carried out. The aim is to find the bias and the uncertainty inherent in the theoretical model [46]. The method presented in the EN 1990 and also in [46], was used for this purpose.

The probabilistic model of the resistance is set up as:

$$r = br_t\delta$$

6-5

With:

- r_t = Theoretical resistance
- b = Correction factor or model bias
- δ = Error term or model uncertainty

The correction factor is a way of predicting the model's tendency to systematically over or under estimate the resistance [46]. It is calculated by finding the best fit to the slope as given in the scatter plots above.

$$b = \frac{\sum r_e r_t}{\sum r_t^2} \quad 6-6$$

With:

- r_e = Experimental resistance

The error term indicates the scatter of the results. The uncertainty can be found in the coefficient of variation of the error term. The error term can be calculated from the following equation:

$$\delta_i = \frac{r_{ei}}{br_{ti}} \quad 6-7$$

An estimate of the coefficient of variation of the error term, V_δ , is found by defining Δ such that:

$$V_\delta = \sqrt{\exp(s_\Delta^2) - 1} \quad 6-8$$

$$\Delta_i = \ln(\delta_i) \quad 6-9$$

The estimate for the expected value, $E(\Delta)$, is given as:

$$\bar{\Delta} = \frac{1}{n} \sum_{i=1}^n \Delta_i \quad 6-10$$

The estimate for the variance, σ_Δ^2 , is given as:

$$s_\Delta^2 = \frac{1}{n-1} \sum_{i=1}^n (\Delta_i - \bar{\Delta})^2 \quad 6-11$$

The bias and coefficient of variation of the error term can be used to evaluate the model's accuracy. A value of $b < 1$ indicates an un-conservative resistance model. This means that the model over estimates the resistance of the member. Naturally, a value of $b > 1$ indicates the opposite.

The coefficient of variation of the error term, V_δ , indicates the scatter of the results. This means that a very high value for the coefficient of variation indicates that the model cannot very accurately predict strength over the range of situations studied. This also means that the model probably needs to be re-assessed and a possible solution for the variation should be found.

The calculations above were done for each of the beams tested and the results can be seen in the Table below.

Table 6-3: Statistical Values for Model Predictions

	Phase 1			Phase 2			Phase 3		
	b	δ	V_{δ}	b	δ	V_{δ}	b	δ	V_{δ}
April B1a	1.707	1.364	0.365	1.130	1.038	0.080	1.072	1.000	0.015
April B1b	1.287	1.063	0.086	0.914	1.034	0.107	0.994	1.003	0.031
April B2a	1.430	1.182	0.219	1.167	1.020	0.043	1.131	0.999	0.011
April B2b	1.300	1.102	0.135	1.040	1.024	0.046	1.092	0.990	0.053
April B3a	1.545	1.158	0.214	1.316	1.015	0.030	1.180	1.028	0.092
April B3b	1.261	1.101	0.151	1.160	1.008	0.016	1.136	1.001	0.009
Nov B1a	0.564	1.123	0.182	0.699	0.898	0.165	0.946	0.999	0.043
Nov B1b	1.024	1.056	0.081	0.808	1.043	0.074	0.950	0.992	0.090
Nov B2a	1.424	1.057	0.089	1.259	1.009	0.024	1.252	1.006	0.034
Nov B2b	1.585	1.109	0.413	1.346	1.020	0.039	1.291	1.008	0.029
Nov B3a	0.863	0.847	0.334	0.825	1.076	0.106	0.841	0.983	0.086
Nov B3b	0.601	1.222	0.311	0.681	0.980	0.051	0.722	0.983	0.075

From Equation 6-5, it can be seen that the real resistance is given by the modelled resistance multiplied by the bias, b , and the error term, δ . In other words, the bias can be multiplied with the error term to find a model factor. In Table 6-3, the values of each of these model factors are given for each of the beams tested. However, a single model factor is needed. To find this factor, the average of the product of the bias and the error term for each phase were found. The average is used because it seems over conservative to again apply the process of reliability on the calculated model factors in order to obtain a single factor. This is shown in Table 6-4.

Phase 1 of the model is not really a concern as it will not be used for design purposes. However, for completeness, the standard deviation of the model factors is 0.115. Phase 2 and 3 will; however, be used for designing the reinforcement needed in a flexural member of a given size with a particular moment applied to it. The factors above should be applied to equations 4-54, 4-55, 4-56 and 4-57. The standard deviation for the model factors for Phases 2 and 3 respectively comes to 0.164 and 0.135. These equations are used to calculate the amount of tensile reinforcement needed in the particular element.

Table 6-4: Model Factors for Phase 1, 2, and 3

Phase 1				Phase 2				Phase 3			
b	δ	$b*\delta$	V_δ	b	δ	$b*\delta$	V_δ	b	δ	$b*\delta$	V_δ
0.564	1.123	0.633	0.182	0.699	0.898	0.628	0.165	0.722	0.983	0.710	0.075
0.863	0.847	0.731	0.334	0.681	0.980	0.667	0.051	0.841	0.983	0.827	0.086
0.601	1.222	0.734	0.311	0.808	1.043	0.843	0.074	0.950	0.992	0.942	0.090
1.024	1.056	1.081	0.081	0.825	1.076	0.888	0.106	0.946	0.999	0.945	0.043
1.287	1.063	1.368	0.086	0.914	1.034	0.945	0.107	0.994	1.003	0.997	0.031
1.261	1.101	1.388	0.151	1.040	1.024	1.065	0.046	1.072	1.000	1.072	0.015
1.3	1.102	1.433	0.135	1.160	1.008	1.169	0.016	1.092	0.990	1.081	0.053
1.424	1.057	1.505	0.089	1.130	1.038	1.173	0.080	1.131	0.999	1.130	0.011
1.43	1.182	1.690	0.219	1.167	1.020	1.190	0.043	1.136	1.001	1.137	0.009
1.585	1.109	1.758	0.143	1.259	1.009	1.270	0.024	1.180	1.028	1.213	0.092
1.545	1.158	1.789	0.214	1.316	1.015	1.336	0.030	1.252	1.006	1.260	0.034
1.707	1.364	2.328	0.365	1.346	1.020	1.373	0.039	1.291	1.008	1.301	0.029
Model		1.562				1.125				1.082	
Standard deviation		0.115				0.164				0.135	
St. deviation as % of mean		7.36%				14.58%				12.48%	

6.4 Conclusion

Partial factors are added to design models in order to ensure structural safety in design. These factors are normally calibrated on practical experiences but in the case of SHCC, no such data exists and reliability calibration methods have to be used.

Calculating design values for the different material properties was done by finding characteristic values and combining them with material factors. The material factor is calculated by multiplying the conversion factor with the coefficient of variation of the characteristic value. It was decided to only apply these material factors to the strength parameters of the material and then impose limits on the strain parameters. This was done in order to not be over conservative in finding the design values.

The limit on the ultimate compression strain is imposed via the Elasticity Modulus and Equation 2-3. A design value is needed for the Elasticity Modulus which is then used in correlation with the ultimate compressive stress to derive the ultimate compressive strain. In order to define this design value for the Elasticity Modulus, more research into the compression behaviour of SHCC is needed, in particular for the different material strengths available.

For the tensile strain limits, the E-value of 10.5GPa is proposed as a starting point. This is in accordance with Naaman and Reinhardt's study [39]. This might not be true for all strengths of SHCC and further study is needed in this field as well. For the ultimate tensile strain, a limit of 0.0246 is proposed. This limit ties in with the material tested during this study but might not be viable for other strengths of SHCC. Again further study is needed.

The model predictions seem to be conservative in most cases and a model factor is derived for each phase of the model. This model factor will increase the reliability of the design model further.

7. DESIGN

7.1 Material Classification

In Chapter 2, a discussion of the tensile and compression properties of SHCC can be found. From this discussion it is clear that the material is quite complex and in order to classify it, all aspects of the material must be taken into account.

According to Naaman and Reinhardt's classification [39] the tensile elasticity modulus of SHCC can be pinned to 10.5GPa. This eliminates the difficulty in finding the first cracking stress and strain point on the tensile response spectrum. This theory is also discussed in Chapter 6.4.2.

The compression properties of SHCC have not been widely studied and it is mostly assumed that SHCC acts in a similar way as normal concrete in compression. In Chapter 2 of this study, the compression properties were discussed. From this discussion the compression response was found to be similar to that of normal concrete, but not the same. To be able to fully exploit the materials properties it is necessary to classify the material in terms of its compression behaviour as well as its tensile behaviour. There is still some work to be done before this will be achieved fully.

To be able to use the proposed design model, the following material parameters are required:

- ultimate tensile stress
- ultimate tensile strain
- ultimate compressive stress
- ultimate compressive strain
- Elasticity modulus for SHCC in tension
- Elasticity modulus for SHCC in compression.
- first cracking tensile stress
- first cracking tensile strain

It is not sufficient to have only the elasticity modulus for the tensile part of the response. However, if the elasticity modulus is known, and either the stress or the strain at first cracking is also available, the missing parameter could be calculated from the equations available; Equation 2-1 for the tensile Elasticity modulus and Equation 2-6 for the compressive Elasticity modulus.

7.2 Limitations

SHCC is known for its ductility and although this is one of its outstanding qualities, it can also be a negative quality when looking at the deflection of a flexural member. It is known that SHCC can

safely take much more deflection than normal concrete, but this might not be a serviceable situation. It is therefore important to closely monitor the deflection of flexural members constructed from SHCC.

The design model was calibrated by using simply supported beams loaded with a single point load in the centre. The basic deflection rule of limiting the length of the simply supported beam to 16 times the effective depth was used in all cases. However, it was found that for beams of more than 10m length, the deflection sometimes exceeded the value of 30mm, which is the limit set down by SANS0100 [47]. This was found when the calculations were done for Material 1, as per Table 4-1, which had the lowest strength of the three materials considered in this dissertation. The 10m limit is also used in the concrete code when using the span/depth ratios. For beam lengths of more than 10m, the deflection for normal RC beams must be proved.

Material 3, the UHPCC, showed few deflection problems even for beam depths of 1m, where beam lengths of 15m were used. Material 2, which was a medium strength SHCC, also showed more deflection resistance than Material 1, but not as much as the ultra-high performance material. With this in mind, there is need for more tests to be done on the actual deflection limits for the various types and strengths of materials in order to define clear and precise rules that can safely be followed. For different materials with different elasticity moduli it might be necessary to have different rules regarding the span/depth ratios, in order to ensure deflections falling with the SLS criteria.

Further to that, the calibration, discussed in Chapter 4.3, was done on beams with widths ranging from 200mm to 350mm and depths ranging from 200mm to 750mm. The reinforcement ranged from 0.1% of the concrete area to 2.5% of the concrete area in both the compression and tensile areas. Within this range, any combination of compression and tensile steel was used. It was found, however, that for high amounts of tensile reinforcement, higher amounts of compressive reinforcement was needed to keep the beam deflection in check. When low amounts of compressive reinforcement was used with high amounts of tensile reinforcement, the compressive reinforcement would fail before the tensile reinforcement could reach its yield strength and normally the deflection of the member would then be more than the limits applied.

During the calibration of the simplified model, the deflection was also used as a cut off for values added into the sample from where the simplified equations were deduced. When a specific beam was tested and it was found that for a specific amount of tensile reinforcement and compressive reinforcement, the beam would deflect too much under service loads; those values were discarded from the sample and were not used. This was done in order to find a simplified model that could be used without having to check the deflections of the beams as well. The upside of this is that any beam with a length shorter than 10m and a span/depth ratio of not more than 16, can be designed with the simplified model without having to check the deflection in order to make sure that it is within

the allowable limits. The downside to this is that there is already a safety factor built into the simplified model which might result in over conservative amounts of steel being introduced for shorter beams.

7.3 Calculations

For calculating the reinforcement needed in a specified beam with a specified load, the following information is needed:

- h = The height of the proposed beam
- b = The width of the proposed beam
- L = The length of the proposed beam
- d = The cover to the tensile reinforcement measured from the top of the beam
- d' = The cover to the compressive reinforcement measured from the top of the beam
- M_u = The ultimate moment to be applied to the beam
- σ_{ct1} = The tensile stress at first cracking for the material to be used
- σ_{ctu} = The ultimate tensile stress for the material to be used
- σ_{ccu} = The ultimate compressive stress for the material to be used
- ϵ_{ct1} = The tensile strain at first cracking for the material to be used
- ϵ_{ctu} = The ultimate tensile strain for the material to be used
- ϵ_{ccu} = The ultimate compressive strain of the material to be used

This information can then be applied to the following equations:

For finding the tensile strain at the point of design, Equations 4-31, 4-33, 4-35, 4-37, 4-39, 4-41, 4-43, 4-44, 4-46, 4-48, 4-50, or 4-52 is used; depending on the height of the beam and whether the design falls within Phase 2 or 3. It is probably best to assume a design in Phase 3 at first as this is the most common phase for designs to fall, unless the material is an ultra-high performance material. It was found that because of the very high compressive strength of this material, the design rarely ventures into the third phase as the compressive strain never reaches the point of 0.317 times the ultimate compressive strain.

Similarly, the position of the neutral axis can be obtained from Equations 4-30, 4-32, 4-34, 4-36, 4-38, 4-40, 4-42, 4-45, 4-47, 4-49, 4-51, or 4-53; depending on the height of the member and the phase of the design.

For Phase 2 and $h = 200\text{mm}$

$$x = 0.01512Ln\left(\frac{Mu}{bd^2\sigma_{ctu}}\right) + 0.06962 \quad 4-30$$

$$\varepsilon_{ct2} = 0.1912 \left(\frac{Mu}{bd^2\sigma_{ctu}} \right)^{0.0262} 0.01456 \quad 4-31$$

For h = 250mm:

$$x = 0.017375Ln \left(\frac{Mu}{bd^2\sigma_{ctu}} \right) + 0.0884 \quad 4-32$$

$$\varepsilon_{ct2} = 0.1828 \left(\frac{Mu}{bd^2\sigma_{ctu}} \right)^{0.0188} 0.01456 \quad 4-33$$

For h = 300mm:

$$x = 0.02004Ln \left(\frac{Mu}{bd^2\sigma_{ctu}} \right) + 0.10737 \quad 4-34$$

$$\varepsilon_{ct2} = 0.1776 \left(\frac{Mu}{bd^2\sigma_{ctu}} \right)^{0.015} 0.01456 \quad 4-35$$

For h = 400mm:

$$x = 0.02536Ln \left(\frac{Mu}{bd^2\sigma_{ctu}} \right) + 0.3625 \quad 4-36$$

$$\varepsilon_{ct2} = 0.1714 \left(\frac{Mu}{bd^2\sigma_{ctu}} \right)^{0.0105} 0.01456 \quad 4-37$$

For h = 500mm:

$$x = 0.02985Ln \left(\frac{Mu}{bd^2\sigma_{ctu}} \right) + 0.18285 \quad 4-38$$

$$\varepsilon_{ct2} = 0.1678 \left(\frac{Mu}{bd^2\sigma_{ctu}} \right)^{0.0078} 0.01456 \quad 4-39$$

For h = 600mm:

$$x = 0.03768Ln \left(\frac{Mu}{bd^2\sigma_{ctu}} \right) + 0.22098 \quad 4-40$$

$$\varepsilon_{ct2} = 0.1655 \left(\frac{Mu}{bd^2\sigma_{ctu}} \right)^{0.0068} 0.01456 \quad 4-41$$

For h = 750mm:

$$x = 0.057975 \ln \left(\frac{Mu}{bd^2 \sigma_{ctu}} \right) + 0.279525 \quad 4-42$$

$$\varepsilon_{ct2} = 0.1632 \left(\frac{Mu}{bd^2 \sigma_{ctu}} \right)^{0.0061} 0.01456 \quad 4-43$$

For h = 200mm:

$$\varepsilon_{ct2} = 0.1935 \left(\frac{Mu}{bd^2 \sigma_{ctu}} \right)^{0.0227} 0.01456 \quad 4-44$$

$$x = 0.01 \ln \left(\frac{Mu}{bd^2 \sigma_{ctu}} \right) + 0.0759 \quad 4-45$$

For Phase 3 and h = 250mm:

$$\varepsilon_{ct2} = 0.1846 \left(\frac{Mu}{bd^2 \sigma_{ctu}} \right)^{0.0146} 0.01456 \quad 4-46$$

$$x = 0.0105 \ln \left(\frac{Mu}{bd^2 \sigma_{ctu}} \right) + 0.0967 \quad 4-47$$

For h = 300mm:

$$\varepsilon_{ct2} = 0.1792 \left(\frac{Mu}{bd^2 \sigma_{ctu}} \right)^{0.0095} 0.01456 \quad 4-48$$

$$x = 0.0099 \ln \left(\frac{Mu}{bd^2 \sigma_{ctu}} \right) + 0.1182 \quad 4-49$$

For h = 400mm:

$$\varepsilon_{ct2} = 0.1725 \left(\frac{Mu}{bd^2 \sigma_{ctu}} \right)^{0.0052} 0.01456 \quad 4-50$$

$$x = 0.01 \ln \left(\frac{Mu}{bd^2 \sigma_{ctu}} \right) + 0.1599 \quad 4-51$$

For h = 500mm:

$$\varepsilon_{ct2} = 0.1687 \left(\frac{Mu}{bd^2 \sigma_{ctu}} \right)^{0.0028} 0.01456 \quad 4-52$$

$$x = 0.0086Ln\left(\frac{Mu}{bd^2\sigma_{ctu}}\right) + 0.2028 \quad 4-53$$

For finding the compressive strain at the point of the design, Equation 4-5 can be used.

$$\varepsilon_{cc} = -x/h - x\varepsilon_{ct} \quad 4-5$$

If the compressive strain at the point of design, calculated above is less than 0.317 of the ultimate compressive strain, the design is based in the second phase of the base model and Equations 4-54 and 4-55 are used to find the areas of tensile reinforcement and the compressive reinforcement respectively.

$$A_s = \frac{\frac{M(h-x)}{\varepsilon_{ct2}} - 1/6 E_{cc} x^2 b (3d' - x) - 1/6 E_{ct} b (h-x)^2 (k(h-x) + 3g(x-d'))}{E_s(d-x)(d-d')} \quad 4-54$$

$$A'_s = \frac{\frac{M(h-x)}{\varepsilon_{ct2}} - 1/6 E_{cc} x^2 b (3d-x) - 1/6 E_{ct} b (h-x)^2 (k(h-x) - 3g(d-x))}{E_s(x-d')(d-d')} \quad 4-55$$

In order to take the model factors into account, Equation 4-54 can be rewritten to Equation 7-1 and Equation 4-55 into Equation 7-2.

$$A_s = \frac{\frac{1.125M(h-x)}{\varepsilon_{ct2}} - 1/6 E_{cc} x^2 b (3d' - x) - 1/6 E_{ct} b (h-x)^2 (k(h-x) + 3g(x-d'))}{E_s(d-x)(d-d')} \quad 7-1$$

$$A'_s = \frac{\frac{1.125M(h-x)}{\varepsilon_{ct2}} - 1/6 E_{cc} x^2 b (3d-x) - 1/6 E_{ct} b (h-x)^2 (k(h-x) - 3g(d-x))}{E_s(x-d')(d-d')} \quad 7-2$$

Where:

$$E_{ct} = \frac{\sigma_{ct1}}{\varepsilon_{ct1}} \quad 7-3$$

$$E_{cc} = 1.681 \frac{\sigma_{ccu}}{\varepsilon_{ccu}} \quad 7-4$$

$$g = \beta^2 + 2\beta(1 - \beta) + \alpha(1 - \beta)^2 \quad 7-5$$

$$k = 2\beta^3 + 3\beta(1 - \beta)(\beta + 1) + \alpha(1 - \beta)^2(\beta + 2) \quad 7-6$$

With:

$$\beta = \frac{\varepsilon_{ct1}}{\varepsilon_{ct2}} \quad 7-7$$

$$\alpha = \frac{\sigma_{ctu} - \sigma_{ct1}}{\varepsilon_{ctu} - \varepsilon_{ct1}} \frac{1}{E_{ct}} \quad 7-8$$

The model factor of 1.125 is applied to the ultimate moment. The derivation of the model factor can be found in Chapter 6 and the model factors for the three phases are given in Table 6-4.

If the compressive strain at the point of design, as calculated by Equation 4-5 is more than 0.317 of the ultimate compressive strain, the design is done in Phase 3 of the base model and Equation 4-56, 4-57 can be used.

$$A_s = \frac{\frac{M(h-x)}{\varepsilon_{ct2}} - 1/6 E_{cc} b x^2 (x n - 3 m (x - d')) - 1/6 E_{ct} (h-x)^2 b (k(h-x) + 3g(x-d'))}{E_s (d-x)(d-d')} \quad 4-56$$

$$A'_s = \frac{\frac{M(h-x)}{\varepsilon_{ct2}} - 1/6 E_{cc} b x^2 (x n - 3 m (d-x)) - 1/6 E_{ct} (h-x)^2 b (k(h-x) - 3g(d-x))}{E_s (x-d')(d-d')} \quad 4-57$$

When adding the model factor, Equation 4-56 changes as into Equation 7-9 and Equation 4-57 into Equation 7-10:

$$A_s = \frac{\frac{1.082M(h-x)}{\varepsilon_{ct2}} - 1/6 E_{cc} b x^2 (x n - 3 m (x - d')) - 1/6 E_{ct} (h-x)^2 b (k(h-x) + 3g(x-d'))}{E_s (d-x)(d-d')} \quad 7-9$$

$$A'_s = \frac{\frac{1.082M(h-x)}{\varepsilon_{ct2}} - 1/6 E_{cc} b x^2 (x n - 3 m (d-x)) - 1/6 E_{ct} (h-x)^2 b (k(h-x) - 3g(d-x))}{E_s (x-d')(d-d')} \quad 7-10$$

With:

$$n = 2\gamma^3 + 3\gamma(1-\gamma)(\gamma+1) + \delta(1-\gamma)^2(\gamma+2) \quad 7-11$$

$$m = \gamma^2 + 2\gamma(1-\gamma) + \delta(1-\gamma)^2 \quad 7-12$$

Where:

$$\gamma = \frac{0.317\varepsilon_{ccu}}{\varepsilon_{cc2}} \quad 7-13$$

$$\delta = \frac{\sigma_{ccu} - 0.533\sigma_{ccu}}{\varepsilon_{ccu} - 0.317\varepsilon_{ccu}} \frac{1}{E_{cc}} = 0.407 \quad 7-14$$

The model factor of 1.082 is again applied to the ultimate moment used to calculate the amount of tensile reinforcement.

Two more calculation examples are given in Annexure B. One is for a simply supported beam with a line load and one is for a one way spanning roof slab with up stand beams on the edges. These examples show the diversity of the design model in that it is not only applicable to simply supported beams with a single point load in the centre of the beam.

7.4 Comparison with Normal R/C

The properties of SHCC imply that it should be a more effective material when used in bending as it contains tensile strength and the idea is that less reinforcement should be needed. This would make it ideal for use in long span flexural members where the tensile reinforcement sometimes becomes cumbersome to fit into the beam. The durability of this material further promotes its use in flexural members, especially in severe environmental conditions such as close to the sea or in factories. However, the ductility of the material implies that it might deflect more than normal reinforced concrete and so, more reinforcement might be needed in order to stiffen it enough to limit the deflection to acceptable limits.

The following example is done in order to see what the differences are in the design of a simply supported beam constructed of reinforced SHCC and the same beam constructed of normal reinforced concrete.

A simply supported beam with dimensions 300x300mm and a length of 2.8m is loaded with a single point load in the centre of the beam. The ultimate applied moment is 150kNm.

For a normal reinforced concrete beam, the calculations will take the following form. The material parameters are as follows:

- Concrete design compressive strength = 30MPa
- Reinforcement yield strength = 450MPa
- Cover to the tensile reinforcement = 275mm (measured from the top of the beam)
- Cover to the compressive reinforcement = 25mm

According to SANS 0100 [47]:

$K' = 0.156$ (no redistribution of moments)

$$K = \frac{M}{bd^2 f_{cu}} = \frac{150}{0.3 * 0.275^2 * 30e3} = 0.220$$

This means that $K > K'$ and thus both compressive and tensile reinforcement is required in this member.

$$\frac{z}{d} = 0.5 + \sqrt{\left(0.25 - \frac{K'}{0.9}\right)} = 0.777$$

For $d = 0.275$, $z = 0.214$

The amount of compressive reinforcement is calculated first from the following equation:

$$A'_s = \frac{(K - K') f_{cu} b d^2}{f_{yc} (d - d')}$$

With:

$$f_{yc} = \frac{f_y}{\gamma_m + f_y/2000} = 327 \text{ MPa}$$

The material factor, γ_m , for the reinforcement steel is 1.15.

Then:

$$\begin{aligned} A'_s &= 0.00054 \text{ m}^2 \\ &= 540 \text{ mm}^2 \text{ which can be related to 3Y16 bars.} \end{aligned}$$

The tensile reinforcement can be calculated from the following:

$$A_s = \frac{K' f_{cu} b d^2}{0.87 f_y z} + \frac{A'_s f_{yc}}{0.87 f_y}$$

$$\begin{aligned} A_s &= 0.00172 \text{ m}^2 \\ &= 1720 \text{ mm}^2 \text{ which can be related to 2Y32 + 1Y20 bars.} \end{aligned}$$

In the above equation, the yield strength of the reinforcement is factored by the material factor for reinforcement steel of $1/1.15 = 0.87$.

For beam lengths of less than 10m, the span over effective depth for a simply supported beam must be less than or equal to 16. The beam length in this case is 2.8m which is less than 16 times the effective depth of 275mm. According to the code it is not necessary to check the deflection of this beam.

The same calculation can be done for SHCC:

Assuming that the design will fall within the Phase 3, Equation 4-48 is used to find the tensile strain at the point of design:

$$\varepsilon_{ct2} = 0.00263$$

From Equation 4-49 the distance to the neutral axis is.

$$x = 0.126\text{m}$$

Equation 4-5 is used to find the compressive strain at the point of design.

$$\varepsilon_{cc} = -0.00191$$

The characteristic properties of the SHCC material are as follows:

- $\varepsilon_{ct1} = 0.00024$
- $\varepsilon_{ctu} = 0.01456$
- $\sigma_{ctu} = 2.937\text{MPa}$
- $\sigma_{ct1} = 2.054\text{MPa}$
- $\varepsilon_{ccu} = -0.00508$
- $\sigma_{ccd} = -30.589\text{MPa}$

The design of this flexural member will thus be in the third phase of the model as $0.317 * \varepsilon_{ccu} = 0.00161 < \varepsilon_{cc} = 0.00191$. That means we have assumed correctly and the design falls within Phase 3.

From Equations 7-3, and 7-4, the elasticity modulus for the tensile part and the compression part of the beams respectively are:

$$E_{ct} = 8.558\text{GPa}$$

$$E_{cc} = 10.112\text{GPa}$$

From Equations 7-7, 7-8, 7-13, and 7-14 the values for β , α , γ , and δ are:

$$\beta = 0.256$$

$$\alpha = 0.00857$$

$$\gamma = 0.843$$

$$\delta = 0.407$$

Then g , k , m , and n can be found from equations 7-5, 7-6, 7-12, and 7-11.

$$g = 0.451$$

$$k = 0.762$$

$$m = 0.985$$

$$n = 1.958$$

The amount of tensile and compressive reinforcement can be calculated by using Equations 7-9 and 7-10 respectively.

$$A_s = 0.00113\text{m}^2$$

$$= 1130\text{mm}^2 \text{ which can be supplied by using 3Y25 bars.}$$

$$A'_s = 0.00110\text{m}^2$$

$$= 1100 \text{ mm}^2 \text{ which can be supplied by using 2Y25 + 1Y16 bars.}$$

More of the same calculations were done for different beam sizes loaded with different moments and the results are shown in Figure 7-1.

From the figure and the above calculations it is clear that the reinforced SHCC beam needs considerably less tensile reinforcement than the normal R/C beam. The compressive reinforcement needed in the R/SHCC is, on the other hand, more than that needed in the normal R/C. The reason for this is to keep the R/SHCC member from deflecting too much.

When looking at the total amount of reinforcement in the member, the SHCC and the R/C works out almost exactly the same. There is thus, no significant saving on the longitudinal reinforcement used in these members. The shear design of the member was not part of this study, and due to the confining effect of SHCC, there might be a saving on the amount of shear reinforcement needed in flexural members. This will, however, have to be studied in more depth elsewhere.

In an article by Bandelt and Billington [53] it was found that the bond strength between HPFRCC and steel reinforcement is around 39% higher than for normal reinforced concrete. Further to this, it was found that an increase in cover and/or confinement, in the form of shear reinforcement, did not increase the bond strength of the reinforcement as is the case for normal R/C. The higher bond strength means that reinforcement lap lengths can be smaller. It is estimated that this can lead to a reduction of 30% in the length of reinforcement used for laps [53].

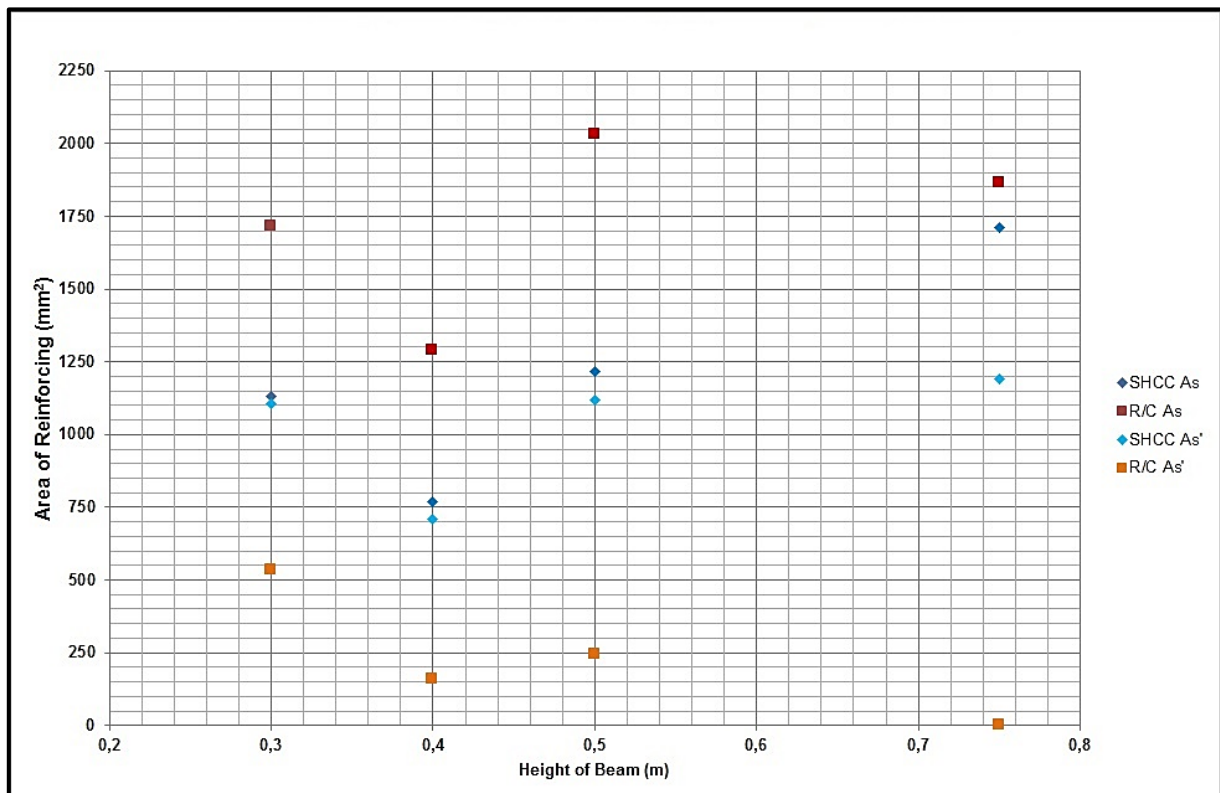


Figure 7-1: Comparison between Reinforcement needed in SHCC and normal R/C beams

The downside of the increase in the bond strength is that delamination does not easily occur along the length of tensile reinforcement. The multiple micro cracking in the SHCC keeps the concrete and the reinforcement together, forcing them to deflect in the same way. When the concrete delaminates from the steel, as is the case in normal R/C, a longer piece of steel is allowed to yield, which spreads the tension force out a bit. In SHCC, this is not allowed to happen, which could lead to the premature breaking of the tension reinforcement, due to the localization of the force and thus the yielding in the rebar. It has also been found that an increase in tensile strength leads to lower deformation capacity

due to deformation being concentrated at a localized area instead of spreading out along the length of the member [53].

However, as the SHCC shows multiple cracks at small spacing, the tension forces are spread out somewhat. This load spreading should in turn allow the reinforcement to yield along its length within the cracked area and not just at the point where the first crack starts. During the testing done for this study, only the longitudinal steel in the least reinforced beams could be loaded until failure. The larger diameter bars did not rupture, even at very large deflections. There was also some delamination present in these tests, which could probably then explain why the tensile reinforcement could not be pushed to breaking point.

7.5 Conclusion

The design of a flexural member constructed from reinforced SHCC is fairly simple as long as all the material parameters for the material to be used are available. When looking at the properties of SHCC compared to that of normal concrete, it seems logical that the design of the R/SHCC member would involve less reinforcement than the design of the conventional R/C member for the same loads. This does seem to be the case for the tensile reinforcement, but not for the compressive reinforcement. This is mainly due to the R/SHCC member's proneness to relative large deflection due to its ductility. The economy of R/SHCC is based on the fact that it is assumed to need less reinforcement for the same amount of concrete and load. The assumption is based on the tensile properties of the material. Unfortunately, that does not seem to be true. However, R/SHCC might still be the more economic choice in the long run due to its enhanced durability, which normal R/C does not have. This is, however, hard to demonstrate as there are no buildings constructed from R/SHCC that can be compared with normal R/C buildings.

The deflection for both the materials will need checking for lengths of more than 10m. This is because the rule for the ratio between the length and the depth of the beam is only valid for beam lengths under 10m.

8. SUMMARY, CONCLUSION AND RECOMMENDATIONS

8.1 Summary

8.1.1 Introduction

While SHCC shows much promise in reducing the need for rehabilitation of reinforced concrete structures, developments to reduce the environmental impact of the material are required. Reducing the carbon footprint of this material will enhance its worth in the construction industry.

As cracking and crack widths are the most important aspects of durability, these properties of SHCC need to be researched in greater depth. While average crack widths are shown to be small, maximum crack widths can reach up to the normal limits set in conventional concrete structures. During this study it was found that the crack widths at the service limit state were too small to see with the naked eye.

There are currently no models for estimating the crack widths in SHCC. The specific crack width limits that need to be applied in order to protect reinforcement against ingress of harmful substances are also lacking. In the absence of these limits, the supposedly higher durability found in R/SHCC than in normal R/C cannot be proven.

8.1.2 Material Description

Both the tensile and compressive behaviours of SHCC are complex and difficult to model. In order to simplify the process, a bi-linear approach was adopted in both cases. Quantifying the tensile response requires the definition of the first cracking stress and strain as well as the ultimate stress and strain. For the compression response, only the ultimate stress and strain is needed since the stress-state point marking the onset of inelastic response is expressed as fractions of the ultimate stress-strain pair.

8.1.3 Testing and Verification of the Model

The model seems to be most sensitive to the compression characteristics of the material used. This behaviour is expected, as only the ultimate compression stress and strain is used to describe all the different compression characteristics.

Two sets of six beams each were tested. The test setup consisted of a simply supported beam loaded with a point load in the centre of the beam. Tensile and compression test specimens were also made for each of the beams in order to minimize the uncertainties in the prediction model. No compression strain values were measured for the first set of tests. Both tests used the same mix design but different approaches were used in the actual mixing of the material.

The first set of tests showed very good correlation with the predicted model values and even the stiffness of the material was closely predicted. The model showed mostly conservative results in this case.

For the second set of tests there seems to have been a slight difference in the stiffness of the actual material versus the stiffness assumed in the model prediction. In some instances the prediction was conservative and in other it was not. This difference is assumed to be due to uncertainties in the elasticity modulus for the material used. Further research into this characteristic of SHCC is needed in order to propose a more accurate model for the elasticity modulus for SHCC.

8.1.4 Analysis Model

The original design model is based on three phases in order to incorporate the different phases of the tensile and compressive responses for this material. The first phase is known as the elastic phase and during this phase both the tensile and compressive responses are linear and no cracks have formed in the member. The second phase starts with the first cracks forming in the tensile zone of the member. This phase takes into account the tensile strain hardening of the material but assumes that the compression response is still elastic. When the compressive strain reaches the limit of 0.317 times its ultimate compressive strain, phase 2 ends and phase 3 starts. During phase 3, both responses are assumed plastic and this phase ends in either tensile crack localization or compression crushing at the top of the flexural member.

Because of the intrinsic nature of the base model, a simplified model is needed. In order to simplify the base model, certain information needs to be estimated from the base model in order to be able to establish enough information to do a flexural design. The design tensile strain value is found by calculating various different scenarios of beams and loads, and then assessing the information gathered into a single equation. The distance to the neutral axis is also calculated from an equation developed in the same way and for different heights of beams. Eventually the design compressive strain can be found from known relationships and with this information, the tensile and compressive steel can be calculated. It was found that the simplified model gives accurate results without a model factor being added to the equations. If the model factor is incorporated, a measure of conservancy is added to the answers. If the realistic steel values are used to establish the resisting moments, the safety factor on the resisting moments becomes quite big in some cases.

A major drawback of the simplified model is that it is related to the depth of the member and equations are only available for depths up to 750mm for Phase 2 design and 500mm for Phase 3 design. Interpolation can be used for values in between the available design values, but to estimate for depths higher than these are not possible at this stage.

To prove that the model is applicable to all strain hardening materials, the simplified model was tested with two more materials of different strengths. The tensile strain values were found to be remarkably similar and again the simplified model gave highly accurate results. It does show, however, that the model is applicable to other types of SHCC. More material types should be tested in order to establish a more accurate way of calculating the design tensile strain. This would improve the accuracy of the simplified model.

8.1.5 Deflection Model

The deflection of the SHCC member is found by applying the same principles as for conventional RC. When the material is elastic, an elastic approach can be adopted, but for a cracked section, the deflection must be found by means of analytical or numerical integration.

Deflection calculations are important in order to establish the serviceability level of the member. Too much deflection can lead to unsightly cracking in structures and visible deflections makes occupants feel unsafe. The serviceability limits as set out for conventional concrete were adopted for SHCC in this instance.

8.1.6 Reliability

Partial factors are added to design models in order to ensure structural safety in design. These factors are normally calibrated on practical experiences but in the case of SHCC, no such data exists and reliability calibration methods have to be used.

Finding design values for the different material properties was done by finding characteristic values and combining them with material factors. The material factor is calculated by multiplying the conversion factor with the coefficient of variation of the characteristic value. It was decided to only apply these material factors to the strength parameters of the material and then impose limits on the strain parameters. This was done in order to not be over conservative in finding the design values.

The limit on the ultimate compression strain is imposed via the Elasticity Modulus and Equation 2-3. A design value is needed for the Elasticity Modulus which is then used in correlation with the ultimate compressive stress to derive the ultimate compressive strain. In order to define this design value for the Elasticity Modulus, more research into the compression behaviour of SHCC is needed, in particular for the different material strengths available.

For the tensile strain limits, the E-value of 10.5GPa is proposed as a starting point. This is in accordance with Naaman and Reinhardt's study [38]. This value might not be true for all strengths of SHCC and further study is needed in this field as well. For the ultimate tensile strain, a limit of

0.0246 is proposed. This limit ties in with the material tested during this study but might not be viable for other strengths of SHCC. Again further study is needed.

The model predictions seem to be conservative in most cases and a model factor is derived for each phase of the model.

8.1.7 Design

The design of a flexural member constructed from reinforced SHCC is fairly simple as long as all the material parameters for the material to be used are available. When looking at the properties of SHCC compared to that of normal concrete, it seems logical that the design of the R/SHCC member would involve less reinforcement than the design of the conventional R/C member for the same loads. This does seem to be the case for the tensile reinforcement, but not for the compressive reinforcement. This is mainly due to the R/SHCC member's proneness to relative large deflection due to its ductility.

The deflection for both the materials will need checking for lengths of more than 10m. This is because the rule for the ratio between the length and the depth of the beam is only valid for beam lengths under 10m.

8.2 Conclusion

8.2.1 Compression and Tensile Response Models

The compression and tensile response models used in deriving the design model requires that the tensile yield stress and strain as well as ultimate stress and strain is known. It also requires the ultimate compressive stress and strain values to be known. Currently there is still a lot of variation in these values, even for materials mixed with the same constituents and in the same way. This results in a lot of uncertainty in the material properties, which in turns relates to very high material factors.

As both the tensile and compressive responses are quite complex, a bilinear approach was used in both cases. These approaches were tested against the materials used in this study, and also used for the verification of the simplified model with the two other materials, but more study is required in order to ensure that these approaches apply to other SHCC materials as well.

8.2.2 Design Model

The novelty of this work lies in the analytical and simplified design model. The base model is broken into three phases. The first represents the elastic phase for both the compression and tension parts of the flexural member. During the second phase, the tension part of the member has passed into the strain hardening phase but the compression part is still considered in its elastic state. During the

last phase, the tensile response is still in the strain hardening state, and the compressive response is considered to have passed into a plastic state.

The exact point of transition between the three phases was calibrated for the material used in this study. It was applied to Materials 2 and 3 as well, but as there are no material data to compare this assumption with, it is not known how accurate it is. The base model shows good correlation with the tests done and is considered accurate.

The simplified model shows good correlation with the base model and is therefore also considered accurate. One of the main limitations of the simplified model is that it cannot be applied to any size beam. It is limited to the sizes tested in this study and further study will be needed to expand the range of the model. Though interpolation is possible between the set sizes, the model is not applicable to sizes bigger than those tested.

Deflection can be a problem in the design of flexural members and unless the designer complies with the rules stated within this dissertation, the deflection will have to be calculated to ensure that it complies with serviceability limit state regulations.

8.2.3 Comparing R/SHCC with R/C

Due to the enhanced tensile capacity of SHCC over normal concrete, the expectation is that R/SHCC will require less reinforcement than normal R/C design. This was found to be true for the tensile part of the member, but not the compressive part. In general it was found that the tensile reinforcing required for a flexural member, as calculated with the simplified model, is less than the requirement for a normal R/C member of the same size and under the same loading conditions. However, the compressive reinforcing calculated for the SHCC member exceeds the compressive reinforcing required for the normal R/C member. The total volume of reinforcing needed in R/SHCC and normal R/C is about equal.

8.3 Recommendations

8.3.1 Material properties

In order to minimise uncertainties in the design model, more accurate tensile and compressive response models are required. This should be done for a wide variety of different SHCC material types and strengths in order to ensure that all possible varieties are covered in the design.

Special attention should be given to finding a relationship between the Elasticity Modulus and the strength of the material. A study should also be conducted into whether there should be a different Elasticity Modulus for the compression part of the member than for the tensile part, or whether there

should be only one for a type of material. This information could simplify the design model considerably.

8.3.2 Deflection Model

A lot of uncertainty exists around the calculation of the deflection of the R/SHCC flexural member. It will be prudent to devote more study into finding a more accurate model for calculating the deflected shape of a flexural member. It was found during this study that the deflection of this material could potentially become a problem and therefore it is important to ensure that an accurate and true model exist for the calculation of the short and long term deflection of this material.

8.3.3 Shear Design

The shear design of the flexural member was not included in this study. It is however, an important part of the design of flexural members and should be studied as well.

9. BIBLIOGRAPHY

- [1] G. P. A. G. Van Zijl and W. P. Boshoff, "FRC in South Africa - application fields, new developments and outlook," in *Proceedings of International Conference ICCX*, 2008.
- [2] Japan Society of Civil Engineers, "Recommendations for Design and Construction of High Performance Fiber Reinforced Cement Composites with Multiple Fine Cracks (HPFRCC)," 2008.
- [3] V. C. Li and T. Kanada, "Engineered Cementitious Composites for Structural Applications," *Journal of Materials in Civil Engineering*, vol. 10, pp. 66-69, 1998.
- [4] G. P. A. G. Van Zijl, "Improved mechanical performance: Shear behaviour of strain hardening cement based composites (SHCC)," *Cement and Concrete Research*, pp. 1241 - 1247, 2007.
- [5] G. J. Parra-Montesinos, "High-Performance Fiber-Reinforced Cement Composites: An alternative for seismic design of structures," *ACI Structural Journal*, vol. 102, pp. 668 - 675, 2005.
- [6] G. Fischer and V. C. Li, "Effect of matrix ductility on deformation behaviour of steel reinforced ECC flexural members under reversed cyclic loading conditions," *ACI Structural Journal*, vol. 99, pp. 781-790, 2002.
- [7] V. C. Li and H. Stang, "Interface Property Characterisation and Strengthening Mechanism in Fiber Reinforced Cement-base composites," *Advanced Cement Based Materials*, vol. 6, pp. 1-20, 1997.
- [8] V. C. Li, H. Horii, P. Kabele, T. Kanda and Y. Lim, "Repair and Retrofit with Engineered Cementitious Composites," *Engineering Fracture Mechanics*, vol. 65, pp. 317-344, 2000.

- [9] V. C. Li, "From Micromechanics to Structural Engineering - The design of cementitious composites for Civil Engineering applications," *JSCE Journal of Structural Mechanics and Earthquake Engineering*, vol. 10, pp. 37-48, 1993.
- [10] S. Wang and V. C. Li, "Polyvinyl Alcohol reinforced engineered cementitious composites: Material design and performances," in *Proceedings on international workshop on HPFRCC in Structural Applications*, Honolulu, 2006.
- [11] V. C. Li, "Tailoring ECC for Special Attributes: A review," *International Journal of Concrete Structures and Materials*, vol. 6, no. 3, pp. 135 - 144, 2012.
- [12] M. D. Lepech, "Improving Infrastructure sustainability using nanoparticle engineered cementitious composites," in *Advances in Cement-Based Materials*, 2010.
- [13] V. C. Li, "Driving infrastructure sustainability with Strain Hardening Cementitious Composites," in *Advances in Cement-Based Materials*, 2010.
- [14] G. P. A. G. Van Zijl, V. Slowik, R. D. T. Filho, F. H. Whittmann and H. Mihashi, "Comparative testing of crack formation in strain-hardening cement-based composites (SHCC)," *Materials and Structures*, vol. 49, pp. 1175 - 1189, 2016.
- [15] M. Sahmaran, M. Li and V. C. Li, "Transport properties of Engineered Cementitious Composites (ECC) under chlorine exposure," *ACI Materials Journal*, vol. 104, pp. 604-611, 2007.
- [16] G. A. Keoleian, A. Kendall, J. Dettling, V. Smith, R. Chandler, M. Lepech and V. Li, "Life cycle modeling of concrete bridge design: Comparison of ECC link slab and conventional steel expansion joint," *Journal of Infrastructure Systems ASCE*, vol. March 2005, pp. 51-60, 2005a.
- [17] G. A. Keoleian, A. Kendall, M. Lepech and V. Li, "Guiding the design and application of new materials for enhancing sustainable performance: Framework and Infrastructure application," in *Proceedings of MRS Symposium*, 2005b.

- [18] W.-C. Choi, H.-D. Yun, J.-W. Kang and S.-W. Kim, "Development of recycled strain-hardening cement-based composite (SHCC) for sustainable infrastructure," *Composites*, vol. 43, pp. 627-635, 2012.
- [19] G. P. A. G. Van Zijl and F. Wittmann, "Durability of Strain-Hardening Fiber Reinforced Cement-Based Composites (SHCC)," Springer, 2011.
- [20] N. Carino and J. Clifton, "Prediction of cracking in reinforced concrete structures.," Building and Fire Research Laboratory National INstitution of Standards and Technology, Gaithersburg, 1995.
- [21] P. Kabele, J. Memecek, L. Novak and L. Kopecky, "Effects of calcium leaching o interfacial properties of PVA fibers in cementitious matrix," *Engineering Mechanics*, vol. 13, no. 4, pp. 285-295, 2006a.
- [22] P. Kabele, J. Memecek, L. Novak and L. Kopecky, "Effects of chemical exposure on bond between synthetic fiber and cementitious matrix," in *Proceedings of ICTRC*, 2006b.
- [23] V. Mechtherine and P. Jun, "Stress-strain behaviour of strain hardening cement based composites (SHCC) under repeated tensile loading," in *Fracture Mechanics of Concrete Structures*, 2007, pp. 1441 - 1448.
- [24] F. Altman, V. Mechtherine and U. Reuter, "A novel durability design approach for new cementitious materials: Modeling chlorine ingress in strain hardening cement based composites," in *Proceedings on second international conference on concrete repair, rehabilitation and retrofit (ICCRRR)*, 2008.
- [25] M. S. Magalhaes, R. D. Toledo Filho and E. M. Fairbairn, "Physical and mechanical properties of Strain-Hardening Cement-based Composites (SHCC)after exposure to elevated temperatures," in *Advances in Cment-Based Materials*, 2010.

- [26] S. C. Paul, G. P. A. G. Van Zijl, J. Babafemi and T. Ming Jen, "Chloride ingress in cracked and uncracked specimens made from strain hardening cement-based composite (SHCC)," *Construction and Building Materials*, vol. 114, pp. 232-240, 2016.
- [27] S. C. Paul and G. P. A. G. Van Zijl, "Chloride -induced corrosion modeling of cracked reinforced SHCC," *Archives of Civil and Mechanical Engineering (ACME)*, vol. 16, pp. 734-742, 2016.
- [28] N. Neithalath, "Analysis of moisture transport in mortars and concrete. Sorptio-bifusion approach," *ACI Materials Journal*, vol. 103, no. 3, pp. 209-217, 2006.
- [29] Z. P. Bazant and L. J. Najjar, "Drying of concrete as a non-linear Diffusion Problem," *Cement and Concrete Research*, vol. 1, pp. 461 - 473, 1971.
- [30] M. Kuneida, E. Denorie, E. Bruhwiler and H. Nakamura, "Challenges for SHCC deformability versus matrix density," in *Pro 53 HPRFCC5*, Mainz, 2007.
- [31] L. V. Lepech M, "Water permeability of cracked cementitious composites," in *Proceedings of ICFII*, Turin, 2005.
- [32] K. Wang, D. C. Jansen, S. Shoh and A. F. Karr, "Permeability study of cracked concrete," *Cement and Concrete Research*, vol. 27, no. 3, pp. 381 - 393, 1997.
- [33] V. C. Li and H. Stang, "Elevating FRC material ductility to infrastructure durability," in *Proceedings 6th RILEM Symposium on Fiber Reinforced Concretes*, 2004.
- [34] G. P. A. G. van Zijl, S. C. Paul and J. P. Rens, "Corrosion of steel reinforcing bars in strain hardening cement-based specimens under sustained load," 2014.
- [35] C. J. Adendorff, W. P. Boshoff and G. P. A. G. Van Zijl, "Characterisation of crack distribution of Strain-Hardening Cement Composites (SHCC) under imposed strain," in *Advances in Cement-Based Materials*, 2010, pp. 215-221.

- [36] G. P. A. G. Van Zijl, V. Slowik, R. D, T. Filho, F. H. Wittmann and H. Mihashi, "Comparative testing of crack formation in strain-hardening cement-based composites (SHCC)," *Materials and Structures*, vol. 49, pp. 1175-1189, 2016.
- [37] M. B. Weimann and V. C. Li, "Drying shrinkage and Crack width of Engineered Cementitious Composites (ECC)," in *Brittle Matrix Composites*, Warsaw, 2003.
- [38] V. C. Li, S. Wang and C. Wu, "Tensile Strain Hardening Behaviour of Polyvinyl Alcohol Engineered Cementitious Composites (PVA-ECC)," *ACI Structural Journal*, pp. 483 - 492, 2001.
- [39] A. E. Naaman and H. W. Reinhardt, "Proposed classification of HPFRC composites based on their tensile response," *Materials and Structures*, vol. 39, pp. 547 - 555, 2006.
- [40] C. Visser, *Mechanical and Structural Characterisation of Extrusion Moulded SHCC*, Thesis presented for the degree of Master of Science at the Department of Civil Engineering of the University of Stellenbosch, 2007.
- [41] G. P. A. G. Van Zijl, *The role of aggregate in high performance fiber reinforced cement-based composites*, Department of Civil Engineering, University of Stellenbosch, 2005.
- [42] W. P. Boshoff and G. P. A. G. van Zijl, "Time-dependant response of ECC: Characterisation of creep and rate dependance," *Cement and Concrete Research*, vol. 37, pp. 725-734, 2007.
- [43] I. Paegle and G. Fischer, "Shear behavior of reinforced Engineered Cementitious Composites (ECC) beams," in *Advances in Cement-Based Materials*, 2010.
- [44] M. Maalej, V. C. Li and M. ASCE, "Flexural/Tensile-Strength Ratio in Engineered Cementitious Composites," *Journal of Materials in Civil Engineering*, pp. 513 - 527, November 1994.
- [45] K. T. Molapo, *The behaviour of Strain-hardening cement composites under biaxial compression*, Stellenbosch, 2010.

- [46] J. S. Dymond and J. V. Retief, "Towards a reliability based development program for SHCC design procedures," in *Advances in Cement-Based Materials*, 2010, pp. 297-306.
- [47] S. 10100-1, *Structural use of Concrete. Part 1 - Design*, 2000.
- [48] K. Wille, S. El-Tawil and A. E. Naaman, "Properties of strain hardening ultra high performance fiber reinforced concrete (UHP-FRC) under direct tensile loading," *Cement and Concrete Composites*, vol. 48, pp. 53-66, 2014.
- [49] E. 1992-1-2, *Eurocode 2: Design of Concrete Structures - Part 1-2*, 2004.
- [50] D. M. Moreno, W. Trono, G. Jen, C. Ostertag and S. L. Billington, "Tension stiffening in reinforced high performance fiber reinforced cement-based composites," *Cement and Concrete Composites*, vol. 50, pp. 36-46, 2014.
- [51] S. C. Paul, *The Role of Cracks and Chlorides in Corrosion of Reinforced Strain Hardening Cement-Based Composite (R/SHCC)*, Dissertation, Stellenbosch University, 2015.
- [52] E. 1. (2002), *Eurocode - Basis of structural Design*, 2002.
- [53] M. J. Bandelt and S. L. Billington, "Bond behavior of steel reinforcement in high-performance fiber-reinforced cementitious composite flexural members," *Materials and Structures*, vol. 49, pp. 71 - 86, 2016.
- [54] C. Soranakom and B. Mobasher, "Flexural Modelling of strain softening and strain hardening fiber reinforced concrete," in *High Performance Fiber Reinforced Cement Composites - HPFRCC5*, Cachan, France, 2007.
- [55] E. N. Periera, J. A. De Oliviera Barros and G. Fischer, *Processes of Cracking in Strain Hardening Cement Composites*, 2012.
- [56] V. C. Li and K. Rokugo, "Task Group D Conclusions - HPFRCC design assumptions," 2004.

- [57] F. H. Wittmann, T. Zhao, L. Tian, F. Wang and L. Wang, "Aspects of durability of strain hardening cement-based composites under imposed strain," in *Advances in Cement-Based Materials*, 2010.
- [58] B. G. Salvoldi, M. E. Gillmer and H. Beushausen, "Determining the durability of SHCC using the South African early age Durability Index tests," in *Advances in Cement-Based Materials*, 2010.
- [59] J. Zhang and V. C. Li, "Monotonic and fatigue performance in bending of fiber-reinforced engineered cementitious composite in overlay system," *Cement and Concrete Research*, vol. 32, pp. 415-523, 2002.
- [60] V. C. Li and T. Matsumoto, "Fatigue crack growth analysis of fiber reinforced concrete with effect of interfacial bond degradation," *Cement and Concrete Composites*, vol. 20, pp. 338-351, 1998.
- [61] F. Altmann and V. Mechtcherine, "Modelling the influence of cracking on chloride ingress into Strain-Hardening Cement-based Composites (SHCC)," in *Advances in Cement-Based Materials*, 2010, pp. 193-202.
- [62] F. Altmann and V. Mechtcherine, "Durability design strategies for new cementitious materials," *Cement and Concrete Research*, vol. 54, pp. 114-125, 2013.
- [63] C. R. Visser and G. P. A. G. Van Zijl, "Mechanical Characteristics of extruded SHCC," in *Fifth international RILEM workshop on High Performance Fiber Reinforced Cement Composites (HPFRCC5)*, 2014.
- [64] G. P. A. G. Van Zijl and L. De Beer, "An SHCC overlay retrofitting strategy for unreinforced load bearing masonry," in *9th International Conference on Fracture Mechanics of Concrete and Concrete Structures*, 2016.
- [65] G. P. A. G. Van Zijl, "Durability under mechanical load- micro-crack formation (Ductility)," in *Durability of Strain-Hardening Fiber Reinforced Cement-Based Composites (SHCC)*, 2011.

- [66] G. Fischer and V. Li, "Effect of Fiber Reinforcement on the response of Structural Members," in *Fracture Mechanics of Concrete Structures*, Ia - FraMCoS, 2004, pp. 831 - 838.
- [67] G. Fischer and V. Li, "Structural Composites with ECC," in *Proceedings of the ASCCS -6*, 2000.
- [68] G. P. A. G. Van Zijl and W. P. Boshoff, "Crack distribution and durability of SHCC," 2016.
- [69] J. Zang and van Zijl G.P.A.G, "Developing non-heat treated UHPC with local materials," *Concrete Beton Journal*, vol. 142, pp. 12 - 23, 2015.
- [70] P. Jun and V. Mechtcherine, "Behaviour of Strain-hardening Cement-based Composites (SHCC) under monotonic and cyclic tensile loading," *Cement and Concrete Composites*, vol. 32, pp. 801-809, 2010.
- [71] L.-I. Kan and H.-s. Shi, "Investigation of self-healing behavior of Engineered Cementitious Composites (ECC) materials," *Construction and Building Materials*, vol. 29, pp. 348-356, 2012.
- [72] D. J. Kim, K. Wille, A. E. Naaman and S. El-Tawil, "Strength dependant tensile behavior of strain hardening fiber reinforced concrete," in *High Performance Fiber Reinforced Cement Composites 6*, 2012, pp. 3-10.
- [73] J. M. Rouse and S. L. Billington, "Creep and Shrinkage of High Performance Fiber-Reinforced Cementitious Composites," *ACI Materials Journal*, vol. 104, pp. 71-86, 2007.
- [74] K. Sirijaroonchai, S. El-Tawil and G. Parra- Montesinos, "Behaviour of high performance fiber reinforced cement composites under multi-axial compressive loading," *Cement and Concrete Composites*, vol. 32, pp. 62-72, 2010.
- [75] S. A. Peerapong, T. Matsumoto and T. Kanda, "Flexural Fatigue Failure Characteristics of an Engineered Cementitious Composite and Polymer Cement Mortars," *JSCE*, vol. 57, no. 718, pp. 121-134, 2002.

- [76] S. C. Paul, G. P. A. G. Van Zijl, A. J. Babafemi and M. J. Tan, "Chloride ingress in cracked and uncracked SHCC under cyclic wetting-drying exposure," *Construction and Building Materials*, vol. 114, pp. 232 - 240, 2016.
- [77] J.-L. Tailhan, P. Rossi and C. Boulay, "Tensile and bending behaviour of a strain hardening cement-based composite: Experimental and numerical analysis," *Cement and Concrete Composites*, vol. 34, pp. 166-171, 2012.
- [78] W. P. Boshoff and G. P. A. G. Van Zijl, "Time-dependant response of ECC: Characterisation of creep and rate dependance," *Cement and Concrete Research*, vol. 37, pp. 725 - 734, 2007.
- [79] K. Wille, S. El-Tawil and A. E. Naaman, "Properties of UHPFRC under direct tensile loading," *Cement and Concrete Composites*, vol. 48, pp. 53-66, 2014.
- [80] M. Lepech and V. Li, "Size effect in ECC structural members in flexure," in *Fracture Mechanics of Concrete Structures*, Ia - FraCos, 2004, pp. 1059 - 1066.
- [81] V. C. Li, "Advances in ECC research," *Material Science tp Application*, vol. ACI Special Publication on Concrete, pp. 373-400, 2002.
- [82] V. C. Li, "On Engineered Cementitious Composites (ECC) - A Review of the Material and Its Applications," *Journal of Advanced Concrete Technology*, vol. 1, pp. 215-230, 2003.
- [83] M. J. Bandelt and S. L. Billington, "Influence of HPFRCC tensile properties on numerical simulation of reinforced HPFRCC component bahviour," in *9th RILEM International Symposium on Fiber Reinforced Concrete BEFIB*, Vancouver, 2016.
- [84] V. C. Li, "Integrated structures and material design," *Materials and Structures*, vol. 40, pp. 387-396, 2007.
- [85] D.-Y. Yoo and N. Banthia, "Mechanical properties of ultra-high-performance fiber-reinforced concrete: A review," *Cement and Concrete Composites*, vol. 73, pp. 267-280, 2016.

- [86] V. Afrouhsabet, L. Biolzi and T. Ozbakkaloglu, "High-performance Fiber-reinforced concrete: a review," *Journal of Material Science*, vol. 51, pp. 6517-6551, 2016.
- [87] C.-C. Hung, W.-M. Yen and K.-H. Yu, "Vulnerability and improvement of reinforced ECC flexural members under displacement reversals: Experimental investigation and computational analysis," *Construction and building materials*, vol. 107, pp. 287-298, 2016.
- [88] S. B. Keskin, O. K. Keskin, O. Anil, M. Sahmaran, A. Alyousif, M. Lachemi, L. Amleh and A. F. Ashour, "Self-healing capability of large-scale engineered cementitious composites beams," *Composites Part B*, vol. 101, pp. 1-13, 2016.
- [89] T. Huang and Y. X. Zhang, "Numerical modelling of mechanical behaviour of engineered cementitious composites under axial tension," *Computers and Structures*, vol. 173, pp. 95-108, 2016.
- [90] B. Gencturk, "Life-cycle cost assessment of RC and ECC frames using structural optimization," *Earthquake Engineering and Structural Dynamics*, vol. 42, pp. 61-79, 2013.
- [91] J. Zhou, J. Pan, A. M. ASCE, C. K. Leung and F. ASCE, "Mechanical Behaviour of Fiber-Reinforced Engineered Cementitious Composites in Uniaxial Compression," *Journal of Materials in Civil Engineering*, vol. 27, pp. 1-10, 2014.
- [92] J. Vorel and W. P. Boshoff, "Computational modelling of real structures made of Strain-hardening Cement-based Composites," *Applied Mathematics and Computation*, vol. 267, pp. 562-570, 2015.
- [93] J. Vorel and W. P. Boshoff, "Numerical simulation of ductile fiber-reinforced cement-based composite," *Journal of Computational and Applied Mathematics*, vol. 270, pp. 433-442, 2014.
- [94] S. H. Said, H. A. Razak and I. Othman, "Flexural behaviour of engineered cementitious composite (ECC) slabs with polyvinyl alcohol fibers," *Construction and Building Materials*, vol. 75, pp. 176-188, 2015.

- [95] E. B. Pereira, G. Fischer and J. A. Barros, "Direct assessment of tensile stress-crack opening behaviour of Strain Hardening Cementitious Composites (SHCC)," *Cement and Concrete Research*, vol. 42, pp. 834-846, 2012.
- [96] Z. Pan, C. Wu, J. Liu, W. Wang and J. Liu, "Study on mechanical properties of cost-effective polyvinyl alcohol engineered cementitious composites (PVA-ECC)," *Construction and Building Materials*, vol. 78, pp. 397-404, 2015.
- [97] C. Lu and C. K. Leung, "A new model for the cracking process and tensile ductility of Strain Hardening Cementitious Composites (SHCC)," *Cement and Concrete Research*, vol. 79, pp. 353-365, 2016.
- [98] S. W. Lee, S.-B. Kang, K. H. Tan and E.-H. Yang, "Experimental and analytical investigation on bond-slip behaviour of deformed bars embedded in engineered cementitious composites," *Construction and Building Materials*, vol. 127, pp. 494-503, 2016.
- [99] A. P. Fantilli, H. Mihashi and P. Vallini, "Strain compatibility between HPFRCC and steel reinforcement," *Materials and Structures*, vol. 38, pp. 495-503, 2005.
- [100] C. Soranakom and B. Mobasher, "Modeling of tension stiffening in reinforced cement composites: Part 1 Theoretical modeling," *Materials and Structures*, vol. 43, pp. 1217-1230, 2010.

ANNEXURE A: ALGORITHM FOR CALCULATION OF NUMERICAL MODEL

This Annexure endeavours to explain the calculation process of the numerical model in such a way as to enable the reader to do a flexural design without further consulting the main text.

Information that must be known:

Material Properties

The following material properties must be known:

- ϵ_{ct1} – First cracking tensile strain
- ϵ_{ctu} – Ultimate tensile strain
- σ_{ct1} – First cracking tensile stress
- σ_{ctu} – Ultimate tensile stress
- ϵ_{ccu} – Ultimate compressive strain
- σ_{ccu} – Ultimate compressive stress

Loading

The ultimate moment, M_u , applied to the member is needed as well as the serviceability moment, M_s . The ultimate moment is used to find the right amount of reinforcement and the serviceability moment is used to check the deflection of the member. If the service loads are unknown, the ultimate load can be divided by 1.4 to approximate the service load.

Structural element dimensions

The following dimensions for the structural member to be design are needed:

- h – Height of the member
- b – Width of the member
- l – Length of the member
- d – Distance to the tensile steel (measured from the top of the member)
- d' – Distance to the compressive steel (measured from the top of the member)

To be calculated up front

By using the information above, the following needs to be calculated:

- $E_{ct} = \frac{\sigma_{ct1}}{\varepsilon_{ct1}}$
- $E_{cc} = 1.681 \frac{\sigma_{cu}}{\varepsilon_{cu}}$
- $\alpha = \frac{\sigma_{ctu} - \sigma_{ct1}}{\varepsilon_{ctu} - \varepsilon_{ct1}} \frac{\varepsilon_{ct1}}{\sigma_{ct1}}$
- $\delta = \frac{\sigma_{ctu} - \sigma_{ct1}}{\varepsilon_{ctu} - \varepsilon_{ct1}} \frac{\varepsilon_{ct1}}{\sigma_{ct1}} = \frac{\sigma_{ctu} - 0.533\sigma_{ctu}}{\varepsilon_{ctu} - 0.317\varepsilon_{ctu}} \frac{0.317\varepsilon_{ctu}}{0.533\sigma_{ctu}} = 0.4067$

Where:

- E_{ct} – Elastic Modulus for the material in tension
- E_{cc} – Elastic Modulus for the material in compression
- α – The factor with which the Elastic Modulus for the material in tension must be applied to find the slope of the strain hardening part of the stress-strain graph
- δ – The factor with which the Elastic Modulus for the material in compression must be applied to find the slope of the second part of the stress-strain graph

Design Process

- 1) Guess the amount of tensile (A_s) and compressive (A'_s) reinforcement in the beam.
- 2) The following equations will need to be solved simultaneously:

- $$x = \frac{E_s(A_s + A'_s) + E_{ct}A_c g \pm \sqrt{(-E_s(A_s + A'_s) - E_{ct}A_c g)^2 - (2E_{ct}bg - 2E_{cc}b)(E_s(A'_s + A_s) + \frac{1}{2}E_{ct}bh^2g)}}{E_{ct}bg - E_{cc}b}$$
- $$\varepsilon_{ct2} = \frac{M_u(h-x)}{\frac{1}{3}E_{cc}bx^3 + \frac{1}{6}E_{ct}b(h-x)^3k + E_s(A'_s(x-d) + A_s(d-x))^2}$$
- $$\beta = \frac{\varepsilon_{ct1}}{\varepsilon_{ct2}}$$
- $$g = \beta^2 + 2\beta(1 - \beta) + \alpha(1 - \beta)^2$$
- $$k = 2\beta^3 + 3\beta(\beta + 1)(1 - \beta) + \alpha(1 - \beta)^2(\beta + 2)$$
- $$\varepsilon_{cc2} = \frac{-x}{h-x} \varepsilon_{ct2}$$

- 3) If $\varepsilon_{cc2} < 0.317\varepsilon_{ccu}$ the design is based in Phase 2. If $\varepsilon_{cc2} > 0.317\varepsilon_{ccu}$ the design falls within phase 3 and the process from point number 7 should be followed.
- 4) The amount of tensile and compressive reinforcement then needs to be changed until the strain the tensile reinforcement just reaches 0.00225 at the ultimate moment applied.
- 5) Now the deflection needs to be checked for the above amounts of reinforcement at the serviceability moment. This is done as follows:
 - Find the part of the beam that is cracked. (see Figure A1)

$$\alpha = 1 - \frac{M_e}{M_y}$$

with M_e = Moment at the first cracking stress

M_y = Applied Moment (serviceability limit state)

- Find the curvature at each of the points indicated in Figure A1

$$\rho_y = \frac{\epsilon_c}{x}$$

with ϵ_c = Compressive strain at the point in question

x = Distance to the neutral axis at the point in question

- The deflection at each point can then be found as follows:

$$\Delta_1 = \frac{1}{3} L_1^2 \rho_1$$

$$\Delta_2 = \Delta_1 + \frac{1}{2} \rho_1 (L_2 - L_1) (L_1 + L_2) + \frac{1}{6} (L_2 - L_1) (\rho_2 - \rho_1) (L_1 + 2L_2)$$

$$\Delta_3 = \Delta_2 + \frac{1}{2} \rho_2 (L_3 - L_2) (L_2 + L_3) + \frac{1}{6} (L_3 - L_2) (\rho_3 - \rho_2) (L_2 + 2L_3)$$

$$\Delta_4 = \Delta_3 + \frac{1}{2} \rho_3 (L_4 - L_3) (L_3 + L_4) + \frac{1}{6} (L_4 - L_3) (\rho_4 - \rho_3) (L_3 + 2L_4)$$

$$\Delta_5 = \Delta_4 + \frac{1}{2} \rho_4 (L_5 - L_4) (L_4 + L_5) + \frac{1}{6} (L_5 - L_4) (\rho_5 - \rho_4) (L_4 + 2L_5)$$

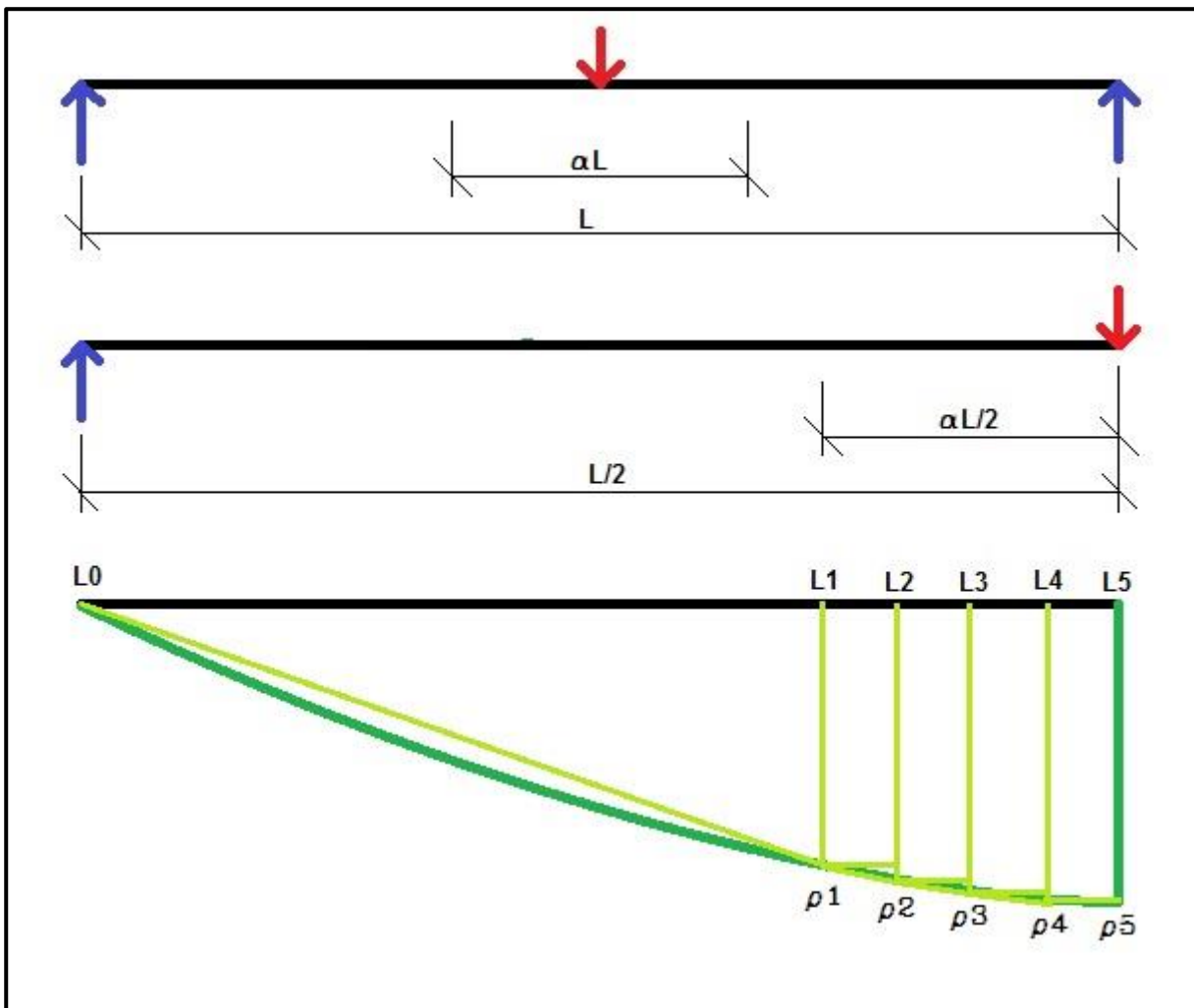


Figure A1: Deflection Calculation Diagram

6) If the deflection is more than $L/250$ or 30mm, whichever is the smaller, the tensile and compressive reinforcement must be increased until the deflection is ok, or the depth of the beam needs to be increased and the calculations start from the beginning.

7) If the design falls in Phase 3 of the model, the following equations become valid:

- $$x = \frac{E_{ct}A_c g + E_s(A'_s + A_s) \pm \sqrt{(-E_{ct}A_c g - E_s(A'_s + A_s))^2 - (2E_{ct}b g - 2E_{cc}b m) \left(\frac{1}{2}E_{ct}b h^2 g + E_s(A'_s d' + A_s d) \right)}}{b(E_{ct}g - E_{cc}m)}$$
- $$\varepsilon_{ct2} = \frac{M_u(h-x)}{\frac{1}{6}E_{cc}b x^3 n + \frac{1}{6}E_{ct}b(h-x)^3 k + E_s(A'_s(x-dr)^2 + A_s(d-x)^2)}$$
- $$g = \beta^2 + 2\beta(1 - \beta) + \alpha(1 - \beta)^2$$
- $$m = \gamma^2 + 2\gamma(1 - \gamma) + \delta(1 - \gamma)^2$$
- $$n = 2\gamma^3 + 3\gamma(1 - \gamma)(\gamma + 1) + \delta(1 - \gamma)^2(\gamma + 2)$$
- $$k = 2\beta^3 + 3\beta(1 - \beta)(\beta + 1) + \alpha(1 - \beta)^2(\beta + 2)$$
- $$\varepsilon_{cc2} = \frac{-x}{h-x} \varepsilon_{ct2}$$

8) Again the amounts of compressive and tensile steel needs to be varied until the tensile strain of the tensile reinforcement is equal to 0.00225 at the ultimate moment applied.

9) Check the deflection as per point number 5. If the deflection is more than $L/250$ or 30mm, whichever is smaller, the compressive and tensile reinforcement needs to be increased until the deflection is in order, or the depth of the beams needs to be increased and the calculation start from the beginning.

ANNEXURE B: COMPLETE ILLUSTRATIVE DESIGN

The following examples endeavour to illustrate the applicability of the design model in the industry.

Example 1 – Simply supported beam with line load

Consider the following beam to be designed:

- 250x550deep and 6.0m long
- simply supported on both ends
- ultimate limit state line load, w , of 55kN/m applied to length of beam

The moment is then calculated as follows:

$$Mu = \frac{wl^2}{8} = 247.5kNm$$

Properties of material to be used:

- $\epsilon_{ct1} = 0.00024$
- $\sigma_{ct1} = 2.054MPa$
- $\epsilon_{ctu} = 0.01456$
- $\sigma_{ctu} = 2.937MPa$
- $\epsilon_{ccu} = -0.00508$
- $\sigma_{ccu} = -30.559MPa$

From this the following can be calculated:

$$E_{ct} = \frac{\sigma_{ct1}}{\epsilon_{ct1}} = 8.558GPa$$

$$E_{cc} = 1.681 \frac{\sigma_{ccu}}{\epsilon_{ccu}} = 10.112GPa$$

$$\alpha = \frac{\sigma_{ctu} - \sigma_{ct1}}{\epsilon_{ctu} - \epsilon_{ct1}} \frac{\epsilon_{ct1}}{\epsilon_{ctu}} = 0.00720$$

$$\delta = 0.407$$

$$0.317\epsilon_{ccu} = 0.00161$$

$$\frac{Mu}{bd^2\sigma_{ctu}} = 1.247$$

For $h = 500\text{mm}$

$$x = 0.02988 \text{Ln} \left(\frac{Mu}{bd^2\sigma_{ctu}} \right) + 0.18285 = 0.1894$$

$$\varepsilon_{ct2} = 0.1678 \left(\frac{Mu}{bd^2\sigma_{ctu}} \right)^{0.0078} 0.01456 = 0.002447$$

For $h = 600\text{mm}$

$$x = 0.03768 \text{Ln} \left(\frac{Mu}{bd^2\sigma_{ctu}} \right) + 0.22098 = 0.2293$$

$$\varepsilon_{ct2} = 0.1655 \left(\frac{Mu}{bd^2\sigma_{ctu}} \right)^{0.0068} 0.01456 = 0.002413$$

That means that for $h = 550\text{mm}$, the values can be interpolated, giving:

$$\varepsilon_{ct2} = 0.00243$$

$$x = 0.209\text{m}$$

This can now be used to determine the compressive strain in the top of the beam via:

$$\varepsilon_{ccu} = \frac{-x}{(h-x)} \varepsilon_{ct2} = -0.00149 < 0.317 \varepsilon_{ccu} = 0.00161$$

The design is thus in Phase 2 and the reinforcement can now be calculated.

First we need to calculate the following:

$$\beta = \frac{\varepsilon_{ct1}}{\varepsilon_{ct2}} = 0.0988$$

$$g = \beta^2 + 2\beta(1-\beta) + \alpha(1-\beta)^2 = 0.1937$$

$$k = 2\beta^3 + 3\beta(1-\beta)(\beta+1) + \alpha(1-\beta)^2(\beta+2) = 0.3077$$

$$A_s = \frac{1.125M(h-x)/\varepsilon_{ct2} - 1/6 E_{cc}x^2b(3d' - x) - 1/6 E_{ct}b(h-x)^2(k(h-x) + 3g(x-d'))}{E_s(d-x)(d-d')} = 1043\text{mm}^2$$

$$A'_s = \frac{1.125M(h-x)/\varepsilon_{ct2} - 1/6 E_{cc}x^2b(3d - x) - 1/6 E_{ct}b(h-x)^2(k(h-x) - 3g(d-x))}{E_s(x-d')(d-d')} = 834\text{mm}^2$$

That means that we can use 2xY20's with 1 Y25 in the bottom of the beam and 3xY20's in the top of the beam. That gives us 1119mm² for tensile reinforcement and 942mm² for compressive reinforcement. The resisting moment of the beam can then be calculated as follows:

$$M_r = \frac{\varepsilon_{ct2} \left(\frac{1}{3} E_{cc}bx^3 + \frac{1}{6} E_{ct}b(h-x)^3k + E_s(A'_s(d-d')^2 + A_s(d-x)^2) \right)}{h-x} = 267.71\text{kNm}$$

This is more than the 247.5kNm that is the ultimate moment, so the design is safe.

As the length of the beam is less than 10m, the deflection does not need to be checked.

Example 2 – Roof slab with upstand beams

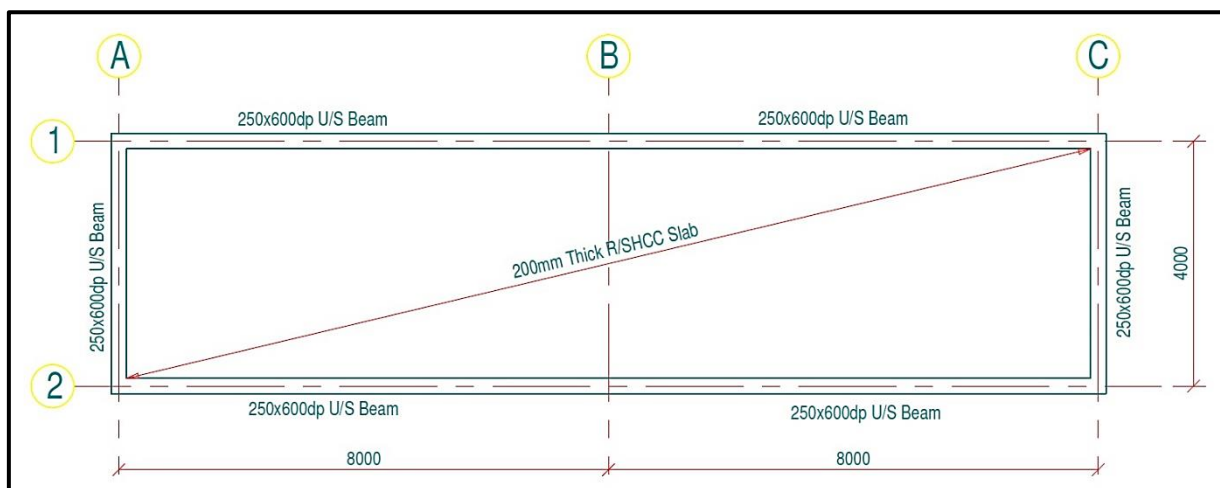


Figure C1 - Roof slab and beam layout

Loading on Slab:

Dead Load = 13.95kPa

$$\text{Live Load} = 1.0\text{kPa}$$

$$\text{ULS} = 1.35\text{DL} + 1.0\text{xLL}$$

$$= 19.833\text{kPa}$$

$$\text{SLS} = \text{DL} + \text{LL}$$

$$= 14.95\text{kPa}$$

Slab is one way spanning so we take a 1m strip to do design.

$$M_{\text{ult}} = w\ell^2/8$$

$$= 39.665\text{kNm/m}$$

The same material as per Example 1 is used.

First we assume that the design is in phase 2. Then:

$$x = 0.01512Ln\left(\frac{M_u}{bd^2\sigma_{ctu}}\right) + 0.06962$$

$$= 0.058\text{m}$$

And

$$\varepsilon_{ct2} = 0.1912\left(\frac{M_u}{bd^2\sigma_{ctu}}\right)^{0.0262} * 0.01456$$

$$= 0.00273$$

Then

$$\varepsilon_{cc} = \frac{-x}{h-x}\varepsilon_{ct2}$$

$$0.00112 < 0.00161$$

Thus the design is indeed in Phase 2.

The reinforcing can then be calculated from the following equations:

$$A_s = \frac{1.125M_u(h-x)/\varepsilon_{ct2} - 1/6 E_{cc}x^2b(3d'-x) - 1/6 E_{ct}b(h-x)^2(k(h-x) + 3g(x-d'))}{E_s(d-x)(d-d')}$$

$$A'_s = \frac{1.125M(h-x)/\varepsilon_{ct2} - 1/6 E_{cc}x^2b(3d-x) - 1/6 E_{ct}b(h-x)^2(k(h-x) - 3g(d-x))}{E_s(x-d')(d-d')}$$

With:

$$g = \beta^2 + 2\beta(1-\beta) + \alpha(1-\beta)^2$$

$$k = 2\beta^3 + 3\beta(1-\beta)(\beta+1) + \alpha(1-\beta)^2(\beta+2)$$

The tensile reinforcement calculated from above comes to 0.000121m² which is very little steel. For the 200mm thick slab. Y8@175mm, 0.000287m², conforms to the minimum tensile reinforcing specified for normal reinforced concrete by the SANS 10100. This is 0.13% of the concrete area which in this case is 0.00026m². As there are no minimum reinforcement limits set for SHCC this limit is used.

The compression reinforcement calculated comes to 0.000065m², which is even less than the tensile reinforcement. The minimum compression reinforcement rule given by SANS 10100 is 0.2% of the concrete area. In this case it works out to 0.0004m². Y10@175 will provide 0.000449m² and so this is used.

The span of the slab does not really necessitate checking the deflection, but if it is done according to chapter 4, the deflection at mid span is 7.197mm.

The reinforcing for the up-stand beams can now be calculated.

For the continuous beams on gridlines 1 and 2, the moments are calculated via Prokon and are given below:

$$M_{ab} = 193\text{kNm} = M_{bc}$$

$$M_b = 345\text{kNm}$$

No redistribution of moments were allowed. Seeing that deflection can be a problem for this material more research is needed to establish what amounts of redistribution should be allowed, if any. At this stage it is considered safe to not apply any redistribution.

From the moments above, and assuming the design falls within Phase 2, the tensile and compressive reinforcement for each part of the beam can be calculated using the following formulas:

$$\varepsilon_{ct2} = 0.1655 \left(\frac{M_u}{bd^2\sigma_{ctu}} \right)^{0.0068} - 0.01456$$

$$x = 0.03768Ln \left(\frac{M_u}{bd^2\sigma_{ctu}} \right) + 0.22098$$

From the above the following is calculated:

$$\varepsilon_{ct2} = 0.00241$$

$$x = 0.213m$$

$$\varepsilon_{cc} = -0.00132$$

Which confirms that the design is indeed within Phase 2.

Now the reinforcement can be calculated from the equations used for the slab design and the following is calculated:

$$A_s = 0.000620m^2$$

$$A'_s = 0.000409m^2$$

The tensile reinforcement is changed to 2Y20's which relates back to 0.000628m² and the compressive reinforcement is changed to 2Y16's which is equivalent to 0.000402m². The deflection calculated for this beam is then 17.586mm which is smaller than the 30mm limit imposed on deflection by SANS 10160.

To calculate the reinforcement needed for the hogging moment, the calculations have to be repeated from the start. The design is again assumed to be in Phase 2 and the tensile strain, the distance to the neutral axis and the compressive strain is calculated as follows:

$$\varepsilon_{ct2} = 0.00242$$

$$x = 0.235m$$

$$\varepsilon_{cc} = -0.00155$$

Confirming the design is indeed in Phase 2, the reinforcement can be calculated as follows:

$$A_s = 0.001382m^2$$

$$A'_s = 0.001108m^2$$

The actual reinforcement for the hogging moment will then be 3Y25's as tensile reinforcement. This is equivalent to 0.001473m². The compressive reinforcement used will be 2Y20's + 1Y25, which results in 0.001119m² of reinforcement. Deflection is not a problem for the hogging moment so there is no sense in calculating it.

The short beam can be calculated in a similar way.

From this example it is clear that the design model is not just applicable to single span simply supported beams with a single point load in the centre of the beam. As long as the material parameters is known and the moment is calculated, the model is applicable to all flexural members bending in one direction only.

ANNEXURE C: VERIFICATION OF DESIGN MODEL VIA DIFFERENT MATERIALS

These tables show the analysis done on a beam in order to establish the ultimate moment resistance for a specific size beam reinforced with a specific amount of reinforcing. The first Table is done for Material 2 and the second one for Material 3.

Material 2

200x200x2800 (Phase 2)																						
h	0,200																					
b	0,2																					
d	0,175																					
d'	0,030																					
l	2,8	11,2																				
As	0,001																					
As'	0,001																					
Ect	15000000																					
Ecc	17444340																					
Es	200000000																					
εct1	0,000236																					
σct1	3540																					
εctu	0,01270																					
σctu	5000																					
εccu	-0,00530	-0,00168																				
σccu	-55000	-29308																				
α	0,00781																					
δ	0,407																					
εct2	β	g	k	x	εct2	P	εcc	εsc	εst	σct2	σcc	f_{sc}	%Ac	As'	Es	f_{st}	%Ac	As	Es	Mu	Δ	
0,0027314	0,086	0,172	0,272	0,058	0,00273	20,152	-0,0011195	-0,00054	0,002250	3,832	-19,529	-108,376	0,100	0,00004	200000000	450,000	0,100	0,00004	199999512	14,106	3,812	
0,002744	0,086	0,171	0,271	0,061	0,00274	23,821	-0,0012083	-0,00062	0,002250	3,834	-21,079	-123,097	0,100	0,00004	200000000	450,000	0,200	0,00008	200000000	16,675	4,783	
0,0027407	0,086	0,171	0,271	0,060	0,00274	23,839	-0,001185	-0,00060	0,002250	3,833	-20,672	-119,236	0,200	0,00008	200000000	450,000	0,200	0,00008	200000000	16,687	4,707	
0,0027564	0,086	0,170	0,270	0,064	0,00276	27,463	-0,0012949	-0,00069	0,002250	3,835	-22,588	-137,436	0,100	0,00004	200000000	449,999	0,300	0,00012	200000000	19,224	5,631	
0,0027528	0,086	0,171	0,270	0,063	0,00275	27,491	-0,0012695	-0,00067	0,002250	3,835	-22,145	-133,228	0,200	0,00008	200000000	450,000	0,300	0,00012	200000000	19,244	5,550	
0,0027493	0,086	0,171	0,270	0,062	0,00275	27,516	-0,0012454	-0,00065	0,002250	3,834	-21,726	-129,243	0,300	0,00012	200000000	450,000	0,300	0,00012	200000000	19,261	5,473	
0,0027685	0,085	0,170	0,269	0,067	0,00277	31,083	-0,0013794	-0,00076	0,002250	3,837	-24,063	-151,446	0,100	0,00004	200000000	450,000	0,400	0,00016	200000000	21,758	6,356	
0,0027646	0,085	0,170	0,269	0,066	0,00276	31,121	-0,001352	-0,00073	0,002250	3,836	-23,585	-146,906	0,200	0,00008	200000000	450,000	0,400	0,00016	200000000	21,785	6,271	
0,0027609	0,085	0,170	0,269	0,065	0,00276	31,155	-0,001326	-0,00071	0,002250	3,836	-23,132	-142,603	0,300	0,00012	200000000	450,000	0,400	0,00016	200000000	21,808	6,189	
0,0027573	0,086	0,170	0,270	0,064	0,00276	31,185	-0,0013014	-0,00069	0,002250	3,835	-22,702	-138,520	0,400	0,00016	200000000	450,000	0,400	0,00016	200000000	21,829	6,112	
0,0027803	0,085	0,169	0,268	0,069	0,00278	34,680	-0,0014622	-0,00083	0,002250	3,838	-25,507	-165,168	0,100	0,00004	200000000	450,000	0,500	0,00020	199999924	24,276	6,979	

0,0027761	0,085	0,169	0,268	0,068	0,00278	34,729	-0,0014329	-0,00080	0,002250	3,838	-24,996	-160,310	0,200	0,00008	200000000	450,000	0,500	0,00020	199999448	24,310	6,890
0,0027721	0,085	0,170	0,268	0,067	0,00277	34,772	-0,0014051	-0,00078	0,002250	3,837	-24,511	-155,699	0,300	0,00012	200000000	449,991	0,500	0,00020	200000000	24,341	6,804
0,0027684	0,085	0,170	0,269	0,066	0,00277	34,812	-0,0013787	-0,00076	0,002250	3,837	-24,050	-151,324	0,400	0,00016	200000000	450,000	0,500	0,00020	199999408	24,369	6,723
0,0027648	0,085	0,170	0,269	0,066	0,00276	34,847	-0,0013536	-0,00074	0,002250	3,836	-23,612	-147,162	0,500	0,00020	200000000	450,000	0,500	0,00020	199999835	24,393	6,645
0,0027919	0,085	0,168	0,267	0,071	0,00279	38,256	-0,0015435	-0,00089	0,002250	3,839	-26,925	-178,637	0,100	0,00004	200000000	450,000	0,600	0,00024	199999050	26,779	7,521
0,0027875	0,085	0,169	0,267	0,070	0,00279	38,317	-0,0015123	-0,00087	0,002250	3,839	-26,382	-173,472	0,200	0,00008	200000000	450,000	0,600	0,00024	200000000	26,822	7,428
0,0027832	0,085	0,169	0,267	0,070	0,00278	38,372	-0,0014827	-0,00084	0,002250	3,838	-25,865	-168,568	0,300	0,00012	200000000	450,000	0,600	0,00024	200000000	26,860	7,339
0,0027792	0,085	0,169	0,268	0,069	0,00278	38,421	-0,0014546	-0,00082	0,002250	3,838	-25,375	-163,907	0,400	0,00016	200000000	450,000	0,600	0,00024	199998986	26,895	7,255
0,0027754	0,085	0,169	0,268	0,068	0,00278	38,466	-0,0014278	-0,00080	0,002250	3,837	-24,908	-159,471	0,500	0,00020	200000000	450,000	0,600	0,00024	200000000	26,926	7,174
0,0027718	0,085	0,170	0,268	0,067	0,00277	38,506	-0,0014024	-0,00078	0,002250	3,837	-24,463	-155,247	0,600	0,00024	200000000	450,000	0,600	0,00024	200000000	26,954	7,096
0,0028033	0,084	0,168	0,266	0,073	0,00280	41,814	-0,0016234	-0,00096	0,002250	3,841	-28,319	-191,880	0,100	0,00004	200000000	450,000	0,700	0,00028	199999869	29,270	8,002
0,0027986	0,084	0,168	0,266	0,072	0,00280	41,887	-0,0015905	-0,00093	0,002250	3,840	-27,745	-186,419	0,200	0,00008	200000000	450,000	0,700	0,00028	199999564	29,321	7,905
0,0027942	0,084	0,168	0,266	0,072	0,00279	41,953	-0,0015591	-0,00091	0,002250	3,840	-27,198	-181,230	0,300	0,00012	200000000	450,000	0,700	0,00028	200000000	29,367	7,812
0,0027899	0,085	0,169	0,267	0,071	0,00279	42,013	-0,0015294	-0,00088	0,002250	3,839	-26,679	-176,292	0,400	0,00016	200000000	450,000	0,700	0,00028	200000000	29,409	7,724
0,0027859	0,085	0,169	0,267	0,070	0,00279	42,067	-0,001501	-0,00086	0,002250	3,839	-26,184	-171,592	0,500	0,00020	200000000	450,000	0,700	0,00028	199999896	29,447	7,640
0,002782	0,085	0,169	0,268	0,069	0,00278	42,116	-0,0014739	-0,00084	0,002250	3,838	-25,712	-167,111	0,600	0,00024	200000000	450,000	0,700	0,00028	200000000	29,481	7,559
0,0027783	0,085	0,169	0,268	0,069	0,00278	42,161	-0,0014482	-0,00081	0,002250	3,838	-25,262	-162,838	0,700	0,00028	200000000	450,000	0,700	0,00028	199999911	29,513	7,482
0,0028096	0,084	0,167	0,265	0,074	0,00281	45,439	-0,0016674	-0,00100	0,002250	3,841	-29,087	-199,173	0,200	0,00008	200000000	450,000	0,800	0,00032	199999820	31,808	8,333
0,0028049	0,084	0,168	0,265	0,074	0,00280	45,517	-0,0016344	-0,00097	0,002250	3,841	-28,512	-193,706	0,300	0,00012	200000000	450,000	0,800	0,00032	199999074	31,862	8,237
0,0028004	0,084	0,168	0,266	0,073	0,00280	45,588	-0,001603	-0,00094	0,002250	3,840	-27,964	-188,501	0,400	0,00016	200000000	450,000	0,800	0,00032	200000000	31,912	8,145
0,0027962	0,084	0,168	0,266	0,072	0,00280	45,653	-0,0015731	-0,00092	0,002250	3,840	-27,442	-183,542	0,500	0,00020	200000000	450,000	0,800	0,00032	199999232	31,957	8,057
0,0027921	0,085	0,168	0,267	0,071	0,00279	45,711	-0,0015446	-0,00089	0,002250	3,839	-26,944	-178,812	0,600	0,00024	200000000	450,000	0,800	0,00032	199999961	31,998	7,973
0,0027882	0,085	0,169	0,267	0,070	0,00279	45,765	-0,0015173	-0,00087	0,002250	3,839	-26,469	-174,299	0,700	0,00028	200000000	450,000	0,800	0,00032	200000000	32,035	7,893
0,0027845	0,085	0,169	0,267	0,070	0,00278	45,814	-0,0014913	-0,00085	0,002250	3,839	-26,015	-169,987	0,800	0,00032	200000000	450,000	0,800	0,00032	199999640	32,069	7,816
0,0028108	0,084	0,167	0,265	0,075	0,00281	49,148	-0,0016757	-0,00100	0,002250	3,842	-29,232	-200,548	0,400	0,00016	200000000	450,000	0,900	0,00036	200000000	34,403	8,527
0,0028063	0,084	0,168	0,265	0,074	0,00281	49,223	-0,0016443	-0,00098	0,002250	3,841	-28,683	-195,338	0,500	0,00020	200000000	450,000	0,900	0,00036	199999076	34,456	8,436
0,002802	0,084	0,168	0,266	0,073	0,00280	49,292	-0,0016143	-0,00095	0,002250	3,841	-28,160	-190,365	0,600	0,00024	200000000	450,000	0,900	0,00036	199999728	34,504	8,349
0,0027979	0,084	0,168	0,266	0,072	0,00280	49,354	-0,0015856	-0,00093	0,002250	3,840	-27,660	-185,617	0,700	0,00028	200000000	450,000	0,900	0,00036	200000000	34,548	8,266
0,002794	0,084	0,168	0,266	0,072	0,00279	49,412	-0,0015582	-0,00091	0,002250	3,840	-27,182	-181,079	0,800	0,00032	200000000	450,000	0,900	0,00036	199999838	34,588	8,186
0,0027903	0,085	0,169	0,267	0,071	0,00279	49,465	-0,001532	-0,00088	0,002250	3,839	-26,725	-176,738	0,900	0,00036	200000000	450,000	0,900	0,00036	199999567	34,625	8,109
0,0028076	0,084	0,168	0,265	0,074	0,00281	52,931	-0,0016531	-0,00098	0,002250	3,841	-28,838	-196,806	0,700	0,00028	200000000	450,000	1,000	0,00040	199999836	37,051	8,608
0,0028035	0,084	0,168	0,266	0,073	0,00280	52,997	-0,0016244	-0,00096	0,002250	3,841	-28,337	-192,046	0,800	0,00032	200000000	450,000	1,000	0,00040	199999083	37,098	8,525
0,0027996	0,084	0,168	0,266	0,073	0,00280	53,059	-0,0015969	-0,00094	0,002250	3,840	-27,857	-187,491	0,900	0,00036	200000000	450,000	1,000	0,00040	200000000	37,141	8,445
0,0027958	0,084	0,168	0,266	0,072	0,00280	53,115	-0,0015706	-0,00092	0,002250	3,840	-27,398	-183,129	1,000	0,00040	200000000	450,000	1,000	0,00040	200000000	37,180	8,369
0,0028087	0,084	0,168	0,265	0,074	0,00281	56,640	-0,0016612	-0,00099	0,002250	3,841	-28,978	-198,133	0,900	0,00036	200000000	450,000	1,100	0,00044	199999221	39,648	8,756
0,0028048	0,084	0,168	0,265	0,074	0,00280	56,705	-0,0016336	-0,00097	0,002250	3,841	-28,497	-193,568	1,000	0,00040	200000000	450,000	1,100	0,00044	200000000	39,693	8,677
0,002801	0,084	0,168	0,266	0,073	0,00280	56,765	-0,0016072	-0,00095	0,002250	3,840	-28,036	-189,192	1,100	0,00044	200000000	450,000	1,100	0,00044	199999607	39,735	8,601
0,0028098	0,084	0,167	0,265	0,075	0,00281	60,351	-0,0016684	-0,00100	0,002250	3,841	-29,105	-199,340	1,100	0,00044	200000000	450,000	1,200	0,00048	200000000	42,246	8,886

0,002806	0,084	0,168	0,265	0,074	0,00281	60,414	-0,001642	-0,00097	0,002250	3,841	-28,643	-194,955	1,200	0,00048	200000000	450,000	1,200	0,00048	200000000	42,290	8,811
0,0028107	0,084	0,167	0,265	0,075	0,00281	64,064	-0,0016751	-0,00100	0,002250	3,842	-29,221	-200,442	1,300	0,00052	200000000	450,000	1,300	0,00052	200000000	44,845	9,001

200x200x2800 (Phase 3)																								
h	0,200																							
b	0,2																							
d	0,175																							
d'	0,030																							
l	2,8	11,2																						
As	0,001																							
As'	0,001																							
Ect	15000000																							
Ecc	17444340																							
Es	200000000																							
Ect1	0,000236																							
σct1	3540																							
Ectu	0,01270																							
σctu	5000																							
Eccu	-0,00530	-0,00168																						
σccu	-55000	-29308																						
α	0,00781																							
δ	0,407																							
εct2	β	g	p	γ	m	n	x	εct2	P	εcc	εsc	εst	σct2	σcc	fsc	%Ac	As'	Es	fst	%Ac	As	Es	Mu	Δ
0,00281	0,084	0,167	0,265	0,987	1,000	2,000	0,075	0,00281	45,352	-0,00170	-0,00102	0,00225	3,842	-29,465	-204,938	0,100	0,00004	200000000	449,999	0,800	0,00032	200000000	31,747	8,219
0,00283	0,084	0,167	0,264	0,943	0,998	1,994	0,077	0,00283	48,852	-0,00178	-0,00109	0,00225	3,843	-30,030	-218,112	0,100	0,00004	200000000	449,999	0,900	0,00036	200000000	34,197	8,579
0,00282	0,084	0,167	0,264	0,963	0,999	1,998	0,076	0,00282	48,966	-0,00174	-0,00106	0,00225	3,843	-29,763	-211,882	0,200	0,00008	200000000	449,999	0,900	0,00036	200000000	34,276	8,482
0,00282	0,084	0,167	0,265	0,983	1,000	1,999	0,076	0,00282	49,064	-0,00171	-0,00103	0,00225	3,842	-29,512	-206,040	0,300	0,00012	200000000	449,999	0,900	0,00036	200000000	34,344	8,389
0,00284	0,083	0,166	0,263	0,902	0,994	1,983	0,079	0,00284	52,308	-0,00186	-0,00116	0,00225	3,845	-30,604	-231,507	0,100	0,00004	200000000	450,000	1,000	0,00040	199999570	36,616	8,907
0,00283	0,083	0,166	0,263	0,922	0,996	1,989	0,078	0,00283	52,450	-0,00182	-0,00112	0,00225	3,844	-30,316	-224,788	0,200	0,00008	200000000	449,999	1,000	0,00040	200000000	36,715	8,810
0,00283	0,084	0,167	0,264	0,942	0,998	1,994	0,077	0,00283	52,574	-0,00178	-0,00109	0,00225	3,843	-30,046	-218,496	0,300	0,00012	200000000	449,999	1,000	0,00040	200000000	36,802	8,715
0,00282	0,084	0,167	0,264	0,961	0,999	1,997	0,077	0,00282	52,682	-0,00175	-0,00106	0,00225	3,843	-29,793	-212,588	0,400	0,00016	200000000	450,000	1,000	0,00040	200000000	36,877	8,624
0,00282	0,084	0,167	0,264	0,980	1,000	1,999	0,076	0,00282	52,776	-0,00171	-0,00104	0,00225	3,842	-29,555	-207,028	0,500	0,00020	200000000	449,999	1,000	0,00040	200000000	36,943	8,535
0,00281	0,084	0,167	0,265	0,998	1,000	2,000	0,075	0,00281	52,858	-0,00168	-0,00101	0,00225	3,842	-29,330	-201,783	0,600	0,00024	200000000	449,999	1,000	0,00040	200000000	37,001	8,448
0,00285	0,083	0,165	0,262	0,864	0,989	1,969	0,081	0,00285	55,722	-0,00194	-0,00123	0,00225	3,846	-31,187	-245,119	0,100	0,00004	200000000	449,999	1,100	0,00044	200000000	39,006	9,210
0,00284	0,083	0,166	0,262	0,884	0,992	1,977	0,080	0,00284	55,894	-0,00190	-0,00119	0,00225	3,845	-30,877	-237,896	0,200	0,00008	200000000	450,000	1,100	0,00044	200000000	39,126	9,112
0,00284	0,083	0,166	0,263	0,903	0,994	1,984	0,079	0,00284	56,045	-0,00186	-0,00116	0,00225	3,845	-30,588	-231,138	0,300	0,00012	200000000	449,999	1,100	0,00044	200000000	39,231	9,017
0,00283	0,083	0,166	0,263	0,922	0,996	1,989	0,078	0,00283	56,178	-0,00182	-0,00112	0,00225	3,844	-30,316	-224,800	0,400	0,00016	200000000	449,999	1,100	0,00044	200000000	39,325	8,924
0,00283	0,083	0,167	0,264	0,941	0,998	1,994	0,077	0,00283	56,296	-0,00179	-0,00109	0,00225	3,843	-30,061	-218,840	0,500	0,00020	200000000	450,000	1,100	0,00044	200000000	39,407	8,834
0,00282	0,084	0,167	0,264	0,959	0,999	1,997	0,077	0,00282	56,399	-0,00175	-0,00107	0,00225	3,843	-29,820	-213,223	0,600	0,00024	200000000	450,000	1,100	0,00044	200000000	39,479	8,746

0,00282	0,084	0,167	0,264	0,977	1,000	1,999	0,076	0,00282	56,490	-0,00172	-0,00104	0,00225	3,842	-29,593	-207,919	0,700	0,00028	200000000	450,000	1,100	0,00044	200000000	39,543	8,662
0,00281	0,084	0,167	0,265	0,994	1,000	2,000	0,075	0,00281	56,570	-0,00169	-0,00101	0,00225	3,842	-29,378	-202,900	0,800	0,00032	200000000	450,000	1,100	0,00044	200000000	39,599	8,579
0,00286	0,082	0,165	0,261	0,828	0,983	1,951	0,083	0,00286	59,097	-0,00203	-0,00129	0,00225	3,848	-31,779	-258,947	0,100	0,00004	200000000	450,000	1,200	0,00048	200000000	41,368	9,493
0,00285	0,083	0,165	0,261	0,848	0,986	1,961	0,082	0,00285	59,299	-0,00198	-0,00126	0,00225	3,847	-31,447	-251,201	0,200	0,00008	200000000	449,999	1,200	0,00048	200000000	41,509	9,394
0,00285	0,083	0,165	0,262	0,867	0,990	1,970	0,081	0,00285	59,479	-0,00194	-0,00122	0,00225	3,846	-31,137	-243,963	0,300	0,00012	200000000	449,999	1,200	0,00048	200000000	41,635	9,297
0,00284	0,083	0,166	0,262	0,886	0,992	1,978	0,080	0,00284	59,639	-0,00190	-0,00119	0,00225	3,845	-30,847	-237,181	0,400	0,00016	200000000	449,999	1,200	0,00048	200000000	41,747	9,204
0,00284	0,083	0,166	0,263	0,904	0,995	1,984	0,079	0,00284	59,780	-0,00186	-0,00115	0,00225	3,845	-30,574	-230,809	0,500	0,00020	200000000	449,999	1,200	0,00048	200000000	41,846	9,112
0,00283	0,083	0,166	0,263	0,922	0,996	1,989	0,078	0,00283	59,907	-0,00182	-0,00112	0,00225	3,844	-30,317	-224,810	0,600	0,00024	200000000	450,000	1,200	0,00048	200000000	41,935	9,024
0,00283	0,083	0,167	0,264	0,940	0,998	1,994	0,077	0,00283	60,018	-0,00179	-0,00110	0,00225	3,843	-30,074	-219,149	0,700	0,00028	200000000	449,999	1,200	0,00048	200000000	42,013	8,938
0,00282	0,084	0,167	0,264	0,957	0,999	1,997	0,077	0,00282	60,118	-0,00176	-0,00107	0,00225	3,843	-29,845	-213,797	0,800	0,00032	200000000	450,000	1,200	0,00048	200000000	42,082	8,854
0,00282	0,084	0,167	0,264	0,974	1,000	1,999	0,076	0,00282	60,205	-0,00173	-0,00104	0,00225	3,842	-29,628	-208,727	0,900	0,00036	200000000	450,000	1,200	0,00048	200000000	42,144	8,773
0,00281	0,084	0,167	0,265	0,991	1,000	2,000	0,075	0,00281	60,283	-0,00170	-0,00102	0,00225	3,842	-29,421	-203,916	1,000	0,00040	200000000	450,000	1,200	0,00048	200000000	42,198	8,695
0,00287	0,082	0,164	0,260	0,795	0,975	1,930	0,085	0,00287	62,435	-0,00211	-0,00136	0,00225	3,849	-32,381	-272,988	0,100	0,00004	200000000	449,999	1,300	0,00052	200000000	43,704	9,759
0,00287	0,082	0,164	0,260	0,814	0,980	1,943	0,084	0,00287	62,669	-0,00206	-0,00132	0,00225	3,848	-32,026	-264,703	0,200	0,00008	200000000	449,999	1,300	0,00052	200000000	43,868	9,659
0,00286	0,083	0,165	0,261	0,833	0,984	1,953	0,083	0,00286	62,878	-0,00202	-0,00128	0,00225	3,847	-31,694	-256,969	0,300	0,00012	200000000	449,999	1,300	0,00052	200000000	44,015	9,562
0,00285	0,083	0,165	0,261	0,852	0,987	1,963	0,082	0,00285	63,065	-0,00197	-0,00125	0,00225	3,847	-31,384	-249,729	0,400	0,00016	200000000	449,999	1,300	0,00052	200000000	44,146	9,467
0,00285	0,083	0,165	0,262	0,870	0,990	1,971	0,081	0,00285	63,232	-0,00193	-0,00121	0,00225	3,846	-31,093	-242,934	0,500	0,00020	200000000	449,999	1,300	0,00052	200000000	44,263	9,374
0,00284	0,083	0,166	0,262	0,888	0,993	1,978	0,080	0,00284	63,382	-0,00189	-0,00118	0,00225	3,845	-30,819	-236,541	0,600	0,00024	200000000	449,999	1,300	0,00052	200000000	44,367	9,284
0,00284	0,083	0,166	0,263	0,905	0,995	1,984	0,079	0,00284	63,515	-0,00186	-0,00115	0,00225	3,845	-30,561	-230,514	0,700	0,00028	200000000	449,999	1,300	0,00052	200000000	44,461	9,197
0,00283	0,083	0,166	0,263	0,922	0,996	1,989	0,078	0,00283	63,635	-0,00182	-0,00112	0,00225	3,844	-30,317	-224,820	0,800	0,00032	200000000	450,000	1,300	0,00052	199999625	44,544	9,112
0,00283	0,083	0,167	0,264	0,939	0,998	1,993	0,078	0,00283	63,742	-0,00179	-0,00110	0,00225	3,844	-30,086	-219,429	0,900	0,00036	200000000	449,999	1,300	0,00052	200000000	44,619	9,030
0,00282	0,084	0,167	0,264	0,955	0,999	1,996	0,077	0,00282	63,837	-0,00176	-0,00107	0,00225	3,843	-29,867	-214,317	1,000	0,00040	200000000	449,999	1,300	0,00052	200000000	44,686	8,950
0,00282	0,084	0,167	0,264	0,971	1,000	1,999	0,076	0,00282	63,922	-0,00173	-0,00105	0,00225	3,843	-29,659	-209,462	1,100	0,00044	200000000	450,000	1,300	0,00052	200000000	44,745	8,873
0,00281	0,084	0,167	0,265	0,987	1,000	2,000	0,075	0,00281	63,997	-0,00170	-0,00102	0,00225	3,842	-29,461	-204,843	1,200	0,00048	200000000	449,999	1,300	0,00052	200000000	44,798	8,798
0,00289	0,082	0,163	0,259	0,764	0,967	1,909	0,086	0,00289	65,737	-0,00220	-0,00144	0,00225	3,850	-32,991	-287,239	0,100	0,00004	200000000	449,999	1,400	0,00056	200000000	46,016	10,011
0,00288	0,082	0,164	0,259	0,783	0,972	1,922	0,085	0,00288	66,005	-0,00215	-0,00139	0,00225	3,849	-32,613	-278,398	0,200	0,00008	200000000	449,999	1,400	0,00056	200000000	46,203	9,910
0,00287	0,082	0,164	0,260	0,802	0,977	1,935	0,084	0,00287	66,245	-0,00210	-0,00135	0,00225	3,849	-32,259	-270,154	0,300	0,00012	200000000	450,000	1,400	0,00056	199999643	46,371	9,812
0,00286	0,082	0,165	0,260	0,820	0,981	1,946	0,083	0,00286	66,460	-0,00205	-0,00131	0,00225	3,848	-31,929	-262,443	0,400	0,00016	200000000	449,999	1,400	0,00056	200000000	46,522	9,716
0,00286	0,083	0,165	0,261	0,838	0,984	1,956	0,082	0,00286	66,653	-0,00201	-0,00128	0,00225	3,847	-31,619	-255,212	0,500	0,00020	200000000	449,999	1,400	0,00056	200000000	46,657	9,622
0,00285	0,083	0,165	0,261	0,855	0,988	1,964	0,082	0,00285	66,827	-0,00196	-0,00124	0,00225	3,846	-31,328	-248,416	0,600	0,00024	200000000	450,000	1,400	0,00056	200000000	46,779	9,531
0,00285	0,083	0,166	0,262	0,872	0,990	1,972	0,081	0,00285	66,983	-0,00193	-0,00121	0,00225	3,846	-31,054	-242,012	0,700	0,00028	200000000	449,999	1,400	0,00056	200000000	46,888	9,442
0,00284	0,083	0,166	0,262	0,889	0,993	1,979	0,080	0,00284	67,123	-0,00189	-0,00118	0,00225	3,845	-30,795	-235,967	0,800	0,00032	200000000	450,000	1,400	0,00056	200000000	46,986	9,356
0,00284	0,083	0,166	0,263	0,906	0,995	1,985	0,079	0,00284	67,250	-0,00185	-0,00115	0,00225	3,845	-30,550	-230,247	0,900	0,00036	200000000	449,999	1,400	0,00056	200000000	47,075	9,273
0,00283	0,083	0,166	0,263	0,922	0,996	1,989	0,078	0,00283	67,363	-0,00182	-0,00112	0,00225	3,844	-30,317	-224,828	1,000	0,00040	200000000	450,000	1,400	0,00056	200000000	47,154	9,192
0,00283	0,083	0,167	0,264	0,938	0,998	1,993	0,078	0,00283	67,465	-0,00179	-0,00110	0,00225	3,844	-30,097	-219,683	1,100	0,00044	200000000	449,999	1,400	0,00056	200000000	47,226	9,113
0,00282	0,084	0,167	0,264	0,954	0,999	1,996	0,077	0,00282	67,557	-0,00176	-0,00107	0,00225	3,843	-29,887	-214,792	1,200	0,00048	200000000	449,999	1,400	0,00056	200000000	47,290	9,036
0,00282	0,084	0,167	0,264	0,969	0,999	1,998	0,076	0,00282	67,639	-0,00173	-0,00105	0,00225	3,843	-29,688	-210,134	1,300	0,00052	200000000	449,999	1,400	0,00056	200000000	47,347	8,962
0,00282	0,084	0,167	0,265	0,984	1,000	2,000	0,075	0,00282	67,712	-0,00171	-0,00103	0,00225	3,842	-29,498	-205,693	1,400	0,00056	200000000	449,999	1,400	0,00056	200000000	47,398	8,890
0,00290	0,081	0,163	0,257	0,735	0,958	1,886	0,088	0,00290	69,007	-0,00229	-0,00151	0,00225	3,852	-33,611	-301,697	0,100	0,00004	200000000	449,999	1,500	0,00060	200000000	48,305	10,251
0,00289	0,082	0,163	0,258	0,754	0,964	1,901	0,087	0,00289	69,309	-0,00223	-0,00146	0,00225	3,851	-33,207	-292,283	0,200	0,00008	200000000	449,999	1,500	0,00060	200000000	48,516	10,149
0,00288	0,082	0,164	0,259	0,772	0,969	1,915	0,086	0,00288	69,580	-0,00218	-0,00142	0,00225	3,850	-32,832	-283,513	0,300	0,00012	200000000	449,999	1,500	0,00060	200000000	48,706	10,050

0,00288	0,082	0,164	0,259	0,790	0,974	1,927	0,085	0,00288	69,824	-0,00213	-0,00138	0,00225	3,849	-32,481	-275,319	0,400	0,00016	200000000	450,000	1,500	0,00060	200000000	48,877	9,953
0,00287	0,082	0,164	0,260	0,808	0,978	1,938	0,084	0,00287	70,044	-0,00208	-0,00134	0,00225	3,848	-32,152	-267,641	0,500	0,00020	200000000	449,999	1,500	0,00060	200000000	49,031	9,858
0,00286	0,082	0,165	0,260	0,825	0,982	1,949	0,083	0,00286	70,243	-0,00204	-0,00130	0,00225	3,848	-31,843	-260,430	0,600	0,00024	200000000	449,999	1,500	0,00060	200000000	49,170	9,766
0,00286	0,083	0,165	0,261	0,842	0,985	1,958	0,082	0,00286	70,422	-0,00200	-0,00127	0,00225	3,847	-31,552	-253,641	0,700	0,00028	200000000	450,000	1,500	0,00060	200000000	49,296	9,676
0,00285	0,083	0,165	0,261	0,858	0,988	1,966	0,081	0,00285	70,584	-0,00196	-0,00124	0,00225	3,846	-31,277	-247,236	0,800	0,00032	200000000	449,999	1,500	0,00060	200000000	49,409	9,588
0,00285	0,083	0,166	0,262	0,875	0,991	1,973	0,081	0,00285	70,731	-0,00192	-0,00121	0,00225	3,846	-31,018	-241,181	0,900	0,00036	200000000	450,000	1,500	0,00060	200000000	49,512	9,503
0,00284	0,083	0,166	0,262	0,891	0,993	1,980	0,080	0,00284	70,864	-0,00189	-0,00118	0,00225	3,845	-30,772	-235,446	1,000	0,00040	200000000	449,999	1,500	0,00060	200000000	49,605	9,421
0,00284	0,083	0,166	0,263	0,906	0,995	1,985	0,079	0,00284	70,983	-0,00185	-0,00115	0,00225	3,845	-30,539	-230,005	1,100	0,00044	200000000	449,999	1,500	0,00060	200000000	49,688	9,341
0,00283	0,083	0,166	0,263	0,922	0,996	1,989	0,078	0,00283	71,092	-0,00182	-0,00112	0,00225	3,844	-30,318	-224,835	1,200	0,00048	200000000	449,999	1,500	0,00060	200000000	49,764	9,263
0,00283	0,083	0,167	0,263	0,937	0,998	1,993	0,078	0,00283	71,189	-0,00179	-0,00110	0,00225	3,844	-30,107	-219,915	1,300	0,00052	200000000	449,999	1,500	0,00060	200000000	49,833	9,187
0,00282	0,084	0,167	0,264	0,952	0,999	1,996	0,077	0,00282	71,277	-0,00176	-0,00108	0,00225	3,843	-29,906	-215,226	1,400	0,00056	200000000	449,999	1,500	0,00060	200000000	49,894	9,114
0,00282	0,084	0,167	0,264	0,967	0,999	1,998	0,076	0,00282	71,357	-0,00174	-0,00105	0,00225	3,843	-29,714	-210,751	1,500	0,00060	200000000	449,999	1,500	0,00060	200000000	49,950	9,043
0,00291	0,081	0,162	0,256	0,708	0,949	1,863	0,090	0,00291	72,246	-0,00237	-0,00158	0,00225	3,853	-34,239	-316,359	0,100	0,00004	200000000	449,999	1,600	0,00064	200000000	50,572	10,481
0,00290	0,081	0,163	0,257	0,726	0,955	1,879	0,089	0,00290	72,583	-0,00231	-0,00153	0,00225	3,852	-33,810	-306,355	0,200	0,00008	200000000	449,999	1,600	0,00064	200000000	50,808	10,378
0,00289	0,082	0,163	0,258	0,744	0,961	1,893	0,088	0,00289	72,886	-0,00226	-0,00149	0,00225	3,851	-33,411	-297,045	0,300	0,00012	200000000	449,999	1,600	0,00064	200000000	51,020	10,278
0,00289	0,082	0,163	0,258	0,762	0,966	1,907	0,087	0,00289	73,160	-0,00221	-0,00144	0,00225	3,850	-33,039	-288,355	0,400	0,00016	200000000	450,000	1,600	0,00064	200000000	51,212	10,180
0,00288	0,082	0,164	0,259	0,779	0,971	1,920	0,086	0,00288	73,408	-0,00216	-0,00140	0,00225	3,850	-32,691	-280,218	0,500	0,00020	200000000	449,999	1,600	0,00064	200000000	51,385	10,084
0,00287	0,082	0,164	0,260	0,796	0,975	1,931	0,085	0,00287	73,632	-0,00211	-0,00136	0,00225	3,849	-32,363	-272,582	0,600	0,00024	200000000	449,999	1,600	0,00064	200000000	51,542	9,990
0,00287	0,082	0,164	0,260	0,813	0,979	1,942	0,084	0,00287	73,835	-0,00207	-0,00133	0,00225	3,848	-32,056	-265,398	0,700	0,00028	200000000	449,999	1,600	0,00064	200000000	51,685	9,899
0,00286	0,082	0,165	0,261	0,829	0,983	1,951	0,083	0,00286	74,020	-0,00203	-0,00129	0,00225	3,847	-31,765	-258,625	0,800	0,00032	200000000	449,999	1,600	0,00064	200000000	51,814	9,810
0,00286	0,083	0,165	0,261	0,845	0,986	1,960	0,082	0,00286	74,187	-0,00199	-0,00126	0,00225	3,847	-31,491	-252,227	0,900	0,00036	200000000	449,999	1,600	0,00064	200000000	51,931	9,724
0,00285	0,083	0,165	0,262	0,861	0,989	1,967	0,081	0,00285	74,339	-0,00195	-0,00123	0,00225	3,846	-31,232	-246,170	1,000	0,00040	200000000	449,999	1,600	0,00064	200000000	52,038	9,640
0,00285	0,083	0,166	0,262	0,877	0,991	1,974	0,080	0,00285	74,477	-0,00192	-0,00120	0,00225	3,846	-30,986	-240,427	1,100	0,00044	200000000	449,999	1,600	0,00064	200000000	52,134	9,558
0,00284	0,083	0,166	0,262	0,892	0,993	1,980	0,080	0,00284	74,603	-0,00188	-0,00117	0,00225	3,845	-30,752	-234,973	1,200	0,00048	200000000	450,000	1,600	0,00064	200000000	52,222	9,479
0,00284	0,083	0,166	0,263	0,907	0,995	1,985	0,079	0,00284	74,717	-0,00185	-0,00115	0,00225	3,845	-30,530	-229,785	1,300	0,00052	200000000	449,999	1,600	0,00064	200000000	52,302	9,402
0,00283	0,083	0,166	0,263	0,922	0,996	1,989	0,078	0,00283	74,820	-0,00182	-0,00112	0,00225	3,844	-30,318	-224,843	1,400	0,00056	200000000	450,000	1,600	0,00064	200000000	52,374	9,327
0,00283	0,083	0,167	0,263	0,937	0,998	1,993	0,078	0,00283	74,914	-0,00179	-0,00110	0,00225	3,844	-30,116	-220,128	1,500	0,00060	200000000	450,000	1,600	0,00064	200000000	52,440	9,255
0,00282	0,084	0,167	0,264	0,951	0,999	1,996	0,077	0,00282	74,999	-0,00177	-0,00108	0,00225	3,843	-29,923	-215,625	1,600	0,00064	200000000	450,000	1,600	0,00064	200000000	52,499	9,184
0,00291	0,081	0,162	0,256	0,700	0,947	1,856	0,090	0,00291	75,829	-0,00240	-0,00160	0,00225	3,854	-34,421	-320,612	0,200	0,00008	200000000	449,999	1,700	0,00068	200000000	53,080	10,599
0,00291	0,081	0,162	0,257	0,718	0,953	1,872	0,089	0,00291	76,165	-0,00234	-0,00155	0,00225	3,853	-33,999	-310,748	0,300	0,00012	200000000	450,000	1,700	0,00068	200000000	53,315	10,498
0,00290	0,081	0,163	0,257	0,735	0,958	1,886	0,088	0,00290	76,469	-0,00229	-0,00151	0,00225	3,852	-33,604	-301,547	0,400	0,00016	200000000	449,999	1,700	0,00068	200000000	53,528	10,398
0,00289	0,082	0,163	0,258	0,752	0,964	1,900	0,087	0,00289	76,745	-0,00223	-0,00146	0,00225	3,851	-33,236	-292,941	0,500	0,00020	200000000	449,999	1,700	0,00068	200000000	53,722	10,301
0,00288	0,082	0,164	0,259	0,769	0,968	1,912	0,086	0,00288	76,996	-0,00218	-0,00142	0,00225	3,850	-32,890	-284,870	0,600	0,00024	200000000	450,000	1,700	0,00068	200000000	53,897	10,206
0,00288	0,082	0,164	0,259	0,786	0,973	1,924	0,085	0,00288	77,223	-0,00214	-0,00139	0,00225	3,849	-32,565	-277,283	0,700	0,00028	200000000	450,000	1,700	0,00068	200000000	54,056	10,114
0,00287	0,082	0,164	0,260	0,802	0,977	1,935	0,084	0,00287	77,431	-0,00210	-0,00135	0,00225	3,849	-32,258	-270,133	0,800	0,00032	200000000	449,999	1,700	0,00068	200000000	54,202	10,024
0,00286	0,082	0,165	0,260	0,818	0,980	1,944	0,084	0,00286	77,620	-0,00205	-0,00132	0,00225	3,848	-31,969	-263,384	0,900	0,00036	200000000	450,000	1,700	0,00068	200000000	54,334	9,936
0,00286	0,083	0,165	0,261	0,833	0,984	1,953	0,083	0,00286	77,792	-0,00202	-0,00128	0,00225	3,847	-31,696	-256,998	1,000	0,00040	200000000	449,999	1,700	0,00068	200000000	54,454	9,850
0,00285	0,083	0,165	0,261	0,849	0,986	1,961	0,082	0,00285	77,948	-0,00198	-0,00125	0,00225	3,847	-31,436	-250,947	1,100	0,00044	200000000	449,999	1,700	0,00068	200000000	54,564	9,767
0,00285	0,083	0,165	0,262	0,864	0,989	1,968	0,081	0,00285	78,092	-0,00195	-0,00123	0,00225	3,846	-31,190	-245,203	1,200	0,00048	200000000	450,000	1,700	0,00068	200000000	54,664	9,687
0,00284	0,083	0,166	0,262	0,879	0,991	1,975	0,080	0,00284	78,222	-0,00191	-0,00120	0,00225	3,846	-30,956	-239,742	1,300	0,00052	200000000	450,000	1,700	0,00068	200000000	54,756	9,608
0,00284	0,083	0,166	0,262	0,893	0,993	1,980	0,080	0,00284	78,341	-0,00188	-0,00117	0,00225	3,845	-30,734	-234,541	1,400	0,00056	200000000	449,999	1,700	0,00068	200000000	54,839	9,532
0,00284	0,083	0,166	0,263	0,908	0,995	1,985	0,079	0,00284	78,450	-0,00185	-0,00115	0,00225	3,845	-30,521	-229,583	1,500	0,00060	200000000	450,000	1,700	0,00068	200000000	54,915	9,458
0,00283	0,083	0,166	0,263	0,922	0,996	1,989	0,078	0,00283	78,549	-0,00182	-0,00112													

0,00283	0,083	0,167	0,263	0,936	0,998	1,993	0,078	0,00283	78,639	-0,00180	-0,00110	0,00225	3,844	-30,124	-220,324	1,700	0,00068	200000000	449,999	1,700	0,00068	200000000	55,047	9,316
0,00292	0,081	0,162	0,256	0,693	0,944	1,849	0,091	0,00292	79,418	-0,00242	-0,00162	0,00225	3,854	-34,593	-324,617	0,300	0,00012	200000000	449,999	1,800	0,00072	200000000	55,593	10,710
0,00291	0,081	0,162	0,257	0,710	0,950	1,865	0,090	0,00291	79,753	-0,00237	-0,00157	0,00225	3,853	-34,176	-314,894	0,400	0,00016	200000000	449,999	1,800	0,00072	200000000	55,827	10,609
0,00290	0,081	0,163	0,257	0,727	0,956	1,880	0,089	0,00290	80,058	-0,00231	-0,00153	0,00225	3,852	-33,787	-305,807	0,500	0,00020	200000000	449,999	1,800	0,00072	200000000	56,041	10,511
0,00289	0,082	0,163	0,258	0,744	0,961	1,893	0,088	0,00289	80,335	-0,00226	-0,00149	0,00225	3,851	-33,422	-297,291	0,600	0,00024	200000000	449,999	1,800	0,00072	200000000	56,235	10,415
0,00289	0,082	0,163	0,258	0,760	0,966	1,906	0,087	0,00289	80,588	-0,00221	-0,00145	0,00225	3,851	-33,079	-289,291	0,700	0,00028	200000000	449,999	1,800	0,00072	200000000	56,412	10,321
0,00288	0,082	0,164	0,259	0,776	0,970	1,917	0,086	0,00288	80,819	-0,00217	-0,00141	0,00225	3,850	-32,756	-281,758	0,800	0,00032	200000000	449,999	1,800	0,00072	200000000	56,573	10,229
0,00287	0,082	0,164	0,259	0,791	0,974	1,928	0,085	0,00287	81,029	-0,00212	-0,00137	0,00225	3,849	-32,452	-274,650	0,900	0,00036	200000000	450,000	1,800	0,00072	200000000	56,720	10,140
0,00287	0,082	0,164	0,260	0,807	0,978	1,938	0,084	0,00287	81,222	-0,00208	-0,00134	0,00225	3,848	-32,164	-267,929	1,000	0,00040	200000000	450,000	1,800	0,00072	200000000	56,855	10,053
0,00286	0,082	0,165	0,260	0,822	0,981	1,947	0,083	0,00286	81,398	-0,00204	-0,00131	0,00225	3,848	-31,891	-261,563	1,100	0,00044	200000000	450,000	1,800	0,00072	200000000	56,979	9,969
0,00286	0,083	0,165	0,261	0,837	0,984	1,955	0,083	0,00286	81,559	-0,00201	-0,00128	0,00225	3,847	-31,633	-255,524	1,200	0,00048	200000000	450,000	1,800	0,00072	200000000	57,091	9,887
0,00285	0,083	0,165	0,261	0,852	0,987	1,963	0,082	0,00285	81,707	-0,00197	-0,00125	0,00225	3,847	-31,387	-249,784	1,300	0,00052	200000000	450,000	1,800	0,00072	200000000	57,195	9,807
0,00285	0,083	0,165	0,262	0,866	0,989	1,970	0,081	0,00285	81,842	-0,00194	-0,00122	0,00225	3,846	-31,153	-244,321	1,400	0,00056	200000000	450,000	1,800	0,00072	200000000	57,289	9,729
0,00284	0,083	0,166	0,262	0,880	0,992	1,976	0,080	0,00284	81,965	-0,00191	-0,00120	0,00225	3,846	-30,929	-239,115	1,500	0,00060	200000000	450,000	1,800	0,00072	200000000	57,376	9,654
0,00284	0,083	0,166	0,262	0,894	0,993	1,981	0,080	0,00284	82,079	-0,00188	-0,00117	0,00225	3,845	-30,717	-234,146	1,600	0,00064	200000000	450,000	1,800	0,00072	199999273	57,455	9,581
0,00284	0,083	0,166	0,263	0,908	0,995	1,985	0,079	0,00284	82,182	-0,00185	-0,00115	0,00225	3,845	-30,513	-229,398	1,700	0,00068	200000000	450,000	1,800	0,00072	200000000	57,528	9,509
0,00283	0,083	0,166	0,263	0,922	0,996	1,989	0,078	0,00283	82,277	-0,00182	-0,00112	0,00225	3,844	-30,319	-224,855	1,800	0,00072	200000000	450,000	1,800	0,00072	200000000	57,594	9,440
0,00291	0,081	0,162	0,256	0,703	0,948	1,859	0,090	0,00291	83,348	-0,00239	-0,00159	0,00225	3,854	-34,344	-318,814	0,500	0,00020	200000000	449,999	1,900	0,00076	200000000	58,343	10,714
0,00291	0,081	0,162	0,257	0,719	0,953	1,873	0,089	0,00291	83,652	-0,00234	-0,00155	0,00225	3,853	-33,960	-309,843	0,600	0,00024	200000000	449,999	1,900	0,00076	200000000	58,557	10,617
0,00290	0,081	0,163	0,258	0,735	0,958	1,886	0,088	0,00290	83,930	-0,00228	-0,00151	0,00225	3,852	-33,599	-301,421	0,700	0,00028	200000000	449,999	1,900	0,00076	200000000	58,751	10,521
0,00289	0,082	0,163	0,258	0,751	0,963	1,899	0,087	0,00289	84,185	-0,00224	-0,00147	0,00225	3,851	-33,259	-293,496	0,800	0,00032	200000000	449,999	1,900	0,00076	200000000	58,929	10,429
0,00288	0,082	0,164	0,259	0,767	0,968	1,911	0,086	0,00288	84,418	-0,00219	-0,00143	0,00225	3,850	-32,939	-286,022	0,900	0,00036	200000000	449,999	1,900	0,00076	200000000	59,092	10,338
0,00288	0,082	0,164	0,259	0,782	0,972	1,921	0,085	0,00288	84,631	-0,00215	-0,00139	0,00225	3,850	-32,637	-278,959	1,000	0,00040	200000000	449,999	1,900	0,00076	200000000	59,242	10,250
0,00287	0,082	0,164	0,260	0,797	0,976	1,932	0,085	0,00287	84,827	-0,00211	-0,00136	0,00225	3,849	-32,350	-272,273	1,100	0,00044	200000000	449,999	1,900	0,00076	200000000	59,379	10,164
0,00287	0,082	0,164	0,260	0,812	0,979	1,941	0,084	0,00287	85,006	-0,00207	-0,00133	0,00225	3,848	-32,078	-265,933	1,200	0,00048	200000000	449,999	1,900	0,00076	200000000	59,504	10,080
0,00286	0,082	0,165	0,261	0,826	0,982	1,949	0,083	0,00286	85,171	-0,00203	-0,00130	0,00225	3,848	-31,820	-259,910	1,300	0,00052	200000000	450,000	1,900	0,00076	200000000	59,620	9,999
0,00286	0,083	0,165	0,261	0,840	0,985	1,957	0,082	0,00286	85,323	-0,00200	-0,00127	0,00225	3,847	-31,575	-254,180	1,400	0,00056	200000000	450,000	1,900	0,00076	200000000	59,726	9,920
0,00285	0,083	0,165	0,261	0,854	0,987	1,964	0,082	0,00285	85,462	-0,00197	-0,00124	0,00225	3,846	-31,341	-248,721	1,500	0,00060	200000000	449,999	1,900	0,00076	200000000	59,823	9,843
0,00285	0,083	0,165	0,262	0,868	0,990	1,970	0,081	0,00285	85,590	-0,00193	-0,00122	0,00225	3,846	-31,118	-243,513	1,600	0,00064	200000000	450,000	1,900	0,00076	200000000	59,913	9,769
0,00294	0,080	0,161	0,254	0,870	0,990	1,971	0,079	0,00294	85,906	-0,00193	-0,00120	0,00233	3,857	-31,090	-240,045	1,700	0,00068	200000000	450,000	1,900	0,00076	192929877	60,134	9,721
0,00284	0,083	0,166	0,262	0,895	0,994	1,981	0,080	0,00284	85,815	-0,00188	-0,00117	0,00225	3,845	-30,701	-233,782	1,800	0,00072	200000000	450,000	1,900	0,00076	200000000	60,071	9,625
0,00284	0,083	0,166	0,263	0,909	0,995	1,986	0,079	0,00284	85,914	-0,00185	-0,00115	0,00225	3,845	-30,506	-229,227	1,900	0,00076	200000000	450,000	1,900	0,00076	200000000	60,140	9,557
0,00292	0,081	0,162	0,256	0,697	0,945	1,853	0,091	0,00292	86,948	-0,00241	-0,00161	0,00225	3,854	-34,503	-322,524	0,600	0,00024	200000000	450,000	2,000	0,00080	200000000	60,864	10,813
0,00291	0,081	0,162	0,257	0,712	0,951	1,867	0,090	0,00291	87,252	-0,00236	-0,00157	0,00225	3,853	-34,124	-313,672	0,700	0,00028	200000000	449,999	2,000	0,00080	200000000	61,076	10,716
0,00290	0,081	0,163	0,257	0,728	0,956	1,880	0,089	0,00290	87,530	-0,00231	-0,00153	0,00225	3,852	-33,767	-305,346	0,800	0,00032	200000000	449,999	2,000	0,00080	200000000	61,271	10,622
0,00289	0,082	0,163	0,258	0,743	0,961	1,893	0,088	0,00289	87,786	-0,00226	-0,00149	0,00225	3,851	-33,431	-297,499	0,900	0,00036	200000000	449,999	2,000	0,00080	200000000	61,450	10,530
0,00289	0,082	0,163	0,258	0,758	0,965	1,904	0,087	0,00289	88,020	-0,00222	-0,00145	0,00225	3,851	-33,113	-290,089	1,000	0,00040	200000000	450,000	2,000	0,00080	200000000	61,614	10,440
0,00288	0,082	0,164	0,259	0,773	0,969	1,915	0,086	0,00288	88,236	-0,00217	-0,00142	0,00225	3,850	-32,813	-283,076	1,100	0,00044	200000000	449,999	2,000	0,00080	200000000	61,765	10,353
0,00288	0,082	0,164	0,259	0,787	0,973	1,925	0,085	0,00288	88,434	-0,00213	-0,00138	0,00225	3,849	-32,528	-276,429	1,200	0,00048	200000000	449,999	2,000	0,00080	200000000	61,904	10,268
0,00287	0,082	0,164	0,260	0,802	0,977	1,935	0,084	0,00287	88,617	-0,00210	-0,00135	0,00225	3,849	-32,258	-270,118	1,300	0,00052	200000000	449,999	2,000	0,00080	200000000	62,032	10,186
0,00287	0,082	0,165	0,260	0,816	0,980	1,943	0,084	0,00287	88,785	-0,00206	-0,00132	0,00225	3,848	-32,001	-264,117	1,400	0,00056	200000000	450,000	2,000	0,00080	200000000	62,150	10,105
0,00286	0,082	0,165	0,261	0,830	0,983	1,951	0,083	0,00286	88,940	-0,00202	-0,00129	0,00225	3,847	-31,756	-258,401	1,500	0,00060	200000000	449,999	2,000	0,00080	200000000	62,258	10,027

0,00286	0,083	0,165	0,261	0,843	0,985	1,959	0,082	0,00286	89,083	-0,00199	-0,00126	0,00225	3,847	-31,522	-252,951	1,600	0,00064	200000000	449,999	2,000	0,00080	200000000	62,358	9,951
0,00285	0,083	0,165	0,261	0,857	0,988	1,965	0,081	0,00285	89,215	-0,00196	-0,00124	0,00225	3,846	-31,299	-247,747	1,700	0,00068	200000000	450,000	2,000	0,00080	199999658	62,450	9,877
0,00285	0,083	0,165	0,262	0,870	0,990	1,971	0,081	0,00285	89,336	-0,00193	-0,00121	0,00225	3,846	-31,086	-242,771	1,800	0,00072	200000000	450,000	2,000	0,00080	200000000	62,535	9,805
0,00284	0,083	0,166	0,262	0,883	0,992	1,977	0,080	0,00284	89,448	-0,00190	-0,00119	0,00225	3,845	-30,882	-238,009	1,900	0,00076	200000000	450,000	2,000	0,00080	200000000	62,614	9,735
0,00284	0,083	0,166	0,262	0,896	0,994	1,982	0,080	0,00284	89,551	-0,00187	-0,00117	0,00225	3,845	-30,687	-233,446	2,000	0,00080	200000000	450,000	2,000	0,00080	199999562	62,686	9,666
0,00292	0,081	0,162	0,256	0,691	0,943	1,847	0,091	0,00292	90,554	-0,00243	-0,00163	0,00225	3,854	-34,654	-326,039	0,700	0,00028	200000000	449,999	2,100	0,00084	200000000	63,388	10,906
0,00291	0,081	0,162	0,256	0,706	0,949	1,861	0,090	0,00291	90,857	-0,00238	-0,00159	0,00225	3,853	-34,280	-317,307	0,800	0,00032	200000000	450,000	2,100	0,00084	200000000	63,600	10,810
0,00290	0,081	0,163	0,257	0,721	0,954	1,874	0,089	0,00290	91,135	-0,00233	-0,00155	0,00225	3,853	-33,927	-309,080	0,900	0,00036	200000000	449,999	2,100	0,00084	200000000	63,794	10,717
0,00290	0,081	0,163	0,258	0,736	0,959	1,887	0,088	0,00290	91,391	-0,00228	-0,00151	0,00225	3,852	-33,594	-301,314	1,000	0,00040	200000000	449,999	2,100	0,00084	200000000	63,974	10,626
0,00289	0,082	0,163	0,258	0,750	0,963	1,898	0,087	0,00289	91,627	-0,00224	-0,00147	0,00225	3,851	-33,280	-293,970	1,100	0,00044	200000000	449,999	2,100	0,00084	200000000	64,139	10,537
0,00289	0,082	0,163	0,259	0,765	0,967	1,909	0,086	0,00289	91,844	-0,00220	-0,00144	0,00225	3,850	-32,982	-287,012	1,200	0,00048	200000000	450,000	2,100	0,00084	200000000	64,291	10,451
0,00288	0,082	0,164	0,259	0,779	0,971	1,919	0,086	0,00288	92,045	-0,00216	-0,00140	0,00225	3,850	-32,699	-280,408	1,300	0,00052	200000000	450,000	2,100	0,00084	200000000	64,431	10,367
0,00287	0,082	0,164	0,259	0,793	0,974	1,929	0,085	0,00287	92,230	-0,00212	-0,00137	0,00225	3,849	-32,430	-274,130	1,400	0,00056	200000000	450,000	2,100	0,00084	200000000	64,561	10,285
0,00287	0,082	0,164	0,260	0,806	0,978	1,938	0,084	0,00287	92,401	-0,00208	-0,00134	0,00225	3,848	-32,174	-268,154	1,500	0,00060	200000000	449,999	2,100	0,00084	200000000	64,681	10,205
0,00286	0,082	0,165	0,260	0,820	0,981	1,946	0,083	0,00286	92,559	-0,00205	-0,00131	0,00225	3,848	-31,930	-262,457	1,600	0,00064	200000000	449,999	2,100	0,00084	200000000	64,791	10,128
0,00286	0,083	0,165	0,261	0,833	0,983	1,953	0,083	0,00286	92,705	-0,00202	-0,00129	0,00225	3,847	-31,697	-257,019	1,700	0,00068	200000000	449,999	2,100	0,00084	200000000	64,894	10,052
0,00286	0,083	0,165	0,261	0,846	0,986	1,960	0,082	0,00286	92,841	-0,00199	-0,00126	0,00225	3,847	-31,474	-251,823	1,800	0,00072	200000000	450,000	2,100	0,00084	200000000	64,988	9,979
0,00285	0,083	0,165	0,261	0,859	0,988	1,966	0,081	0,00285	92,965	-0,00196	-0,00123	0,00225	3,846	-31,261	-246,849	1,900	0,00076	200000000	449,999	2,100	0,00084	200000000	65,076	9,907
0,00285	0,083	0,166	0,262	0,872	0,990	1,972	0,081	0,00285	93,081	-0,00193	-0,00121	0,00225	3,846	-31,057	-242,086	2,000	0,00080	200000000	449,999	2,100	0,00084	200000000	65,157	9,838
0,00284	0,083	0,166	0,262	0,885	0,992	1,977	0,080	0,00284	93,188	-0,00190	-0,00119	0,00225	3,845	-30,861	-237,518	2,100	0,00084	200000000	449,999	2,100	0,00084	200000000	65,232	9,770
0,00291	0,081	0,162	0,256	0,700	0,947	1,856	0,090	0,00291	94,466	-0,00240	-0,00160	0,00225	3,854	-34,428	-320,761	0,900	0,00036	200000000	449,999	2,200	0,00088	200000000	66,126	10,900
0,00291	0,081	0,162	0,257	0,714	0,952	1,869	0,089	0,00291	94,744	-0,00235	-0,00156	0,00225	3,853	-34,079	-312,635	1,000	0,00040	200000000	450,000	2,200	0,00088	200000000	66,321	10,807
0,00290	0,081	0,163	0,257	0,729	0,956	1,881	0,089	0,00290	95,000	-0,00231	-0,00152	0,00225	3,852	-33,750	-304,953	1,100	0,00044	200000000	449,999	2,200	0,00088	200000000	66,500	10,717
0,00289	0,082	0,163	0,258	0,743	0,961	1,892	0,088	0,00289	95,237	-0,00226	-0,00149	0,00225	3,851	-33,439	-297,678	1,200	0,00048	200000000	449,999	2,200	0,00088	200000000	66,666	10,629
0,00289	0,082	0,163	0,258	0,757	0,965	1,903	0,087	0,00289	95,456	-0,00222	-0,00145	0,00225	3,851	-33,143	-290,776	1,300	0,00052	200000000	449,999	2,200	0,00088	200000000	66,819	10,543
0,00288	0,082	0,164	0,259	0,770	0,969	1,913	0,086	0,00288	95,658	-0,00218	-0,00142	0,00225	3,850	-32,862	-284,218	1,400	0,00056	200000000	449,999	2,200	0,00088	200000000	66,961	10,460
0,00288	0,082	0,164	0,259	0,784	0,972	1,923	0,085	0,00288	95,846	-0,00214	-0,00139	0,00225	3,849	-32,595	-277,978	1,500	0,00060	200000000	449,999	2,200	0,00088	200000000	67,092	10,379
0,00287	0,082	0,164	0,260	0,797	0,976	1,932	0,085	0,00287	96,019	-0,00211	-0,00136	0,00225	3,849	-32,340	-272,031	1,600	0,00064	200000000	449,999	2,200	0,00088	200000000	67,213	10,300
0,00287	0,082	0,164	0,260	0,811	0,979	1,940	0,084	0,00287	96,180	-0,00207	-0,00133	0,00225	3,848	-32,097	-266,356	1,700	0,00068	200000000	450,000	2,200	0,00088	200000000	67,326	10,223
0,00286	0,082	0,165	0,260	0,824	0,982	1,948	0,083	0,00286	96,329	-0,00204	-0,00130	0,00225	3,848	-31,864	-260,934	1,800	0,00072	200000000	449,999	2,200	0,00088	200000000	67,430	10,149
0,00286	0,083	0,165	0,261	0,836	0,984	1,955	0,083	0,00286	96,467	-0,00201	-0,00128	0,00225	3,847	-31,642	-255,748	1,900	0,00076	200000000	449,999	2,200	0,00088	200000000	67,527	10,076
0,00285	0,083	0,165	0,261	0,849	0,986	1,961	0,082	0,00285	96,596	-0,00198	-0,00125	0,00225	3,847	-31,429	-250,782	2,000	0,00080	200000000	449,999	2,200	0,00088	200000000	67,617	10,005
0,00285	0,083	0,165	0,262	0,862	0,989	1,967	0,081	0,00285	96,714	-0,00195	-0,00123	0,00225	3,846	-31,225	-246,021	2,100	0,00084	200000000	450,000	2,200	0,00088	200000000	67,700	9,936
0,00285	0,083	0,166	0,262	0,874	0,991	1,973	0,081	0,00285	96,825	-0,00192	-0,00121	0,00225	3,846	-31,030	-241,452	2,200	0,00088	200000000	449,999	2,200	0,00088	200000000	67,777	9,869
0,00292	0,081	0,162	0,256	0,694	0,944	1,850	0,091	0,00292	98,081	-0,00242	-0,00162	0,00225	3,854	-34,568	-324,049	1,000	0,00040	200000000	449,999	2,300	0,00092	200000000	68,656	10,984
0,00291	0,081	0,162	0,256	0,708	0,949	1,863	0,090	0,00291	98,358	-0,00237	-0,00158	0,00225	3,853	-34,225	-316,024	1,100	0,00044	200000000	450,000	2,300	0,00092	199999926	68,850	10,893
0,00290	0,081	0,163	0,257	0,722	0,954	1,875	0,089	0,00290	98,614	-0,00233	-0,00154	0,00225	3,853	-33,899	-308,427	1,200	0,00048	200000000	450,000	2,300	0,00092	200000000	69,030	10,803
0,00290	0,081	0,163	0,258	0,736	0,959	1,887	0,088	0,00290	98,851	-0,00228	-0,00151	0,00225	3,852	-33,590	-301,223	1,300	0,00052	200000000	449,999	2,300	0,00092	200000000	69,196	10,716
0,00289	0,082	0,163	0,258	0,749	0,963	1,898	0,087	0,00289	99,071	-0,00224	-0,00147	0,00225	3,851	-33,297	-294,380	1,400	0,00056	200000000	450,000	2,300	0,00092	200000000	69,350	10,631
0,00289	0,082	0,163	0,258	0,763	0,967	1,908	0,087	0,00289	99,275	-0,00220	-0,00144	0,00225	3,850	-33,018	-287,871	1,500	0,00060	200000000	449,999	2,300	0,00092	200000000	69,492	10,549
0,00288	0,082	0,164	0,259	0,776	0,970	1,917	0,086	0,00288	99,464	-0,00217	-0,00141	0,00225	3,850	-32,753	-281,671	1,600	0,00064	200000000	450,000	2,300	0,00092	200000000	69,625	10,469
0,00288	0,082	0,164	0,259	0,789	0,974	1,926	0,085	0,00288	99,640	-0,00213	-0,00138	0,00225	3,849	-32,499	-275,755	1,700	0,00068	200000000	449,999	2,300	0,00092	200000000	69,748	10,390

0,00287	0,082	0,164	0,260	0,802	0,977	1,935	0,084	0,00287	99,803	-0,00210	-0,00135	0,00225	3,849	-32,257	-270,106	1,800	0,00072	200000000	449,999	2,300	0,00092	200000000	69,862	10,314
0,00287	0,082	0,164	0,260	0,814	0,980	1,943	0,084	0,00287	99,955	-0,00206	-0,00132	0,00225	3,848	-32,026	-264,704	1,900	0,00076	200000000	449,999	2,300	0,00092	200000000	69,968	10,240
0,00286	0,082	0,165	0,261	0,827	0,982	1,950	0,083	0,00286	100,096	-0,00203	-0,00130	0,00225	3,848	-31,804	-259,532	2,000	0,00080	200000000	449,999	2,300	0,00092	200000000	70,067	10,168
0,00286	0,083	0,165	0,261	0,839	0,985	1,957	0,082	0,00286	100,227	-0,00200	-0,00127	0,00225	3,847	-31,592	-254,575	2,100	0,00084	200000000	449,999	2,300	0,00092	200000000	70,159	10,098
0,00285	0,083	0,165	0,261	0,852	0,987	1,963	0,082	0,00285	100,348	-0,00197	-0,00125	0,00225	3,847	-31,388	-249,820	2,200	0,00088	200000000	450,000	2,300	0,00092	200000000	70,244	10,029
0,00285	0,083	0,165	0,262	0,864	0,989	1,968	0,081	0,00285	100,462	-0,00195	-0,00123	0,00225	3,846	-31,192	-245,253	2,300	0,00092	200000000	449,999	2,300	0,00092	200000000	70,323	9,963
0,00292	0,081	0,162	0,256	0,689	0,942	1,845	0,091	0,00292	101,699	-0,00244	-0,00164	0,00225	3,854	-34,703	-327,179	1,100	0,00044	200000000	449,999	2,400	0,00096	200000000	71,190	11,064
0,00291	0,081	0,162	0,256	0,702	0,947	1,858	0,090	0,00291	101,975	-0,00239	-0,00160	0,00225	3,854	-34,363	-319,256	1,200	0,00048	200000000	449,999	2,400	0,00096	200000000	71,383	10,974
0,00291	0,081	0,162	0,257	0,716	0,952	1,870	0,089	0,00291	102,231	-0,00235	-0,00156	0,00225	3,853	-34,041	-311,745	1,300	0,00052	200000000	449,999	2,400	0,00096	200000000	71,562	10,885
0,00290	0,081	0,163	0,257	0,729	0,957	1,881	0,089	0,00290	102,469	-0,00230	-0,00152	0,00225	3,852	-33,736	-304,614	1,400	0,00056	200000000	449,999	2,400	0,00096	200000000	71,728	10,799
0,00289	0,082	0,163	0,258	0,742	0,961	1,892	0,088	0,00289	102,689	-0,00226	-0,00149	0,00225	3,851	-33,445	-297,833	1,500	0,00060	200000000	449,999	2,400	0,00096	200000000	71,883	10,715
0,00289	0,082	0,163	0,258	0,756	0,965	1,902	0,087	0,00289	102,894	-0,00222	-0,00146	0,00225	3,851	-33,169	-291,375	1,600	0,00064	200000000	449,999	2,400	0,00096	200000000	72,026	10,633
0,00288	0,082	0,164	0,259	0,768	0,968	1,912	0,086	0,00288	103,085	-0,00219	-0,00143	0,00225	3,850	-32,905	-285,216	1,700	0,00068	200000000	449,999	2,400	0,00096	200000000	72,160	10,554
0,00288	0,082	0,164	0,259	0,781	0,972	1,921	0,086	0,00288	103,263	-0,00215	-0,00140	0,00225	3,850	-32,653	-279,336	1,800	0,00072	200000000	449,999	2,400	0,00096	200000000	72,284	10,476
0,00287	0,082	0,164	0,260	0,794	0,975	1,929	0,085	0,00287	103,428	-0,00212	-0,00137	0,00225	3,849	-32,412	-273,715	1,900	0,00076	200000000	449,999	2,400	0,00096	200000000	72,399	10,401
0,00287	0,082	0,164	0,260	0,806	0,978	1,937	0,084	0,00287	103,582	-0,00208	-0,00134	0,00225	3,848	-32,181	-268,335	2,000	0,00080	200000000	449,999	2,400	0,00096	200000000	72,507	10,327
0,00286	0,082	0,165	0,260	0,818	0,980	1,945	0,084	0,00286	103,725	-0,00205	-0,00132	0,00225	3,848	-31,961	-263,180	2,100	0,00084	200000000	449,999	2,400	0,00096	200000000	72,608	10,256
0,00286	0,083	0,165	0,261	0,830	0,983	1,952	0,083	0,00286	103,859	-0,00202	-0,00129	0,00225	3,847	-31,749	-258,236	2,200	0,00088	200000000	449,999	2,400	0,00096	200000000	72,701	10,186
0,00286	0,083	0,165	0,261	0,842	0,985	1,958	0,082	0,00286	103,983	-0,00200	-0,00127	0,00225	3,847	-31,545	-253,490	2,300	0,00092	200000000	450,000	2,400	0,00096	200000000	72,788	10,118
0,00285	0,083	0,165	0,261	0,854	0,987	1,964	0,082	0,00285	104,100	-0,00197	-0,00124	0,00225	3,846	-31,350	-248,928	2,400	0,00096	200000000	450,000	2,400	0,00096	200000000	72,870	10,052
0,00292	0,081	0,162	0,256	0,697	0,946	1,853	0,091	0,00292	105,597	-0,00241	-0,00161	0,00225	3,854	-34,495	-322,343	1,300	0,00052	200000000	449,999	2,500	0,00100	200000000	73,918	11,051
0,00291	0,081	0,162	0,257	0,710	0,950	1,865	0,090	0,00291	105,852	-0,00237	-0,00157	0,00225	3,853	-34,177	-314,919	1,400	0,00056	200000000	450,000	2,500	0,00100	200000000	74,097	10,963
0,00290	0,081	0,163	0,257	0,723	0,955	1,876	0,089	0,00290	106,090	-0,00232	-0,00154	0,00225	3,852	-33,875	-307,861	1,500	0,00060	200000000	450,000	2,500	0,00100	200000000	74,263	10,878
0,00290	0,081	0,163	0,258	0,736	0,959	1,887	0,088	0,00290	106,311	-0,00228	-0,00151	0,00225	3,852	-33,587	-301,143	1,600	0,00064	200000000	450,000	2,500	0,00100	200000000	74,418	10,795
0,00289	0,082	0,163	0,258	0,749	0,963	1,897	0,087	0,00289	106,517	-0,00224	-0,00147	0,00225	3,851	-33,313	-294,738	1,700	0,00068	200000000	450,000	2,500	0,00100	200000000	74,562	10,714
0,00289	0,082	0,163	0,258	0,761	0,966	1,907	0,087	0,00289	106,709	-0,00221	-0,00144	0,00225	3,851	-33,051	-288,624	1,800	0,00072	200000000	450,000	2,500	0,00100	200000000	74,696	10,635
0,00288	0,082	0,164	0,259	0,774	0,970	1,916	0,086	0,00288	106,888	-0,00217	-0,00141	0,00225	3,850	-32,800	-282,781	1,900	0,00076	200000000	450,000	2,500	0,00100	200000000	74,821	10,558
0,00288	0,082	0,164	0,259	0,786	0,973	1,924	0,085	0,00288	107,055	-0,00214	-0,00139	0,00225	3,849	-32,561	-277,190	2,000	0,00080	200000000	450,000	2,500	0,00100	200000000	74,938	10,483
0,00287	0,082	0,164	0,260	0,798	0,976	1,932	0,085	0,00287	107,211	-0,00211	-0,00136	0,00225	3,849	-32,331	-271,835	2,100	0,00084	200000000	450,000	2,500	0,00100	200000000	75,048	10,410
0,00287	0,082	0,164	0,260	0,810	0,979	1,940	0,084	0,00287	107,356	-0,00207	-0,00133	0,00225	3,848	-32,111	-266,700	2,200	0,00088	200000000	450,000	2,500	0,00100	200000000	75,149	10,339
0,00286	0,082	0,165	0,260	0,821	0,981	1,947	0,083	0,00286	107,492	-0,00205	-0,00131	0,00225	3,848	-31,900	-261,771	2,300	0,00092	200000000	450,000	2,500	0,00100	200000000	75,245	10,270
0,00286	0,083	0,165	0,261	0,833	0,983	1,953	0,083	0,00286	107,619	-0,00202	-0,00129	0,00225	3,847	-31,697	-257,035	2,400	0,00096	200000000	450,000	2,500	0,00100	200000000	75,333	10,203
0,00286	0,083	0,165	0,261	0,845	0,986	1,959	0,082	0,00286	107,738	-0,00199	-0,00126	0,00225	3,847	-31,502	-252,481	2,500	0,00100	200000000	450,000	2,500	0,00100	200000000	75,417	10,137

Material 3

200x200x2800 (Phase 2)																					
h	0,200																				
b	0,2																				
d	0,175																				
d'	0,030																				
l	2,8	11,2																			
As	0,001																				
As'	0,001																				
Ect	55924171																				
Ecc	57965517																				
Es	200000000																				
ε_{ct1}	0,000211																				
σ_{ct1}	11800																				
ε_{ctu}	0,00390																				
σ_{ctu}	15000																				
ε_{ccu}	-0,00725	-0,00230																			
σ_{ccu}	-250000	-133219																			
α	0,01551																				
δ	0,407																				
ε_{ct2}	β	g	k	x	ε_{ct2}	P	ε_{cc}	ε_{sc}	ε_{st}	σ_{ct2}	σ_{cc}	f_{sc}	%Ac	As'	Es	f_{st}	%Ac	As	Es	Mu	Δ
0,0027294	0,077	0,162	0,259	0,058	0,00273	61,439	-0,0011058	-0,00053	0,002250	13,985	-64,097	-106,101	0,000	0,00000	200000000	450,000	0,100	0,00004	200000000	43,007	3,183
0,0027285	0,077	0,162	0,259	0,057	0,00273	61,450	-0,0010992	-0,00053	0,002250	13,984	-63,718	-105,016	0,100	0,00004	200000000	450,000	0,100	0,00004	199999996	43,015	3,166
0,0027334	0,077	0,162	0,259	0,059	0,00273	65,113	-0,0011337	-0,00055	0,002250	13,988	-65,714	-110,722	0,000	0,00000	200000000	450,000	0,200	0,00008	199999997	45,579	3,639
0,0027324	0,077	0,162	0,259	0,058	0,00273	65,127	-0,0011269	-0,00055	0,002250	13,987	-65,321	-109,601	0,100	0,00004	200000000	450,000	0,200	0,00008	199999997	45,589	3,617
0,0027301	0,077	0,162	0,259	0,058	0,00273	65,130	-0,0011199	-0,00054	0,002249	13,985	-64,917	-108,483	0,200	0,00008	200000000	449,770	0,200	0,00008	200000000	45,591	3,595
0,0027373	0,077	0,161	0,258	0,060	0,00274	68,778	-0,0011613	-0,00058	0,002250	13,991	-67,316	-115,302	0,000	0,00000	200000000	450,000	0,300	0,00012	199999884	48,144	3,950
0,0027363	0,077	0,161	0,258	0,059	0,00274	68,795	-0,0011543	-0,00057	0,002250	13,991	-66,911	-114,144	0,100	0,00004	200000000	450,000	0,300	0,00012	199999922	48,156	3,928
0,0027353	0,077	0,162	0,258	0,059	0,00274	68,811	-0,0011475	-0,00057	0,002250	13,990	-66,513	-113,007	0,200	0,00008	200000000	449,999	0,300	0,00012	200000000	48,168	3,906
0,0027344	0,077	0,162	0,258	0,059	0,00273	68,826	-0,0011407	-0,00056	0,002250	13,989	-66,122	-111,890	0,300	0,00012	200000000	450,000	0,300	0,00012	199999292	48,178	3,885
0,0027413	0,077	0,161	0,258	0,060	0,00274	72,434	-0,0011887	-0,00060	0,002250	13,995	-68,903	-119,841	0,000	0,00000	200000000	450,000	0,400	0,00016	199999007	50,704	4,254
0,0027402	0,077	0,161	0,258	0,060	0,00274	72,454	-0,0011815	-0,00059	0,002250	13,994	-68,486	-118,648	0,100	0,00004	200000000	450,000	0,400	0,00016	199999522	50,718	4,231
0,0027392	0,077	0,161	0,258	0,060	0,00274	72,473	-0,0011744	-0,00059	0,002250	13,993	-68,076	-117,476	0,200	0,00008	200000000	450,000	0,400	0,00016	199999231	50,731	4,208
0,0027382	0,077	0,161	0,258	0,060	0,00274	72,491	-0,0011675	-0,00058	0,002250	13,992	-67,673	-116,324	0,300	0,00012	200000000	450,000	0,400	0,00016	199999514	50,744	4,186
0,0027372	0,077	0,161	0,258	0,060	0,00274	72,508	-0,0011606	-0,00058	0,002250	13,991	-67,277	-115,193	0,400	0,00016	200000000	450,000	0,400	0,00016	199999505	50,756	4,164
0,0027451	0,077	0,161	0,258	0,061	0,00275	76,083	-0,0012159	-0,00062	0,002250	13,998	-70,478	-124,341	0,000	0,00000	200000000	450,000	0,500	0,00020	199999308	53,258	4,546
0,0027441	0,077	0,161	0,258	0,061	0,00274	76,105	-0,0012084	-0,00062	0,002250	13,997	-70,048	-123,113	0,100	0,00004	200000000	450,000	0,500	0,00020	199999930	53,274	4,522
0,002743	0,077	0,161	0,258	0,061	0,00274	76,127	-0,0012012	-0,00061	0,002250	13,996	-69,626	-121,907	0,200	0,00008	200000000	450,000	0,500	0,00020	199999617	53,289	4,499

0,002742	0,077	0,161	0,258	0,061	0,00274	76,148	-0,001194	-0,00060	0,002250	13,996	-69,212	-120,722	0,300	0,00012	200000000	450,000	0,500	0,00020	199999649	53,304	4,476
0,002741	0,077	0,161	0,258	0,060	0,00274	76,168	-0,001187	-0,00060	0,002250	13,995	-68,804	-119,557	0,400	0,00016	200000000	450,000	0,500	0,00020	199999692	53,317	4,454
0,00274	0,077	0,161	0,258	0,060	0,00274	76,187	-0,0011801	-0,00059	0,002250	13,994	-68,404	-118,412	0,500	0,00020	200000000	450,000	0,500	0,00020	199999687	53,331	4,431
0,002749	0,077	0,161	0,257	0,062	0,00275	79,723	-0,0012428	-0,00064	0,002250	14,002	-72,039	-128,805	0,000	0,00000	200000000	449,999	0,600	0,00024	200000000	55,806	4,825
0,0027479	0,077	0,161	0,257	0,062	0,00275	79,749	-0,0012352	-0,00064	0,002250	14,001	-71,598	-127,543	0,100	0,00004	200000000	450,000	0,600	0,00024	199999612	55,824	4,801
0,0027468	0,077	0,161	0,257	0,062	0,00275	79,774	-0,0012277	-0,00063	0,002250	14,000	-71,164	-126,303	0,200	0,00008	200000000	450,000	0,600	0,00024	199999406	55,841	4,777
0,0027458	0,077	0,161	0,258	0,062	0,00275	79,797	-0,0012203	-0,00063	0,002250	13,999	-70,738	-125,085	0,300	0,00012	200000000	450,000	0,600	0,00024	199999805	55,858	4,754
0,0027447	0,077	0,161	0,258	0,061	0,00274	79,820	-0,0012131	-0,00062	0,002250	13,998	-70,319	-123,887	0,400	0,00016	200000000	450,000	0,600	0,00024	199999630	55,874	4,731
0,0027437	0,077	0,161	0,258	0,061	0,00274	79,841	-0,001206	-0,00061	0,002250	13,997	-69,907	-122,710	0,500	0,00020	200000000	450,000	0,600	0,00024	199999654	55,889	4,708
0,0027427	0,077	0,161	0,258	0,061	0,00274	79,862	-0,001199	-0,00061	0,002250	13,996	-69,502	-121,552	0,600	0,00024	200000000	450,000	0,600	0,00024	199999600	55,903	4,686
0,0027528	0,077	0,161	0,257	0,063	0,00275	83,355	-0,0012695	-0,00067	0,002250	14,005	-73,588	-133,233	0,000	0,00000	200000000	450,000	0,700	0,00028	200000000	58,349	5,091
0,0027517	0,077	0,161	0,257	0,063	0,00275	83,384	-0,0012617	-0,00066	0,002250	14,004	-73,135	-131,938	0,100	0,00004	200000000	450,000	0,700	0,00028	200000000	58,369	5,066
0,0027506	0,077	0,161	0,257	0,063	0,00275	83,412	-0,001254	-0,00065	0,002250	14,003	-72,690	-130,666	0,200	0,00008	200000000	450,000	0,700	0,00028	199999713	58,388	5,042
0,0027495	0,077	0,161	0,257	0,062	0,00275	83,439	-0,0012465	-0,00065	0,002250	14,002	-72,252	-129,415	0,300	0,00012	200000000	450,000	0,700	0,00028	199999693	58,407	5,018
0,0027484	0,077	0,161	0,257	0,062	0,00275	83,464	-0,001239	-0,00064	0,002250	14,001	-71,822	-128,185	0,400	0,00016	200000000	450,000	0,700	0,00028	199999672	58,425	4,994
0,0027474	0,077	0,161	0,257	0,062	0,00275	83,489	-0,0012317	-0,00063	0,002250	14,000	-71,399	-126,975	0,500	0,00020	200000000	450,000	0,700	0,00028	199999691	58,442	4,971
0,0027464	0,077	0,161	0,257	0,062	0,00275	83,512	-0,0012246	-0,00063	0,002250	13,999	-70,983	-125,786	0,600	0,00024	200000000	450,000	0,700	0,00028	199999623	58,459	4,948
0,0027454	0,077	0,161	0,258	0,061	0,00275	83,535	-0,0012175	-0,00062	0,002250	13,998	-70,574	-124,617	0,700	0,00028	200000000	450,000	0,700	0,00028	199999716	58,474	4,926
0,0027566	0,077	0,160	0,257	0,064	0,00276	86,980	-0,001296	-0,00069	0,002250	14,008	-75,125	-137,629	0,000	0,00000	200000000	450,000	0,800	0,00032	199999834	60,886	5,342
0,0027554	0,077	0,161	0,257	0,064	0,00276	87,012	-0,001288	-0,00068	0,002250	14,007	-74,661	-136,301	0,100	0,00004	200000000	450,000	0,800	0,00032	200000000	60,909	5,317
0,0027543	0,077	0,161	0,257	0,063	0,00275	87,043	-0,0012801	-0,00067	0,002250	14,006	-74,204	-134,996	0,200	0,00008	200000000	450,000	0,800	0,00032	199999902	60,930	5,293
0,0027532	0,077	0,161	0,257	0,063	0,00275	87,073	-0,0012724	-0,00067	0,002250	14,005	-73,755	-133,712	0,300	0,00012	200000000	450,000	0,800	0,00032	199999790	60,951	5,269
0,0027521	0,077	0,161	0,257	0,063	0,00275	87,102	-0,0012648	-0,00066	0,002250	14,004	-73,314	-132,451	0,400	0,00016	200000000	450,000	0,800	0,00032	199999903	60,971	5,245
0,002751	0,077	0,161	0,257	0,063	0,00275	87,129	-0,0012573	-0,00066	0,002250	14,003	-72,880	-131,210	0,500	0,00020	200000000	450,000	0,800	0,00032	199999810	60,990	5,221
0,00275	0,077	0,161	0,257	0,062	0,00275	87,155	-0,0012499	-0,00065	0,002250	14,002	-72,453	-129,990	0,600	0,00024	200000000	450,000	0,800	0,00032	199999718	61,009	5,198
0,002749	0,077	0,161	0,257	0,062	0,00275	87,180	-0,0012427	-0,00064	0,002250	14,002	-72,034	-128,790	0,700	0,00028	200000000	450,000	0,800	0,00032	199999940	61,026	5,175
0,0027479	0,077	0,161	0,257	0,062	0,00275	87,205	-0,0012356	-0,00064	0,002250	14,001	-71,621	-127,609	0,800	0,00032	200000000	450,000	0,800	0,00032	199999944	61,043	5,152
0,0027603	0,076	0,160	0,256	0,065	0,00276	90,597	-0,0013224	-0,00071	0,002250	14,011	-76,652	-141,992	0,000	0,00000	200000000	450,000	0,900	0,00036	199999957	63,418	5,581
0,0027592	0,076	0,160	0,256	0,065	0,00276	90,633	-0,0013142	-0,00070	0,002250	14,010	-76,176	-140,632	0,100	0,00004	200000000	450,000	0,900	0,00036	200000000	63,443	5,556
0,002758	0,077	0,160	0,257	0,064	0,00276	90,667	-0,0013061	-0,00070	0,002250	14,009	-75,708	-139,295	0,200	0,00008	200000000	450,000	0,900	0,00036	199999917	63,467	5,531
0,0027569	0,077	0,160	0,257	0,064	0,00276	90,700	-0,0012982	-0,00069	0,002250	14,008	-75,248	-137,980	0,300	0,00012	200000000	450,000	0,900	0,00036	199999988	63,490	5,506
0,0027558	0,077	0,160	0,257	0,064	0,00276	90,732	-0,0012904	-0,00068	0,002250	14,007	-74,796	-136,687	0,400	0,00016	200000000	450,000	0,900	0,00036	199999935	63,512	5,482
0,0027547	0,077	0,161	0,257	0,064	0,00275	90,762	-0,0012827	-0,00068	0,002250	14,006	-74,351	-135,415	0,500	0,00020	200000000	450,000	0,900	0,00036	200000000	63,533	5,458
0,0027536	0,077	0,161	0,257	0,063	0,00275	90,791	-0,0012751	-0,00067	0,002250	14,006	-73,914	-134,164	0,600	0,00024	200000000	450,000	0,900	0,00036	199999948	63,554	5,434
0,0027525	0,077	0,161	0,257	0,063	0,00275	90,819	-0,0012677	-0,00066	0,002250	14,005	-73,483	-132,934	0,700	0,00028	200000000	450,000	0,900	0,00036	199999904	63,573	5,411
0,0027515	0,077	0,161	0,257	0,063	0,00275	90,846	-0,0012604	-0,00066	0,002250	14,004	-73,060	-131,724	0,800	0,00032	200000000	450,000	0,900	0,00036	200000000	63,592	5,388
0,0027505	0,077	0,161	0,257	0,063	0,00275	90,872	-0,0012532	-0,00065	0,002250	14,003	-72,643	-130,533	0,900	0,00036	200000000	450,000	0,900	0,00036	199999961	63,610	5,365
0,0027641	0,076	0,160	0,256	0,066	0,00276	94,207	-0,0013485	-0,00073	0,002250	14,015	-78,167	-146,325	0,000	0,00000	200000000	449,999	1,000	0,00040	200000000	65,945	5,806
0,0027629	0,076	0,160	0,256	0,065	0,00276	94,246	-0,0013401	-0,00072	0,002250	14,014	-77,680	-144,933	0,100	0,00004	200000000	450,000	1,000	0,00040	200000000	65,972	5,781
0,0027617	0,076	0,160	0,256	0,065	0,00276	94,284	-0,0013319	-0,00072	0,002250	14,013	-77,201	-143,564	0,200	0,00008	200000000	450,000	1,000	0,00040	199999970	65,999	5,755

0,0027605	0,076	0,160	0,256	0,065	0,00276	94,320	-0,0013237	-0,00071	0,002250	14,012	-76,731	-142,218	0,300	0,00012	200000000	450,000	1,000	0,00040	200000000	66,024	5,731
0,0027594	0,076	0,160	0,256	0,065	0,00276	94,355	-0,0013157	-0,00070	0,002250	14,011	-76,268	-140,894	0,400	0,00016	200000000	450,000	1,000	0,00040	200000000	66,048	5,706
0,0027583	0,076	0,160	0,257	0,064	0,00276	94,388	-0,0013079	-0,00070	0,002250	14,010	-75,812	-139,592	0,500	0,00020	200000000	450,000	1,000	0,00040	200000000	66,072	5,682
0,0027572	0,077	0,160	0,257	0,064	0,00276	94,420	-0,0013002	-0,00069	0,002250	14,009	-75,364	-138,311	0,600	0,00024	200000000	450,000	1,000	0,00040	200000000	66,094	5,658
0,0027561	0,077	0,160	0,257	0,064	0,00276	94,451	-0,0012925	-0,00069	0,002250	14,008	-74,923	-137,051	0,700	0,00028	200000000	450,000	1,000	0,00040	200000000	66,116	5,634
0,002755	0,077	0,161	0,257	0,064	0,00276	94,481	-0,0012851	-0,00068	0,002250	14,007	-74,490	-135,811	0,800	0,00032	200000000	450,000	1,000	0,00040	200000000	66,137	5,611
0,002754	0,077	0,161	0,257	0,063	0,00275	94,510	-0,0012777	-0,00067	0,002250	14,006	-74,063	-134,591	0,900	0,00036	200000000	450,000	1,000	0,00040	200000000	66,157	5,588
0,0027529	0,077	0,161	0,257	0,063	0,00275	94,537	-0,0012705	-0,00067	0,002250	14,005	-73,643	-133,391	1,000	0,00040	200000000	450,000	1,000	0,00040	200000000	66,176	5,566
0,0027678	0,076	0,160	0,256	0,066	0,00277	97,810	-0,0013745	-0,00075	0,002250	14,018	-79,673	-150,629	0,000	0,00000	200000000	450,000	1,100	0,00044	199999531	68,467	6,020
0,0027666	0,076	0,160	0,256	0,066	0,00277	97,853	-0,0013659	-0,00075	0,002250	14,017	-79,175	-149,205	0,100	0,00004	200000000	450,000	1,100	0,00044	199999486	68,497	5,994
0,0027653	0,076	0,160	0,256	0,066	0,00277	97,894	-0,0013574	-0,00074	0,002250	14,016	-78,685	-147,805	0,200	0,00008	200000000	450,000	1,100	0,00044	200000000	68,526	5,968
0,0027642	0,076	0,160	0,256	0,066	0,00276	97,933	-0,0013491	-0,00073	0,002250	14,015	-78,203	-146,428	0,300	0,00012	200000000	450,000	1,100	0,00044	200000000	68,553	5,943
0,002763	0,076	0,160	0,256	0,065	0,00276	97,971	-0,001341	-0,00073	0,002250	14,014	-77,730	-145,074	0,400	0,00016	200000000	450,000	1,100	0,00044	200000000	68,580	5,918
0,0027618	0,076	0,160	0,256	0,065	0,00276	98,008	-0,0013329	-0,00072	0,002250	14,013	-77,264	-143,742	0,500	0,00020	200000000	450,000	1,100	0,00044	200000000	68,605	5,894
0,0027607	0,076	0,160	0,256	0,065	0,00276	98,043	-0,001325	-0,00071	0,002250	14,012	-76,805	-142,431	0,600	0,00024	200000000	450,000	1,100	0,00044	200000000	68,630	5,870
0,0027596	0,076	0,160	0,256	0,065	0,00276	98,077	-0,0013172	-0,00071	0,002250	14,011	-76,354	-141,142	0,700	0,00028	200000000	450,000	1,100	0,00044	200000000	68,654	5,846
0,0027585	0,076	0,160	0,256	0,064	0,00276	98,110	-0,0013096	-0,00070	0,002250	14,010	-75,910	-139,873	0,800	0,00032	200000000	450,000	1,100	0,00044	200000000	68,677	5,822
0,0027574	0,077	0,160	0,257	0,064	0,00276	98,141	-0,001302	-0,00069	0,002250	14,009	-75,474	-138,624	0,900	0,00036	200000000	450,000	1,100	0,00044	200000000	68,699	5,799
0,0027564	0,077	0,160	0,257	0,064	0,00276	98,171	-0,0012946	-0,00069	0,002250	14,008	-75,044	-137,396	1,000	0,00040	200000000	450,000	1,100	0,00044	200000000	68,720	5,776
0,0027553	0,077	0,161	0,257	0,064	0,00276	98,201	-0,0012873	-0,00068	0,002250	14,007	-74,621	-136,186	1,100	0,00044	200000000	450,000	1,100	0,00044	200000000	68,741	5,754
0,0027715	0,076	0,160	0,255	0,067	0,00277	101,406	-0,0014003	-0,00077	0,002250	14,021	-81,168	-154,905	0,000	0,00000	200000000	450,000	1,200	0,00048	199999568	70,985	6,222
0,0027702	0,076	0,160	0,256	0,067	0,00277	101,452	-0,0013915	-0,00077	0,002250	14,020	-80,659	-153,450	0,100	0,00004	200000000	450,000	1,200	0,00048	199999734	71,017	6,196
0,002769	0,076	0,160	0,256	0,067	0,00277	101,497	-0,0013829	-0,00076	0,002250	14,019	-80,159	-152,019	0,200	0,00008	200000000	450,000	1,200	0,00048	199999796	71,048	6,170
0,0027678	0,076	0,160	0,256	0,066	0,00277	101,539	-0,0013744	-0,00075	0,002250	14,018	-79,667	-150,611	0,300	0,00012	200000000	450,000	1,200	0,00048	200000000	71,078	6,144
0,0027666	0,076	0,160	0,256	0,066	0,00277	101,581	-0,001366	-0,00075	0,002250	14,017	-79,182	-149,227	0,400	0,00016	200000000	450,000	1,200	0,00048	200000000	71,107	6,119
0,0027654	0,076	0,160	0,256	0,066	0,00277	101,621	-0,0013578	-0,00074	0,002250	14,016	-78,706	-147,865	0,500	0,00020	200000000	450,000	1,200	0,00048	200000000	71,134	6,095
0,0027642	0,076	0,160	0,256	0,066	0,00276	101,659	-0,0013497	-0,00073	0,002250	14,015	-78,237	-146,525	0,600	0,00024	200000000	450,000	1,200	0,00048	200000000	71,161	6,070
0,0027631	0,076	0,160	0,256	0,065	0,00276	101,696	-0,0013418	-0,00073	0,002250	14,014	-77,776	-145,207	0,700	0,00028	200000000	450,000	1,200	0,00048	200000000	71,187	6,046
0,002762	0,076	0,160	0,256	0,065	0,00276	101,732	-0,0013339	-0,00072	0,002250	14,013	-77,322	-143,909	0,800	0,00032	200000000	450,000	1,200	0,00048	200000000	71,212	6,022
0,0027609	0,076	0,160	0,256	0,065	0,00276	101,766	-0,0013262	-0,00071	0,002250	14,012	-76,876	-142,633	0,900	0,00036	200000000	450,000	1,200	0,00048	200000000	71,236	5,999
0,0027598	0,076	0,160	0,256	0,065	0,00276	101,799	-0,0013186	-0,00071	0,002250	14,011	-76,436	-141,376	1,000	0,00040	200000000	450,000	1,200	0,00048	200000000	71,259	5,976
0,0027587	0,076	0,160	0,256	0,064	0,00276	101,831	-0,0013112	-0,00070	0,002250	14,010	-76,003	-140,139	1,100	0,00044	200000000	450,000	1,200	0,00048	200000000	71,282	5,953
0,0027577	0,077	0,160	0,257	0,064	0,00276	101,862	-0,0013038	-0,00069	0,002250	14,009	-75,577	-138,921	1,200	0,00048	200000000	450,000	1,200	0,00048	200000000	71,304	5,930
0,0027751	0,076	0,160	0,255	0,068	0,00278	104,996	-0,0014259	-0,00080	0,002250	14,024	-82,654	-159,153	0,000	0,00000	200000000	450,000	1,300	0,00052	199999871	73,497	6,414
0,0027739	0,076	0,160	0,255	0,068	0,00277	105,045	-0,001417	-0,00079	0,002250	14,023	-82,135	-157,668	0,100	0,00004	200000000	450,000	1,300	0,00052	199999575	73,532	6,387
0,0027726	0,076	0,160	0,255	0,067	0,00277	105,093	-0,0014081	-0,00078	0,002250	14,022	-81,624	-156,206	0,200	0,00008	200000000	450,000	1,300	0,00052	199999310	73,565	6,361
0,0027714	0,076	0,160	0,255	0,067	0,00277	105,139	-0,0013995	-0,00077	0,002250	14,021	-81,121	-154,769	0,300	0,00012	200000000	450,000	1,300	0,00052	199999549	73,598	6,335
0,0027701	0,076	0,160	0,256	0,067	0,00277	105,184	-0,0013909	-0,00077	0,002250	14,020	-80,626	-153,355	0,400	0,00016	200000000	450,000	1,300	0,00052	200000000	73,629	6,310
0,0027689	0,076	0,160	0,256	0,067	0,00277	105,227	-0,0013825	-0,00076	0,002250	14,019	-80,140	-151,964	0,500	0,00020	200000000	450,000	1,300	0,00052	199999833	73,659	6,285
0,0027678	0,076	0,160	0,256	0,066	0,00277	105,269	-0,0013743	-0,00075	0,002250	14,018	-79,661	-150,595	0,600	0,00024	200000000	450,000	1,300	0,00052	200000000	73,688	6,260
0,0027666	0,076	0,160	0,256	0,066	0,00277	105,309	-0,0013662	-0,00075	0,002250	14,017	-79,190	-149,248	0,700	0,00028	200000000	450,000	1,300	0,00052	200000000	73,716	6,236
0,0027654	0,076	0,160	0,256	0,066	0,00277	105,347	-0,0013582	-0,00074	0,002250	14,016	-78,726	-147,922	0,800	0,00032	200000000	450,000	1,300	0,00052	200000000	73,743	6,212

0,0027643	0,076	0,160	0,256	0,066	0,00276	105,385	-0,0013503	-0,00073	0,002250	14,015	-78,269	-146,617	0,900	0,00036	200000000	450,000	1,300	0,00052	200000000	73,769	6,188
0,0027632	0,076	0,160	0,256	0,065	0,00276	105,421	-0,0013425	-0,00073	0,002250	14,014	-77,820	-145,333	1,000	0,00040	200000000	450,000	1,300	0,00052	200000000	73,795	6,165
0,0027621	0,076	0,160	0,256	0,065	0,00276	105,456	-0,0013349	-0,00072	0,002250	14,013	-77,378	-144,069	1,100	0,00044	200000000	450,000	1,300	0,00052	200000000	73,819	6,142
0,0027611	0,076	0,160	0,256	0,065	0,00276	105,490	-0,0013274	-0,00071	0,002250	14,012	-76,943	-142,824	1,200	0,00048	200000000	450,000	1,300	0,00052	200000000	73,843	6,119
0,00276	0,076	0,160	0,256	0,065	0,00276	105,522	-0,00132	-0,00071	0,002250	14,011	-76,514	-141,598	1,300	0,00052	200000000	450,000	1,300	0,00052	200000000	73,865	6,097
0,0027788	0,076	0,159	0,255	0,069	0,00278	108,578	-0,0014514	-0,00082	0,002250	14,027	-84,131	-163,376	0,000	0,00000	200000000	450,000	1,400	0,00056	200000000	76,005	6,596
0,0027775	0,076	0,159	0,255	0,068	0,00278	108,632	-0,0014423	-0,00081	0,002250	14,026	-83,601	-161,860	0,100	0,00004	200000000	450,000	1,400	0,00056	199999363	76,042	6,570
0,0027762	0,076	0,159	0,255	0,068	0,00278	108,683	-0,0014333	-0,00080	0,002250	14,025	-83,080	-160,369	0,200	0,00008	200000000	450,000	1,400	0,00056	199999289	76,078	6,543
0,0027749	0,076	0,160	0,255	0,068	0,00277	108,733	-0,0014244	-0,00079	0,002250	14,024	-82,566	-158,902	0,300	0,00012	200000000	450,000	1,400	0,00056	200000000	76,113	6,517
0,0027737	0,076	0,160	0,255	0,068	0,00277	108,781	-0,0014157	-0,00079	0,002250	14,023	-82,062	-157,458	0,400	0,00016	200000000	450,000	1,400	0,00056	200000000	76,147	6,491
0,0027724	0,076	0,160	0,255	0,067	0,00277	108,827	-0,0014071	-0,00078	0,002250	14,022	-81,565	-156,038	0,500	0,00020	200000000	450,000	1,400	0,00056	200000000	76,179	6,466
0,0027712	0,076	0,160	0,255	0,067	0,00277	108,872	-0,0013987	-0,00077	0,002250	14,021	-81,076	-154,641	0,600	0,00024	200000000	450,000	1,400	0,00056	200000000	76,210	6,441
0,0027701	0,076	0,160	0,256	0,067	0,00277	108,915	-0,0013904	-0,00077	0,002250	14,020	-80,595	-153,265	0,700	0,00028	200000000	450,000	1,400	0,00056	200000000	76,241	6,416
0,0027689	0,076	0,160	0,256	0,067	0,00277	108,957	-0,0013822	-0,00076	0,002250	14,019	-80,121	-151,912	0,800	0,00032	200000000	450,000	1,400	0,00056	200000000	76,270	6,392
0,0027677	0,076	0,160	0,256	0,066	0,00277	108,998	-0,0013742	-0,00075	0,002250	14,018	-79,655	-150,579	0,900	0,00036	200000000	450,000	1,400	0,00056	200000000	76,298	6,368
0,0027666	0,076	0,160	0,256	0,066	0,00277	109,037	-0,0013663	-0,00075	0,002250	14,017	-79,196	-149,267	1,000	0,00040	200000000	450,000	1,400	0,00056	200000000	76,326	6,344
0,0027655	0,076	0,160	0,256	0,066	0,00277	109,074	-0,0013585	-0,00074	0,002250	14,016	-78,745	-147,976	1,100	0,00044	200000000	450,000	1,400	0,00056	200000000	76,352	6,321
0,0027644	0,076	0,160	0,256	0,066	0,00276	109,111	-0,0013508	-0,00073	0,002250	14,015	-78,300	-146,705	1,200	0,00048	200000000	450,000	1,400	0,00056	200000000	76,378	6,298
0,0027633	0,076	0,160	0,256	0,065	0,00276	109,146	-0,0013432	-0,00073	0,002250	14,014	-77,862	-145,453	1,300	0,00052	200000000	450,000	1,400	0,00056	200000000	76,402	6,275
0,0027623	0,076	0,160	0,256	0,065	0,00276	109,180	-0,0013358	-0,00072	0,002250	14,013	-77,431	-144,220	1,400	0,00056	200000000	450,000	1,400	0,00056	199999526	76,426	6,253
0,0027824	0,076	0,159	0,255	0,069	0,00278	112,155	-0,0014767	-0,00084	0,002250	14,031	-85,600	-167,574	0,000	0,00000	200000000	450,000	1,500	0,00060	199999452	78,508	6,770
0,0027811	0,076	0,159	0,255	0,069	0,00278	112,212	-0,0014674	-0,00083	0,002250	14,029	-85,059	-166,028	0,100	0,00004	200000000	450,000	1,500	0,00060	199999675	78,548	6,743
0,0027797	0,076	0,159	0,255	0,069	0,00278	112,267	-0,0014582	-0,00082	0,002250	14,028	-84,527	-164,507	0,200	0,00008	200000000	450,000	1,500	0,00060	200000000	78,587	6,716
0,0027785	0,076	0,159	0,255	0,069	0,00278	112,320	-0,0014492	-0,00082	0,002250	14,027	-84,004	-163,010	0,300	0,00012	200000000	450,000	1,500	0,00060	200000000	78,624	6,690
0,0027772	0,076	0,159	0,255	0,068	0,00278	112,371	-0,0014403	-0,00081	0,002250	14,026	-83,489	-161,538	0,400	0,00016	200000000	450,000	1,500	0,00060	200000000	78,660	6,664
0,0027759	0,076	0,159	0,255	0,068	0,00278	112,421	-0,0014316	-0,00080	0,002250	14,025	-82,982	-160,089	0,500	0,00020	200000000	450,000	1,500	0,00060	200000000	78,695	6,638
0,0027747	0,076	0,160	0,255	0,068	0,00277	112,469	-0,001423	-0,00079	0,002250	14,024	-82,483	-158,664	0,600	0,00024	200000000	450,000	1,500	0,00060	200000000	78,729	6,613
0,0027735	0,076	0,160	0,255	0,068	0,00277	112,516	-0,0014145	-0,00079	0,002250	14,023	-81,992	-157,260	0,700	0,00028	200000000	450,000	1,500	0,00060	200000000	78,761	6,588
0,0027723	0,076	0,160	0,255	0,067	0,00277	112,561	-0,0014062	-0,00078	0,002250	14,022	-81,509	-155,879	0,800	0,00032	200000000	450,000	1,500	0,00060	200000000	78,793	6,563
0,0027711	0,076	0,160	0,255	0,067	0,00277	112,604	-0,001398	-0,00077	0,002250	14,021	-81,033	-154,519	0,900	0,00036	200000000	450,000	1,500	0,00060	200000000	78,823	6,539
0,00277	0,076	0,160	0,256	0,067	0,00277	112,646	-0,0013899	-0,00077	0,002250	14,020	-80,565	-153,180	1,000	0,00040	200000000	450,000	1,500	0,00060	200000000	78,853	6,515
0,0027688	0,076	0,160	0,256	0,067	0,00277	112,687	-0,0013819	-0,00076	0,002250	14,019	-80,104	-151,862	1,100	0,00044	200000000	450,000	1,500	0,00060	200000000	78,881	6,492
0,0027677	0,076	0,160	0,256	0,066	0,00277	112,727	-0,0013741	-0,00075	0,002250	14,018	-79,650	-150,564	1,200	0,00048	200000000	450,000	1,500	0,00060	200000000	78,909	6,468
0,0027666	0,076	0,160	0,256	0,066	0,00277	112,765	-0,0013664	-0,00075	0,002250	14,017	-79,203	-149,286	1,300	0,00052	200000000	450,000	1,500	0,00060	200000000	78,935	6,445
0,0027655	0,076	0,160	0,256	0,066	0,00277	112,802	-0,0013588	-0,00074	0,002250	14,016	-78,763	-148,027	1,400	0,00056	200000000	450,000	1,500	0,00060	200000000	78,961	6,423
0,0027645	0,076	0,160	0,256	0,066	0,00276	112,837	-0,0013513	-0,00073	0,002250	14,015	-78,329	-146,787	1,500	0,00060	200000000	450,000	1,500	0,00060	200000000	78,986	6,400
0,002786	0,076	0,159	0,254	0,070	0,00279	115,725	-0,0015019	-0,00086	0,002250	14,034	-87,060	-171,747	0,000	0,00000	200000000	450,000	1,600	0,00064	200000000	81,007	6,936
0,0027846	0,076	0,159	0,254	0,070	0,00278	115,785	-0,0014924	-0,00085	0,002250	14,032	-86,509	-170,172	0,100	0,00004	200000000	450,000	1,600	0,00064	199999850	81,050	6,908
0,0027833	0,076	0,159	0,254	0,070	0,00278	115,844	-0,0014831	-0,00084	0,002250	14,031	-85,966	-168,622	0,200	0,00008	200000000	450,000	1,600	0,00064	200000000	81,091	6,881
0,002782	0,076	0,159	0,255	0,069	0,00278	115,901	-0,0014739	-0,00084	0,002250	14,030	-85,433	-167,096	0,300	0,00012	200000000	450,000	1,600	0,00064	200000000	81,131	6,855
0,0027807	0,076	0,159	0,255	0,069	0,00278	115,956	-0,0014648	-0,00083	0,002250	14,029	-84,908	-165,595	0,400	0,00016	200000000	450,000	1,600	0,00064	200000000	81,169	6,828
0,0027794	0,076	0,159	0,255	0,069	0,00278	116,009	-0,0014559	-0,00082	0,002250	14,028	-84,391	-164,118	0,500	0,00020	200000000	450,000	1,600	0,00064	200000000	81,206	6,802

0,0027782	0,076	0,159	0,255	0,068	0,00278	116,061	-0,0014471	-0,00081	0,002250	14,027	-83,883	-162,664	0,600	0,00024	200000000	450,000	1,600	0,00064	200000000	81,242	6,777
0,0027769	0,076	0,159	0,255	0,068	0,00278	116,110	-0,0014385	-0,00081	0,002250	14,026	-83,382	-161,233	0,700	0,00028	200000000	450,000	1,600	0,00064	200000000	81,277	6,752
0,0027757	0,076	0,159	0,255	0,068	0,00278	116,159	-0,00143	-0,00080	0,002250	14,025	-82,889	-159,825	0,800	0,00032	200000000	450,000	1,600	0,00064	200000000	81,311	6,727
0,0027745	0,076	0,160	0,255	0,068	0,00277	116,205	-0,0014216	-0,00079	0,002250	14,024	-82,404	-158,438	0,900	0,00036	200000000	450,000	1,600	0,00064	200000000	81,344	6,702
0,0027733	0,076	0,160	0,255	0,068	0,00277	116,251	-0,0014134	-0,00079	0,002250	14,023	-81,927	-157,072	1,000	0,00040	200000000	450,000	1,600	0,00064	200000000	81,375	6,678
0,0027722	0,076	0,160	0,255	0,067	0,00277	116,294	-0,0014053	-0,00078	0,002250	14,022	-81,456	-155,728	1,100	0,00044	200000000	450,000	1,600	0,00064	200000000	81,406	6,654
0,002771	0,076	0,160	0,255	0,067	0,00277	116,337	-0,0013973	-0,00077	0,002250	14,021	-80,993	-154,404	1,200	0,00048	200000000	450,000	1,600	0,00064	200000000	81,436	6,631
0,0027699	0,076	0,160	0,256	0,067	0,00277	116,378	-0,0013894	-0,00077	0,002250	14,020	-80,537	-153,100	1,300	0,00052	200000000	450,000	1,600	0,00064	200000000	81,464	6,608
0,0027688	0,076	0,160	0,256	0,067	0,00277	116,417	-0,0013816	-0,00076	0,002250	14,019	-80,088	-151,815	1,400	0,00056	200000000	450,000	1,600	0,00064	200000000	81,492	6,585
0,0027677	0,076	0,160	0,256	0,066	0,00277	116,456	-0,001374	-0,00075	0,002250	14,018	-79,645	-150,550	1,500	0,00060	200000000	450,000	1,600	0,00064	200000000	81,519	6,562
0,0027666	0,076	0,160	0,256	0,066	0,00277	116,493	-0,0013665	-0,00075	0,002250	14,017	-79,209	-149,304	1,600	0,00064	200000000	450,000	1,600	0,00064	200000000	81,545	6,540
0,0027896	0,076	0,159	0,254	0,071	0,00279	119,288	-0,001527	-0,00088	0,002250	14,037	-88,512	-175,898	0,000	0,00000	200000000	450,000	1,700	0,00068	200000000	83,502	7,094
0,0027882	0,076	0,159	0,254	0,070	0,00279	119,353	-0,0015173	-0,00087	0,002250	14,036	-87,950	-174,293	0,100	0,00004	200000000	450,000	1,700	0,00068	199999630	83,547	7,067
0,0027868	0,076	0,159	0,254	0,070	0,00279	119,415	-0,0015078	-0,00086	0,002250	14,034	-87,398	-172,714	0,200	0,00008	200000000	450,000	1,700	0,00068	200000000	83,591	7,039
0,0027855	0,076	0,159	0,254	0,070	0,00279	119,476	-0,0014984	-0,00086	0,002250	14,033	-86,854	-171,160	0,300	0,00012	200000000	450,000	1,700	0,00068	200000000	83,633	7,012
0,0027842	0,076	0,159	0,254	0,070	0,00278	119,534	-0,0014892	-0,00085	0,002250	14,032	-86,319	-169,631	0,400	0,00016	200000000	450,000	1,700	0,00068	200000000	83,674	6,986
0,0027829	0,076	0,159	0,255	0,069	0,00278	119,591	-0,0014801	-0,00084	0,002250	14,031	-85,793	-168,126	0,500	0,00020	200000000	450,000	1,700	0,00068	200000000	83,714	6,959
0,0027816	0,076	0,159	0,255	0,069	0,00278	119,646	-0,0014711	-0,00083	0,002250	14,030	-85,275	-166,644	0,600	0,00024	200000000	450,000	1,700	0,00068	200000000	83,752	6,934
0,0027803	0,076	0,159	0,255	0,069	0,00278	119,699	-0,0014623	-0,00083	0,002250	14,029	-84,765	-165,186	0,700	0,00028	200000000	450,000	1,700	0,00068	200000000	83,790	6,908
0,0027791	0,076	0,159	0,255	0,069	0,00278	119,751	-0,0014537	-0,00082	0,002250	14,028	-84,262	-163,750	0,800	0,00032	200000000	450,000	1,700	0,00068	200000000	83,826	6,883
0,0027779	0,076	0,159	0,255	0,068	0,00278	119,801	-0,0014451	-0,00081	0,002250	14,027	-83,768	-162,336	0,900	0,00036	200000000	450,000	1,700	0,00068	200000000	83,860	6,858
0,0027767	0,076	0,159	0,255	0,068	0,00278	119,849	-0,0014367	-0,00080	0,002250	14,026	-83,281	-160,944	1,000	0,00040	200000000	450,000	1,700	0,00068	200000000	83,894	6,834
0,0027755	0,076	0,160	0,255	0,068	0,00278	119,896	-0,0014285	-0,00080	0,002250	14,025	-82,801	-159,574	1,100	0,00044	200000000	450,000	1,700	0,00068	200000000	83,927	6,810
0,0027743	0,076	0,160	0,255	0,068	0,00277	119,941	-0,0014203	-0,00079	0,002250	14,024	-82,329	-158,224	1,200	0,00048	200000000	450,000	1,700	0,00068	200000000	83,959	6,786
0,0027732	0,076	0,160	0,255	0,067	0,00277	119,985	-0,0014123	-0,00078	0,002250	14,023	-81,864	-156,894	1,300	0,00052	200000000	450,000	1,700	0,00068	200000000	83,989	6,762
0,0027721	0,076	0,160	0,255	0,067	0,00277	120,027	-0,0014044	-0,00078	0,002250	14,022	-81,406	-155,584	1,400	0,00056	200000000	450,000	1,700	0,00068	200000000	84,019	6,739
0,0027709	0,076	0,160	0,255	0,067	0,00277	120,069	-0,0013966	-0,00077	0,002250	14,021	-80,955	-154,294	1,500	0,00060	200000000	450,000	1,700	0,00068	200000000	84,048	6,716
0,0027698	0,076	0,160	0,256	0,067	0,00277	120,109	-0,0013889	-0,00077	0,002250	14,020	-80,510	-153,023	1,600	0,00064	200000000	450,000	1,700	0,00068	200000000	84,076	6,694
0,0027688	0,076	0,160	0,256	0,067	0,00277	120,147	-0,0013814	-0,00076	0,002250	14,019	-80,072	-151,771	1,700	0,00068	200000000	450,000	1,700	0,00068	200000000	84,103	6,672
0,0027931	0,076	0,159	0,254	0,071	0,00279	122,846	-0,0015519	-0,00090	0,002250	14,040	-89,956	-180,026	0,000	0,00000	200000000	450,000	1,800	0,00072	200000000	85,992	7,246
0,0027917	0,076	0,159	0,254	0,071	0,00279	122,915	-0,001542	-0,00089	0,002250	14,039	-89,384	-178,392	0,100	0,00004	200000000	450,000	1,800	0,00072	199999394	86,040	7,218
0,0027903	0,076	0,159	0,254	0,071	0,00279	122,981	-0,0015323	-0,00088	0,002250	14,037	-88,822	-176,785	0,200	0,00008	200000000	450,000	1,800	0,00072	199999646	86,087	7,191
0,002789	0,076	0,159	0,254	0,071	0,00279	123,045	-0,0015228	-0,00088	0,002250	14,036	-88,268	-175,202	0,300	0,00012	200000000	450,000	1,800	0,00072	199999475	86,132	7,163
0,0027876	0,076	0,159	0,254	0,070	0,00279	123,107	-0,0015134	-0,00087	0,002250	14,035	-87,724	-173,645	0,400	0,00016	200000000	450,000	1,800	0,00072	199999792	86,175	7,136
0,0027863	0,076	0,159	0,254	0,070	0,00279	123,167	-0,0015041	-0,00086	0,002250	14,034	-87,187	-172,112	0,500	0,00020	200000000	449,999	1,800	0,00072	200000000	86,217	7,110
0,002785	0,076	0,159	0,254	0,070	0,00279	123,226	-0,001495	-0,00085	0,002250	14,033	-86,660	-170,603	0,600	0,00024	200000000	450,000	1,800	0,00072	199999869	86,258	7,084
0,0027837	0,076	0,159	0,254	0,070	0,00278	123,283	-0,0014861	-0,00085	0,002250	14,032	-86,140	-169,118	0,700	0,00028	200000000	450,000	1,800	0,00072	199999518	86,298	7,058
0,0027825	0,076	0,159	0,255	0,069	0,00278	123,337	-0,0014772	-0,00084	0,002250	14,031	-85,628	-167,655	0,800	0,00032	200000000	450,000	1,800	0,00072	200000000	86,336	7,033
0,0027812	0,076	0,159	0,255	0,069	0,00278	123,391	-0,0014685	-0,00083	0,002250	14,030	-85,125	-166,215	0,900	0,00036	200000000	450,000	1,800	0,00072	199999480	86,373	7,007
0,00278	0,076	0,159	0,255	0,069	0,00278	123,442	-0,00146	-0,00082	0,002250	14,028	-84,629	-164,797	1,000	0,00040	200000000	450,000	1,800	0,00072	199999562	86,409	6,983
0,0027788	0,076	0,159	0,255	0,069	0,00278	123,492	-0,0014516	-0,00082	0,002250	14,027	-84,140	-163,400	1,100	0,00044	200000000	450,000	1,800	0,00072	200000000	86,444	6,958
0,0027776	0,076	0,159	0,255	0,068	0,00278	123,540	-0,0014433	-0,00081	0,002250	14,026	-83,659	-162,025	1,200	0,00048	200000000	450,000	1,800	0,00072	199999650	86,478	6,934
0,0027764	0,076	0,159	0,255	0,068	0,00278	123,587	-0,0014351	-0,00080	0,002250	14,025	-83,185	-160,669	1,300	0,00052	200000000	449,999	1,800	0,00072	200000000	86,511	6,911

0,0027753	0,076	0,160	0,255	0,068	0,00278	123,633	-0,001427	-0,00080	0,002250	14,024	-82,718	-159,335	1,400	0,00056	200000000	450,000	1,800	0,00072	199999559	86,543	6,887
0,0027742	0,076	0,160	0,255	0,068	0,00277	123,676	-0,0014191	-0,00079	0,002250	14,023	-82,258	-158,020	1,500	0,00060	200000000	450,000	1,800	0,00072	200000000	86,574	6,864
0,002773	0,076	0,160	0,255	0,067	0,00277	123,719	-0,0014113	-0,00078	0,002250	14,022	-81,805	-156,724	1,600	0,00064	200000000	450,000	1,800	0,00072	200000000	86,603	6,841
0,0027719	0,076	0,160	0,255	0,067	0,00277	123,760	-0,0014036	-0,00078	0,002250	14,021	-81,358	-155,448	1,700	0,00068	200000000	450,000	1,800	0,00072	200000000	86,632	6,819
0,0027709	0,076	0,160	0,255	0,067	0,00277	123,801	-0,001396	-0,00077	0,002250	14,021	-80,918	-154,190	1,800	0,00072	200000000	450,000	1,800	0,00072	199999013	86,660	6,797
0,0027967	0,075	0,158	0,253	0,072	0,00280	126,398	-0,0015767	-0,00092	0,002250	14,043	-91,392	-184,133	0,000	0,00000	200000000	450,000	1,900	0,00076	199999573	88,479	7,392
0,0027952	0,075	0,159	0,254	0,072	0,00280	126,470	-0,0015666	-0,00091	0,002250	14,042	-90,811	-182,470	0,100	0,00004	200000000	450,000	1,900	0,00076	199999512	88,529	7,364
0,0027938	0,076	0,159	0,254	0,072	0,00279	126,540	-0,0015568	-0,00090	0,002250	14,040	-90,238	-180,834	0,200	0,00008	200000000	450,000	1,900	0,00076	200000000	88,578	7,336
0,0027924	0,076	0,159	0,254	0,071	0,00279	126,609	-0,001547	-0,00090	0,002250	14,039	-89,675	-179,224	0,300	0,00012	200000000	450,000	1,900	0,00076	199999418	88,626	7,308
0,0027911	0,076	0,159	0,254	0,071	0,00279	126,674	-0,0015375	-0,00089	0,002250	14,038	-89,121	-177,639	0,400	0,00016	200000000	450,000	1,900	0,00076	199999675	88,672	7,281
0,0027897	0,076	0,159	0,254	0,071	0,00279	126,738	-0,0015281	-0,00088	0,002250	14,037	-88,575	-176,078	0,500	0,00020	200000000	450,000	1,900	0,00076	200000000	88,717	7,254
0,0027884	0,076	0,159	0,254	0,071	0,00279	126,800	-0,0015188	-0,00087	0,002250	14,036	-88,037	-174,542	0,600	0,00024	200000000	450,000	1,900	0,00076	199999678	88,760	7,228
0,0027871	0,076	0,159	0,254	0,070	0,00279	126,860	-0,0015097	-0,00087	0,002250	14,035	-87,509	-173,030	0,700	0,00028	200000000	450,000	1,900	0,00076	199999557	88,802	7,202
0,0027858	0,076	0,159	0,254	0,070	0,00279	126,918	-0,0015007	-0,00086	0,002250	14,034	-86,988	-171,541	0,800	0,00032	200000000	450,000	1,900	0,00076	199999465	88,843	7,176
0,0027846	0,076	0,159	0,254	0,070	0,00278	126,975	-0,0014918	-0,00085	0,002250	14,032	-86,475	-170,075	0,900	0,00036	200000000	450,000	1,900	0,00076	199999159	88,882	7,151
0,0027833	0,076	0,159	0,254	0,070	0,00278	127,030	-0,0014831	-0,00084	0,002250	14,031	-85,970	-168,631	1,000	0,00040	200000000	450,000	1,900	0,00076	199999086	88,921	7,126
0,002782	0,076	0,159	0,255	0,069	0,00278	127,081	-0,0014745	-0,00084	0,002250	14,030	-85,471	-167,206	1,100	0,00044	200000000	449,992	1,900	0,00076	200000000	88,957	7,101
0,0027809	0,076	0,159	0,255	0,069	0,00278	127,134	-0,0014661	-0,00083	0,002250	14,029	-84,982	-165,807	1,200	0,00048	200000000	450,000	1,900	0,00076	200000000	88,994	7,077
0,0027797	0,076	0,159	0,255	0,069	0,00278	127,184	-0,0014577	-0,00082	0,002250	14,028	-84,499	-164,427	1,300	0,00052	200000000	450,000	1,900	0,00076	200000000	89,029	7,053
0,0027785	0,076	0,159	0,255	0,069	0,00278	127,232	-0,0014495	-0,00082	0,002250	14,027	-84,024	-163,067	1,400	0,00056	200000000	450,000	1,900	0,00076	200000000	89,063	7,029
0,0027774	0,076	0,159	0,255	0,068	0,00278	127,279	-0,0014415	-0,00081	0,002250	14,026	-83,555	-161,728	1,500	0,00060	200000000	450,000	1,900	0,00076	199999557	89,095	7,006
0,0027762	0,076	0,159	0,255	0,068	0,00278	127,325	-0,0014335	-0,00080	0,002250	14,025	-83,093	-160,408	1,600	0,00064	200000000	450,000	1,900	0,00076	199999993	89,127	6,983
0,0027751	0,076	0,160	0,255	0,068	0,00278	127,369	-0,0014257	-0,00080	0,002250	14,024	-82,639	-159,108	1,700	0,00068	200000000	450,000	1,900	0,00076	199999327	89,158	6,960
0,002774	0,076	0,160	0,255	0,068	0,00277	127,412	-0,0014179	-0,00079	0,002250	14,023	-82,190	-157,826	1,800	0,00072	200000000	450,000	1,900	0,00076	199999426	89,188	6,938
0,0027729	0,076	0,160	0,255	0,067	0,00277	127,453	-0,0014103	-0,00078	0,002250	14,022	-81,748	-156,563	1,900	0,00076	200000000	450,000	1,900	0,00076	199999651	89,217	6,915
0,0028002	0,075	0,158	0,253	0,073	0,00280	129,944	-0,0016013	-0,00094	0,002250	14,046	-92,822	-188,219	0,000	0,00000	200000000	450,000	2,000	0,00080	199999697	90,961	7,533
0,0027987	0,075	0,158	0,253	0,072	0,00280	130,020	-0,0015911	-0,00093	0,002250	14,045	-92,230	-186,528	0,100	0,00004	200000000	450,000	2,000	0,00080	200000000	91,014	7,504
0,0027973	0,075	0,158	0,253	0,072	0,00280	130,094	-0,0015811	-0,00092	0,002250	14,043	-91,648	-184,864	0,200	0,00008	200000000	450,000	2,000	0,00080	199999866	91,066	7,476
0,0027959	0,075	0,158	0,253	0,072	0,00280	130,166	-0,0015712	-0,00092	0,002250	14,042	-91,075	-183,225	0,300	0,00012	200000000	450,000	2,000	0,00080	200000000	91,116	7,448
0,0027945	0,076	0,159	0,254	0,072	0,00279	130,236	-0,0015615	-0,00091	0,002250	14,041	-90,511	-181,613	0,400	0,00016	200000000	450,000	2,000	0,00080	199999653	91,165	7,421
0,0027931	0,076	0,159	0,254	0,071	0,00279	130,303	-0,0015519	-0,00090	0,002250	14,040	-89,955	-180,025	0,500	0,00020	200000000	450,000	2,000	0,00080	200000000	91,212	7,393
0,0027918	0,076	0,159	0,254	0,071	0,00279	130,369	-0,0015424	-0,00089	0,002250	14,039	-89,409	-178,462	0,600	0,00024	200000000	450,000	2,000	0,00080	199999930	91,258	7,367
0,0027905	0,076	0,159	0,254	0,071	0,00279	130,432	-0,0015332	-0,00088	0,002250	14,038	-88,870	-176,923	0,700	0,00028	200000000	450,000	2,000	0,00080	199999784	91,303	7,340
0,0027891	0,076	0,159	0,254	0,071	0,00279	130,494	-0,001524	-0,00088	0,002250	14,036	-88,340	-175,408	0,800	0,00032	200000000	450,000	2,000	0,00080	199999800	91,346	7,314
0,0027879	0,076	0,159	0,254	0,070	0,00279	130,554	-0,001515	-0,00087	0,002250	14,035	-87,818	-173,915	0,900	0,00036	200000000	450,000	2,000	0,00080	200000000	91,388	7,289
0,0027866	0,076	0,159	0,254	0,070	0,00279	130,612	-0,0015061	-0,00086	0,002250	14,034	-87,304	-172,446	1,000	0,00040	200000000	450,000	2,000	0,00080	199999803	91,428	7,263
0,0027853	0,076	0,159	0,254	0,070	0,00279	130,668	-0,0014974	-0,00085	0,002250	14,033	-86,798	-170,998	1,100	0,00044	200000000	450,000	2,000	0,00080	200000000	91,467	7,238
0,0027841	0,076	0,159	0,254	0,070	0,00278	130,723	-0,0014888	-0,00085	0,002250	14,032	-86,299	-169,572	1,200	0,00048	200000000	450,000	2,000	0,00080	199999646	91,506	7,214
0,0027829	0,076	0,159	0,255	0,069	0,00278	130,775	-0,0014803	-0,00084	0,002250	14,031	-85,807	-168,167	1,300	0,00052	200000000	450,000	2,000	0,00080	200000000	91,543	7,189
0,0027817	0,076	0,159	0,255	0,069	0,00278	130,827	-0,001472	-0,00083	0,002250	14,030	-85,323	-166,783	1,400	0,00056	200000000	450,000	2,000	0,00080	199999494	91,579	7,165
0,0027805	0,076	0,159	0,255	0,069	0,00278	130,877	-0,0014637	-0,00083	0,002250	14,029	-84,846	-165,419	1,500	0,00060	200000000	450,000	2,000	0,00080	199999808	91,614	7,142
0,0027794	0,076	0,159	0,255	0,069	0,00278	130,925	-0,0014556	-0,00082	0,002250	14,028	-84,376	-164,075	1,600	0,00064	200000000	450,000	2,000	0,00080	199999866	91,648	7,119
0,0027782	0,076	0,159	0,255	0,069	0,00278	130,972	-0,0014476	-0,00081	0,002250	14,027	-83,913	-162,751	1,700	0,00068	200000000	450,000	2,000	0,00080	200000000	91,680	7,096

0,002777	0,076	0,159	0,255	0,068	0,00278	131,012	-0,0014397	-0,00081	0,002250	14,026	-83,453	-161,440	1,800	0,00072	200000000	449,974	2,000	0,00080	200000000	91,709	7,072
0,002776	0,076	0,159	0,255	0,068	0,00278	131,062	-0,001432	-0,00080	0,002250	14,025	-83,006	-160,159	1,900	0,00076	200000000	450,000	2,000	0,00080	200000000	91,743	7,050
0,0027749	0,076	0,160	0,255	0,068	0,00277	131,105	-0,0014243	-0,00079	0,002250	14,024	-82,563	-158,891	2,000	0,00080	200000000	450,000	2,000	0,00080	200000000	91,773	7,028
0,0028037	0,075	0,158	0,253	0,073	0,00280	133,484	-0,0016259	-0,00096	0,002250	14,049	-94,244	-192,285	0,000	0,00000	200000000	450,000	2,100	0,00084	199999249	93,439	7,669
0,0028022	0,075	0,158	0,253	0,073	0,00280	133,565	-0,0016155	-0,00095	0,002250	14,048	-93,642	-190,566	0,100	0,00004	200000000	450,000	2,100	0,00084	200000000	93,495	7,640
0,0028008	0,075	0,158	0,253	0,073	0,00280	133,643	-0,0016053	-0,00094	0,002250	14,046	-93,050	-188,873	0,200	0,00008	200000000	450,000	2,100	0,00084	199999592	93,550	7,611
0,0027993	0,075	0,158	0,253	0,073	0,00280	133,718	-0,0015952	-0,00094	0,002250	14,045	-92,468	-187,207	0,300	0,00012	200000000	450,000	2,100	0,00084	200000000	93,603	7,583
0,0027979	0,075	0,158	0,253	0,072	0,00280	133,792	-0,0015853	-0,00093	0,002250	14,044	-91,894	-185,568	0,400	0,00016	200000000	450,000	2,100	0,00084	199999910	93,654	7,555
0,0027965	0,075	0,158	0,253	0,072	0,00280	133,863	-0,0015756	-0,00092	0,002250	14,043	-91,329	-183,953	0,500	0,00020	200000000	450,000	2,100	0,00084	200000000	93,704	7,527
0,0027951	0,075	0,159	0,254	0,072	0,00280	133,932	-0,001566	-0,00091	0,002250	14,042	-90,773	-182,364	0,600	0,00024	200000000	450,000	2,100	0,00084	200000000	93,752	7,500
0,0027938	0,076	0,159	0,254	0,072	0,00279	133,999	-0,0015565	-0,00090	0,002250	14,040	-90,226	-180,798	0,700	0,00028	200000000	450,000	2,100	0,00084	199999685	93,799	7,474
0,0027925	0,076	0,159	0,254	0,071	0,00279	134,064	-0,0015472	-0,00090	0,002250	14,039	-89,687	-179,257	0,800	0,00032	200000000	450,000	2,100	0,00084	199999605	93,845	7,447
0,0027912	0,076	0,159	0,254	0,071	0,00279	134,127	-0,0015381	-0,00089	0,002250	14,038	-89,156	-177,739	0,900	0,00036	200000000	450,000	2,100	0,00084	199999711	93,889	7,421
0,0027899	0,076	0,159	0,254	0,071	0,00279	134,189	-0,0015291	-0,00088	0,002250	14,037	-88,632	-176,243	1,000	0,00040	200000000	450,000	2,100	0,00084	200000000	93,932	7,396
0,0027886	0,076	0,159	0,254	0,071	0,00279	134,248	-0,0015202	-0,00087	0,002250	14,036	-88,117	-174,771	1,100	0,00044	200000000	450,000	2,100	0,00084	199999675	93,974	7,371
0,0027874	0,076	0,159	0,254	0,070	0,00279	134,306	-0,0015114	-0,00087	0,002250	14,035	-87,610	-173,320	1,200	0,00048	200000000	450,000	2,100	0,00084	199999265	94,014	7,346
0,0027861	0,076	0,159	0,254	0,070	0,00279	134,362	-0,0015028	-0,00086	0,002250	14,034	-87,110	-171,890	1,300	0,00052	200000000	450,000	2,100	0,00084	199999209	94,053	7,321
0,0027849	0,076	0,159	0,254	0,070	0,00278	134,416	-0,0014943	-0,00085	0,002250	14,033	-86,617	-170,482	1,400	0,00056	200000000	450,000	2,100	0,00084	200000000	94,091	7,297
0,0027837	0,076	0,159	0,254	0,070	0,00278	134,469	-0,0014859	-0,00085	0,002250	14,032	-86,132	-169,094	1,500	0,00060	200000000	450,000	2,100	0,00084	199999925	94,128	7,273
0,0027825	0,076	0,159	0,255	0,069	0,00278	134,520	-0,0014777	-0,00084	0,002250	14,031	-85,653	-167,726	1,600	0,00064	200000000	450,000	2,100	0,00084	200000000	94,164	7,249
0,0027814	0,076	0,159	0,255	0,069	0,00278	134,570	-0,0014695	-0,00083	0,002250	14,030	-85,182	-166,378	1,700	0,00068	200000000	450,000	2,100	0,00084	199999461	94,199	7,226
0,0027802	0,076	0,159	0,255	0,069	0,00278	134,619	-0,0014615	-0,00083	0,002250	14,029	-84,717	-165,050	1,800	0,00072	200000000	450,000	2,100	0,00084	199999753	94,233	7,203
0,0027791	0,076	0,159	0,255	0,069	0,00278	134,665	-0,0014536	-0,00082	0,002250	14,028	-84,259	-163,740	1,900	0,00076	200000000	450,000	2,100	0,00084	200000000	94,266	7,180
0,002778	0,076	0,159	0,255	0,068	0,00278	134,711	-0,0014458	-0,00081	0,002250	14,027	-83,807	-162,449	2,000	0,00080	200000000	450,000	2,100	0,00084	199999582	94,298	7,158
0,0027769	0,076	0,159	0,255	0,068	0,00278	134,755	-0,0014381	-0,00081	0,002250	14,026	-83,362	-161,177	2,100	0,00084	200000000	450,000	2,100	0,00084	199999886	94,329	7,136
0,0028072	0,075	0,158	0,253	0,074	0,00281	137,019	-0,0016503	-0,00098	0,002250	14,052	-95,659	-196,332	0,000	0,00000	200000000	450,000	2,200	0,00088	199999572	95,913	7,800
0,0028057	0,075	0,158	0,253	0,074	0,00281	137,104	-0,0016397	-0,00097	0,002250	14,051	-95,048	-194,584	0,100	0,00004	200000000	450,000	2,200	0,00088	200000000	95,973	7,771
0,0028042	0,075	0,158	0,253	0,074	0,00280	137,186	-0,0016294	-0,00096	0,002250	14,049	-94,446	-192,864	0,200	0,00008	200000000	450,000	2,200	0,00088	200000000	96,030	7,742
0,0028027	0,075	0,158	0,253	0,073	0,00280	137,265	-0,0016191	-0,00096	0,002250	14,048	-93,854	-191,171	0,300	0,00012	200000000	450,000	2,200	0,00088	200000000	96,086	7,713
0,0028012	0,075	0,158	0,253	0,073	0,00280	137,339	-0,001609	-0,00095	0,002250	14,047	-93,269	-189,500	0,400	0,00016	200000000	449,985	2,200	0,00088	200000000	96,137	7,685
0,0027999	0,075	0,158	0,253	0,073	0,00280	137,417	-0,0015992	-0,00094	0,002250	14,046	-92,697	-187,863	0,500	0,00020	200000000	450,000	2,200	0,00088	199999514	96,192	7,657
0,0027985	0,075	0,158	0,253	0,072	0,00280	137,490	-0,0015894	-0,00093	0,002250	14,044	-92,132	-186,247	0,600	0,00024	200000000	450,000	2,200	0,00088	200000000	96,243	7,630
0,0027971	0,075	0,158	0,253	0,072	0,00280	137,561	-0,0015798	-0,00092	0,002250	14,043	-91,575	-184,655	0,700	0,00028	200000000	450,000	2,200	0,00088	200000000	96,292	7,603
0,0027958	0,075	0,159	0,254	0,072	0,00280	137,629	-0,0015704	-0,00092	0,002250	14,042	-91,027	-183,088	0,800	0,00032	200000000	450,000	2,200	0,00088	200000000	96,340	7,576
0,0027944	0,076	0,159	0,254	0,072	0,00279	137,696	-0,001561	-0,00091	0,002250	14,041	-90,487	-181,545	0,900	0,00036	200000000	450,000	2,200	0,00088	199999560	96,387	7,550
0,0027931	0,076	0,159	0,254	0,071	0,00279	137,761	-0,0015519	-0,00090	0,002250	14,040	-89,955	-180,024	1,000	0,00040	200000000	450,000	2,200	0,00088	199999891	96,432	7,524
0,0027918	0,076	0,159	0,254	0,071	0,00279	137,823	-0,0015428	-0,00089	0,002250	14,039	-89,431	-178,526	1,100	0,00044	200000000	450,000	2,200	0,00088	199999832	96,476	7,498
0,0027906	0,076	0,159	0,254	0,071	0,00279	137,884	-0,0015339	-0,00089	0,002250	14,038	-88,915	-177,051	1,200	0,00048	200000000	450,000	2,200	0,00088	199999470	96,519	7,473
0,0027893	0,076	0,159	0,254	0,071	0,00279	137,944	-0,0015252	-0,00088	0,002250	14,037	-88,406	-175,597	1,300	0,00052	200000000	450,000	2,200	0,00088	199999391	96,560	7,448
0,0027881	0,076	0,159	0,254	0,070	0,00279	138,001	-0,0015165	-0,00087	0,002250	14,035	-87,905	-174,164	1,400	0,00056	200000000	450,000	2,200	0,00088	200000000	96,601	7,424
0,0027869	0,076	0,159	0,254	0,070	0,00279	138,057	-0,001508	-0,00086	0,002250	14,034	-87,411	-172,752	1,500	0,00060	200000000	450,000	2,200	0,00088	199999648	96,640	7,399
0,0027857	0,076	0,159	0,254	0,070	0,00279	138,111	-0,0014996	-0,00086	0,002250	14,033	-86,925	-171,361	1,600	0,00064	200000000	450,000	2,200	0,00088	199999812	96,678	7,375
0,0027845	0,076	0,159	0,254	0,070	0,00278	138,164	-0,0014913	-0,00085	0,002250	14,032	-86,445	-169,990	1,700	0,00068	200000000	450,000	2,200	0,00088	199999302	96,715	7,352

0,0027833	0,076	0,159	0,254	0,070	0,00278	138,215	-0,0014832	-0,00084	0,002250	14,031	-85,972	-168,638	1,800	0,00072	200000000	450,000	2,200	0,00088	199999388	96,750	7,329
0,0027822	0,076	0,159	0,255	0,069	0,00278	138,265	-0,0014751	-0,00084	0,002250	14,030	-85,506	-167,306	1,900	0,00076	200000000	450,000	2,200	0,00088	200000000	96,785	7,306
0,002781	0,076	0,159	0,255	0,069	0,00278	138,313	-0,0014672	-0,00083	0,002250	14,029	-85,047	-165,992	2,000	0,00080	200000000	450,000	2,200	0,00088	199999341	96,819	7,283
0,0027799	0,076	0,159	0,255	0,069	0,00278	138,360	-0,0014594	-0,00082	0,002250	14,028	-84,594	-164,697	2,100	0,00084	200000000	450,000	2,200	0,00088	199999711	96,852	7,261
0,0027788	0,076	0,159	0,255	0,069	0,00278	138,405	-0,0014517	-0,00082	0,002250	14,027	-84,147	-163,420	2,200	0,00088	200000000	450,000	2,200	0,00088	199999789	96,884	7,239
0,0028107	0,075	0,158	0,252	0,075	0,00281	140,549	-0,0016746	-0,00100	0,002250	14,055	-97,068	-200,359	0,000	0,00000	200000000	450,000	2,300	0,00092	199999847	98,384	7,927
0,0028091	0,075	0,158	0,252	0,074	0,00281	140,637	-0,0016639	-0,00099	0,002250	14,054	-96,447	-198,584	0,100	0,00004	200000000	450,000	2,300	0,00092	199999674	98,446	7,897
0,0028076	0,075	0,158	0,253	0,074	0,00281	140,723	-0,0016533	-0,00098	0,002250	14,052	-95,836	-196,837	0,200	0,00008	200000000	450,000	2,300	0,00092	200000000	98,506	7,868
0,0028061	0,075	0,158	0,253	0,074	0,00281	140,807	-0,0016429	-0,00098	0,002250	14,051	-95,234	-195,117	0,300	0,00012	200000000	450,000	2,300	0,00092	199999597	98,565	7,839
0,0028047	0,075	0,158	0,253	0,074	0,00280	140,888	-0,0016327	-0,00097	0,002250	14,050	-94,642	-193,423	0,400	0,00016	200000000	450,000	2,300	0,00092	200000000	98,621	7,810
0,0028032	0,075	0,158	0,253	0,073	0,00280	140,966	-0,0016227	-0,00096	0,002250	14,049	-94,058	-191,755	0,500	0,00020	200000000	450,000	2,300	0,00092	200000000	98,676	7,782
0,0028018	0,075	0,158	0,253	0,073	0,00280	141,043	-0,0016128	-0,00095	0,002250	14,047	-93,484	-190,113	0,600	0,00024	200000000	450,000	2,300	0,00092	199999875	98,730	7,755
0,0028004	0,075	0,158	0,253	0,073	0,00280	141,117	-0,001603	-0,00094	0,002250	14,046	-92,918	-188,496	0,700	0,00028	200000000	450,000	2,300	0,00092	200000000	98,782	7,727
0,0027991	0,075	0,158	0,253	0,073	0,00280	141,189	-0,0015934	-0,00093	0,002250	14,045	-92,361	-186,903	0,800	0,00032	200000000	450,000	2,300	0,00092	200000000	98,832	7,700
0,0027977	0,075	0,158	0,253	0,072	0,00280	141,259	-0,0015839	-0,00093	0,002250	14,044	-91,812	-185,334	0,900	0,00036	200000000	450,000	2,300	0,00092	200000000	98,881	7,674
0,0027964	0,075	0,158	0,253	0,072	0,00280	141,327	-0,0015746	-0,00092	0,002250	14,043	-91,272	-183,788	1,000	0,00040	200000000	450,000	2,300	0,00092	200000000	98,929	7,648
0,0027951	0,075	0,159	0,254	0,072	0,00280	141,393	-0,0015654	-0,00091	0,002250	14,042	-90,739	-182,265	1,100	0,00044	200000000	450,000	2,300	0,00092	200000000	98,975	7,622
0,0027938	0,076	0,159	0,254	0,072	0,00279	141,458	-0,0015563	-0,00090	0,002250	14,040	-90,214	-180,765	1,200	0,00048	200000000	450,000	2,300	0,00092	199999854	99,020	7,596
0,0027925	0,076	0,159	0,254	0,071	0,00279	141,520	-0,0015474	-0,00090	0,002250	14,039	-89,697	-179,287	1,300	0,00052	200000000	450,000	2,300	0,00092	200000000	99,064	7,571
0,0027912	0,076	0,159	0,254	0,071	0,00279	141,581	-0,0015386	-0,00089	0,002250	14,038	-89,188	-177,831	1,400	0,00056	200000000	450,000	2,300	0,00092	199999812	99,107	7,546
0,00279	0,076	0,159	0,254	0,071	0,00279	141,640	-0,00153	-0,00088	0,002250	14,037	-88,686	-176,395	1,500	0,00060	200000000	450,000	2,300	0,00092	199999563	99,148	7,522
0,0027888	0,076	0,159	0,254	0,071	0,00279	141,697	-0,0015214	-0,00087	0,002250	14,036	-88,191	-174,981	1,600	0,00064	200000000	450,000	2,300	0,00092	199999561	99,188	7,497
0,0027876	0,076	0,159	0,254	0,070	0,00279	141,752	-0,001513	-0,00087	0,002250	14,035	-87,703	-173,586	1,700	0,00068	200000000	450,000	2,300	0,00092	200000000	99,227	7,474
0,0027864	0,076	0,159	0,254	0,070	0,00279	141,807	-0,0015047	-0,00086	0,002250	14,034	-87,222	-172,211	1,800	0,00072	200000000	450,000	2,300	0,00092	200000000	99,265	7,450
0,0027852	0,076	0,159	0,254	0,070	0,00279	141,859	-0,0014965	-0,00085	0,002250	14,033	-86,748	-170,856	1,900	0,00076	200000000	450,000	2,300	0,00092	199999655	99,301	7,427
0,0027841	0,076	0,159	0,254	0,070	0,00278	141,910	-0,0014885	-0,00085	0,002250	14,032	-86,281	-169,521	2,000	0,00080	200000000	450,000	2,300	0,00092	199999714	99,337	7,404
0,0027829	0,076	0,159	0,255	0,069	0,00278	141,960	-0,0014805	-0,00084	0,002250	14,031	-85,820	-168,203	2,100	0,00084	200000000	450,000	2,300	0,00092	199999739	99,372	7,381
0,0027818	0,076	0,159	0,255	0,069	0,00278	142,008	-0,0014727	-0,00083	0,002250	14,030	-85,366	-166,905	2,200	0,00088	200000000	450,000	2,300	0,00092	199999465	99,406	7,359
0,0027807	0,076	0,159	0,255	0,069	0,00278	142,055	-0,001465	-0,00083	0,002250	14,029	-84,918	-165,624	2,300	0,00092	200000000	450,000	2,300	0,00092	200000000	99,438	7,337
0,0028141	0,075	0,158	0,252	0,075	0,00281	144,073	-0,0016988	-0,00102	0,002250	14,058	-98,471	-204,369	0,000	0,00000	200000000	450,000	2,400	0,00096	199999646	100,851	8,050
0,0028126	0,075	0,158	0,252	0,075	0,00281	144,165	-0,0016879	-0,00101	0,002250	14,057	-97,840	-202,566	0,100	0,00004	200000000	450,000	2,400	0,00096	200000000	100,916	8,020
0,002811	0,075	0,158	0,252	0,075	0,00281	144,255	-0,0016772	-0,00100	0,002250	14,055	-97,219	-200,792	0,200	0,00008	200000000	450,000	2,400	0,00096	200000000	100,979	7,990
0,0028095	0,075	0,158	0,252	0,074	0,00281	144,343	-0,0016666	-0,00100	0,002250	14,054	-96,608	-199,044	0,300	0,00012	200000000	450,000	2,400	0,00096	200000000	101,040	7,961
0,002808	0,075	0,158	0,253	0,074	0,00281	144,428	-0,0016563	-0,00099	0,002250	14,053	-96,006	-197,324	0,400	0,00016	200000000	450,000	2,400	0,00096	199999510	101,100	7,932
0,0028066	0,075	0,158	0,253	0,074	0,00281	144,510	-0,001646	-0,00098	0,002250	14,052	-95,414	-195,630	0,500	0,00020	200000000	450,000	2,400	0,00096	199999822	101,157	7,904
0,0028051	0,075	0,158	0,253	0,074	0,00281	144,591	-0,001636	-0,00097	0,002250	14,050	-94,830	-193,962	0,600	0,00024	200000000	450,000	2,400	0,00096	199999831	101,213	7,876
0,0028037	0,075	0,158	0,253	0,073	0,00280	144,668	-0,0016261	-0,00096	0,002250	14,049	-94,256	-192,319	0,700	0,00028	200000000	450,000	2,400	0,00096	200000000	101,268	7,848
0,0028023	0,075	0,158	0,253	0,073	0,00280	144,744	-0,0016163	-0,00095	0,002250	14,048	-93,690	-190,701	0,800	0,00032	200000000	450,000	2,400	0,00096	199999742	101,321	7,821
0,002801	0,075	0,158	0,253	0,073	0,00280	144,818	-0,0016067	-0,00095	0,002250	14,047	-93,132	-189,107	0,900	0,00036	200000000	450,000	2,400	0,00096	199999798	101,372	7,794
0,0027996	0,075	0,158	0,253	0,073	0,00280	144,889	-0,0015972	-0,00094	0,002250	14,045	-92,583	-187,536	1,000	0,00040	200000000	450,000	2,400	0,00096	199999205	101,423	7,767
0,0027983	0,075	0,158	0,253	0,072	0,00280	144,959	-0,0015879	-0,00093	0,002250	14,044	-92,041	-185,989	1,100	0,00044	200000000	450,000	2,400	0,00096	199999853	101,471	7,741
0,002797	0,075	0,158	0,253	0,072	0,00280	145,026	-0,0015787	-0,00092	0,002250	14,043	-91,508	-184,465	1,200	0,00048	200000000	450,000	2,400	0,00096	199999722	101,518	7,715
0,0027957	0,075	0,159	0,254	0,072	0,00280	145,092	-0,0015696	-0,00091	0,002250	14,042	-90,983	-182,962	1,300	0,00052	200000000	450,000	2,400	0,00096	199999666	101,564	7,690

0,0027944	0,076	0,159	0,254	0,072	0,00279	145,156	-0,0015607	-0,00091	0,002250	14,041	-90,465	-181,482	1,400	0,00056	200000000	450,000	2,400	0,00096	199999572	101,609	7,665
0,0027931	0,076	0,159	0,254	0,071	0,00279	145,218	-0,0015519	-0,00090	0,002250	14,040	-89,955	-180,023	1,500	0,00060	200000000	450,000	2,400	0,00096	199999719	101,652	7,640
0,0027919	0,076	0,159	0,254	0,071	0,00279	145,278	-0,0015432	-0,00089	0,002250	14,039	-89,452	-178,585	1,600	0,00064	200000000	450,000	2,400	0,00096	199999446	101,695	7,616
0,0027907	0,076	0,159	0,254	0,071	0,00279	145,337	-0,0015346	-0,00089	0,002250	14,038	-88,956	-177,168	1,700	0,00068	200000000	450,000	2,400	0,00096	199999592	101,736	7,591
0,0027895	0,076	0,159	0,254	0,071	0,00279	145,394	-0,0015262	-0,00088	0,002250	14,037	-88,467	-175,770	1,800	0,00072	200000000	450,000	2,400	0,00096	199999695	101,776	7,568
0,0027883	0,076	0,159	0,254	0,070	0,00279	145,449	-0,0015179	-0,00087	0,002250	14,036	-87,985	-174,393	1,900	0,00076	200000000	450,000	2,400	0,00096	200000000	101,814	7,544
0,0027871	0,076	0,159	0,254	0,070	0,00279	145,503	-0,0015097	-0,00087	0,002250	14,035	-87,510	-173,035	2,000	0,00080	200000000	450,000	2,400	0,00096	200000000	101,852	7,521
0,0027859	0,076	0,159	0,254	0,070	0,00279	145,555	-0,0015016	-0,00086	0,002250	14,034	-87,042	-171,696	2,100	0,00084	200000000	450,000	2,400	0,00096	199999901	101,889	7,498
0,0027848	0,076	0,159	0,254	0,070	0,00278	145,606	-0,0014936	-0,00085	0,002250	14,033	-86,580	-170,375	2,200	0,00088	200000000	450,000	2,400	0,00096	200000000	101,924	7,475
0,0027837	0,076	0,159	0,254	0,070	0,00278	145,656	-0,0014858	-0,00085	0,002250	14,032	-86,124	-169,073	2,300	0,00092	200000000	450,000	2,400	0,00096	200000000	101,959	7,453
0,0027826	0,076	0,159	0,255	0,069	0,00278	145,704	-0,001478	-0,00084	0,002250	14,031	-85,675	-167,788	2,400	0,00096	200000000	450,000	2,400	0,00096	199998964	101,993	7,431
0,0028176	0,075	0,157	0,252	0,076	0,00282	147,591	-0,0017229	-0,00104	0,002250	14,061	-99,867	-208,361	0,000	0,00000	200000000	450,000	2,500	0,00100	199999712	103,314	8,170
0,002816	0,075	0,158	0,252	0,076	0,00282	147,688	-0,0017118	-0,00103	0,002250	14,060	-99,227	-206,531	0,100	0,00004	200000000	450,000	2,500	0,00100	199999806	103,382	8,139
0,0028144	0,075	0,158	0,252	0,075	0,00281	147,783	-0,001701	-0,00102	0,002250	14,058	-98,597	-204,729	0,200	0,00008	200000000	450,000	2,500	0,00100	199999874	103,448	8,109
0,0028129	0,075	0,158	0,252	0,075	0,00281	147,874	-0,0016902	-0,00101	0,002250	14,057	-97,976	-202,956	0,300	0,00012	200000000	450,000	2,500	0,00100	199999737	103,512	8,080
0,0028114	0,075	0,158	0,252	0,075	0,00281	147,963	-0,0016797	-0,00101	0,002250	14,056	-97,365	-201,209	0,400	0,00016	200000000	450,000	2,500	0,00100	200000000	103,574	8,051
0,0028099	0,075	0,158	0,252	0,075	0,00281	148,049	-0,0016693	-0,00100	0,002250	14,054	-96,764	-199,489	0,500	0,00020	200000000	450,000	2,500	0,00100	199999924	103,635	8,022
0,0028084	0,075	0,158	0,253	0,074	0,00281	148,133	-0,0016591	-0,00099	0,002250	14,053	-96,171	-197,795	0,600	0,00024	200000000	450,000	2,500	0,00100	199999730	103,693	7,993
0,002807	0,075	0,158	0,253	0,074	0,00281	148,215	-0,001649	-0,00098	0,002250	14,052	-95,587	-196,126	0,700	0,00028	200000000	450,000	2,500	0,00100	200000000	103,750	7,965
0,0028056	0,075	0,158	0,253	0,074	0,00281	148,294	-0,0016391	-0,00097	0,002250	14,051	-95,012	-194,483	0,800	0,00032	200000000	450,000	2,500	0,00100	199999927	103,806	7,938
0,0028042	0,075	0,158	0,253	0,074	0,00280	148,371	-0,0016294	-0,00096	0,002250	14,049	-94,446	-192,864	0,900	0,00036	200000000	450,000	2,500	0,00100	200000000	103,860	7,911
0,0028028	0,075	0,158	0,253	0,073	0,00280	148,446	-0,0016197	-0,00096	0,002250	14,048	-93,888	-191,269	1,000	0,00040	200000000	450,000	2,500	0,00100	199999897	103,912	7,884
0,0028015	0,075	0,158	0,253	0,073	0,00280	148,519	-0,0016102	-0,00095	0,002250	14,047	-93,339	-189,697	1,100	0,00044	200000000	450,000	2,500	0,00100	199999341	103,963	7,857
0,0028001	0,075	0,158	0,253	0,073	0,00280	148,590	-0,0016009	-0,00094	0,002250	14,046	-92,797	-188,148	1,200	0,00048	200000000	449,999	2,500	0,00100	200000000	104,013	7,831
0,0027988	0,075	0,158	0,253	0,073	0,00280	148,659	-0,0015917	-0,00093	0,002250	14,045	-92,263	-186,622	1,300	0,00052	200000000	450,000	2,500	0,00100	200000000	104,061	7,805
0,0027975	0,075	0,158	0,253	0,072	0,00280	148,726	-0,0015826	-0,00093	0,002250	14,044	-91,737	-185,119	1,400	0,00056	200000000	450,000	2,500	0,00100	199999670	104,108	7,780
0,0027962	0,075	0,158	0,253	0,072	0,00280	148,791	-0,0015737	-0,00092	0,002250	14,043	-91,218	-183,636	1,500	0,00060	200000000	450,000	2,500	0,00100	200000000	104,154	7,755
0,002795	0,075	0,159	0,254	0,072	0,00279	148,855	-0,0015649	-0,00091	0,002250	14,041	-90,707	-182,175	1,600	0,00064	200000000	450,000	2,500	0,00100	199999697	104,198	7,730
0,0027937	0,076	0,159	0,254	0,072	0,00279	148,916	-0,0015562	-0,00090	0,002250	14,040	-90,204	-180,735	1,700	0,00068	200000000	450,000	2,500	0,00100	199999282	104,241	7,706
0,0027925	0,076	0,159	0,254	0,071	0,00279	148,976	-0,0015476	-0,00090	0,002250	14,039	-89,707	-179,315	1,800	0,00072	200000000	450,000	2,500	0,00100	199999876	104,283	7,682
0,0027913	0,076	0,159	0,254	0,071	0,00279	149,034	-0,0015391	-0,00089	0,002250	14,038	-89,217	-177,915	1,900	0,00076	200000000	450,000	2,500	0,00100	200000000	104,324	7,658
0,0027901	0,076	0,159	0,254	0,071	0,00279	149,091	-0,0015308	-0,00088	0,002250	14,037	-88,735	-176,535	2,000	0,00080	200000000	450,000	2,500	0,00100	199999235	104,364	7,634
0,0027889	0,076	0,159	0,254	0,071	0,00279	149,146	-0,0015226	-0,00088	0,002250	14,036	-88,258	-175,174	2,100	0,00084	200000000	450,000	2,500	0,00100	200000000	104,402	7,611
0,0027878	0,076	0,159	0,254	0,070	0,00279	149,200	-0,0015145	-0,00087	0,002250	14,035	-87,789	-173,832	2,200	0,00088	200000000	450,000	2,500	0,00100	200000000	104,440	7,588
0,0027866	0,076	0,159	0,254	0,070	0,00279	149,252	-0,0015065	-0,00086	0,002250	14,034	-87,326	-172,508	2,300	0,00092	200000000	450,000	2,500	0,00100	200000000	104,476	7,566
0,0027855	0,076	0,159	0,254	0,070	0,00279	149,303	-0,0014986	-0,00086	0,002250	14,033	-86,869	-171,203	2,400	0,00096	200000000	450,000	2,500	0,00100	200000000	104,512	7,543
0,0027844	0,076	0,159	0,254	0,070	0,00278	149,352	-0,0014909	-0,00085	0,002250	14,032	-86,419	-169,915	2,500	0,00100	200000000	450,000	2,500	0,00100	200000000	104,547	7,521

200x200x2800 (Phase 3)																					
h	0,200																				
b	0,2																				
d	0,175																				
d'	0,030																				

